UNIWERSYTET MARII CURIE-SKŁODOWSKIEJ
W LUBLINIE
Szkoła Doktorska Nauk Ścisłych i Przyrodniczych

Dziedzina: **nauki rolnicze**
Dyscyplina: **rolnictwo i ogrodnictwo**

Nataliia Kutyrieva-Nowak
nr albumu: 252404

Badania białek arabinogalaktanowych (AGP) jako istotnych składników ściany komórkowej w procesie dojrzewania owoców

(Studies on arabinogalactan proteins (AGPs) as significant components of cell wall in the fruit ripening process)

Rozprawa doktorska przygotowywana pod kierunkiem naukowym
promotora: dr hab. Agaty Leszczuk

w Instytucie Agrofizyki im. Bohdana Dobrzańskiego
Polskiej Akademii Nauk

LUBLIN, 2025

Składam serdeczne podziękowania
Pani dr hab. Agacie Leszczuk za nieocenioną pomoc
przy realizacji niniejszej pracy,
za opiekę metodyczną i merytoryczną,
za wszystkie inspiracje oraz
za okazaną życzliwość i wyrozumiałość.

OŚWIADCZENIE PROMOTORA ROZPRAWY

Oświadczam, że niniejsza rozprawa została przygotowania pod moim kierunkiem i stwierdzam, że spełnia ona warunki do przestawienia jej w postępowaniu o nadanie stopnia naukowego.

Data …… Podpis promotora rozprawy ……..…..…

OŚWIADCZENIE AUTORA ROZPRAWY

Świadoma odpowiedzialności prawnej oświadczam, że niniejsza rozprawa została napisana przeze mnie samodzielnie i nie zawiera treści uzyskanych w sposób niezgodny z obowiązującymi przepisami.

Oświadczam również, że przedstawiona rozprawa nie była wcześniej przedmiotem procedur związanych z uzyskaniem stopnia naukowego w wyższej uczelni.

Oświadczam ponadto, że niniejsza rozprawa jest identyczna z załączoną wersją elektroniczną.

Data …… Podpis autora rozprawy ……..……

NARODOWE CENTRUM NAUKI

Badania do rozprawy doktorskiej zostały wykonane w ramach projektu finansowanego przez Narodowe Centrum Nauki, pt. „Badania białek arabinogalaktanowych (AGP) jako istotnych składników ściany komórkowej podczas procesu dojrzewania owoców” (Sonata 16, nr 2020/39/D/NZ9/00232).

CIHEAM
MAI CHANIA

Badania opisane w rozprawie doktorskiej zostały zrealizowane w ścisłej współpracy z zespołem badawczym kierowanym przez dr Panagiotis Kalaitzis z Horticultural Genetics & Biotechnology Department w Mediterranean Agronomic Institute of Chania w Grecji.

Streszczenie

Ściana komórkowa jest zewnętrzną warstwą komórki roślinnej, a jej struktura oraz wiązania pomiędzy poszczególnymi składnikami są kluczowe dla funkcjonowania całego organizmu. Ważnymi składnikami odpowiedzialnymi za współtworzenie amorficznej macierzy zewnątrzkomórkowej są białka arabinogalaktanowe (AGP). AGP są proteoglikanami, należącymi do rodziny glikoprotein bogatych w hydroksyprolinę. Zbudowane są z domeny białkowej połączonej z łańcuchami węglowodanowymi. Zaburzenia podczas poszczególnych etapów biosyntezy AGP są krytyczne dla ich budowy i rozmieszczenia w komórce, co z kolei może oddziaływać na ich funkcjonalność podczas zachodzących procesów fizjologicznych, w tym w procesie dojrzewania owoców.

W związku z tym, w niniejszej rozprawie doktorskiej sformułowano hipotezę, zgodnie, z którą **proces dojrzewania owoców pomidora jest ściśle skorelowany ze zmianami dystrybucji i cechami molekularnymi AGP**. Powyższa hipoteza została zweryfikowana w ramach badań *in situ* i *ex situ,* które polegały na analizie zmian w strukturze, zawartości i lokalizacji AGP w trakcie procesu dojrzewania owoców pomidora (*Solanum lycopersicum* L.) roślin „dzikiego typu" oraz linii ze zmodyfikowaną ekspresją genu *SlP4H3*. **Głównym celem niniejszej rozprawy doktorskiej było zbadanie roli AGP w formowaniu struktury ściany komórkowej, ze szczególnym uwzględnieniem czasowo-przestrzennej dystrybucji pozostałych jej składników w trakcie procesu dojrzewania owoców.**

Rozprawa doktorska obejmuje trzy zasadnicze etapy badawcze. Pierwszy etap badań umożliwił wyodrębnienie AGP jako potencjalnych markerów procesu dojrzewania. Zaobserwowano stopniowe zmniejszenie zawartości AGP w miarę postępu dojrzewania owoców. W początkowych stadiach procesu dominowały frakcje AGP o masie molekularnej 60-120 kDa. Podczas gdy w fazach kończących proces odnotowano dominację frakcji o masie molekularnej 20-25 kDa. Ponadto, w finalnych stadiach procesu zaobserwowano obecność AGP o masie molekularnej 30 kDa, które uznano za marker zakończenia procesu dojrzewania. Badania mikroskopowe tkanki owoców potwierdziły występowanie zmian ilościowych, jak i czasowo-przestrzennych modyfikacji specyficznych epitopów AGP w miarę postępującego procesu dojrzewania. W owocach we wstępnych stadiach procesu, epitopy AGP, rozpoznawane przez przeciwciała JIM13 i LM2, zlokalizowano w przestrzeni

pomiędzy ścianą a błoną komórkową. W miarę postępu dojrzewania zaobserwowano zaburzenie charakterystycznego wzorca dystrybucji AGP.

Kolejny etap badań umożliwił określenie zmian w zawartości oraz lokalizacji epitopów AGP w owocach linii transgenicznych, w których zmodyfikowano ekspresję genu *SlP4H3*. Przeprowadzone badania ujawniły zależności pomiędzy zmianami ekspresji genu *SlP4H3* a ilością AGP w owocach. Stwierdzono brak charakterystycznej frakcji AGP – markerów zakończenia procesu dojrzewania, a rozkład mas molekularnych analizowanych epitopów AGP był odmienny niż w owocach „dzikiego typu". Zaobserwowano występowanie nieprawidłowości anatomicznych i morfologicznych w owocach linii transgenicznych. Epitopy AGP w owocach znajdowały się głównie w zdegradowanych kompartymentach ściany komórkowej, w cytoplazmie.

Ostatni etap badań umożliwił określenie bezpośredniego wpływu zmian w strukturze AGP oraz ich lokalizacji na montaż ściany komórkowej. Ilość i czasowo-przestrzenna dystrybucja ekstensyn, ksylanu, ramnogalakturonanu typu I, nisko i wysoko estryfikowanego homogalakturonanu uległy modyfikacji. Dodatkowo, w owocach linii transgenicznych, aberracje w organizacji ściany komórkowej spowodowały zmiany w tkance owoców, które uwidoczniono na poziomie tkankowym, komórkowym oraz subkomórkowym.

Podsumowując, zaburzenia struktury, zawartości i czasowo-przestrzennej dystrybucji AGP stanowią czynnik zakłócający prawidłowy przebieg procesu dojrzewania owoców. W związku z powyższym, **wyniki uzyskane w ramach niniejszej rozprawy doktorskiej potwierdzają hipotezę, że AGP mają kluczowe znaczenie dla procesu dojrzewania owoców.**

Słowa kluczowe: białka arabinogalaktanowe, ściana komórkowa, proces dojrzewania, owoce pomidora

Abstract

The cell wall is the outer layer of a plant cell, and its structure and the bonds between components are crucial to the function of the whole organism. Arabinogalactan proteins (AGPs) are important components responsible for co-forming the amorphous extracellular matrix. AGPs are glycoproteins belonging to the hydroxyproline-rich glycoprotein family. They consist of a protein domain linked to sugar chains. Disruption of the various stages of AGP biosynthesis is critical to their structure and distribution in cells, which can affect their functional properties during the occurring physiological processes, including fruit ripening.

Accordingly, this thesis proposes the hypothesis that **tomato fruit ripening is closely correlated with changes in the distribution and molecular characteristics of AGPs**. The above hypothesis was verified through *in situ* and *ex situ* studies, which investigated changes in the structure, content, and localisation of AGPs during the ripening of tomato (*Solanum lycopersicum* L.) fruit from wild-type plants and lines with modified expression of the *SlP4H3* gene. **The main objective was to study the role of AGP in the formation of the cell wall structure, with a particular focus on the spatio-temporal distribution of its other components during the fruit ripening process**.

The thesis consists of three main research phases. The first phase of the study enabled the identification of AGPs as potential markers indicating the progression of the ripening process. A gradual decrease in AGP content was observed as the fruit ripened. In the early stages of the process, AGP fractions with a molecular weight of 60-120 kDa dominated, while in the later stages, fractions with a molecular weight of 20-25 kDa became more dominant. In addition, bands indicating the presence of AGP with a molecular weight of 30 kDa were observed in the final stages of the process, which can be considered as a marker for the finalisation of the ripening process. Microscopic analysis of fruit tissues confirmed the presence of quantitative changes as well as spatio-temporal modifications of specific AGP epitopes as the ripening process progressed. In fruit at the beginning of ripening, AGP epitopes recognised by JIM13 and LM2 antibodies were mainly localised in the space between the cell wall and the plasma membrane. As ripening progressed, a disruption of the characteristic AGP distribution pattern was observed.

The next stage of the study allowed the determination of changes in the content and localisation of AGP in the fruit of transgenic lines in which the expression of the *SlP4H3*

gene had been modified. The study demonstrated correlations between changes in *SlP4H3* gene expression and AGP content in fruit during the ripening process. The characteristic AGP fraction, which marks the finalisation of the ripening, was absent, and the layout of molecular masses of the AGP epitopes analysed differed from that observed in wild-type fruit. Anatomical and morphological changes in the fruit of transgenic lines were observed. AGP epitopes in fruit were mainly located in degraded cell wall compartments, in the cytoplasm.

In the final stage of the study, it was possible to determine the direct effect of changes in AGP structure and localisation on cell wall assembly. The amount and spatio-temporal distribution of extensin, xylan, rhamnogalacturonan type I, low and high esterified homogalacturonan were modified. In the fruit of transgenic lines, disruption of polysaccharide and proteoglycan networks in the cell wall was noted as ripening progressed. Additionally, aberrations in cell wall organization led to changes in fruit tissues, observed at the tissue, cellular and subcellular levels.

In conclusion, changes in the structure, content and spatio-temporal distribution of AGPs represent a disruptive factor in fruit ripening. Accordingly, **the results obtained in this thesis support the hypothesis that AGPs are crucial for the fruit ripening process**.

Keywords: arabinogalactan proteins, cell wall, ripening process, tomato fruit

Spis treści

Lista publikacji stanowiących podstawę rozprawy doktorskiej

Niniejsza rozprawa doktorska jest oparta na cyklu publikacji pod tytułem:

„Badania białek arabinogalaktanowych (AGP) jako istotnych składników ściany komórkowej w procesie dojrzewania owoców”

P.1: **Kutyrieva-Nowak N.**, Leszczuk A., Zdunek A. 2023. A practical guide to *in situ* and *ex situ* characterisation of arabinogalactan proteins (AGPs) in fruits. Plant Methods, 19: 117.

Wskaźnik Impact Factor (2023): 4.7; punktacja MNiSW: 140 punktów.

P.2: **Kutyrieva-Nowak N.**, Leszczuk A., Zając A., Kalaitzis P., Zdunek A. 2023. Arabinogalactan protein is a molecular and cytological marker of particular stages of the tomato fruit ripening process. Scientia Horticulturae, 310: 111718.

Wskaźnik Impact Factor (2023): 3.9; punktacja MNiSW: 140 punktów.

P.3: **Kutyrieva-Nowak N.**, Leszczuk A., Ezzat L., Kaloudas D., Zając A., Szymańska-Chargot M., Skrzypek T., Krokida A., Mekkaoui K., Lampropoulou E., Kalaitzis P., Zdunek A. 2024. The modified activity of prolyl 4 hydroxylases reveals the effect of arabinogalactan proteins on changes in the cell wall during the tomato ripening process. Frontiers in Plant Science, 15: 1365490.

Wskaźnik Impact Factor (2023): 4.1; punktacja MNiSW: 100 punktów.

P.4: **Kutyrieva-Nowak N.**, Leszczuk A., Denic D., Bellaidi S., Blazakis K., Gemeliari P., Lis M., Kalaitzis P., Zdunek A. 2024. *In vivo* and *ex vivo* study on cell wall components as part of the network in tomato fruit during the ripening process. Horticulture Research, 11: uhae145.

Wskaźnik Impact Factor (2023): 7.6; punktacja MNiSW: 200 punktów.

Opis indywidualnego wkładu do publikacji stanowiących podstawę rozprawy doktorskiej

P.1: Kutyrieva-Nowak N., Leszczuk A., Zdunek A. 2023. A practical guide to *in situ* and *ex situ* characterisation of arabinogalactan proteins (AGPs) in fruits. Plant Methods, 19: 117.

Indywidualny wkład: przegląd literatury dotyczącej technik analizy białek arabinogalaktanowych (AGP), analiza protokołów metod badawczych, przygotowanie manuskryptu, udział w edycji i korekcie manuskryptu oraz uczestnictwo w odpowiedziach na recenzje

P.2: Kutyrieva-Nowak N., Leszczuk A., Zając A., Kalaitzis P., Zdunek A. 2023. Arabinogalactan protein is a molecular and cytological marker of particular stages of the tomato fruit ripening process. Scientia Horticulturae, 310: 111718.

Indywidualny wkład: przeprowadzenie badań laboratoryjnych, analiza uzyskanych wyników, statystyczne i graficzne opracowanie danych, przygotowanie manuskryptu, udział w edycji i korekcie manuskryptu oraz uczestnictwo w odpowiedziach na recenzje

P.3: Kutyrieva-Nowak N., Leszczuk A., Ezzat L., Kaloudas D., Zając A., Szymańska-Chargot M., Skrzypek T., Krokida A., Mekkaoui K., Lampropoulou E., Kalaitzis P., Zdunek A. 2024. The modified activity of prolyl 4 hydroxylases reveals the effect of arabinogalactan proteins on changes in the cell wall during the tomato ripening process. Frontiers in Plant Science, 15: 1365490.

Indywidualny wkład: przeprowadzenie badań laboratoryjnych, analiza uzyskanych wyników, statystyczne i graficzne opracowanie danych, przygotowanie manuskryptu, udział w edycji i korekcie manuskryptu oraz uczestnictwo w odpowiedziach na recenzje

P.4: Kutyrieva-Nowak N., Leszczuk A., Denic D., Bellaidi S., Blazakis K., Gemeliari P., Lis M., Kalaitzis P., Zdunek A. 2024. *In vivo* and *ex vivo* study on cell wall components as part of the network in tomato fruit during the ripening process. Horticulture Research, 11: uhae145.

Indywidualny wkład: przeprowadzenie badań laboratoryjnych, analiza uzyskanych wyników, statystyczne i graficzne opracowanie danych, przygotowanie manuskryptu, udział w edycji i korekcie manuskryptu oraz uczestnictwo w odpowiedziach na recenzje

Wykaz skrótów

Skrót	Wyjaśnienie skrótu	Objaśnienie z języka angielskiego
2-ODD	Dioksygenaza zależna od 2-oksoglutaranu	*2-oxoglutarate-dependent dioxygenase*
4-Me-GlcA	Kwas 4-O-metylo-D-glukuronowy	*4-O-methyl-D-glucuronic acid*
AG	Arabinogalaktan	*Arabinogalactan*
AGP	Białka arabinogalaktanowe	*Arabinogalactan proteins*
Ala	Alanina	*Alanine*
APAP1	Kompleks składający z arabinoksylanu, pektyn i białek arabinogalaktanowych	*Arabinoxylan Pectin Arabinogalactan Protein 1 Complex*
L-Ara	L-arabinoza	*L-arabinose*
Asn	Asparagina	*Asparagine*
AZ	Strefa odcięcia owocu	*Fruit abscission zone*
CLSM	Skanujący laserowy mikroskop konfokalny	*Confocal laser scanning microscope*
CWP	Białka ściany komórkowej	*Cell wall proteins*
Cys	Cysteina	*Cysteine*
DHP	3,4-dehydroprolina	*3,4-dehydroproline*
ELISA	Test immunoenzymatyczny	*Enzyme-linked immunosorbent assay*
FLA	AGP podobne do fascyklin	*Fasciclin-like AGPs*
L-Fuc	L-fukoza	*L-fucose*
Gal	D-galaktoza	*D-galactose*
GalA	Kwas D-galakturonowy	*D-galacturonic acid*
GAP	Białka zakotwiczone kotwicą GPI	*GPI-anchored proteins*
Glc	D-glukoza	*D-glucose*
GlcA	Kwas D-glukuronowy	*D-glucuronic acid*
GlcN	D-glukozamina	*D-glucosamine*
GPI	Kotwica glikozylofosfatydyloinozytolu	*Glycosylphosphatidyl inositol anchor*

Skrót	Wyjaśnienie skrótu	Objaśnienie z języka angielskiego
HG	Homogalakturonan	*Homogalacturonan*
HRGP	Glikoproteiny bogate w hydroksyprolinę	*Hydroxyproline-rich glycoproteins*
Hyp	Hydroksyprolina	*Hydroxyproline*
Lys	Lizyna	*Lysine*
Man	D-mannoza	*D-mannose*
P4H	Hydroksylaza 4-prolinowa	*Prolyl 4-hydroxylase*
PCR	Łańcuchowa reakcja polimerazy	*Polymerase chain reaction*
PDCA	2,4-dikarboksylan pirydyny	*Pyridine 2,4-dicarboxylate*
L-Rha	L-ramnoza	*L-rhamnose*
Pro	Prolina	*Proline*
PVDF	Polifluorek winylidenu	*Polyvinylidene difluoride*
RG-I	Ramnogalakturonan typu I	*Rhamnogalacturonan type I*
SDS-PAGE	Elektroforeza w żelu poliakrylamidowym w warunkach denaturujących białko w obecności soli sodowej siarczanu dodecylu	*Sodium dodecyl sulphate-polyacrylamide gel electrophoresis*
SEM	Skaningowy mikroskop elektronowy	*Scanning electron microscope*
SEM-EDS	SEM z mikroanalizą EDS – spektroskopia dyspersji energii	*SEM with energy dispersive spectroscopy*
Ser	Seryna	*Serine*
SlP4H	Gen kodujący hydroksylazę 4-prolinową w roślinie pomidora	*Solanum lycopersicum Prolyl 4-Hydroxylase*
TEM	Transmisyjny mikroskop elektronowy	*Transmission electron microscope*
Thr	Treonina	*Threonine*
Val	Walina	*Valine*
Xyl	D-ksyloza	*D-xylose*

Wykaz skrótów – opis materiału badawczego

Skrót	Wyjaśnienie skrótu	Objaśnienie z języka angielskiego
cGFP	Linia transgeniczna z nadekspresją genu *SlP4H3* ze znacznikiem GFP znajdującym się na C-końcu DNA	*Transgenic line with overexpression SlP4H3 gene with the GFP tag at the C-terminus DNA*
nGFP	Linia transgeniczna z nadekspresją genu *SlP4H3* ze znacznikiem GFP znajdującym się na N-końcu DNA	*Transgenic line with overexpression SlP4H3 gene with the GFP tag at the N-terminus DNA*
OEX#1	Linia transgeniczna z nadekspresją genu *SlP4H3* nr 1	*Transgenic line with overexpression SlP4H3 gene*
OEX#2	Linia transgeniczna z nadekspresją genu *SlP4H3* nr 2	*Transgenic line with overexpression SlP4H3 gene*
RNAi#1	Linia transgeniczna z wyciszoną ekspresją genu *SlP4H3* nr 1	*Transgenic line with silenced SlP4H3 gene*
RNAi#7	Linia transgeniczna z wyciszoną ekspresją genu *SlP4H3* nr 7	*Transgenic line with silenced SlP4H3 gene*
WT	Roślina „dzikiego typu”	*‘Wild type’ plants*

Wykaz skrótów – opis stadiów procesu dojrzewania owoców

Skrót	Wyjaśnienie skrótu	Objaśnienie z języka angielskiego
BR	Początek procesu dojrzewania, stadium początku wybarwienia, tzw. stadium „przełamania”	*Breaker stage*
TU	Zaawansowane wybarwienie owoców, stadium słabo „zapalone”	*Turning stage*
PINK	Stadium różowe	*Pink stage*
RR	Zakończenie procesu dojrzewania, stadium czerwone	*Red Ripe stage*

1. Wprowadzenie

1.1 Ściana komórkowa podczas procesu dojrzewania owoców

Dojrzewanie owoców jest złożonym procesem rozwojowym obejmującym zmiany fizjologiczne, morfologiczne oraz anatomiczne tkanki (Kalaitzis i in., 2023; Osorio i in., 2013). Postęp procesu dojrzewania owoców prowadzi do istotnych zmian w ich kolorze, smaku, teksturze i aromacie (Klee i Giovannoni, 2011), a jakość dojrzałych owoców jest kluczowa dla producentów żywności i konsumentów (Brummell, 2006). Znaczącą ilość badań dotyczących procesu dojrzewania owoców prowadzono z wykorzystaniem układu modelowego – owoców pomidora (*Solanum lycopersicum* L.) (Feder i in., 2020; Hyodo i in., 2013). Ważnym aspektem branym pod uwagę w wyborze wspomnianego obiektu badań jest również znaczenie pomidora jako rośliny uprawnej (Skolik i in., 2019). Na całym świecie co roku produkuje się około 182 mln ton owoców pomidora (Quinet i in., 2019).

Molekularne podstawy procesu dojrzewania owoców są złożone i związane z cechami strukturalnymi ściany komórkowej (Hyodo i in., 2013; Seymour i in., 2013). Zaobserwowano, że podczas dojrzewania owoców dochodzi do degradacji polisacharydów i proteoglikanów ściany komórkowej, jak również do modyfikacji wiązań pomiędzy jej składnikami (Brummell, 2006). Postępująca degradacja ściany komórkowej powoduje rozluźnienie struktury tkanki owoców oraz stanowi końcowe stadium procesu dojrzewania (Kalaitzis i in., 2023). Pektyny blaszki środkowej stają się słabiej związane z macierzą zewnątrzkomórkową, co prowadzi do powstawania pustych przestrzeni międzykomórkowych (Orfila i in., 2001; Paniagua i in., 2014; Posé i in., 2019; Wang i Seymour, 2022). Ponadto, ich degradacja przyczynia się do wzrostu ilości wolnych jonów wapnia (Ca^{2+}) w apoplaście (Ortiz i in., 2011), regulujących aktywność enzymów, w tym pektynoesteraz, celulaz, poligalakturonaz, β-galaktozydaz i liaz pektynowych (Gao i in., 2019). Zaś, aktywność wspomnianych enzymów powoduje nie tylko rozkład poszczególnych składników ściany komórkowej (Seymour i in., 2013), ale również wpływa na postęp wnikania wody do przestrzeni między fibrylami celulozowymi, powodując jej pęcznienie i pękanie (Brummell, 2006; Posé i in., 2018, 2019).

Ściana komórkowa jest najbardziej zewnętrzną warstwą komórki roślinnej (Srivastava i in., 2017; Zhang i in., 2021). Jej skład jest zmienny i zależy od gatunku rośliny, typu tkanki i stadium fizjologicznego (Srivastava i in., 2017). Ściana komórkowa składa się z sieci mikrofibryli celulozowych połączonych z innymi polisacharydami,

m.in. hemicelulozami i pektynami (Lampugnani i in., 2018). Według najnowszego modelu budowy ściany komórkowej zwanego kompleksem APAP1 (ang. *Arabinoxylan Pectin Arabinogalactan Protein 1 Complex*), to białka arabinogalaktanowe (ang. *arabinogalactan proteins, AGP*) odgrywają w nim kluczową rolę strukturalną (Tan i in., 2013, 2023). AGP są odpowiedzialne za tworzenie dynamicznej sieci porządkującej polisacharydy i proteoglikany w kontinuum ściana-błona komórkowa. Kompleks APAP1 zbudowany jest z AGP, arabinogalaktanu typu II (ang. *arabinogalactan type II, AG*), homogalakturonanu (ang. *homogalacturonan, HG*), ramnogalakturonanu typu I (ang. *rhamnogalacturonan type I, RG-I*) i ksylanu (ang. *xylan*) (Hijazi i in., 2014a, 2014b; Tan i in., 2013, 2023). Ilość i rozmieszczenie poszczególnych składników kompleksu APAP1 należą do najważniejszych czynników wpływających na funkcję ściany komórkowej podczas przemian fizjologicznych (Srivastava i in., 2017; Tan i in., 2013). Zakłada się, że kompleks APAP1 nie pełni jedynie funkcji strukturalnej, ale również jest zaangażowany w sygnalizację komórkową i adhezję komórka-komórka (Hijazi i in., 2014b; Tan i in., 2013).

1.2 Charakterystyka białek arabinogalaktanowych

AGP są złożonymi proteoglikanami (Ellis i in., 2010; Nothnagel, 1997), należącymi do jednej z dziewięciu funkcjonalnych grup białek zaangażowanych w interakcje z innymi składnikami ściany komórkowej (ang. *cell wall proteins, CWP*) (Hijazi i in., 2014b). Najprostszym sposobem klasyfikacji AGP jest wydzielenie dwóch grup: klasycznych i nieklasycznych AGP (Silva i in., 2020). Klasyczne AGP należą do rodziny glikoprotein bogatych w hydroksyprolinę (ang. *highly glycosylated hydroxyproline-rich glycoproteins, HRGP*) (Ellis i in., 2010; Fragkostefanakis i in., 2012). Zaś, nieklasyczne AGP posiadają zmienną ilość aminokwasów (Showalter, 2001), dzięki czemu można podzielić je dodatkowo na: AGP ubogie w hydroksyprolinę (Hyp) (Baldwin i in., 1993), AGP bogate w cysteinę (Cys), asparaginę (Asn) i/lub lizynę (Lys) (Showalter, 2001), AGP podobne do fascyklin (ang. *fasciclin-like AGPs, FLA*) (Schultz i in., 2002) oraz chimeryczne AGP (Showalter, 2001).

Po kilkudziesięciu latach badań AGP nadal wyzwaniem jest ich ekstrakcja oraz oczyszczanie (Strasser i in., 2021). Najczęściej w celu ich izolacji wykorzystuje się odczynnik Yariv (Hoshing i in., 2020; Yariv i in., 1962). Odczynnik ten selektywnie rozpoznaje i wiąże łańcuchy β-(1→3)-galaktanów, dłuższe niż pięć reszt (Chen i in., 2024;

Kitazawa i in., 2013; Rueda i in., 2023). Wspomniane pentagalaktany zostały zidentyfikowane jako najmniejsze sekwencje AGP wymagane do reaktywności odczynnika Yariv (Hoshing i in., 2022; Paulsen i in., 2014). Analiza kompleksu Yariv-pentagalaktan ujawniła, że stabilność tej struktury jest wynikiem oddziaływań niekowalencyjnych π-π i CH/π. Odziaływania te zachodzą pomiędzy hydrofobowymi domenami odczynnika Yariv a bogatymi w grupy CH obszarami pentagalaktanów (Přerovská i in., 2021). Dzięki zdolności do stabilnego wiązania łańcuchów węglowodanowych, odczynnik Yariv znalazł zastosowanie również w badaniach roli AGP w przemianach fizjologicznych roślin (Chen i in., 2024). Wyniki badań Pérez-Pérez i współpracowników (2019) wykazały, że obecność odczynnika Yariv modyfikuje przebieg embriogenezy somatycznej. Ponadto stwierdzono, że dodanie odczynnika Yariv do pożywki hodowlanej ma istotny wpływ na rozwój struktury łagiewki pyłkowej podczas kiełkowania ziaren pyłku (Leszczuk i in., 2019b).

Typowe klasyczne AGP składają się z części białkowej i rozbudowanej domeny cukrowej. Około 90-95% cząsteczki AGP stanowią łańcuchy węglowodanowe, głównie AG typu II (Kieliszewski, 2001; Popper, 2011), które są wysoce O-glikozylowane do reszt Hyp (Johnson i in., 2017; Tan i in., 2003). Szkielet białkowy, stanowiący N-końcową domenę AGP, składa się z około 100 aminokwasów (Schultz i in., 2000), głównie proliny (Pro), Hyp, alaniny (Ala), seryny (Ser), treoniny (Thr) i waliny (Val) (Ma i Johnson, 2023; Showalter, 2001; Showalter i Basu, 2015). Reszty aminokwasowe ułożone są w powtarzające się motywy dipeptydowe: Ala-Pro, Ser-Pro, Thr-Pro i Val-Pro (Showalter i Basu, 2016). Reszty Pro są hydroksylowane przez wielogenową rodzinę enzymów – hydroksylazy 4-prolinowe (ang. *prolyl 4-hydroxylases, P4H*) (Kalaitzis i in., 2010). Podczas posttranslacyjnej modyfikacji AGP dochodzi również do przyłączenia ugrupowania wiążącego zwanego kotwicą glikozylofosfatydyloinozytolu (ang. *glycosylphosphatidyl inositol (GPI) anchor*) do hydrofobowej C-końcowej domeny (Fragkostefanakis i in., 2012). Pozwala to do umiejscowienia AGP w zewnętrznej warstwie fosfolipidowej błony komórkowej (Silva i in., 2020), a tym samym na sklasyfikowanie AGP do unikatowej klasy białek zakotwiczonych GPI (ang. *GPI-anchored proteins, GAP*) (Liu i in., 2015). Kotwica GPI zbudowana jest z części oligosacharydowej o składzie α-Man(1→2)-α-Man(1→6)-α-Man(1→4)-α-GlcN(1→6)-inozytol oraz części fosfolipidowej (Oxley i Bacic, 1999). Dominującym składnikiem fosfolipidowym jest fitosfingozyna (Svetek i in., 1999), która jest związana

z kwasem tetrakozanowym (Showalter, 2001). Biosynteza części białkowej i kotwicy GPI zachodzi w obrębie retikulum endoplazmatycznego (Silva i in., 2020; Zhou, 2022).

Domena cukrowa AGP to przede wszystkim łańcuchy β-(1→3)-galaktanu oraz łańcuchy boczne β-(1→6)-galaktanu o zmiennej długości, które zakończone są resztami α-(1→3)-arabinozy (Showalter i Basu, 2016; Tan i in., 2024). Uznaje się, że stosunek L-arabinozy (L-Ara) do D-galaktozy (Gal) wynosi około 1:2 (Göllner i in., 2010). Rzadziej występującymi resztami cukrowymi AGP są D-glukoza (Glc), D-mannoza (Man), D-ksyloza (Xyl), L-ramnoza (L-Rha), L-fukoza (L-Fuc), D-glukozamina (GlcN) (Showalter, 2001), kwas D-glukuronowy (GlcA), kwas D-galakturonowy (GalA) i kwas 4-O-metylo-D-glukuronowy (4-Me-GlcA) (Inaba i in., 2015). Detaliczne analizy chemiczne wykazały, że skład łańcuchów węglowodanowych jest specyficzny dla gatunku rośliny, rodzaju tkanki, a także poszczególnych procesów fizjologicznych (Ghosh i in., 2023). Wysoce rozgałęziona część cukrowa przyłączona do domeny białkowej silnie wpływa na właściwości chemiczne i strukturalne AGP oraz ich różnorodność funkcjonalną (Ma i in., 2018). AGP charakteryzują się różnymi masami molekularnymi, które odzwierciedlają zmienne stopnie glikozylacji ich specyficznych rdzeni białkowych (Showalter i Basu, 2016). O-glikozylacja jest dominującą formą glikozylacji klasycznych AGP, katalizowaną przez Hyp-O-galaktozylotransferazy. Reakcja ta zachodzi w aparacie Golgiego (Ma i Johnson, 2023). Zaburzenia podczas poszczególnych etapów biosyntezy AGP są krytyczne dla ich struktury, zawartości, rozmieszczenia *in situ* i funkcji biologicznej (Silva i in., 2020; Strasser i in., 2021). Zaś, specyficzna i zmienna lokalizacja AGP w kontinuum ściana-błona komórkowa jest wykorzystywana do identyfikacji ich roli podczas zachodzących procesów fizjologicznych (Liu i in., 2015). Udział tych cząsteczek w wielu procesach wzrostu i rozwoju roślin jest dobrze poznany (Silva i in., 2020), ale wciąż brakuje informacji na temat ich funkcji w procesie dojrzewania owoców.

1.3 Wpływ hydroksylazy 4-prolinowej na strukturę i funkcje białek arabinogalaktanowych podczas procesu dojrzewania owoców

Roślinne P4H należą do dioksygenaz zależnych od 2-oksoglutaranu (ang. *2-oxoglutarate-dependent dioxygenases, 2-ODDs*) (Vlad i in., 2010), związanych z błoną komórkową (Kawai i in., 2014; Koski i in., 2009). P4H do prawidłowego funkcjonowania wymagają obecności tlenu jako kosubstratu, jonów żelaza (Fe^{2+}) i kwasu

askorbinowego (Koski i in., 2007). P4H katalizują hydroksylację Pro, która jest główną posttranslacyjną modyfikacją HRGP (Ellis i in., 2010; Perrakis i in., 2021). Mechanizm działania P4H polega na dodaniu grup hydroksylowych (-OH) do Pro w obecności O_2, 2-oksoglutaranu i kwasu askorbinowego. Po reakcji enzymatycznej produktem końcowym jest Hyp oraz dwutlenek węgla i kwas bursztynowy (Koski i in., 2007).

Prawidłowy przebieg hydroksylacji Pro jest niezbędny do wzrostu i rozwoju roślin (Duruflé i in., 2017; Silva i in., 2020; Vlad i in., 2007). Aktywność P4H w komórce można zrewidować za pomocą specyficznych inhibitorów, m.in. 3,4-dehydroproliny (ang. *3,4-dehydroproline, DHP*) (Cooper i Varner, 1983; Piński i in., 2021) lub poprzez manipulację ekspresją genów kodujących ten enzym (Kalaitzis i in., 2010; Perrakis i in., 2019). W badaniach z użyciem selektywnego inhibitora aktywności P4H (DHP) odnotowano zahamowanie procesów podziału komórek, ograniczając rozwój korzeni cebuli (*Allium cepa* L.) (de Tullio i in., 1999). Zastosowanie strukturalnego analogu 2-oksoglutaranu – 2,4-dikarboksylanu pirydyny (ang. *pyridine 2,4-dicarboxylate, PDCA*) indukowało zmiany w procesach dojrzewania owoców pomidora, wpływając na znaczne zmniejszenie produkcji etylenu oraz obniżając ilość epitopów AGP rozpoznawanych przez przeciwciało JIM13 (Kalaitzis i in., 2010). Dodatkowo, zastosowanie PDCA skutkowało modyfikacjami w procesie tworzenia komórek korzeniowych roślin pomidora (Fragkostefanakis i in., 2018).

Badania dotyczące roli enzymu P4H w procesie rozwoju i dojrzewania roślin uprawnych zostały po raz pierwszy podjęte w Mediterranean Agronomic Institute of Chania. W tym celu stworzono linie roślin ze zmodyfikowaną ekspresją genów *Solanum lycopersicum Prolyl 4-Hydroxylases* (*SlP4H*) (Perrakis i in., 2019). Utworzono linie zawierające liczne izoformy enzymu P4H, m.in. P4H1, P4H2, P4H3, P4H4, P4H5, P4H6, P4H7, P4H8, P4H9 oraz P4H10 (Fragkostefanakis i in., 2014; Vlad i in., 2007). Biorąc pod uwagę ich aktywność katalityczną, lokalizację w komórkach, ich zdolności do interakcji z białkami oraz rolę w regulacji procesów, takich jak rozwój roślin, odpowiedź na stres, a także tworzenie struktur komórkowych, kolejne badania wykonywano w roślinach linii P4H3. Udowodniono, że izomer P4H3 wykazuje aktywność szczególnie w miejscach związanych z biosyntezą ścian komórkowych, jak również w retikulum endoplazmatycznym (Perrakis i in., 2019). Analiza anatomiczna roślin linii transgenicznych z wyciszoną ekspresją genu *SlP4H3* wskazała liczne aberracje w budowie tkanki w strefie odcięcia (ang. *abscission zone, AZ*), manifestując, że niedobór Hyp prowadzi do opóźnienia terminu

zainicjowania procesu dojrzewania owoców (Perrakis i in., 2019). Podsumowując, w roślinach z zaburzoną aktywnością enzymu P4H3 obserwuje się zmniejszenie zawartości Hyp, co w konsekwencji prowadzi do nieprawidłowej organizacji komórek i zaburzonego wzrostu tkanek (Perrakis i in., 2019, 2021; Vlad i in., 2007).

Niemniej jednak, mechanizm zaobserwowanych zmian strukturalnych związanych z aktywnością P4H3 pozostaje nadal niejasny. Zakłada się, że zawartość Hyp jako głównego aminokwasu budującego białka strukturalne HRGP może pośrednio regulować przebieg procesów wiązania jonów oraz utrzymywać integralność kontinuum ściana-błona komórkowa (Velasquez i in., 2011, 2015). Udowodniono, że brak hydroksylacji Pro lub zaburzony jej prawidłowy przebieg, wynikający ze zmiany ekspresji genu *SlP4H3*, wpływa na modyfikacje procesu O-glikozylacji AGP (Konkina i in., 2021). W przypadku ściany komórkowej korzeni *Arabidopsis thaliana* określono związek między poziomem glikozylacji a funkcjonalnością AGP (Nibbering i in., 2020). Autorzy wykazali, że brak aktywności β-1,3-galaktozydazy, zaangażowanej w biosyntezę AGP, negatywnie wpływa na elastyczność ściany komórkowej korzeni, prowadząc do zmniejszonego tempa wzrostu komórek (Nibbering i in., 2020).

Pierwsze informacje dotyczące roli AGP w procesie dojrzewania owoców zostały przedstawione w badaniach nad owocami winorośli (*Vitis vinifera*) (Moore i in., 2014). Odkrycie obecności AGP w tkankach sugeruje, że białka te mogą stanowić ważny strukturalno-funkcjonalnym składnik wpływający na właściwości owoców. Udowodniono, że specyficzna lokalizacja i struktura AGP w ścianie komórkowej jest skorelowana z poszczególnymi stadiami procesu dojrzewania owoców (Moore i in., 2014). Autorzy zasugerowali, że AGP, rozpoznawane przez przeciwciało LM2, są markerami stadium *véraison* jagód winogron. Odnotowano wyraźnie zwiększoną zawartość AGP we wspomnianym stadium, które jest przejściem od etapu wzrostu owocu do etapu rozpoczęcia dojrzewania winogron (Moore i in., 2014). W innych badaniach wykazano, że wraz z postępem procesu dojrzewania owoców jabłoni (*Malus* × *domestica*) oraz wraz z ich pozbiorczym starzeniem się następuje zmiana dystrybucji specyficznych epitopów AGP (Leszczuk i in., 2018). W owocach jabłoni stwierdzono obecność epitopów AGP, rozpoznawanych przez przeciwciała JIM13, JIM15 i MAC207, w ścianie komórkowej w bezpośrednim połączeniu z błoną komórkową. Wykazano, że obecność epitopów AGP jest ograniczona głównie do błony komórkowej, z ich wyraźną akumulacją wzdłuż granicy ze ścianą komórkową i przestrzeni pomiędzy ścianą a błoną komórkową, w tzw. macierzy

zewnątrzkomórkowej. Natomiast 3-miesięczny proces pozbiorczego starzenia się owoców istotnie wpływa na właściwości AGP. Odnotowano zmniejszoną zawartość AGP w kontinuum ściana-błona komórkowa, a ich obecność potwierdzono również w cytoplazmie (Leszczuk i in., 2019a, 2020a). Co ciekawe, pomimo ogromnego zainteresowania, nadal nie określono mechanizmu działania AGP w procesie rozwoju i dojrzewania owoców (Leszczuk i in., 2020b, 2023; Perrakis i in., 2019).

2. Hipoteza badawcza i cele rozprawy doktorskiej

Hipoteza badawcza

Badania struktury ściany komórkowej i połączeń pomiędzy jej poszczególnymi składnikami stanowią aktywnie rozwijającą się dziedzinę nauki. Dotychczas w badaniach koncentrowano się głównie na celulozie, pektynach i hemicelulozach, ich strukturze oraz funkcjach pełnionych w ścianie komórkowej. Niemniej jednak, wciąż brakuje szczegółowych informacji na temat AGP oraz ich interakcji z innymi składnikami ściany komórkowej, szczególnie w kontekście procesu dojrzewania owoców.

Z uwagi na konieczność dogłębnego zrozumienia roli AGP w procesie dojrzewania owoców oraz ich potencjalnego wpływu na przebieg tego procesu postawiono następującą hipotezę badawczą:

Dojrzewanie owoców pomidora jest ściśle związane
ze zmianami dystrybucji i właściwościami molekularnymi AGP.

Cel rozprawy doktorskiej

Głównym celem badań przedstawionych w niniejszej rozprawie doktorskiej było zrozumienie roli AGP w kształtowaniu struktury ściany komórkowej, a w szczególności ich wpływu na czasowo-przestrzenną dystrybucję jej pozostałych składników w trakcie procesu dojrzewania owoców.

W związku z realizacją celu głównego postawiono następujące cele szczegółowe:

- opracowanie wzorca zmian właściwości molekularnych AGP i ich czasowo-przestrzennej dystrybucji podczas procesu dojrzewania owoców [P.2] z wykorzystaniem metod molekularnych i immunocytochemicznych na poziomie komórkowym i subkomórkowym [P.1];
- wskazanie różnic w zawartości i czasowo-przestrzennym rozmieszczeniu AGP w różnych stadiach procesu dojrzewania w owocach roślin pomidora ze zmodyfikowaną ekspresją genów *SlP4H3*, przeprowadzając kompleksowe badania mikroskopowe i immunocytochemiczne [P.3];
- określenie wpływu zmian ekspresji genu *SlP4H3* na cechy AGP, a następnie na pozostałe składniki kompleksu APAP1 w ścianie komórkowej podczas procesu dojrzewania owoców [P.4].

3. Materiały i metody badawcze

3.1 Materiał badawczy

Materiał badawczy stanowiły owoce pochodzące z homozygotycznych roślin pomidora generacji T2 i T3 (*Solanum lycopersicum* L. cv. ‘Ailsa Craig’) linii z wyciszoną ekspresją genu *SlP4H3* (RNAi#1, RNAi#7) i linii z nadekspresją genu *SlP4H3* (OEX#1, OEX#2) (Perrakis i in., 2021, 2019). Ponadto, analizowano dwie linie z nadekspresją genu *SlP4H3* (cGFP OEX (cGFP) i nGFP OEX (nGFP)), w których dodany znacznik GFP znajdował się na C- lub na N-końcu DNA (Perrakis i in., 2021). Linie transgeniczne roślin zostały przygotowane i scharakteryzowane przez grupę badawczą z Mediterranean Agronomic Institute of Chania (MAICH) w Grecji. Rośliny uprawiano w warunkach szklarniowych w kontrolowanych warunkach temperatury (w zakresie 18-27°C) i wilgotności względnej (w zakresie 60-80%). Kontrolę do przeprowadzonych badań stanowiły owoce pomidora pochodzące z roślin „dzikiego typu” *S. lycopersicum* L. cv. ‘Ailsa Craig’ (ang. *‘wild type’, WT*). Zamierzoną cechą roślin linii RNAi#1 i RNAi#7 była około 50% niższa ekspresja genu *SlP4H3*. Natomiast poziom ekspresji tego genu w owocach roślin linii OEX#1 i OEX#2 stanowił odpowiednio 4- i 8-krotność poziomu ekspresji genu odnotowanego w owocach WT. Ekspresja genu *SlP4H3* w liniach cGFP i nGFP była odpowiednio 92- i 20-krotnie wyższa w porównaniu do owoców roślin z niemodyfikowaną ekspresją genu *SlP4H3*.

Owoce pomidora zbierano w ścisłe określonych stadiach procesu dojrzewania: początek wybarwienia, „przełamania” (ang. *Breaker stage, BR*), słabo „zapalone” (ang. *Turning stage, TU*), różowe (ang. *Pink stage, PINK*) oraz czerwone (ang. *Red Ripe stage, RR*) (Chromiński, 1971; Nakatsuka i in., 1998). Stadia dojrzewania zidentyfikowano na podstawie oceny zmian koloru skórki owoców (Batu, 2004). Poprawność selekcji poszczególnych stadiów dojrzewania zbadano przez grupę badawczą z MAICH metodami genetycznymi (stosując łańcuchową reakcję polimerazy, ang. *polymerase chain reaction, PCR*) oraz metodami biochemicznymi (analizując poziom zawartości etylenu za pomocą chromatografii gazowej). Dodatkowo, sprawdzono poziom likopenu, który jest pigmentem należącym do karotenoidów (Georgiadou i in., 2021), a jego zawartość w owocach pomidora jest charakterystyczna dla każdego stadium procesu dojrzewania (Nagata i Yamashita, 1992). W owocach WT w stadium BR zawartość likopenu odnotowano na poziomie 3,5 µg/g, który stopniowo wzrastał do 28 µg/g świeżej masy tkanki owoców w stadium RR. Natomiast w owocach linii transgenicznych stwierdzono wyższe stężenie likopenu niż

w owocach WT. Na początku procesu dojrzewania stężenie wynosiło około 10 µg/g i wraz z postępem procesu dojrzewania wzrosło do 50-70 µg/g świeżej masy tkanki. W owocach linii nGFP poziom likopenu w ostatnim stadium procesu dojrzewania był dwukrotnie wyższy niż w przypadku pozostałych linii transgenicznych.

Analizy przygotowanego materiału badawczego przeprowadzono technikami *in situ* i *ex situ* (Rysunek 1).

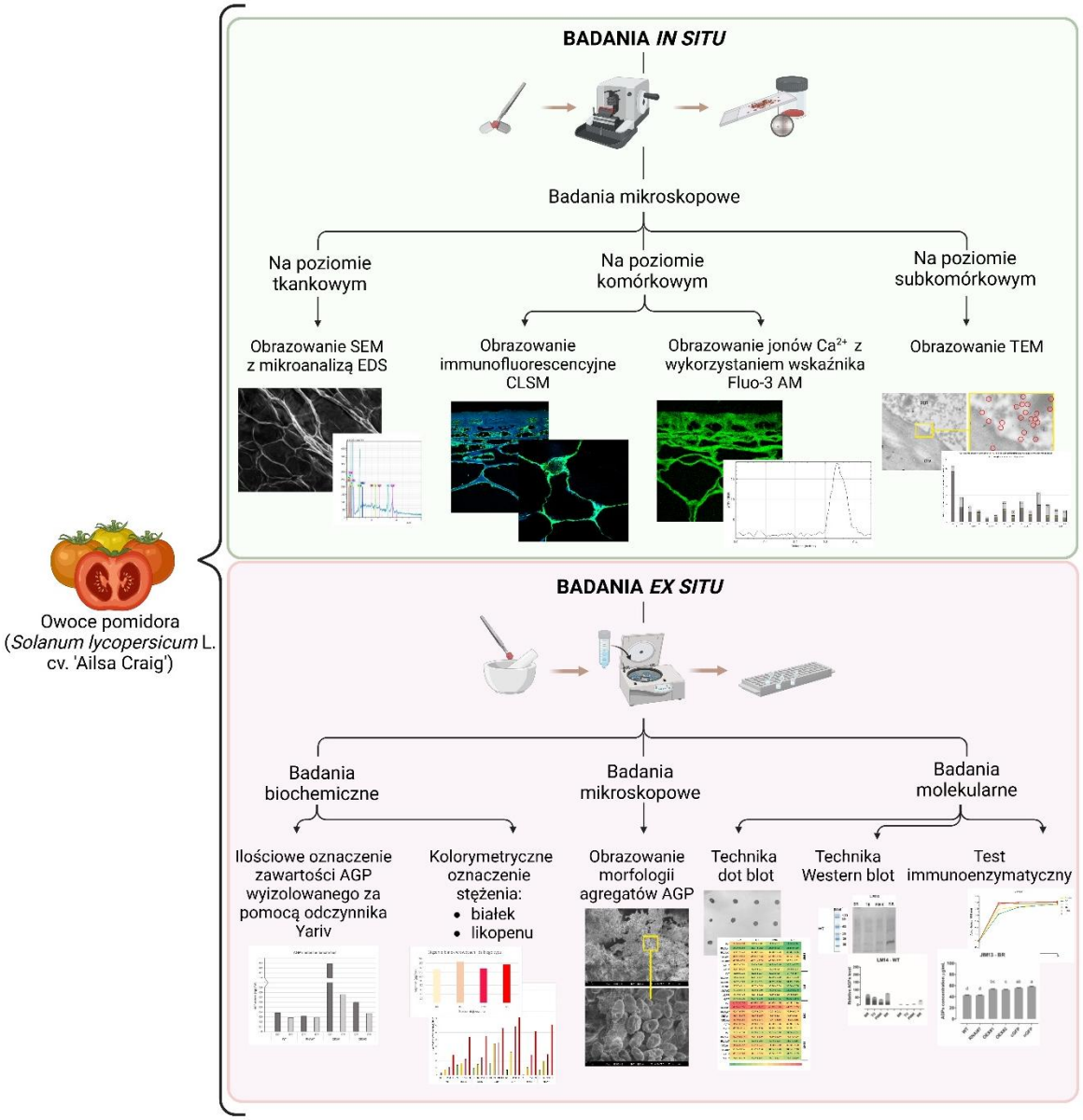

Rysunek 1. Wykorzystane techniki badawcze *in situ* i *ex situ*. Rysunek wykonano w programie BioRender [opracowanie własne].

Sposób przygotowania materiału badawczego oraz dokładne protokoły wykonania wszystkich analiz, liczby powtórzeń technicznych, sposób analizy uzyskanych danych wraz z dodatkowymi technicznymi wskazówkami zostały opisane w poszczególnych

publikacjach [P.1 – P.4]. Przede wszystkim, publikacja P.1 pod tytułem „A practical guide to *in situ* and *ex situ* characterisation of arabinogalactan proteins (AGPs) in fruits" stanowi kompleksowy opis sposobu przeprowadzenia określonych eksperymentów, opisuje nowe i często udoskonalone procedury oraz ich optymalizację konieczną do analiz tkanki owoców. W niniejszej rozprawie przedstawiono wyłącznie krótki opis i cel zastosowanej techniki badawczej.

3.2 Badania molekularne

3.2.1. Analiza składników ściany komórkowej – technika dot blot

Immunocytochemiczna technika dot blot została zastosowana do detekcji obecności wybranych składników ściany komórkowej w analizowanych próbkach. Jest uproszczoną wersją techniki Western blot, w której próbki są nakrapiane bezpośrednio na membranę, bez konieczności przeprowadzania rozdziału elektroforetycznego. Szczegółowy protokół techniki dot blot przedstawiono w publikacji P.2.

Identyfikacja obecności specyficznych epitopów składników ściany komórkowej opierała się na zastosowaniu pierwszorzędowych przeciwciał monoklonalnych (Kerafast, USA). W Tabeli 1 przedstawiono dokładny opis stosowanych przeciwciał.

Tabela 1. Przeciwciała pierwszorzędowe rozpoznające wybrane składniki ściany komórkowej.

Nazwa przeciwciała	Epitop	Bibliografia
JIM13	β-GlcA(1→3)-α-GalA(1→2)-α-Rha; AGP	(Knox i in., 1991; Yates i in., 1996)
JIM15	GlcA; 4-Me-GlcA; AGP	(Yates i in., 1996)
LM2	GlcA; AGP	(Yates i in., 1996)
LM14	Arabinogalaktan typu II; AGP	(Moller i in., 2008)
LM1	Ekstensyny	(Smallwood i in., 1996)
LM11	β-Xyl(1→4)-β-Xyl(1→4)-β-Xyl(1→4)-β-Xyl; ksylan, arabinoksylan	(McCartney i in., 2005)
LM16	Ramnogalakturonan typu I	(Verhertbruggen i in., 2009)
LM19	α-GalA(1→4)-α-GalA(1→4)-α-GalA(1→4)-α-GalA; homogalakturonan	(Verhertbruggen i in., 2009)
LM20	α-MeGalA(1→4)-α-MeGalA(1→4)-α-MeGalA(1→4)-α-MeGalA; homogalakturonan	(Verhertbruggen i in., 2009)

3.2.2. Jakościowa i ilościowa analiza składników ściany komórkowej – technika Western blot

Technikę Western blot wykorzystano w celu molekularnej charakterystyki poszczególnych składników ściany komórkowej. Metoda została przeprowadzona w kilku etapach: elektroforetyczny rozdział wyizolowanych białek w żelu poliakrylamidowym (ang. *sodium dodecyl sulphate–polyacrylamide gel electrophoresis, SDS-PAGE*), transfer białek na membranę PVDF (ang. *polyvinylidene difluoride transfer membranę),* reakcja immunochemiczna oraz kolorymetryczna detekcja wygenerowanego sygnału. Szczegółowy protokół wykonanej analizy przedstawiono w publikacji P.1.

3.2.3. Profilowanie składników ściany komórkowej – test immunoenzymatyczny (ang. *enzyme-linked immunosorbent assay, ELISA*)

Profilowanie składników ściany komórkowej za pomocą testu immunoenzymatycznego (ELISA) to technika, która została zastosowana celem ilościowego oznaczenia składników ściany komórkowej. Test przeprowadzono według metody opisanej przez Pfeifer i in. (2020) na 96-dołkowej płytce (Nunc MaxiSorpTM flat-bottom, Thermo Scientific, Denmark). Szczegółowy protokół wszystkich etapów analizy przedstawiono w publikacji P.1.

3.2.4. Test „wiązania" *in vitro* (ang. *binding assay*) – technika dot blot

Test „wiązania" *in vitro* z zastosowaniem techniki dot blot wykorzystano w celu oceny interakcji pomiędzy poszczególnymi składnikami ściany komórkowej. Określono powinowactwo wyizolowanego z owoców AGP z komercyjnie dostępnymi składnikami ściany komórkowej, m.in. AG, RG, częściowo acetylowany ksylan, ksyloglukan (Megazyme, USA) i celuloza (Sigma-Aldrich, USA). Analizę wykonano zgodnie z metodologią przedstawioną w pracach Hijazi i in. (2014a) oraz Moller i in. (2008). Szczegółowy protokół przeprowadzenia analizy przedstawiono w publikacji P.4.

3.2.5. Test „wiązania” *in vitro* (ang. *binding assay*) – technika ELISA

Testy powinowactwa pomiędzy AGP a pozostałymi składnikami ściany komórkowej zostały wykonane również poprzez zastosowanie detekcji techniką ELISA. Analizy przeprowadzono zgodnie z metodą przestawioną w pracy Biswal i in. (2018). Szczegółowy protokół przeprowadzenia analizy przedstawiono w publikacji P.4.

3.3 Badania mikroskopowe

3.3.1. Preparatyka tkanki do analiz mikroskopowych

Przygotowanie materiału roślinnego do analiz mikroskopowych przeprowadzono zgodnie z wytycznymi opisanymi przez Leszczuk i in. (2019c), a szczegółowy protokół przedstawiono w publikacji P.1.

3.3.2. Technika immunofluorescencyjna – skanujący laserowy mikroskop konfokalny (ang. *confocal laser scanning microscope, CLSM*)

Znakowanie immunofluorescencyjne lokalizacji składników ściany komórkowej na poziomie tkankowym i komórkowym wykonano w celu oceny zmian czasowo-przestrzennej dystrybucji wybranych epitopów w trakcie procesu dojrzewania owoców. Dominantą metody jest zastosowanie przeciwciała drugorzędowego skoniugowanego z fluorochromem Alexa Fluor 488 (ang. *secondary antibody, goat Anti-rat IgM (heavy chain) cross – Alexa Fluor 488*; ThermoFisher Scientific, Denmark). Szczegółowy protokół przedstawiono w publikacji P.1.

3.3.3. Technika immunozłotowa – transmisyjny mikroskop elektronowy (ang. *transmission electron microscope, TEM*)

Znakowanie składników ściany komórkowej z użyciem techniki immunozłotowej miało na celu identyfikację zmian lokalizacji epitopów na poziomie subkomórkowym w wybranych kompartymentach komórkowych: ścianie komórkowej, błonie komórkowej oraz cytoplazmie. W przypadku tej metody, detekcja bazuje na zastosowaniu przeciwciała sprzężonego z nanocząstkami złota (ang. *secondary Anti-rat IgG (whole molecule) – Gold antibody*; Sigma, USA). Szczegółowy protokół przeprowadzenia analizy przedstawiono w publikacji P.1.

3.3.4. Analiza morfologiczna izolowanego AGP – skaningowy mikroskop elektronowy (ang. *scanning electron microscope, SEM*)

AGP izolowano z owoców w dwóch skrajnych stadiach procesu dojrzewania. W tym celu zastosowano zdolność wiązania AGP i odczynnika Yariv. Uzyskane liofilizaty obrazowano z wykorzystaniem mikroskopii elektronowej SEM. Szczegółowy protokół przeprowadzenia analizy przedstawiono w publikacji P.3.

3.3.5. Analiza zawartości jonów wapnia – SEM z mikroanalizą EDS – spektroskopia dyspersji energii (ang. *energy dispersive spectroscopy*)

Do określenia zawartości jonów Ca^{2+} w tkance owoców zastosowano metodę spektroskopii dyspersji energii w połączeniu z mikroskopią SEM. Obrazowanie powierzchni tkanki owoców pozwoliło na identyfikację jonów na poziomie mikroskalowym. Analizy przeprowadzono zgodnie z metodyką zaproponowaną przez Li i in. (2014). Szczegółowy protokół analizy przedstawiono w publikacji P.4.

3.3.6. Analiza dystrybucji jonów wapnia – CLSM z wykorzystaniem wskaźnika Fluo-3 AM

Detekcję jonów wapnia przeprowadzono również na poziomie komórkowym z użyciem wskaźnika Fluo-3 AM (Sigma-Aldrich, USA), wykazującym fluorescencję w obecności jonów Ca^{2} (Tsien, 1980). Poziom intensywności fluorescencji jest proporcjonalny do stężenia jonów Ca^{2+}. Analizę przeprowadzono zgodnie z metodyką zaprezentowaną w pracach Li i in. (2014) oraz Qiu i in. (2020). Szczegółowy protokół przeprowadzenia analizy przedstawiono w publikacji P.4.

3.4 Badania biochemiczne

3.4.1. Ekstrakcja i kolorymetryczne oznaczenie zawartości białek

Ekstrakcję białek przeprowadzono w oparciu o protokół Ling i in. (2021) z zastosowaniem buforu Laemmli'ego (1970) w modyfikacji własnej. Zawartość białka oznaczono metodą kolorymetryczną Bradford (1976) i obliczono na podstawie równania krzywej kalibracyjnej dla albuminy surowicy bydlęcej (ang. *bovine serum albumin, BSA*;

y=0,0013x; R^2 = 0,9935). Stężenie białek wyrażono jako µg/ml. Szczegółowy protokół izolacji przedstawiono w publikacjach P.2, P.3 oraz P.4.

3.4.2. Ekstrakcja i kolorymetryczne oznaczenie zawartości likopenu

Ekstrakcję likopenu i analizę kolorymetryczną przeprowadzono w oparciu o protokół Nagata i Yamashita (1992). Zawartość likopenu obliczono zgodnie z równaniem Nagata i Yamashita (1992) i wyrażono jako µg/g świeżej masy tkanki (Georgiadou i in., 2021).

3.4.3. Izolacja AGP za pomocą odczynnika Yariv

Izolację AGP z tkanki owoców przeprowadzono metodą ekstrakcji opisaną po raz pierwszy przez Derek Lamport (2013) oraz techniką opracowaną dla tkanki owoców zaproponowaną przez Leszczuk i in. (2020c). Dwie wymienione metody ekstrakcji opierają się na użyciu odczynnika Yariv (1,3,5-tri(ρ-glikozyloksyfenylazo)-2,4,6-trihydroksybenzen, β-GlcY; Biosupplies, Australia) (Kitazawa i in., 2013; Yariv i in., 1962). Zawartość wyizolowanego AGP wyrażono jako mg/g świeżej masy tkanki. Szczegółowy protokół izolacji przedstawiono w publikacji P.2.

3.4.4. Test dyfuzji AGP w żelu agarowym z odczynnikiem Yariv

Test dyfuzji radialnej w żelu agarowym przeprowadzono zgodnie z opisem van Holst i Clarke (1985) oraz Castilleux i in. (2020). Test umożliwia określenie stężenia AGP poprzez pomiar strefy reakcji AGP z β-GlcY. Zawartość AGP wyrażono jako mg/ml. Szczegółowy protokół przeprowadzenia analizy przedstawiono w publikacji P.2.

4. Omówienie wyników przedstawionych w publikacjach

W publikacjach P.1, P.2, P.3 i P.4 opisano i przedyskutowano rolę AGP w ścianie komórkowej oraz scharakteryzowano wpływ modyfikacji ekspresji genu *SlP4H3* na proces dojrzewania owoców pomidora. Cykl przedstawionych publikacji (P.1 – P.4) prezentuje ciąg uzupełniających się wiadomości, stanowiący kontynuację ściśle zaplanowanych doświadczeń. Publikacje uporządkowano z uwzględnieniem zależności przyczynowo – skutkowych pomiędzy poszczególnymi etapami badań:

Publikacja P.1 jest kompleksowym praktycznym przewodnikiem w zakresie metod immunocytochemicznych w badaniach AGP w owocach.

W publikacji P.2 zbadano rolę AGP w naturalnym procesie dojrzewania oraz oceniono potencjał tych proteoglikanów jako markerów finalizacji procesu dojrzewania owoców.

W publikacji P.3 omówiono wpływ modyfikowanej ekspresji genu *SlP4H3* na właściwości AGP. Wyniki przedstawione w pracy wskazują, że zmiany w ekspresji genu kodującego enzym P4H3 znacząco oddziałują na zawartość i strukturę AGP.

Publikacja P.4 stanowi kulminacyjny punkt prowadzonych badań, w której szczególną uwagę poświęcono roli AGP w tworzeniu dynamicznej sieci porządkującej polisacharydy i proteoglikany ściany komórkowej zwanej kompleksem APAP1.

4.1. Publikacja P.1

Kutyrieva-Nowak N., Leszczuk A., Zdunek A. 2023. A practical guide to *in situ* and *ex situ* characterisation of arabinogalactan proteins (AGPs) in fruits. Plant Methods, 19: 117.

W publikacji P.1 zaprezentowano opis immunocytochemicznych metod wykorzystywanych do charakterystyki AGP w owocach. Celem niniejszej pracy było stworzenie praktycznego przewodnika metod, zarówno analiz *in situ*, jak i *ex situ*. W publikacji omówiono metody mikroskopowe pozwalające na wizualizację czasowo-przestrzennej dystrybucji AGP, w tym technikę znakowania immunofluorescencyjnego i technikę immunozłotową. Ponadto, opisano metody *ex situ* umożliwiające określenie cech molekularnych AGP oraz przeprowadzenie ich ilościowej analizy, takich jak Western blot i technika ELISA. Niniejsza praca zawiera kluczowe informacje o poszczególnych etapach preparatyki materiału, wykonania reakcji immunocytochemicznych, a także detekcji i identyfikacji sygnału za pomocą odpowiednich narzędzi badawczych.

W publikacji opisano optymalizację techniki immunofluorescencyjnej z wykorzystaniem obrazowania z użyciem mikroskopii konfokalnej skaningowej (CLSM) oraz metodę immunozłotową, której wizualizacja odbywała się za pomocą mikroskopii elektronowej transmisyjnej (TEM). Etapy preparatyki tkanki do badań immunocytochemicznych obejmują szereg procedur, w tym ich utrwalenie, odwodnienie i przeprowadzenie reakcji immunocytochemicznych. Ze względu na wysoką zawartość wody oraz podatność na uszkodzenia mechaniczne, szczególnie pod koniec procesu dojrzewania, przygotowanie tkanki owoców pomidora wymaga licznych modyfikacji standardowych procedur badawczych. Podczas przygotowania tkanek owoców zastosowano utrwalacz składający się z mieszaniny 2% roztworu paraformaldehydu i 2,5% roztworu aldehydu glutarowego w PBS. Taka kombinacja pozwala na zachowanie struktury komórkowej przez stabilizację białek. Podczas etapu zatapiania tkanek owoców wykorzystano żywicę akrylową LR White. Żywica LR White jest nietoksyczną żywicą o niskiej lepkości i minimalnym niespecyficznym barwieniu, co czyni ją odpowiednią do preparatyki i późniejszego obrazowania fluorescencji i uwidocznienie nanocząstek złota. Przygotowane w ten sposób kapsułki z tkankami owoców zostały następnie sekcjonowane z użyciem ultramikrotomu na skrawki o grubości 1 μm i 70 nm w zależności od techniki mikroskopowej. Podczas znakowania immunofluorescencyjnego, skrawki owoców umieszczano na szkiełkach pokrytych poli-L-lizyną, w celu poprawy adhezji próbki do powierzchni szkiełka mikroskopowego. Z kolei, do znakowania immunozłotowego, skrawki owoców umieszczano na heksagonalnych siatkach niklowych pokrytych błoną formwarową. Siatki niklowe pokryte błoną formwarową są mniej reaktywne chemicznie w porównaniu do siatek miedzianych, co minimalizuje ryzyko wystąpienia niespecyficznych interakcji z przeciwciałami. Ponadto, zastosowanie siateczek niklowych minimalizuje zakłócenia od metalicznych artefaktów, zapewniając lepsze warunki do precyzyjnego obrazowania z użyciem mikroskopii elektronowej.

Strategicznym etapem reakcji immunocytochemicznej jest inkubacja próbki z przeciwciałami: pierwszorzędowym monoklonalnym oraz drugorzędowym sprzężonym z odpowiednim znacznikiem: fluorescencyjnym (Alexa Fluor 488) oraz nanocząstkami złota. Do badań tkanki owoców zoptymalizowano rozcieńczenia stosowanych komercyjnych przeciwciał pierwszorzędowych – 1:50 i drugorzędowych – 1:200 dla techniki fluorescencyjnej oraz 1:50 dla techniki immunozłotowej. Dodatkowo, po inkubacji z przeciwciałem drugorzędowym przeprowadzono barwienie za pomocą barwnika

Calcofluor White. Etap ten wprowadzono w celu uwidocznienia celulozy i hemicelulozy obecnej w ścianie komórkowej. Uzyskana kontrastująca wizualizacja umożliwia jednoczesną detekcję AGP oraz precyzyjne określenie ich lokalizacji w strukturach ściany komórkowej.

Opisane w publikacji P.1 techniki molekularne, tj. Western blot oraz test immunoenzymatyczny, pozwalają na określenie zawartości i cech molekularnych AGP. W przypadku analizy AGP z zastosowaniem techniki Western blot wprowadzono szereg modyfikacji, pozwalający na identyfikację epitopów AGP na membranie PVDF. Rozdział elektroforetyczny AGP, jako proteoglikanów, jest bardziej złożony niż rozdział klasycznych białek, ze względu na ich specyficzną strukturę, która obejmuje zarówno domenę białkową, jak i liczne łańcuchy węglowodanowe. W publikacji P.1 zaproponowano elektroforezę w żelu poliakrylamidowym w warunkach denaturujących z wykorzystaniem dodecylosiarczanu sodu (SDS-PAGE) jako preferowaną w analizach AGP. Ponadto, zmodyfikowano stężenie roztworu blokującego – 5% roztwór BSA. Dodatkowo, zoptymalizowano zastosowane stężenia przeciwciał pierwszorzędowych – 1:500 i drugorzędowych związanych z fosfatazą alkaliczną (AP) – 1:1000. W przypadku techniki ELISA zmodyfikowano stężenie przeciwciał pierwszorzędowych – 1:20 i drugorzędowych – 1:500, a także czas ich inkubacji z powszechnie stosowanych 24h na 72h.

Podsumowując, zaprezentowane w publikacji P.1 modyfikacje technik pozwalają na optymalizację analiz AGP, w tym poprawę czułości, specyficzności, szybkości i powtarzalności analiz.

4.2. Publikacja P.2

Kutyrieva-Nowak N., Leszczuk A., Zając A., Kalaitzis P., Zdunek A. 2023. Arabinogalactan protein is a molecular and cytological marker of particular stages of the tomato fruit ripening process. Scientia Horticulturae, 310: 111718.

W publikacji P.2 przedstawiono detaliczny opis zmian cech molekularnych i czasowo-przestrzennej dystrybucji AGP w owocach podczas naturalnie zachodzącego procesu dojrzewania. Do badań wykorzystano owoce pochodzące z roślin pomidora – WT, zebrane w ściśle określonych stadiach. Celem badań zaprezentowanych w publikacji P.2 była analiza AGP jako proteoglikanów, stanowiących potencjalny marker poszczególnych stadiów

procesu dojrzewania. W badaniach wykorzystano wcześniej zoptymalizowane techniki immunocytochemiczne i biochemiczne, tj. znakowanie immunofluorescencyjne, ekstrakcję AGP z użyciem odczynnika Yariv, analizę molekularną Western blot, test immunoenzymatyczny oraz test dyfuzji na żelu agarowym.

Izolacja AGP z użyciem odczynnika Yariv wraz z analizą ilościową pozwoliły na wykazanie znaczących różnic w ich zawartości w poszczególnych stadiach procesu dojrzewania. W tkankach owoców w stadium BR stężenie AGP osiągnęło poziom 0,98 mg/g świeżej masy tkanki. W stadium TU stężenie wzrosło do 3,11 mg/g, z wyraźnym spadkiem w stadiach PINK i RR do stężenia około 1,1 mg/g świeżej masy tkanki. Wyniki testu dyfuzji AGP w żelu agarowym z odczynnikiem Yariv również potwierdziły zmniejszenie stężenia AGP w tkance wraz z postępem procesu dojrzewania.

Wykorzystując półilościową analizę dot blot i test ELISA przeprowadzono rewizję obecności specyficznych epitopów AGP rozpoznawanych przez przeciwciała JIM13, LM2 i LM14 w owocach. Wyniki analizy metodą dot blot wskazują na stopniowy spadek liczby analizowanych epitopów w miarę postępu procesu dojrzewania owoców. W tkankach owoców wykluczono występowanie epitopów AGP rozpoznawanych przez przeciwciało JIM15. Dodatkowo, po zastosowaniu przeciwciała LM2, zaobserwowano najwyższą intensywność sygnału w owocach we wszystkich analizowanych stadiach procesu dojrzewania. Uzyskane wyniki wskazują, że przeciwciało LM2 może pełnić nadrzędną rolę jako narzędzie do detekcji AGP w owocach pomidora. Podobnie analiza przeprowadzona za pomocą techniki ELISA wykazała, że w owocach roślin WT nie występują istotne zmiany w ilości epitopów AGP (JIM13) w trakcie dojrzewania. Natomiast w przypadku analizy reakcji z przeciwciałami LM2 i LM14 stwierdzono wyraźne zmiany w ekspozycji tych epitopów.

Stosując analizę Western blot oszacowano zmiany zawartości poszczególnych frakcji AGP o różnych masach molekularnych podczas procesu dojrzewania owoców. Dowiedziono, że w stadiach BR i TU dominują frakcje AGP o masie molekularnej 60-120 kDa. Natomiast podczas postępu procesu dojrzewania owoców masa molekularna AGP znacznie spada. W stadiach PINK i RR przeważają frakcje AGP o masie molekularnej 20-25 kDa. W ostatnich etapach procesu dojrzewania zaobserwowano obecność AGP o masie molekularnej 30 kDa. Z tego powodu frakcję AGP charakteryzującą się tą masą molekularną uznano za marker finalizacji procesu dojrzewania.

Wyniki badań mikroskopowych ujawniły zmiany anatomiczne w tkankach owoców, które były skorelowane z typowymi, dobrze udokumentowanymi modyfikacjami komórkowych struktur owoców, związanymi z postępującym procesem dojrzewania. Analizy lokalizacji i czasowo-przestrzennej dystrybucji AGP na poziomie tkankowym ujawniły, że na początku dojrzewania epitopy AGP były usytułowane głównie w zewnętrznych częściach owocu, tj. w warstwach epidermalnych. Natomiast wraz z postępem procesu dojrzewania identyfikowane epitopy odnotowano przede wszystkim w warstwie hypodermalnej. Zatem, obecność AGP w poszczególnych tkankach owoców sugeruje ich specyficzność tkankową zależną od stadium procesu dojrzewania.

Analizy na poziomie komórkowym potwierdziły specyficzność lokalizacji AGP, a dokładnie ich występowanie zgodnie ze ściśle określonym wzorcem. Na początku procesu dojrzewania owoców epitopy AGP rozpoznawane przez przeciwciała JIM13 i LM2 znajdowały się głównie w kontinuum ściana-błona komórkowa. W kolejnych stadiach dojrzewania analizowane epitopy AGP uwidoczniono w licznie oderwanych przedziałach ściany komórkowej, usytułowanych w bezpośrednim sąsiedztwie z błoną komórkową. Postępowi procesu dojrzewania również towarzyszyło zmniejszenie intensywności fluorescencji.

Podsumowując, AGP mogą być wykorzystane jako potencjalne wskaźniki procesu dojrzewania, ze względu na obecność specyficznych cech charakterystycznych dla poszczególnych stadiów tego procesu. Wyniki uzyskane w badaniach P.2 dostarczają kluczowych informacji o charakterystycznych właściwościach AGP w różnych stadiach naturalnie zachodzącego procesu dojrzewania owoców pomidora. Uzyskane dane stanowią punkt wyjścia – „wzorzec", na podstawie którego przeprowadzono kolejne badania procesu dojrzewania owoców pomidora ze zmienioną aktywnością P4H.

4.3. Publikacja P.3

Kutyrieva-Nowak N., Leszczuk A., Ezzat L., Kaloudas D., Zając A., Szymańska-Chargot M., Skrzypek T., Krokida A., Mekkaoui K., Lampropoulou E., Kalaitzis P., Zdunek A. 2024. The modified activity of prolyl 4 hydroxylases reveals the effect of arabinogalactan proteins on changes in the cell wall during the tomato ripening process. Frontiers in Plant Science, 15: 1365490.

W publikacji P.3 przedstawiono wyniki badań w zakresie zmian cech AGP w owocach roślin pomidora ze zmodyfikowanym poziomem ekspresji genu *SlP4H3*. Enzym P4H3 jest zaangażowany w posttranslacyjną modyfikację AGP. Zmiany podczas hydroksylacji Pro mogą wpływać na przebieg O-glikozylacji, warunkując występowanie modyfikacji strukturalnych i funkcjonalnych AGP. Celem badań przedstawionych w tej publikacji było scharakteryzowanie struktury molekularnej, cech biochemicznych, zawartości, lokalizacji i czasowo-przestrzennej dystrybucji AGP podczas zaburzonego przebiegu procesu dojrzewania. Badania przeprowadzono w owocach roślin z wyciszoną ekspresją genu *SlP4H3* (RNAi#1, RNAi#7) oraz nadekspresją genu *SlP4H3* (OEX#1, OEX#2, cGFP, nGFP). W pracy opisano kompleksowe analizy porównawcze z użyciem metod *in situ* i *ex situ* w odniesieniu do wcześniej scharakteryzowanych właściwości AGP w owocach roślin WT [P.2].

Przeprowadzone analizy z użyciem techniki dot blot ujawniły zależności pomiędzy zmianami ekspresji genu *SlP4H3* a zawartością AGP w owocach. W owocach linii transgenicznych stwierdzono zmienioną zawartość poszczególnych epitopów AGP w trakcie procesu dojrzewania. W przypadku owoców linii RNAi#7 zaobserwowano 5-20% zmniejszenie intensywności sygnału w reakcji z przeciwciałami JIM13, LM2 i LM14. Natomiast, w owocach linii OEX#1 odnotowano 20-30% wyższy poziom sygnału, nawet w owocach w końcowym stadium procesu dojrzewania. Najwyższy sygnał podczas analizy wszystkich próbek uzyskano w reakcji z przeciwciałem LM2, co wskazuje na brak istotnego wpływu aktywności P4H3 na obecność GlcA w strukturze AGP.

Dzięki zastosowaniu techniki ELISA, w owocach linii z nadekspresją genu *SlP4H3* (OEX#1, OEX#2, cGFP, nGFP) odnotowano stężenie epitopów AGP na poziomie 50-60 µg/ml (JIM13) i 1000-1300 µg/ml (LM2). Badania owoców linii RNAi#7 nie wykazały istotnych różnic w ilości epitopów AGP w porównaniu do owoców roślin WT. W obu przypadkach stężenia wynosiły 40 µg/ml i 900 µg/ml, odpowiednio w reakcji

z przeciwciałem JIM13 i LM2. Natomiast, analiza owoców linii RNAi#1 z wymienionymi przeciwciałami pozwoliła na odnotowanie znacznie niższego stężenia epitopów AGP (około 30 µg/ml (JIM13) i 300 µg/ml (LM2)). Stężenie epitopów AGP rozpoznawanych przez przeciwciało LM14 wynosiło 20 µg/ml i nie stwierdzono istotnych różnic pomiędzy badanymi próbkami.

Analiza molekularna AGP wyizolowanych z owoców linii transgenicznych potwierdziła obecność frakcji AGP w zakresie mas molekularnych 20-120 kDa. W celu określenia względnego poziomu zawartości poszczególnych frakcji AGP przeprowadzono pomiar intensywności sygnału kolorymetrycznego poszczególnych prążków, stosując oprogramowanie Image Lab Software v. 6.1 (Bio-Rad, USA). Otrzymane wartości zsumowano i przedstawiono w trzech zakresach mas molekularnych 20-25 kDa, 25-60 kDa oraz 60-120 kDa. Wykazano, że masa molekularna AGP w poszczególnych stadiach procesu dojrzewania była odmienna od typowego „wzorca" opracowanego na podstawie analiz AGP w owocach roślin WT. Stwierdzono wzrost względnego poziomu zawartości AGP (JIM13 i LM2) w owocach linii cGFP i nGFP, który utrzymywał się do zakończenia procesu dojrzewania. Z kolei najniższy poziom zawartości AGP (JIM13 i LM2) zaobserwowano w owocach linii RNAi#1 i RNAi#7. W owocach linii transgenicznych odnotowano wzrost względnego poziomu zawartości AGP (LM14) o masie molekularnej 60-120 kDa. Interesującym jest fakt, że podczas badań owoców linii ze zmodyfikowaną ekspresją genu *SlP4H3* nie odnotowano obecności charakterystycznej frakcji AGP (bardzo charakterystycznego prążka) o masie molekularnej około 30 kDa, uznaną za marker finalizacji procesu dojrzewania.

Stosując technikę ekstrakcji z użyciem odczynnika Yariv określono stężenie AGP w tkance owoców. W początkowym stadium procesu dojrzewania zawartość AGP w owocach linii OEX#1 wynosiła 4,28 mg/g, w owocach linii OEX#2 – 0,59 mg/g, w owocach linii RNAi#7 – 0,31 mg/g, a w owocach roślin WT – 0,38 mg/g świeżej masy tkanki. Natomiast w ostatnim stadium dojrzewania zaobserwowano istotnie niższą zawartość AGP. W przypadku owoców linii OEX#1 odnotowano zmniejszenie na poziomie 80%, w porównaniu do 26,5% dla owoców roślin WT, 7,48% dla owoców linii RNAi#7 oraz 37,5% dla owoców linii OEX#2.

Analizy histologiczne oraz znakowanie immunofluorescencyjne AGP przeprowadzono w tkance owoców w dwóch skrajnych stadiach procesu dojrzewania, tj. BR i RR. Stwierdzono liczne odstępstwa od typowego obrazu tkanki owoców obserwowanego

wraz z postępem procesu dojrzewania. W tkance linii nGFP odnotowano rozluźnienie ściany komórkowej już na początku procesu dojrzewania. Natomiast, w tkankach linii RNAi#1 i RNAi#7 stwierdzono mniej zintegrowane, nierównomiernie pogrubione i pofałdowane ściany komórkowe. Dodatkowo, w owocach tych linii w obu stadiach procesu dojrzewania odnotowano niski poziom fluorescencji w reakcji z przeciwciałami JIM13, LM2 i LM14. W owocach linii OEX#1 i OEX#2 epitopy AGP rozpoznawane przez przeciwciało JIM13 były widoczne w całym obszarze kontinuum ściana-błona komórkowa, w tym nawet w stadium RR.

Obrazowanie epitopów AGP rozpoznawanych przez przeciwciało JIM13 na poziomie subkomórkowym pozwoliło na odnalezienie korelacji lokalizacji AGP w poszczególnych przedziałach komórkowych a stadiami procesu dojrzewania. Analiza rozmieszczenia AGP polegała na zidentyfikowaniu i przeliczeniu nanocząstek złota (Anti-Rat-IgG – 10 nm colloidal Gold antibody; Sigma, USA) na uzyskanych elektronogramach TEM (2048 × 2048 pikseli) za pomocą oprogramowania ImageJ. Wyniki wyrażono jako liczbę nanocząstek złota na 1 μm^2 powierzchni badanego przedziału komórkowego (Corral-Martínez i in., 2016; Leszczuk i in., 2018).

W owocach linii transgenicznych ze zmodyfikowaną ekspresją genu *SlP4H3* odnotowano nie tylko zaburzenia wzoru czasowo-przestrzennej dystrybucji AGP, ale również ich zmiany ilościowe. W owocach linii OEX#1 i OEX#2 stwierdzono zdecydowanie mniejszą ilość epitopów AGP w kontinuum ściana-błona komórkowa (odpowiednio 0,30 nanocząstek na μm^2 i 0,31 nanocząstek na μm^2) w porównaniu do owoców roślin WT (odpowiednio 1,13 nanocząstek na μm^2). Natomiast w owocach linii RNAi#1 i RNAi#7 w stadium BR stwierdzono odpowiednio 80% i 93% zmniejszenie ilości epitopów AGP w kontinuum ściana-błona komórkowa (0,21 nanocząstek na μm^2 i 0,08 nanocząstek na μm^2). Ponadto, w owocach linii cGFP i nGFP w stadium BR epitopy AGP były rozproszone w kontinuum ściana-błona komórkowa (odpowiednio 0,38 nanocząstek na μm^2 i 0,14 nanocząstek na μm^2) oraz cytoplazmie (0,29 nanocząstek na μm^2 i 0,15 nanocząstek na μm^2). Analizując owoce linii transgenicznych w stadium RR odnotowano mniejsze ilości epitopów AGP w porównaniu do owoców roślin WT (średnio o 50%).

Na podstawie uzyskanych wyników badań sformułowano wniosek, iż zmiany w strukturze AGP oraz ich lokalizacja wywierają bezpośredni wpływ na strukturę ściany komórkowej, znacząco zaburzając charakterystyczną anatomię tkanki owoców, przypisaną

do poszczególnych stadiów procesu dojrzewania. Na ówczesnym etapie analizy postawiono hipotezę, iż zjawisko to związane jest z zakłóceniem występowania również innych składników ściany komórkowej, prowadząc tym samym do modyfikacji cech anatomicznych tkanki owoców.

4.4. Publikacja P.4

Kutyrieva-Nowak N., Leszczuk A., Denic D., Bellaidi S., Blazakis K., Gemeliari P., Lis M., Kalaitzis P., Zdunek A. 2024. *In vivo* and *ex vivo* study on cell wall components as part of the network in tomato fruit during the ripening process. Horticulture Research, 11: uhae145.

W publikacji P.4 zaprezentowano wyniki badań w zakresie analizy zmian zawartości oraz czasowo-przestrzennej dystrybucji poszczególnych składników kompleksu APAP1, z zastosowaniem technik immunocytochemicznych oraz biochemicznych. W ramach badań skoncentrowano się na ksylanie, RG-I oraz nisko i wysoko estryfikowanym HG, które są rozpoznawane odpowiednio przez przeciwciała LM11, LM16, LM19 oraz LM20. Celem niniejszej pracy było określenie wpływu zaburzeń w syntezie jednego ze składników kompleksu APAP1 – AGP, na integralność całej ściany komórkowej. W związku z tym do badań wykorzystano ponownie owoce roślin ze zmodyfikowaną ekspresją genu *SlP4H3* oraz WT w dwóch skrajnych stadiach procesu dojrzewania (BR i RR).

Znakowanie immunofluorescencyjne z użyciem przeciwciała LM11 pozwoliło na zobrazowano epitopów ksylanu w ścianie komórkowej i przestworach międzykomórkowych w owocach roślin WT. W przypadku owoców linii ze zmodyfikowaną ekspresją genu *SlP4H3* stwierdzono podobny wzór rozmieszczenia epitopów LM11. Dodatkowo, odnotowano wyższą intensywność sygnału fluorescencji w porównaniu do owoców roślin WT, która utrzymywała się do zakończenia procesu dojrzewania.

Sygnał immunofluorescencji w reakcji z przeciwciałem LM16, rozpoznającym epitopy RG-I, odnotowano głównie wzdłuż ściany komórkowej we wszystkich analizowanych owocach. Intensywność fluorescencji w owocach linii OEX#1 i OEX#2 była zbliżona do tej w owocach roślin WT. Natomiast w owocach linii RNAi#7 stwierdzono odstępstwo od typowej lokalizacji RG-I. Analizowane epitopy zwizualizowano jako pojedyncze skupiska w obrębie ściany komórkowej.

Znakowanie immunofluorescencyjne HG (LM19) w owocach linii z modyfikowaną ekspresją genu *SlP4H3* wykazało największe różnice w porównaniu do owoców roślin WT. W przypadku owoców roślin WT i linii transgenicznych w stadium BR, epitopy nisko estryfikowanego HG (LM19) zwizualizowano w ścianie komórkowej i przestworach międzykomórkowych. W miarę postępu procesu dojrzewania, w owocach linii OEX#1 i OEX#2 nie stwierdzono zmniejszenia intensywności fluorescencji ani obecności pojedynczych skupisk epitopów HG w obszarze międzykomórkowym, co różniło się od obserwacji w owocach roślin WT. Natomiast, w owocach linii RNAi#7 stwierdzono znaczne zmniejszenie intensywności sygnału wraz z postępującym procesem dojrzewania.

W przypadku znakowania wysoko estryfikowanego HG z użyciem przeciwciała LM20 nie odnotowano istotnych zmian w intensywności fluorescencji w owocach linii transgenicznych w porównaniu do owoców roślin WT. Intensywność zmniejszała się wraz z postępem procesu dojrzewania. Epitopy HG (LM20) zostały oznakowane jako pojedyncze skupiska w ścianie komórkowej i obszarze międzykomórkowym.

Analiza mikroskopowa TEM na poziomie subkomórkowym potwierdziła różnice w dystrybucji poszczególnych składników ściany komórkowej. Analizę gęstości znakowania poszczególnych epitopów przeprowadzono zgodnie z podejściem zaprezentowanym w pracy P.3, polegającym na określeniu ilości nanocząstek złota na 1 μm^2 powierzchni kompartymentu komórkowego. Interpretacja uzyskanych danych opierała się na określeniu stosunku ilościowego pomiędzy obecnością poszczególnych składników w ścianie lub błonie komórkowej a obecnością tych epitopów w cytoplazmie. Dzięki temu możliwe było określenie „stopnia degradacji" ściany komórkowej, przyjmując, że ściana komórkowa ulega strukturalnej dezorganizacji.

Analiza z wykorzystaniem przeciwciała LM11 pozwoliła zlokalizować epitopy ksylanu głównie w obrębie ściany komórkowej. Co ciekawe, wyniki znakowania owoców linii z nadekspresją genu *SlP4H3* wykazały brak analizowanych epitopów w cytoplazmie. W owocach wszystkich analizowanych roślin w stadium RR odnotowano wzrost gęstości epitopów ksylanu (LM11) w kontinuum ściana-błona komórkowa. Wspomniany wzrost wynosił 40% dla owoców roślin WT, 60% dla owoców linii RNAi#7, 80% dla owoców linii OEX#1 oraz 10% dla owoców linii OEX#2.

Epitopy RG-I (LM16) zlokalizowano głównie w kontinuum ściana-błona komórkowa, a wraz z postępem procesu dojrzewaniem ich ilość zwiększała się w cytoplazmie.

Nie odnotowano istotnych różnic pomiędzy owocami linii transgenicznych a owocami roślin WT.

Największą ilość epitopów HG (LM19) stwierdzono w kontinuum ściana-błona komórkowa we wszystkich analizowanych owocach. W owocach linii OEX#1 i OEX#2 zaobserwowano znaczący wzrost ilości analizowanych epitopów w stadium RR (odpowiednio 10-krotny i 24-krotny). Jednakże, nie odnotowano istotnych różnic pomiędzy owocami linii RNAi#7 a owocami roślin WT.

W przypadku analizy HG rozpoznanego przez przeciwciało LM20, w owocach roślin WT zidentyfikowano większą ilość epitopów HG (LM20) w kontinuum ściana-błona komórkowa niż w cytoplazmie. Natomiast, w owocach linii ze zmodyfikowaną ekspresją genu *SlP4H3* odnotowano 1,5-krotny wzrost zawartości epitopów HG (LM20) w cytoplazmie od początkowego stadium procesu dojrzewania.

Profilowanie składników ściany komórkowej z zastosowaniem techniki ELISA umożliwiło na potwierdzenie licznych zaburzeń w ilości analizowanych składników w owocach linii transgenicznych. Do analiz włączono również określenie zawartości ekstensyn, rozpoznawanych przez przeciwciało LM1. Ekstensyny są białkami strukturalnymi ściany komórkowej, należące do rodziny HRGP. Hydroksyprolina w ich strukturze, podobnie jak w przypadku AGP, jest kluczowym składnikiem domeny białkowej. W owocach linii OEX#1 i OEX#2 w stadium BR odnotowano istotny wzrost ilości epitopów ekstensyn rozpoznawanych przez przeciwciało LM1 (odpowiednio 15 mg/ml PNP i 10 mg/ml PNP), w porównaniu do 5 mg/ml PNP w przypadku owoców roślin WT. Nie zidentyfikowano znaczących różnic pomiędzy owocami linii z nadekspresją genu *SlP4H3* a owocami roślin WT w stadium RR (około 15 mg/ml PNP). Natomiast, w owocach linii RNAi#7 stwierdzono 2-krotnie mniejszą ilość epitopów LM1 (8 mg/ml PNP) niż w owocach roślin WT. Zatem, analizy z wykorzystaniem przeciwciała LM1 pozwoliły na potwierdzenie specyficzności ekspresji genu *SlP4H3* względem HRGP.

W przypadku analizy ksylanu rozpoznanego przez przeciwciało LM11 stwierdzono wzrost ilości epitopów (z 5 mg/ml PNP do 15 mg/ml PNP) wraz z postępem procesu dojrzewania we wszystkich owocach linii ze zmodyfikowaną ekspresją genu *SlP4H3*.

W przypadku analizy epitopów RG-I (LM16) nie zidentyfikowano znaczących różnic pomiędzy owocami linii transgenicznych a owocami roślin WT w postępującym procesie dojrzewania.

Stwierdzono niższą zawartość HG rozpoznawanych przez przeciwciało LM19 w owocach linii OEX#1, OEX#2 i RNAi#7 w porównaniu do owocach roślin WT. W owocach linii z nadekspresją genu *SlP4H3* w stadium BR i RR stężenie epitopów HG (LM19) wynosiło około 10 mg/ml PNP. Natomiast w owocach linii RNAi#7 około 15 mg/ml PNP, w porównaniu do 20 mg/ml PNP w owocach roślin WT.

Analiza obecności epitopów HG (LM20) w stadium BR nie wykazała istotnych różnic między owocami linii transgenicznych a owocami roślin WT. We wszystkich owocach odnotowano 2-krotny wzrost ilości epitopów HG (LM20) pod koniec procesu dojrzewania (z 3 mg/ml PNP do 6 mg/ml PNP).

Test „wiązania" *in vitro* za pomocą techniki dot blot na membranie PVDF pozwolił na zbadanie powinowactwa AGP do innych składników ściany komórkowej, tj. AG, RG-I, ksylanu, ksyloglukanu. Analizy objęły również celulozę jako podstawowy budulec szkieletu ściany komórkowej. Stwierdzono zdolność wiązania wyizolowanego AGP z owoców linii transgenicznych i roślin WT z RG-I i celulozą. Testy „wiązania" *in vitro*, których detekcję wykonano za pomocą techniki ELISA również potwierdziły możliwość interakcji AGP ze składnikami ściany komórkowej, głównie z AG, RG-I i celulozą.

Celem wyjaśnienia zmian w montażu ściany komórkowej tkanki owoców roślin ze zmienioną ekspresją genu *SlP4H3* przeprowadzono analizę lokalizacji jonów wapnia w ścianie komórkowej. Wykonano analizy z użyciem SEM-EDS oraz znakowanie jonów Ca^{2+} wskaźnikiem Fluo-3 AM i jego wizualizację z użyciem CLSM. Dane uzyskane dzięki przeprowadzeniu obu metod pozwalają wysnuć generalny wniosek, że ilość jonów Ca^{2+} wzrasta we wszystkich analizowanych owocach wraz z postępem procesu dojrzewania. Zaś, ich poziom w owocach roślin z nadekspresją i wyciszeniem genu *SlP4H3* jest wyższy.

Na wykresach składu pierwiastkowego analizowanych owoców odnotowano obecność jonów Ca^{2+}. W próbkach pochodzących z owoców roślin WT i linii transgenicznych stwierdzono piki odpowiadające jonom Ca^{2+}, znajdującym się w różnych przedziałach komórkowych. Podobnie, analiza owoców wszystkich linii transgenicznych i WT wykazała wzrost intensywności fluorescencji w obecności wskaźnika Fluo-3 AM wraz z postępem procesu dojrzewania. Najwyższą intensywność sygnału uzyskano w komórkach warstwy epidermalnej owoców w stadium RR. Co więcej, poziom fluorescencji w owocach linii OEX#1 i OEX#2 był znacznie wyższy niż w owocach roślin WT. Za pomocą oprogramowania ImageJ oznaczono profile poziomu szarości (ang. *plot profile*) pozwalające

na analizę intensywności sygnału wzdłuż wybranego obszaru ściany komórkowej owoców. W owocach roślin WT w stadium BR odnotowano pojedynczy pik, odpowiadający kumulacji jonów Ca^{2+} w ścianie komórkowej. Natomiast w owocach linii transgenicznych w stadium BR nie odnotowano tego piku, wskazując na większe rozproszenie jonów Ca^{2+}. W stadium RR w owocach roślin WT i linii transgenicznych również zaobserwowano jony Ca^{2+} w całej powierzchni ściany komórkowej.

Na podstawie uzyskanych wyników można wnioskować, że zmiany podczas syntezy jednego ze składników kompleksu APAP1 wpływają na proces tworzenia stabilnej sieci porządkującej kontinuum ściana-błona komórkowa. Zaburzenia strukturalne ściany komórkowej, w szczególności zmiany w organizacji pektyn, są skorelowane ze zmianami w wiązaniu jonów Ca^{2+}. Konsekwencją zaburzeń ilościowych i molekularnych jest zmieniona aranżacja połączeń pomiędzy składnikami ściany komórkowej, skutkująca modyfikacjami w anatomii tkanki owoców.

5. Podsumowanie i wnioski

Metody z zakresu biologii molekularnej i mikroskopii stały się kluczowymi technikami badawczymi stosowanymi w dziedzinie nauk rolniczych. Umożliwiają poszukiwanie rozwiązań pomocnych w podnoszeniu ilości i jakości plonów, co jest szczególnie ważne w obliczu rosnącego zapotrzebowania na żywność, jak również z powodu negatywnych i nieustających zmian klimatycznych. Najnowsze osiągnięcia nauki pozwalają na badanie i modyfikowanie procesów fizjologicznych, które mają bezpośredni związek z uprawą i jakością plonów. W ostatnim czasie opisano rolę AGP w regulacji wzrostu i rozwoju roślin, jak również ich zaangażowanie w procesach zwiększenia odporności upraw na stresy środowiskowe (Ma i in., 2018; Ma i Johnson, 2023). Jednak mniej uwagi poświęcono funkcji AGP w procesie dojrzewania owoców. Jest to nadal temat aktualny i wymagający interdyscyplinarnych badań oraz rozwoju i optymalizacji nowych narzędzi badawczych.

Celem badań zaprezentowanych w niniejszej rozprawie doktorskiej było określenie wpływu AGP na strukturę ściany komórkowej oraz poznanie czasowo-przestrzennej dystrybucji proteoglikanów, jak i pozostałych składników ściany komórkowej na poziomie komórkowym i tkankowym podczas dojrzewania owoców.

Na podstawie wyników przeprowadzonych badań można sformułować następujące wnioski:

- Owoce roślin ze zmodyfikowaną ekspresją genu *SlP4H3* charakteryzują się zmienioną organizacją ściany komórkowej. Zarówno wzrost, jak i zmniejszenie ekspresji genu *SlP4H3* wywołują zmiany zawartości i cech molekularnych AGP.
- Zmiana ekspresji genu *SlP4H3* wpływa na proces hydroksylacji Pro w domenie białkowej AGP, co wpływa na proces „przyłączania" łańcuchów węglowodanowych w kolejnych etapach biosyntezy.
- Istnieje przyczynowo – skutkowy cykl następujących po sobie zmian, wywołanych zaburzeniami natywnej struktury AGP:
    1) Zaburzenia w zawartości i strukturze molekularnej AGP są odpowiedzialne za zmiany lokalizacji tych proteoglikanów w ścianie komórkowej owoców.
    2) Zmiany dystrybucji AGP wpływają na czasowo-przestrzenną dystrybucję pozostałych składników ściany komórkowej.

3) Brak natywnej postaci AGP zaburza wzajemną organizację pozostałych elementów strukturalnych kompleksu APAP1 oraz jonów wapnia.
4) Zmodyfikowana i nieuporządkowana sieć macierzy zewnątrzkomórkowej ma wpływ na zmiany anatomiczne tkanki owoców.
5) Zmiany anatomiczne tkanki owoców są związane z zaburzeniem prawidłowego przebiegu procesu dojrzewania.

Podsumowując, uzyskane wyniki potwierdzają postawioną hipotezę o roli AGP jako kluczowego elementu strukturalnego w prawidłowym przebiegu procesu dojrzewania. Zrozumienie mechanizmów działania AGP jest obiecującą perspektywą badawczą i może stanowić pierwszy krok w kierunku zwiększenia efektywności produkcji roślinnej, a tym samym poprawę jakości owoców.

6. Tekst publikacji P.1

Kutyrieva-Nowak N., Leszczuk A., Zdunek A. 2023.

A practical guide to *in situ* and *ex situ* characterisation of arabinogalactan proteins (AGPs) in fruits.

Plant Methods, 19: 117.

Kutyrieva-Nowak *et al. Plant Methods* (2023) 19:117
https://doi.org/10.1186/s13007-023-01100-3

Plant Methods

REVIEW Open Access

A practical guide to in situ and ex situ characterisation of arabinogalactan proteins (AGPs) in fruits

Nataliia Kutyrieva-Nowak[1], Agata Leszczuk[1*] and Artur Zdunek[1]

Abstract

Background Arabinogalactan proteins (AGPs) are plant cell components found in the extracellular matrix that play crucial roles in fruit growth and development. AGPs demonstrate structural diversity due to the presence of a protein domain and an expanded carbohydrate moiety. Considering their molecular structure, the modification of glycosylation is a primary factor contributing to the functional variety of AGPs.

Main body Immunocytochemical methods are used for qualitative and quantitative analyses of AGPs in fruit tissues. These include in situ techniques such as immunofluorescence and immunogold labelling for visualising AGP distribution at different cellular levels and ex situ methods such as Western blotting and enzyme-linked immunoenzymatic assays (ELISA) for molecular characterisation and quantitative detection of isolated AGPs. The presented techniques were modified by considering the structure of AGPs and the changes that occur in fruit tissues during the development and ripening processes. These methods are based on antibodies that recognise carbohydrate chains, which are the only commercially available highly AGP-specific tools. These probes recognise AGP epitopes and identify structural modifications and changes in spatio-temporal distribution, shedding light on their functions in fruit.

Conclusion This paper provides a concise overview of AGP research methods, emphasising their use in fruit tissue analysis and demonstrating the accessibility gaps in other tools used in such research (e.g. antibodies against protein moieties). It underscores fruit tissue as a valuable source of AGPs and emphasises the potential for future research to understand of AGP synthesis, degradation, and their roles in various physiological processes. Moreover, the application of advanced probes for AGP visualisation is a milestone in obtaining more detailed insights into the localisation and function of these proteins within fruit.

Keywords Arabinogalactan proteins, Cell wall, Glycobiology, Immunocytochemistry, Microscopy, Molecular biology

Background

Arabinogalactan proteins (AGPs) are widely distributed components of the plant cell, where they serve a variety of functions. In general, AGPs have been found in all kinds of tissues, mostly in plasma membranes (PM), cell walls, and intercellular spaces as well as in soluble exudates secreted by plants. Studies at the cellular level have shown that the specific localisation of AGPs facilitates the formation of a continuum between the plasma membrane and the cell wall [1, 2]. AGPs are classified as proteoglycans with several combinations of glycosylated variations (glycoforms) [3, 4]. The AGP polypeptide sequence and the complexity of AG polysaccharide chains (presence of various sugars in varying amounts) are major factors that contribute to the high structural variability of AGPs [2, 5]. About 10% of the total

*Correspondence:
Agata Leszczuk
a.leszczuk@ipan.lublin.pl
[1] Institute of Agrophysics, Polish Academy of Sciences, Doświadczalna 4, 20-290 Lublin, Poland

molecular mass of proteoglycans is made up by the protein moiety [2]. As part of the hydroxyproline-rich glycoprotein family (HRGPs), AGPs contain a large number of hydroxyproline residues [2, 6–8]. Proline/hydroxyproline, alanine, serine, and threonine are also prevalent in their *N*-terminal domain [9–11]. During the biosynthesis and the post-translational modification of AGPs, the enzyme prolyl 4-hydroxylase (P4H) transforms proline (Pro) into hydroxyproline (Hyp), which is necessary for the molecule glycosylation process. AGPs are not properly glycosylated when proline hydroxylation does not occur, and changes in the proline hydroxylation process cause either their breakdown or a shift to lower molecular weight polypeptides [9, 12]. In turn, about 90% of the molecule consists of carbohydrate chains which are rich in arabinose, galactose, and occasionally D-glucuronic acid (GlcA), L-rhamnose (L-Rha), and uronic acids [13]. Most AGPs have one or more hydroxyproline residues that have been *O*-glycosylated by AG type II. They consist mostly of (1 → 3)-β-galactan and (1 → 6)-β-linked galactan chains attached to each other by (1 → 3, 1 → 6)-linked branch points with terminal arabinosyl residues in the *O*-3 and *O*-6 positions. The size of type II AGs varies between AGPs, with estimations typically lying between 30 and 150 sugar residues. The side chains of AGPs vary greatly due to the inclusion of different sugar residues in their structure. L-arabinose (L-Ara) residues are present in the side chains, along with GlcA, Rha, 4-*O*-methyl-glucuronic acid (4-Me-GlcA), D-xylose (Xyl), D-mannose (Man), D-glucose (Glc), D-galacturonic acid (GalA), D-glucosamine (GlcN), and L-fucose (L-Fuc) [4, 13, 14]. Both moieties allow the formation of an AGP molecule ranging in molecular weight from 60 to 300 kDa [15].

Moreover, there is a structure–function relationship in AGPs. The functionality of AGP is based on the direct function of its glycan [15]. It is known that AGPs have been related to various important stages of plant growth and development, including seed germination, somatic embryogenesis, pollen tube formation, cell division, cellular communication, and programmed cell death [4, 16]. AGPs have reportedly been shown as regulators of cell growth and differentiation processes, transducers of cell surface signals, and signalling pathways of responses to the environment [17, 18]. In situ and ex situ studies on AGPs in fruits performed by Leszczuk and coworkers have shown that AGPs are consistently found in fruit tissue and may induce alterations in fruits during the developmental and ripening processes [12, 19]. Analyses of AGP in fruits at the molecular level, i.e. ion binding, the establishment of cell wall-plasma membrane integrity, and cross-linking with other cell wall constituents [20], show that AGPs have an impact on fruit cell wall dissolution and subsequent softening [14].

Therefore, the characterisation of AGPs, particularly in terms of their hypothetical functions in fruit metabolism, necessitates the employment of numerous techniques, such as immunocytochemical methods based on the detection of carbohydrate epitopes. We have compiled a practical guide that includes methods that can be applied in AGPs research in fruits. The aim of the current paper is to provide step-by-step instructions for using and adapting common research techniques in studies on AGPs in fruits with the proviso that these methods should be correctly adjusted and modified before studying the specificity of AGPs in fruit tissue during the development and ripening processes. Moreover, this guide will equip researchers with tools with shown critical gaps which will make it easier to carry out analyses of fruit tissues and will also allow the potential of analyses of AGPs to understand the structure and changes of the cell wall during physiological processes.

Immunocytochemical methods for qualitative and quantitative analyses of AGPs

AGPs can be found, measured, and localised using a variety of in situ and ex situ techniques [10]. However, due to the structural and compositional diversity of both the protein and carbohydrate moieties of AGPs, each technique has some advantages and disadvantages. Also, it is well known that fruit tissue is specific and requires appropriate treatment and selection of adequate methods [21, 22]. In situ research allows the study of biological processes in the context of the actual plant/fruit environment, which is important for understanding the AGP functions and interactions between individual extracellular matrix components as well as their response to all stress factors. However, in situ analyses must be complemented by equivalent ex situ studies. Ex situ studies of isolated AGPs may not accurately reflect processes occurring in the natural environment. The extraction process is always associated with the need to detach AGP molecules from the matrix, and the progress of the degradation process, especially of the protein moiety. Above all, only the analysis of isolated AGP makes it possible to describe the features of AGP that are the result of ongoing processes related to the cell functioning. Currently, one of the most effective approaches for studying AGPs is immunocytochemistry. Ex situ methods like immunoblotting, immunoprinting on the membrane, and enzyme-linked immunosorbent assay (ELISA test), which include molecular characterisation and quantitative detection, can be used to identify AGP epitopes. In turn, in situ methods used for this purpose are typically based on the immunofluorescence technique and immunogold labelling, allowing visualisation of the AGP distribution at the cellular and subcellular levels [23]. Both types of

techniques facilitate a comprehensive description of the presence of AGPs in fruits.

The methods mentioned above are based on individual antibodies specifically recognising the target of interest. The antibody detects and binds to precisely defined antigen epitopes. By using particular monoclonal antibodies (mAbs) that bind to the structurally complex motif present in these proteoglycans, AGPs can be detected in plant tissues [24]. Moreover, the knowledge of the AGP glycan structure obtained via the widespread use of anti-AGP mAbs, such as JIM8, JIM13, JIM14, LM2, and others, demonstrates that AGPs are variably expressed during fruit growth and ripening [13]. Characterisation of commercially available antibodies commonly used in AGP studies is presented in Table 1.

All immunocytochemical techniques are based on a general pattern consisting of sequential steps: material preparation (1), immunocytochemical reaction with primary and secondary antibodies (2), and signal detection and measurement using adequate tools for particular methods (3). First, a properly prepared fruit tissue is subjected to post-fixation membrane-permeabilisation. Although antigen–antibody binding is characterised by high specificity, there is a possibility of non-specific antibody interactions. To prevent and reduce nonspecific background staining, the blocking step is necessary before the immunocytochemical reaction, which involves incubation of the material with immunologically inactive (containing no specific antibodies) serum from another animal species, i.e. 2–10% solution of bovine serum

Table 1 Characterisation of AGP epitopes recognized by specific antibodies

Antibody name	Epitope structure	Characterisation	M.W. of Protein Antigen (kDa)	References
JIM4	β-GlcA(1 → 3)-α-GalA(1 → 2)-Rha	Recognises oligosaccharides; binds to a set of discreet protein bands	70–100	[25–27]
JIM8	Carbohydrate portion of arabinogalactan proteins	Binds to a galactose-rich epitope of agps; the epitope contains one or more galactose residues	68, 84, 160	[25, 28, 29]
JIM13	β-GlcA(1 → 3)-α-GalA(1 → 2)-α-Rha	It is most likely not the complete epitope structure, because it binds to other anti-AGP glycan antibodies	80–100	[25–27]
JIM14	β-Gal(1 → 6)-β-Gal(1 → 6)-β-Gal(1 → 6)	Binds to at least three consecutive galactans with β-1,6-linked galactan; is used to visualise differentially branched galactan in type II AG polysaccharides	80–100	[25–27, 30]
JIM15	D-GlcA, GlcA-β(1-O-Me)	Recognises an epitope distinct from JIM13 and JIM14 but uncharacterised	80–100	[25–27]
JIM16	β-Gal(1 → 3)-β-Gal(1 → 3)-β- Gal(1 → 3)	Binds to a β-1,3-linked galactan backbone when substituted with a single β-1,6-linked Gal residue; used to visualise differentially branched galactan in type II AG	80–100	[25, 26, 30]
JIM101	unknown	Binds strongly to okra rhamnogalacturonan I and seed mucilages from *Sinapus alba* and *Camelina sativa*	No information	[31]
JIM133	β-1,3-linked galactooligosaccharides	Detects the nonreducing ends of the β-1,3-linked galactan backbone in the AG structures of agps	No information	[30, 31]
MAC204	Arabinogalactan (epitope structure unknown)	Binds to arabinogalactan proteins, but the epitope has not been characterised in detail	90–100	[31, 32]
MAC207	β-GlcA(1 → 3)-α-GalA(1 → 2)-Rha	Recognises an arabinose-containing epitope	70–100	[27, 29, 31, 32]
LM2	β-D-GlcA	Recognises a carbohydrate epitope containing β-linked D-glucuronic acid in AGP glycan	No information	[26, 28, 33]
LM14	AG type II arabinogalactan	Recognises arabinose and galactose-rich epitopes	No information	[34]
LM30	Arabinogalactan	Binds to terminal arabinose residues linked to galactan	No information	[35]
PN 16.4B4	Uncharacterised epitope in the carbohydrate part of the glycoprotein	Binds to arabinogalactan glycoproteins	135–180	[31, 36]

albumin (BSA) [37]. In the next step, the examined material is incubated with an unlabelled antibody that recognises the specific antigen (primary antibody). Then, the excess antibody that did not bind to the antigen is washed off and a second incubation step is performed with a so-called secondary antibody conjugated with label molecules, which facilitates detection with well-established methods [38]. Here, protocols of the immunofluorescence labelling imaged with a confocal laser scanning microscope (CLSM), immunogold labelling imaged with the transmission electron microscope (TEM), immunoblotting, and ELISA test are described in detail with an emphasis on essential steps that should be modified in fruit AGP analyses.

In situ studies—microscopic methods

Modern bioimaging methods facilitate the visualisation of epitope distribution at cellular and subcellular levels [39–41]. The presence of AGPs *in planta* is possible to be demonstrated using two immunocytochemical approaches, i.e. immunofluorescence labelling and immunogold labelling (Table 2).

Protocol of tissue preparation for microscopic methods

The tissue of fresh fruit is very delicate, highly hydrated, and prone to damage. Hence, preparation of sufficient thin sections with appropriate preparative steps is typically advantageous. The material should be subjected to the procedure of fixation, resin embedding, and thin or/and ultra-thin sectioning [42, 43]. The basic steps of sample preparation for CLSM and TEM are the same: fixation in a fixative solution, dehydration in gradient series of ethanol solutions, embedding in resin, and polymerisation. The choice of chemical fixative and buffer solutions depends on the purpose of the CLSM and TEM study and requires optimisation of the procedure for fruit tissue for both structural studies and labelling of AGP carbohydrate epitopes. A common problem encountered during the fixation step is the use of glutaraldehyde. Also, the embedding stage and the use of proper resin are fundamental to the final quality of sample blocks and sectioning. Epoxy resins cannot be used for CLSM and TEM imaging of fruit tissues compared with other plant tissues [42, 43]. This is due to its high viscosity and potential to damage cellular structures. Another disadvantage of this resin is its poor staining ability, which is a basic criterion for microscopic analysis of fruit tissues. LR White resin is a low-viscosity and non-toxic acrylic resin with minimal non-specific staining, which makes it an ideal tool for infiltrating fruit tissues. Moreover, LR White resin provides a chance of using one block for both CLSM and TEM, which definitely advances the sectioning step. Also, sections of LR White resin are hydrophilic so that immunocytochemistry reagents can easily penetrate into the section. The scheme of the method is shown in Fig. 1.

Procedure

1. Cut cube-shaped pieces of fruit tissue.
2. Add 2% paraformaldehyde and 2.5% glutaraldehyde in PBS (phosphate-buffered saline) to the fruit tissue.

Table 2 Application, advantages, and disadvantages of microscopic techniques with antibody-based probes in AGPs studies

Technique	Application	Advantage	Disadvantage
Immunofluorescence labelling—Confocal laser scanning microscope (CLSM)	Used to show where AGPs are distributed across labelled cells and tissues; analyses at the tissue/cellular level	AGP location is identified using a fluorescent signal It is possible to see cellular features at a resolution of 1 µm High contrast and resolution images are possible to obtain quickly and non-intrusively Eliminates the problem of glare resulting from preparation of layers lying outside the plane of focus	The fluorescence lessens with time. The fluorescence of samples fades (photobleaching) during observations Results are susceptible to the effects of the environment Resolution is still inferior to that of electron microscopy A high price and a very limited field of view
Immunogold labelling—Transmission electron microscope (TEM)	Used to localise AGPs and other cell wall components at the subcellular level	AGP localisation in ultra-thin sections using a gold-conjugated antibody It is possible to see intracellular features at a resolution of 0.2 nm Analysis and observation of very high-resolution images High magnification	Fixation is needed in cell preparation, which might result in artificial damage Lengthy and complicated methods for preparation of cells and tissues for TEM Requires a conductive coating of gold/palladium alloy, carbon, osmium, etc. for correct imaging Expensive, difficult to access, and complicated to use

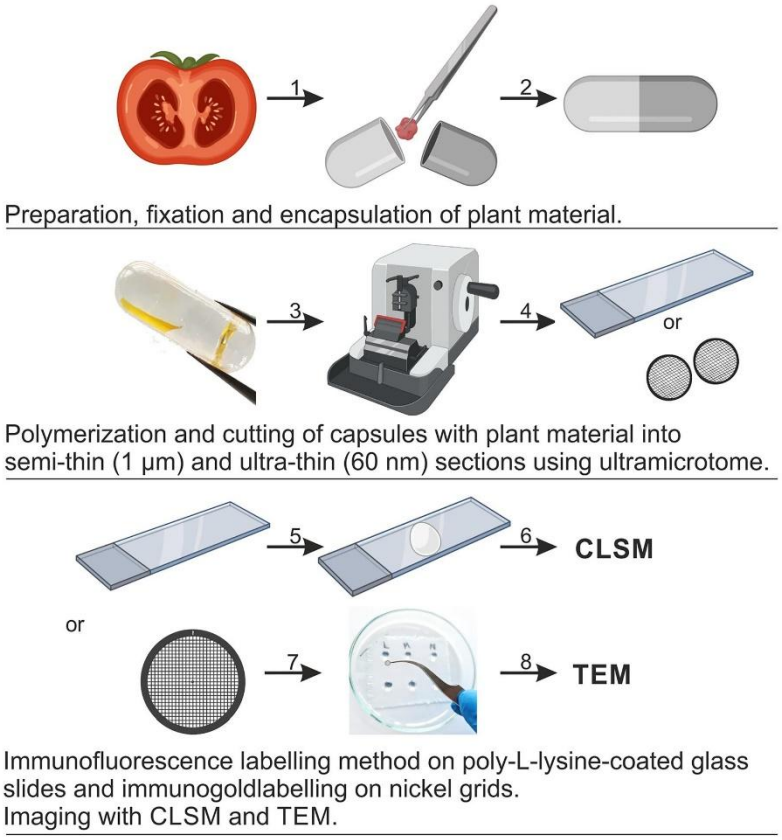

Fig. 1 Scheme of the preparative sequence of microscopic methods. (1) Preparation, fixation, and encapsulation of plant material. (2) Polymerisation of capsules with fixed plant material. (3) Cutting capsules into semi-thin and ultra-thin sections. (4) Mounting the sections on poly-L-lysine-coated glass slices (for CLSM) or nickel grids (for TEM). (5) Immunofluorescence labelling – method on poly-l-lysine-coated slices. (6) Imaging with CLSM. (7) Immunogold labelling – method on grids with formvar film (8) Imaging with TEM. Created with BioRender.com

3. Place the tissue with the fixation solution in a vacuum (0.7 bar) seven times, with breaks after vacuum for 10 min each. Next, place the tissue under vacuum overnight.
4. Wash the sample with PBS three times for 15 min each at RT (room temperature).
5. Remove the solution and wash the sample with distilled water three times for 15 min each at RT.
6. Remove the solution and start the dehydration process with graded series of ethanol solutions. Add 30%, 50%, 70%, 90%, and 96% ethanol for 15 min each at RT.
7. Remove the solution and add 99.8% ethanol twice for 30 min each at RT.
8. Substitute ethanol with 3:1, 1:1, and 1:3 mixtures of 99.8% ethanol and LR White resin for 2 h each at RT and with 100% LR White resin overnight at 4 °C.
9. Remove the solution and replace by 100% LR White resin (infiltration of the sample with LR White resin). Leave the sample for 8 h at RT.
10. Encapsulate the sample in gelatine capsules and start polymerisation for 48 h at 55 °C.

11. Prepare a cutting plane of an appropriate size on blocks containing the embedded material (trimming stage).
12. Cut semi-thin Sects. (1 μm) using a glass knife-equipped ultramicrotome. Mount the sections on poly-L-lysine coated glass slides.
13. Cut ultra-thin Sects. (70 nm) using a diamond knife-equipped ultramicrotome. Mount the sections on formvar film-coated nickel square grids.

Critical

(1) Samples should not be left in 100% resin at RT longer than a few days; otherwise, they will begin to polymerise.
(2) Using LR white to place fruit tissue requires a graded series of ethanol, not acetone, because acetone residues may hinder polymerisation.
(3) The steps of tissue saturation with resin cannot be accelerated, because insufficient time of this step will result in poor fixation of the tissue, which will make it impossible to section it. The block inside will be too soft.
(4) Nickel square mesh grids with formvar, not the more common copper grids, should be used to place the sections for electron microscopy, as they are non-reactive and do not react with antibodies.

Immunofluorescence labelling with antibody-based probes and CLSM imaging at the cellular level

Understanding the precise distribution of AGPs in fruit tissues is of paramount importance because of their pivotal roles in fruit growth, development, and ripening. Immunofluorescence enables researchers to visualise AGPs within fruit tissues, thereby offering insights into their quantity, localisation, dynamics, and interactions with other cellular components [44, 45]. In the immunofluorescence technique, fruit sections are placed on poly-l-lysine-coated slices, which are incubated with primary monoclonal antibodies that recognise AGP carbohydrate moieties (Table 1). To label fruit tissue, we employed antibodies that were more diluted than those typically used in other studies and as recommended by the producer. This 1:10 concentration proved to be too high, resulting in nonspecific binding and poor visualization of the AGP epitopes' distribution [34]. Subsequently, to visualise AGP epitopes, the sections are incubated with secondary antibodies conjugated with a fluorescent label [6, 44, 46]. The intensity of fluorescent signals is determined from CLSM images, which reveals the quantity of AGP epitopes in the sample [44, 47, 48]. Due to the distribution of AGPs at the border of the cell wall and membrane compartments, it is necessary to use Calcofluor White Stain for better visualisation of the AGP epitopes. This fluorescent blue dye staining cellulose allows labelling of the whole surface of the cell wall. In the case of samples from various stages of ripening, quick disappearance of immunofluorescence can be observed at the last stages of the process, which is correlated with the lower content of AGPs and the lower number of epitopes. Dako Fluorescent Mounting Medium, which retards fading of the fluorescence signal and thus allows longer imaging after mounting, can be used to enhance the visualisation of fluorescence. The schematic description of the method is shown in Fig. 2.

Procedure

1. Prepare semi-thin (1 μm) sections using an ultramicrotome and a glass knife.
2. Place the sections on poly-L-lysine coated glass slides and dry at 45 °C.
3. Use a liquid blocker Dako-Pen to draw a hydrophobic barrier around the sections on the glass [49].
4. Wash the slice with PBS twice for 15 min each.
5. Add blocking buffer (2% BSA solution in PBS) and incubate for 30 min at RT.
6. Remove the blocking buffer and wash the slice with PBS for 15 min at RT.
7. Add primary antibody diluted at 1:50 in a 0.1% BSA solution in PBS and incubate overnight at 4 °C. Next day, incubate for 15 min at RT.
8. Remove the solution and wash the slice four times with PBS for 20 min each at RT.
9. Add secondary antibody conjugated with a fluorescent label diluted at 1:200 in a 0.1% BSA solution in PBS and incubate overnight at 4 °C. Next day, incubate for 15 min at RT.
10. Remove the solution and wash the slice with PBS twice for 15 min each at RT.
11. Wash the slice five times with distilled water for 10 min each at RT.
12. Stain the slice with Calcofluor White in order to contrast the image.
13. Visualise the sections using CLSM.
14. Make control reactions without incubation with the primary antibody.

Critical

(1) It is important to place sections onto poly-L-lysine-coated glass slides to prevent their run-off during the next immunolabelling steps.

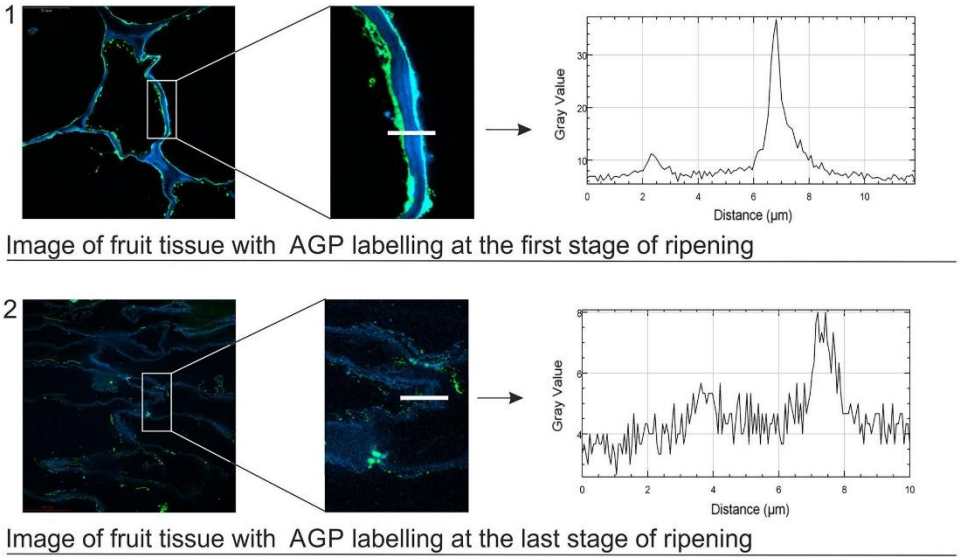

Fig. 2 CLSM image with a magnification of the cell wall in fruits at the first stage of ripening (1) and at the last stage of ripening (2). Results obtained with the immunofluorescence method – plots of the grey value profile from labelled cell walls (marked with a white line)

(2) The drying of slides with sections cannot be accelerated by raising the temperature above 45 °C. This causes rippling of polymerised tissue, which reduces the quality of immunofluorescence labelling and CLSM imaging.
(3) The entire labelling procedure must take place in a wet enclosed space.
(4) A few additional solutions can reduce unspecific binding: adding the detergent Tween to the wash buffer, using excess volumes of wash buffer, and trying to remove all wash buffer by tapping the glass against absorbent paper.
(5) The step with secondary antibody, i.e. Alexa-Fluor 488, should be carried out in the dark.

Immunogold labelling and imaging at the subcellular level using a TEM

The immunogold labelling method, which merges the resolution of electron microscopy with the specificity of immunolabelling, allows for the precise visualization of AGPs at a subcellular level of fruit tissue. By using secondary antibodies conjugated with gold nanoparticles, AGPs can be identified and allowed to reveal their involvement in the cell wall assembly, signalling, and intercellular communication [40, 43]. Like the other immunocytochemical methods, immunogold labelling used for AGP studies require technical modifications in the tissue preparation protocol [50]. Using primary monoclonal antibodies that target particular AGP epitopes, fruit sections are placed on grids covered by a formvar layer [51]. An antibody conjugated with colloidal gold particles specific to the primary antibodies should be used as a secondary antibody. Due to their high electron density and punctate shape, coupled colloidal gold particles are simple to identify as dark dots and count. In contrast to the standard plant sample preparation protocols [50], the osmium tetroxide treatment is excluded. This step is omitted to avoid worsening the quality of the samples, as the use of OsO4-treated often results in a decrease in the intensity of labelled dots during TEM imaging of fruit tissues. Nonetheless, the details within the cells are still well preserved without this solution. The schematic description of the method is shown in Fig. 3.

Procedure

1. Prepare ultra-thin (70 nm) sections using an ultramicrotome and a diamond knife with a 45° angle.
2. Place the sections on formvar film-coated nickel grids.
3. Place parafilm on a Petri dish which is necessary to make immunogold labelling.

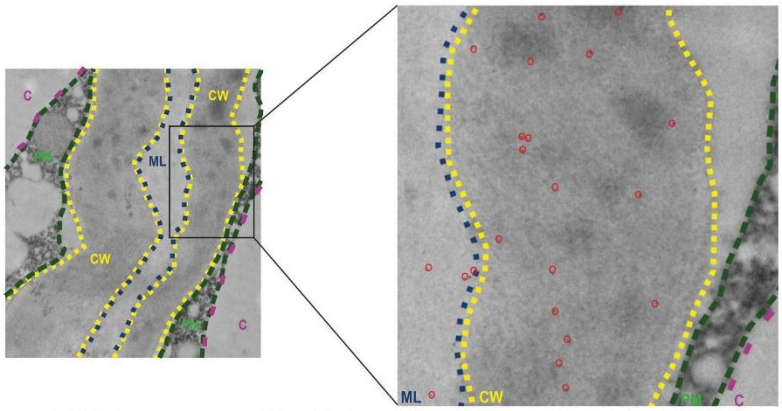

Fig. 3 TEM image with labelled AGPs. Epitopes are visible as dark dots (circled in red colour). Magnification with underlined localisation of AGPs in particular cell compartments. Abbreviations: CW – cell wall (yellow colour), PM – plasma membrane (green colour), ML – middle lamella (blue colour), C – cytoplasm (pink colour)

4. Wash the grids with distilled water three times for 10 min each.
5. Add blocking buffer (1% BSA solution in PBS) and incubate for 30 min at RT.
6. Add primary antibody diluted at 1:10 in a 0.1% BSA solution in PBS and incubate for 3 h at 37 °C.
7. Remove the solution and wash the grids with a 1% BSA solution in PBS three times for 10 min each.
8. Add secondary antibody conjugated to gold particles diluted at 1:50 in a 0.1% BSA solution in PBS and incubate for 1 h at 37 °C.
9. Remove the solution and wash the grids with PBS twice for 10 min each.
10. Wash the grids with distilled water five times for 10 min each.
11. Allow the grids to dry on clean filter paper and next put them into the TEM Grid storage box.
12. Add a filtered aqueous 1% UA solution (uranyl acetate) and incubate for 10 min at RT.
13. Wash the grids with distilled water three times for a few seconds each and allow them to dry.
14. Add filtered Reynold's reagent (triple lead citrate) and incubate for 7 min at RT.
15. Wash the grids three times with distilled water for a few seconds each, allow them to dry, and transfer them to the grid box for storage.
16. Visualise sections and examine the image using TEM.
17. Make control reactions without incubation with the primary antibody.

Critical

(1) Filter both staining solutions using a 0.2 µm filter, as this step will prevent contamination of the grids.
(2) The grid must be floating, not submerged.
(3) To prevent grid contamination, place NaOH pellets around the staining vessel to absorb CO_2 and wetness.

Ex situ studies – molecular methods

Ex situ methods for molecular analysis are an ideal way to analyse AGPs isolated from fruit tissue. These methods are based on investigations of material obtained in the extraction procedure, which allows qualitative and quantitative analyses. Modern molecular methods not only detect the presence of AGPs but also determine their concentration and structural characteristics [52–54]. The ability to demonstrate the presence and amount of AGPs in the sample is possible using two molecular techniques, i.e. Western blotting and ELISA test [55] (Table 3).

Tissue preparation—extraction protocol

Generally, the extraction of AGPs from plant tissue is complicated because the sugar residues of AGPs are linked to other cell wall constituents, which additionally contributes to cell wall stability and resistance to chemical, physical, and biological factors. Therefore, the extraction process must be aggressive enough to access AGPs without irreversible alterations in the protein moiety. Compared to more rigid plant structures, such as stems or leaves, fruit tissue is more hydrated

Table 3 Application, advantages, and disadvantages of molecular techniques with antibody-based probes in AGPs studies

Technique	Application	Advantage	Disadvantage
Western blotting	Used to detect the molecular weight of AGPs	Separation of proteins according to molecular weight High specificity and sensitivity Nice and clean interpretable results Commercially available antibodies	Work-intensive and not quick Medium throughput High cost and technical demand Tissue must be homogenised Low intensity of bands can distort the results
ELISA	Used to detect AGPs qualitatively and quantitatively	High specificity, sensitivity, and efficiency Easy to perform with a simple procedure Commercially available reagents for detection Simultaneous analysis of several samples	High cost Insufficient blocking of immobilised antigens yields false results Results limited to the amount of the antigen in the sample

and changes its biochemical composition throughout physiological processes. These factors make the extraction process more complex, and the concentration of the extraction buffer during AGPs extraction should be considered. Before the extraction process, the fruit tissue is sliced and frozen at − 80 °C. In order to extract proteins from plant tissues, they must be initially homogenised in liquid nitrogen and then added to suitable extraction buffer (i.e. Laemmli's buffer) [42, 56]. Modified Laemmli's buffer is composed of 65 mM Tris–HCl pH 6.8 (tris-(hydroxymethyl)-aminomethane), 2% SDS (sodium dodecyl sulphate), 2 mM EDTA (ethylenediaminetetraacetic acid), 1 mM PMSF (phenylmethylsulphonyl fluoride), 700 mM β-mercaptoethanol, and 1:10 protease inhibitor. This extraction buffer is used to maintain the pH, ionic strength, and stability of AGPs during the extraction procedure. For a less hydrated fruit tissue, a proportion of 1:1 should be used (i.e. 1 mL of extraction buffer per 1 g of tissue). This proportion should be modified (i.e. 0.5 mL of extraction buffer per 1 g of tissue) in the case of a highly hydrated fruit tissue from the last stages of ripening. In order to prevent protein degradation, samples should be kept on ice during the extraction process and extracted quickly with pre-chilled equipment. The homogenates are typically boiled for 5 min at 95 °C and clarified by centrifugation at 14 000 rpm at 4 °C for 20 min. The last step of the extraction process is to collect the supernatant, which is ready for use or/and may be frozen at −80 °C.

Molecular mass characterisation of AGPs using immunoblotting

Immunoblotting enables specific detection and molecular mass characterisation of AGPs in fruit tissues, which allows the demonstration of their structural variations and functional diversity. Western blotting is an analytical technique used in molecular biology to detect and characterise specific antigenic determinants [54, 57, 58]. The technique involves appropriate sample preparation, electrophoretic separation (i.e. SDS-PAGE – sodium dodecyl sulphate polyacrylamide gel electrophoresis) [7, 59, 60], transfer of separated proteins from the gel to the membrane (nitrocellulose, polyvinylidene difluoride (PVDF)) [61, 62], incubation with appropriate antibodies, and detection [63]. Visualisation of these markers can be carried out colorimetrically or with chemiluminescence methods [53, 57]. To optimise the Western blotting technique used to study AGPs, some changes should be done in the concentrations of the reagents used [64]. First of all, the AGP epitope analysis of fruit tissues requires the optimal concentration of the antibody, which is determined by testing a variety of antibody dilutions around the concentration suggested by the producer. To improve the imaging AGP epitopes on the membrane, lower concentrations of antibodies were used than the 1:10 dilution typically used for immunoblotting plant samples, such as from *Brassica napus* (var. Expert) and pea (*Pisum sativum* var. Normand) roots [63]. Also, to improve imaging and minimise a high background, the concentration of the blocking buffer should be modified due to the necessity of more effective blocking of non-specific sites. Additionally, in AGP separation, a wet membrane transfer at 4 °C should be carried out to minimise unwanted effects of generated heat, such as gel distortion. The schematic description of the method is shown in Fig. 4.

Procedure

1. To construct polyacrylamide gel electrophoresis with protein denaturing conditions (SDS-PAGE gel), prepare the resolving gel: mix 6 mL of 12.5% resolving gel (stock: mix 33.28 mL of acrylamide, 25.12 mL of distilled water, 20 mL of 1.5 M Tris pH 8.8, 800 µL of SDS), 60 µL of 10% APS (ammo-

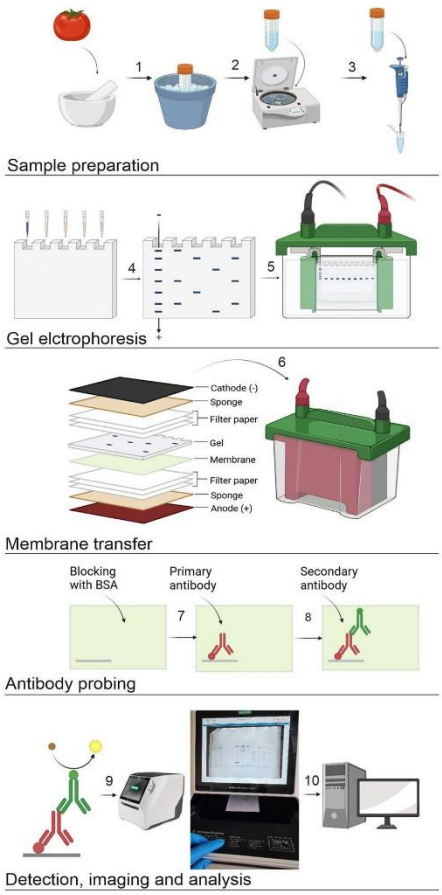

Fig. 4 Scheme of measuring AGPs using Western Blotting. (1) Homogenisation of plant material in liquid nitrogen. (2) Extraction step. (3) Collection of the supernatant. (4) Application of samples and protein leader to electrophoresis gel. (5) SDS-PAGE electrophoretic separation. (6) Preparation of the sandwich. Membrane transfer. (7) Membrane blocking with BSA and incubation with primary antibody. (8) Membrane incubation with secondary antibody. (9) Signal detection and band measurement. (10) Imaging with a scanning machine. Created with BioRender.com

nium persulphate sodium), and 20 µL of TEMED (N,N,N',N'-tetramethylethylene diamine), cast it between two glass plates, pour over ¾ of the volume, and wait for polymerisation for about 30 min. After polymerisation, add 2 mL of isopropanol to leave a flat surface of the resolving gel.

2. Remove the alcohol by touching with the edge of tissue paper. Prepare the stacking gel: mix 3 mL of the stacking gel (stock: mix 5.44 mL of acrylamide, 21.76 mL of distilled water, 4 mL of 1 M Tris pH 6.8, 320 µL of SDS, Bromophenol blue), 30 µL of 10% APS and 15 µL TEMED, cast it between two glass plates, insert a plastic electrophoresis comb to create the wells, and wait for polymerisation for 30 min.
3. Prepare samples: add 3×SDS sample buffer to the total protein amount (according to Bradford's measurement), mix the samples, and heat the mixture to 95 °C for 5 min.
4. Set up the electrophoresis apparatus and add 1×running buffer (mix 14.4 g of glycine, 3 g of Tris Base, 1 g of SDS, and 1 L of distilled water).
5. Load an appropriate protein ladder and samples onto the gel (around 20 µL per well).
6. Turn on the electrophoresis power pack and set it to a low voltage (80 V for 20 min) with a subsequent increase to a higher voltage (120 V for 1 h). Stop the gel running when the protein leader migrates to the appropriate position.
7. Wash PVDF membranes (nitrocellulose membranes) in methanol for 1 min before transfer.
8. Soak sponges and Whatman filter paper in 1×transfer buffer (mix 14.41 g of glycine, 15.14 g of Tris Base, and 4 mL of 10% SDS in 100 mL of distilled water and add 200 mL of methanol and 700 mL of distilled water).
9. Assemble the transfer constituent 'sandwich' sequentially arranging the sponge, 2–3 sheets of wetted filter paper, the membrane, the gel, 2–3 sheets of wetted filter paper, and finally the second sponge, starting to build on the transfer cassette facing the anode (+).
10. Turn on the power pack, set the voltage to low, and use the wet transfer technique (90 V for 80 min).
11. Wash the membrane with TBST (Tris-buffered saline) on a lab shaker for 15 min.
12. Add blocking buffer (5% BSA solution in PBS) and incubate for 1 h at RT on a lab shaker.
13. Remove the blocking buffer and wash the membrane with TBST three times for 5 min each on a lab shaker.
14. After the preincubation step, add the primary antibody diluted in 1:500 in a 2.5% BSA solution in PBS and incubate for 2 h at RT on a lab shaker or overnight at 4 °C.
15. Remove the solution and wash the membrane with TBST three times for 5 min each on a lab shaker.
16. Add secondary antibody with the AP-specific (alkaline phosphatase) enzyme conjugate diluted at

1:1000 in a 2.5% BSA solution in PBS and incubate the mixture for 2 h at RT on a lab shaker.
17. Remove the solution and wash the membrane with TBST three times for 5 min each on a lab shaker.
18. Wash the membrane for 10 min with the AP buffer (mix 12.11 g of Tris Base, 5.84 g of NaCl, 1.01 g of MgCl2, and 1 L of distilled water, pH 9.5).
19. Add a freshly prepared substrate solution for colorimetric detection (20 mL of AP buffer, 1 mL of BCiP (5-bromo-4-chloro-3-indolyl phosphate), and 1 mL of NBT (nitrotetrazolium Blue chloride) to the membrane.
20. Incubate the membrane at RT in the dark on a lab shaker until bands are reached (the average time is 15 min).
21. Wash the membrane twice with distilled water for 10 min each.
22. Membrane imaging using an imaging system with a UV free tray.

Critical

(1) To prevent degradation of AGPs, samples should be kept on ice during preparation and application on the gel.
(2) Prepare and store BCiP and NBT reagents in the dark.
(3) If a too high background is noted on the membrane, it requires shorter incubation with primary antibodies.
(4) If "smiling" bands are observed, the SDS-PAGE electrophoresis was overheated or ran too quickly; in such a case, either the voltage should be lower or the electrophoresis should be run in colder conditions.
(5) Any white spots noted on the membrane suggest that probably air bubbles were left between the gel and the membrane during the folding of the 'sandwich'; to resolve this, moisten the plastic with transfer buffer and use it to roll air bubbles out of the membrane.
(6) Any black spots noted on the membrane suggest that probably the antibodies bound to the blocking reagent; to resolve this, use a different blocking reagent and wash the membrane more precisely before detection.
(7) AGPs (in comparison to typical proteins) do not separate as single bands but as smeared bands. This is a result of the heterogeneity of glycosylation.

Selective glycome profiling of AGPs using enzyme-linked immunosorbent assay—ELISA test

ELISA is an immunoenzymatic test commonly that is used in scientific research. Its advantages include high sensitivity [65] and the ability to evaluate multiple samples at the same time providing highly reproducible results [52, 66]. ELISA is a basic test for the qualitative and quantitative determination of specific epitopes based on the number of antigen–antibody bonds formed. By comparing these bonds to standards, it is possible to estimate their quantity [67, 68]. AGPs can also be analysed qualitatively and quantitatively using ELISA. However, due to the specific structure of AGPs, modification of the protocol is necessary. In the case of fruit tissue, which are highly hydrated, the cover process is extended to 72 h, as opposed to a few hours in traditional ELISA. Additionally, it is run at 37 °C, compared with overnight coating at 4 °C for rice and carrot roots [33]. These modifications have made it possible to optimise the sample covering. Moreover, optimisation of the concentration of the primary antibody was carried out, as the use of the recommended concentration of 1:10 by the producer gave too intense a background signal [25, 34]. The description of the method is shown in Fig. 5.

Procedure

1. Prepare a 96-well microplate and add particular sample per well.
2. Incubate for 72 h at 37 °C with shaking (350 rpm).
3. Wash the plate with 100 µL of PBS three times for 5 min each on a lab shaker.
4. Add 200 µL of blocking buffer (0.1% BSA solution in PBS) per well and incubate for 1 h at 37 °C with shaking (350 rpm).
5. Remove the blocking buffer and wash the plate with 100 µL of PBS three times for 5 min each on a lab shaker.
6. After the preincubation step, add 100 µL of primary antibody diluted at 1:20 in PBS per well.
7. Cover the plate and incubate for 1 h at 37 °C with shaking (350 rpm).
8. Remove the solution and wash the plate with 100 µL of PBS three times for 5 min each on a lab shaker.
9. Add 100 µL of secondary antibody with the enzyme conjugate an AP-specific diluted at 1:500 in PBS per well.
10. Cover the plate and incubate for 1 h at 37 °C with shaking (350 rpm).

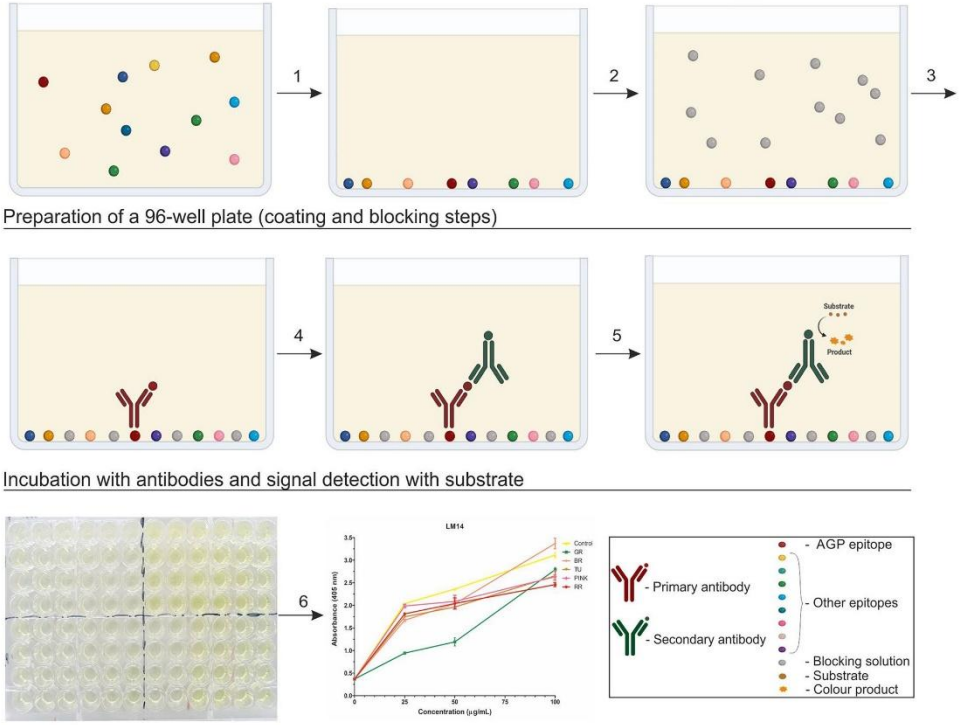

Fig. 5 Scheme of measuring AGPs using ELISA. (1) Coating – sample immobilisation. (2) Blocking with BSA. (3) Incubation with primary antibody. (4) Incubation with secondary antibody. (5) Signal detection using a microplate reader. (6) Measurement and quantitative analysis of the AGP concentration in the sample. Created with BioRender.com

11. Remove the solution and wash the plate with 100 µL of PBS three times for 5 min each on a lab shaker.
12. Add 100 µL of a freshly prepared substrate solution of PNPP (p-nitrophenol phosphate) per well.
13. Incubate the plate at RT in the dark until the desired colour intensity is reached (on average it is 15 min).
14. Add 50 µL of 2 M NaOH to stop the reaction.
15. Measure the absorbance at 405 nm.

Critical

(1) Equilibrate PNPP to room temperature and keep it in the dark before using.
(2) Too strong a signal (no differentiation on the board) most probably indicates that the wrong concentration of antibody or too much substrate was used or the plate was not rinsed properly between the steps.

Briefly, all specific reagents, buffers, and types of equipment that are necessary for immunocytochemical analyses of AGPs are summarised in Table 4. Also, the optimised concentration of primary and secondary antibodies is shown as an integral part of all described methods.

Discussion

AGPs are classified as a family of proteins present in the cell wall structure [15, 69]. Considering their heterogeneous structure, a few types of AGPs should be distinguished [15]. AGPs identified from the *Arabidopsis* genome based on composition, size, and the presence of different domains fall into four distinct classes, like classical AGPs, lysine-rich AGPs, AG peptides, chimeric

Table 4 Reagents and equipment necessary for immunocytochemical techniques

Immunofluorescence labelling	Immunogold labelling	SDS-PAGE Western blotting	ELISA
Reagents			
PBS	PBS	PBS	PBS
BSA	BSA	BSA	BSA
Paraformaldehyde	Uranyl acetate	12.5% Resolving gel*	NaOH
Glutaraldehyde	Reynolds reagent	Stacking gel*	PNPP
NaOH	Paraformaldehyde	10% APS	
Ethanol	Glutaraldehyde	Sample buffer*	
Resin	NaOH	Running buffer*	
	Ethanol	Transfer buffer*	
	Resin	TBST*	
		AP buffer*	
		BCiP*	
		NBT*	
		DMF	
Antibodies			
Primary antibody diluted in BSA (1:50)	Primary antibody diluted in BSA (1:10)	Primary antibody diluted in PBS (1:500)	Primary antibody diluted in PBS (1:20)
Secondary antibody conjugated with a fluorochrome diluted in BSA (1:200)	Secondary antibody conjugated with gold nanoparticles diluted in BSA (1:50)	Secondary antibody with AP diluted in PBS (1:1000)	Secondary antibody with AP diluted in PBS (1:500)
Equipment			
Vacuum pump	Vacuum pump	Electrophoresis apparatus	Microplate washer
Gelatine capsules	Gelatine capsules	Wet transfer module	Microplate shaker
Ultramicrotome	Ultramicrotome	Laboratory shaker	Microplate reader
Glass knife	Diamond knife	Nitrocellulose membrane	
Poly-L-lysine coated glass slides	Nickel grids with formvar film	Scanning machine	
Wet chamber	Petri dishes		
Hydrophobic pen	TEM		
CLSM			

* *Resolving gel*—12.5% (33.28 mL of acrylamide, 25.12 mL of distilled water, 20 mL of 1.5 M Tris pH 8.8, 0.8 mL of 10% SDS)

* *Stacking gel* (5.44 mL of acrylamide, 21.76 mL of distilled water, 4 mL of 1 M Tris pH 6.8, 0.32 mL of 10% SDS, bromophenol blue)

* *Sample buffer* (100 µL of Tris pH 6.8, 480 µL of 10% SDS, 480 µL of 0.5 M DTT, 240 µL of 100% glycerol)

* *Running buffer* (add 14.4 g of glycerine, 3 g of Tris Base, and 1 g of SDS to 1 L of distilled water)

* *Transfer buffer* (add 72.06 g of glycine, 15.14 g of Tris Base, and 20 mL of 10% SDS to 500 mL of distilled water)

* *TBST* (add 2.423 g of Tris Base, 8 g of NaCl, and 1 mL of Tween 20 to 1 L of distilled water and establish pH 7.6)

* *AP buffer* (add 12.11 g of Tris Base, 5.84 g of NaCl, and 1.01 g of $MgCl_2$ to 1 L of distilled water and establish pH 9.5)

* *BCiP* (add 4 mg of BCiP to 1 mL of distilled water)

* *NBT* (add 9 mg of NBT to 0.3 mL of distilled water and 0.7 mL DMF)

fasciclin-like AGPs (FLAs), chimeric plastocyanin (PAGs) and other chimeric AGPs [70]. Although they are composed of 90% of carbohydrate moiety, AGPs are definitely different from other cell wall polysaccharides which constitute up to 90–95% of the cell wall mass [71]. The cell wall polysaccharides include pectin, cellulose, hemicelluloses, and different glycoproteins [34]. Cellulose microfibrils with hemicelluloses such as xyloglucans, xylans and other glucans form a load-bearing matrix. In this matrix, spaces between cellulose skeleton are filled with amorphic gel, composed mainly of pectic constituents, like the most common homogalacturonan (HG), rhamnogalacturonan type I (RGI), rhamnogalacturonan type II (RGII) and xylogalacturonans (XG) [69, 71]. The methods listed in current paper with exquisite specificity of monoclonal antibodies have established some aspects and fine details of cell wall structural modifications and distribution of cell wall components during cell metabolism. The

structure, presence and amounts of cell wall components vary greatly, starting from the variable localisation in the extracellular matrix, the change in distribution and the significant structural variability observed during the physiological processes of plants. Another feature that distinguishes the other carbohydrate components from AGPs is a pattern of their molecular changes. As far as AGPs can be considered as a marker of particular stages of fruit development and ripening, pectins are more permanent and their alternations cannot be linked to individual processes in the cell [72–74]. Glyco profiling of the main pectic epitopes using ELISA assay by Posé and coworkers on the tomato and strawberry fruit at unripe and ripe stages have defined differently in epitope quantities during the ripening process [75]. The mentioned information allows the conclusion that AGPs, although composed of carbohydrate moiety, exhibit distinct characteristics, indicating novel cell wall attribute.

Taking into account the alternations in content and distribution of AGPs across the examined plant organs, also the necessity of molecular features examination should be underlined to gain additional insight into changes in the glycosylation process. All mentioned above properties of AGPs in comparison to features of other cell wall constituents allow concluding that AGPs may be involved in plant molecular mechanisms. As is well-known AGPs are present both free in the apoplast where they act as signalling molecules as well as in strict connection with the extracellular matrix, in the close area of the cell wall and plasma membrane. In the literature, the role of AGPs as signalling molecules in molecular interactions of intercellular signalling is connected with their Ca^{2+} binding capacity and presumptive engagement in the release of cell-surface apoplastic calcium [1, 18]. Another, substantial function of AGPs is the co-creating of the assembly of the cell wall by crosslinking with other cell wall glycopolymers and intermolecular formation of calcium bridges [20, 76]. The classical AGPs have been assumed to form complexes with pectins and hemicelluloses, by covalently attaching with RG-I and HG linked to Rha residues in AG polysaccharides and with arabinoxylan attached to Rha residue in the RG-I [20]. Mentioned conjugate isolated from *Arabidopsis* suspension culture media was distinguished by a significant amount of RG-I – AGP fraction, which indeed covalently linkage between RG-I and AGPs for a functional wall structure [76]. The latest reports confirm the role of AGPs in creating cell wall continuity, by physical interaction with the pectic domains RG-I and homogalacturonan [77]. The most recent results indicate that cationic AGP domains serve a chaperoning role by catalyzing boron bridging and RG-II dimerization. The authors assume that RG-II and specific AGPs are involved in guiding cell-wall assembly [77].

The framework of plant cell wall glycans and the maintenance of interactions between them should be also investigated in the fruit context. Results obtained with the aforementioned methods are compatible and allow a comprehensive analysis of AGPs present in fruits. Currently, antibodies recognising carbohydrate chains are the only commercially available tools maximally specific to AGPs [24, 26, 33, 34]. These antibodies are used to identify epitopes that are useful markers of tissue modification during particular stages of the fruit development and ripening process [13]. Despite the strong emphasis on the involvement of AGPs in plant physiological processes, most studies focus only on their structural rather than functional characteristics. To date, AGPs have been investigated in only a few kinds of fruits, e.g. strawberry—*Fragaria* x *ananassa* [78], grape—*Vitis vinifera* [79], tomato—*Solanum lycopersicum* [80], olive—*Olea europaea* L. [81], apple—*Malus domestica* [5, 23, 82], and pear—*Pyrus communis* [4]. Thus, the aim of the current paper was to gather the optimised protocols, troubleshooting, and experience gained from experimental work on AGPs in fruits. So far, most reports of AGPs in fruits have been based on the use of the presented protocols, i.e. the spatio-temporal pattern of distribution, tissue specificity, concentration in fruit tissue, characterisation of the glycan structure, and differences in the carbohydrate moiety structure. Using these protocols, it was possible to determine the effect of AGPs on fruit physiological processes, such as development, ripening, and senescence during postharvest storage [12, 14, 83]. Immunocytochemical analyses in situ with CLSM and TEM imaging have confirmed the altered distribution of AGPs during the ripening process, noted as a typical spatio-temporal pattern. At the beginning of the process, AGP epitopes are found mainly in the plasma membrane, where they are accumulated along the cell wall border. For example, immunolabelling with JIM13 showed the presence of the β-GlcA-(1→3)-α-GalA-(1→2)-α-Rha epitope in the cell wall-plasma membrane continuum, while their assembly in the mature green and stored fruit tissue was disturbed [5]. The immunogold labelling with JIM13 confirmed the specific arrangement of AGPs in the fruit cell wall. Moreover, the results obtained at the subcellular level using TEM indicated the presence of AGPs in other cellular compartments as well, emphasising that the synthesis of carbohydrate chains and protein moiety takes place in the endoplasmic reticulum [82, 84].

Furthermore, in situ and ex situ immunocytochemical techniques demonstrated a correlation between the level of AGP glycosylation and molecular AGP alterations with advancing cellular processes. Selective glycome profiling of AGPs revealed the decreasing molecular weight and concentration of AGPs with the progress of the ripening

process [85]. Similar changes during the grape ripening process were observed by Moore and co-workers [79]. The quantity of AGP epitopes (JIM8, JIM13, and LM14) gradually increased during ripening, which was followed by reduction and release of AGPs into the apoplast [79]. Our research on tomato fruits as a model organism for ripening analyses have revealed that fruits at the breaker stage contain AGPs with the highest molecular weight with miscellaneous carbohydrate chains, while AGPs with low molecular weight (~ 30 kDa) are mainly noted in fruits at the red ripe stage. These low-molecular AGPs may be regarded as a marker of the end of the ripening process in tomato fruits. Also, the JIM13 antibody, which detects the most frequent AGP epitope with a molecular weight range of 120–20 kDa, can be used as a tool to determine the presence or absence of AGPs in plant tissue [85].

On the other hand, the literature provides information about the frequent use of Yariv reagent to isolate AGP, but so far there has been no unambiguous description with which AGP structural moiety it binds [86, 87]. It is acknowledged that a chemical compound known as the β-glucosyl Yariv reagent (1,3,5-tri(p-glycosyloxyphenylazo)-2,4,6-trihydroxybenzene, β-GlcY) is often used as a cytochemical reagent for detection, quantification, and purification of AGPs as well as modification of the molecular activities of AGPs [80, 87]. Also, a previous study showed that Yariv reactivity is not dependent on the peptide component of AGPs. β-GlcY binds to β-1,3-galactan chains which are longer than five residues. Most likely, this is related to the sequential trimming of the AG moieties of AGPs using sets of specific glycoside hydrolases [88]. In our previous work on apple fruit, the AGPs concentration was estimated at 2 080 µg/g of the parenchyma tissue of red fruits. In comparison to the presence of AGPs in tomato fruits, the concentration was similar, indicating that fruit tissue is a rich source of the examined proteoglycans [42]. For example, during the turning stage of the ripening process, the AGP concentration was determined to be 3 110 µg/g of fresh tissue, suggesting that the presence of AGPs is correlated with the ongoing synthesis of long chains of AGP carbohydrates [85]. For comparison, research carried out by Kaur and coworkers have determined the amount of precipitated AGP in *Arabidopsis thaliana* in different organs. The amount of AGP was 150 µg/g of fresh weight rosette leaf, 450 µg/g from the stem, 610 µg/g from the root, and 1000 µg/g from the flower [89]. Other research conducted by Lamport confirmed the presence of 30–300 µg AGPs per fresh weight of tobacco leaf [90]. Precluding the necessity to clarify the role of AGPs in fruit metabolism and considering the content of AGP in other plant organs, research on AGP in fruits is even more useful to obtain research material. Previous studies on AGPs in fruits allow concluding that fruit tissue is a good research material for isolation as well as structural and molecular characterisation of AGPs as crucial cell wall components.

Conclusions and future perspectives

Immunocytochemical techniques, both in situ and ex situ, offer the opportunity to precisely determine the molecular and structural modifications occurring in fruit tissues during development and ripening processes. Antibody-based methods are the primary tool for studying AGPs. All techniques, i.e. glycome profiling, immunoprinting on a membrane, screening by ELISA, and/or epitope mapping allow characterisation of the carbohydrate moiety of AGPs. Immunocytochemical studies that use antibodies to identify and visualise specific AGP epitopes have their advantages and disadvantages. The advantages of immunocytochemistry include high specificity correlated with qualitative and quantitative analysis. On the other hand, the disadvantage of immunocytochemistry is the sample preparation step associated with difficulties in quantitative analysis and great subjectivity in the interpretation of results. Briefly, microscopic methods using antibody labeling are powerful tools that allow visualisation of AGPs and an understanding of tissue architecture. The immunofluorescence and immunogold methods allow for precise imaging of AGP localisation with high specificity, followed by qualitative and quantitative analysis. Western Blotting has also high specificity and allows for quantitative measurement but also requires several steps, including gel electrophoresis, transfer of proteins to a membrane, and detection with antibodies which can be time-consuming and labor-intensive. Therefore, in parallel, it is worth performing an additional analysis, such as ELISA, which is a method with high sensitivity and specificity. ELISA allows to detection of low levels of the tested molecules in samples, and this is extremely important in the case of hydrated fruit tissue. Moreover, the ELISA technique is scalable, which allows for simultaneous testing of many samples and enables quantitative analysis of the quantity.

The development of new antibodies in future research, including those against the protein domain, will allow a more thorough analysis of changes that occur in AGP molecules, determining the mechanism of AGP synthesis, degradation, and action during physiological processes. Moreover, a thorough study of glycobiology methods to investigate the AGP structure and distribution in cell walls may provide new knowledge for applications in the glycoscience area. Moreover, the latest reports on the construction of an analogue of the Yariv Reagent deserve to be emphasized [91].

The synthesis of an azido analogue of the Yariv reagent which is functionalized with a fluorophore allows to creation of a glycoconjugate that binds AGPs and allows the ability to visualize AGPs using fluorescence microscopy. The new probe for studying AGPs provides an opportunity to carry out more sophisticated imaging of AGP localisation. Moreover, the new way of AGPs visualisation will give the opportunity to compare results provided with immunocytochemistry tools [91].

Abbreviations

AG	Arabinogalactan
AGPs	Arabinogalactan proteins
AP	Alkaline phosphatase
APS	Ammonium persulphate sodium
BCiP	5-Bromo-4-chloro-3-indolyl-phosphate
BSA	Bovine serum albumin
C	Cytoplasm
CLSM	Confocal laser scanning microscope
CW	Cell wall
EDTA	Ethylenediaminetetraacetic acid
ELISA	Enzyme-linked immunosorbent assay
FITC	Fluorescein isothiocyanate
GalA	D-galacturonic acid
Glc	D-glucose
GlcA	D-glucuronic acid
HRGPs	The hydroxyproline-rich glycoproteins family
Hyp	Hydroxyproline
L-Ara	L-arabinose
L-Fuc	L-fucose
L-Rha	L-rhamnose
M.W.	Molecular weight
mAb	Monoclonal antibody
Man	D-mannose
4-Me-GlcA	4-o-methyl-glucuronic acid
ML	Middle lamella
NBT	Nitrotetrazolium Blue chloride
P4H	Prolyl 4-hydroxylase
PBS	Phosphate-buffered saline
PM	Plasma membrane
PMSF	Phenylmethylsulphonyl fluoride
PNPP	P-nitrophenyl phosphate
Pro	Proline
PVDF	Polyvinylidene difluoride
RT	Room temperature
SDS	Sodium dodecyl sulphate
SDS-PAGE	Sodium dodecyl sulphate polyacrylamide gel electrophoresis
TBST	Tris-buffered saline
TEM	Transmission electron microscope
TEMED	N,N,N′,N′-tetramethylethylene diamine
Tris	Tris-(hydroxymethyl)-aminomethane
UA	Uranyl acetate
Xyl	D-xylose

Acknowledgements
The authors gratefully acknowledge financial support by National Science Center Poland: SONATA16 (grant number 2020/39/D/NZ9/00232).

Author contributions
NK compiled the literature and wrote the first draft of a manuscript, AL designed the paper and edited the manuscript, AZ revised the manuscript.

Funding
The authors gratefully acknowledge financial support by National Science Center Poland: SONATA16 (Grant number 2020/39/D/NZ9/00232).

Availability of data and materials
Not applicable.

Declarations

Ethics approval and consent to participate
Not applicable.

Consent for publication
Not applicable.

Competing interests
The authors declare that they have no competing interests.

Received: 21 March 2023 Accepted: 27 October 2023
Published online: 01 November 2023

References

1. Lopez-Hernandez F, Tryfona T, Rizza A, Yu XL, Harris MOB, Webb AAR, et al. Calcium binding by arabinogalactan polysaccharides is important for normal plant development. Plant Cell. 2020;32:3346–69.
2. Showalter A. Arabinogalactan – proteins: structure, expression and function. Cell Mol Life Sci. 2001;58:1399–417.
3. Peng Q, Song J, Lv X, Wang Z, Huang L, Du Y. Structural characterization of an arabinogalactan-protein from the fruits of *Lycium ruthenicum*. J Agric Food Chem. 2012;60:9424–9.
4. Tsumuraya Y, Ozeki E, Ooki Y, Yoshimi Y, Hashizume K, Kotake T. Properties of arabinogalactan-proteins in European pear (*Pyrus communis* L.) fruits. Carbohydr Res. 2019;485:1–9.
5. Leszczuk A, Chylińska M, Zięba E, Skrzypek T, Szczuka E, Zdunek A. Structural network of arabinogalactan proteins (AGPs) and pectins in apple fruit during ripening and senescence processes. Plant Sci. 2018;275:36–48.
6. El-Tantawy A-A, Solís M-T, da Costa ML, Coimbra S, Risueñ M-C, Testillano PS. Arabinogalactan protein profiles and distribution patterns during microspore embryogenesis and pollen development in *Brassica napus*. Plant Reprod. 2013;26:231–43.
7. Castro AJ, Suárez C, Zienkiewicz K, Alché JDD, Zienkiewicz A, Rodríguez-García MI. Electrophoretic profiling and immunocytochemical detection of pectins and arabinogalactan proteins in olive pollen during germination and pollen tube growth. Ann Bot. 2013;112:503–13.
8. Lamport DTA, Northcote DH. Hydroxyproline in primary cell walls of higher plants. Nature. 1960;188:665–6.
9. Showalter AM, Basu D. Extensin and arabinogalactan-protein biosynthesis: Glycosyltransferases, research challenges, and biosensors. Front Plant Sci. 2016;7:1–9.
10. Popper ZA. Extraction and detection of arabinogalactan proteins. Methods Mol Biol. 2011;715:245–54.
11. Schultz CJ, Johnson KL, Currie G, Bacic A. The classical Arabinogalactan protein gene family of *Arabidopsis*. Plant Cell. 2000;12:1751–67.
12. Leszczuk A, Kalaitzis P, Blazakis KN, Zdunek A. The role of arabinogalactan proteins (AGPs) in fruit ripening—a review. Hort Res. 2020;7:1–12.
13. Seifert GJ, Roberts K. The biology of arabinogalactan proteins. Annu Rev Plant Biol. 2007;58:137–61.
14. Leszczuk A, Cybulska J, Skrzypek T, Zdunek A. Properties of arabinogalactan proteins (AGPs) in apple (*Malus* x *domestica*) fruit at different stages of ripening. Biology. 2020;9:1–12.
15. Silva J, Ferraz R, Dupree P, Showalter AM, Coimbra S. Three decades of advances in arabinogalactan-protein biosynthesis. Front Plant Sci. 2020;11:1–18.
16. Losada JM, Herrero M. Arabinogalactan-protein secretion is associated with the acquisition of stigmatic receptivity in the apple flower. Ann Bot. 2012;110:573–84.
17. Hromadova D, Soukup A, Tylova E. Arabinogalactan proteins in plant roots—an update in possible functions. Front Plant Sci. 2021;12:1–15.

18. Lamport DTA, Tan L, Held M, Kieliszewski MJ. Pollen tube growth and guidance: Occam's razor sharpened on a molecular arabinogalactan glycoprotein Rosetta Stone. New Phytol. 2018;217:491–500.
19. Leszczuk A, Szczuka E, Zdunek A. Arabinogalactan proteins: Distribution during the development of male and female gametophytes. Plant Physiol Biochem. 2019;135:9–18.
20. Tan L, Eberhard S, Pattathil S, Warder C, Glushka J, Yuan C, et al. An *Arabidopsis* cell wall proteoglycan consists of pectin and arabinoxylan covalently linked to an arabinogalactan protein. Plant Cell. 2013;25:270–87.
21. Wang D, Seymour GB. Molecular and biochemical basis of softening in tomato. Mol Horticulture. 2022;2:1–10.
22. Feder A, Jensen S, Wang A, Courtney L, Middleton L, van Eck J, et al. Tomato fruit as a model for tissue-specific gene silencing in crop plants. Hort Res. 2020;7:142–8.
23. Leszczuk A, Pieczywek PM, Gryta A, Frąc M, Zdunek A. Immunocytochemical studies on the distribution of arabinogalactan proteins (AGPs) as a response to fungal infection in *Malus* x *domestica* fruit. Sci Rep. 2019;9:1–14.
24. Knox JP. The use of antibodies to study the architecture and developmental regulation of plant cell walls. Int Rev Cytol. 1997;171:79–120.
25. Knox JP, Linstead PJ, Peart J, Cooper C, Roberts K. Developmentally regulated epitopes of cell surface arabinogalactan proteins and their relation to root tissue pattern formation. Plant J. 1991;1:317–26.
26. Yates EA, Valdor J-F, Haslam SM, Morris HR, Dell A, Mackie W, et al. Characterization of carbohydrate structural features recognized by anti-arabinogalactan-protein monoclonal antibodies. Glycobiology. 1996;6:131–9.
27. Yates EA, Knox JP. Investigations into the occurrence of plant cell surface epitopes in exudate gums. Carbohydr Polym. 1994;24:281–6.
28. Yan Y, Takáč T, Li X, Chen H, Wang Y, Xu E, et al. Variable content and distribution of arabinogalactan proteins in banana (*Musa* spp.) under low temperature stress. Front Plant Sci. 2015;6:1–14.
29. Pennell RI, Janniche L, Kjellbom P, Scofield GN, Peart JM, Robertsa K. Developmental regulation of a plasma membrane arabinogalactan protein epitope in oilseed rape flowers. Plant Cell. 1991;3:1317–26.
30. Ruprecht C, Bartetzko MP, Senf D, Dallabernadina P, Boos I, Andersen MCF, et al. A Synthetic Glycan Microarray Enables Epitope Mapping of Plant Cell Wall Glycan-Directed Antibodies. Plant Physiol. 2017;175:1094–104.
31. Pattathil S, Avci U, Baldwin D, Swennes AG, McGill JA, Popper Z, et al. A comprehensive toolkit of plant cell wall glycan-directed monoclonal antibodies. Plant Physiol. 2010;153:514–25.
32. Bradley DJ, Wood EA, Larkins AP, Galfre G, Butcher GW, Brewin NJ. Isolation of monoclonal antibodies reacting with peribacteroid membranes and other components of pea root nodules containing *Rhizobium leguminosarum*. Planta. 1988;173:149–60.
33. Smallwood M, Yates EA, Willats WGT, Martin H, Knox JP. Immunochemical comparison of membrane-associated and secreted arabinogalactan-proteins in rice and carrot. Planta. 1996;198:452–9.
34. Moller I, Marcus SE, Haeger A, Verhertbruggen Y, Verhoef R, Schols H, et al. High-throughput screening of monoclonal antibodies against plant cell wall glycans by hierarchical clustering of their carbohydrate microarray binding profiles. Glycoconj J. 2008;25:37–48.
35. Wilkinson MD, Tosi P, Lovegrove A, Corol DI, Ward JL, Palmer R, et al. The Gsp-1 genes encode the wheat arabinogalactan peptide. J Cereal Sci. 2017;74:155–64.
36. Norman PM, Wingate VPM, Lamb CJ. Monoclonal antibodies to plant plasma-membrane antigens. Planta. 1986;167:452–9.
37. Leszczuk A, Chylińska M, Zdunek A. Enzymes and vitamin C as factors influencing the presence of arabinogalactan proteins (AGPs) in *Solanum lycopersicum* fruit. Plant Physiol Biochem. 2019;139:681–90.
38. Burry RW. Multiple Antibodies from the Same Species. Immunocytochemistry A Practical Guide for Biomedical Research. Burry R W. New York: Springer; 2010. p. 119–38.
39. Bergersen LH, Storm-Mathisen J, Gundersen V. Immunogold quantification of amino acids and proteins in complex subcellular compartments. Nat Protoc. 2008;3:144–52.
40. Palacio-López K, Tinaz B, Holzinger A, Domozych DS. Arabinogalactan proteins and the extracellular matrix of charophytes: a sticky business. Front Plant Sci. 2019;10:1–15.
41. Wilson SM, Bacic A. Preparation of plant cells for transmission electron microscopy to optimize immunogold labeling of carbohydrate and protein epitopes. Nat Protoc. 2012;7:1716–27.
42. Leszczuk A, Zając A, Kurzyna-Szklarek M, Cybulska J, Zdunek A. Investigations of changes in the arabinogalactan proteins (AGPs) structure, size and composition during the fruit ripening process. Sci Rep. 2020;10:1–14.
43. Tremi I, Havaki S, Georgitsopoulou S, Lagopati N, Georgakilas V, Gorgoulis VG, et al. A guide for using transmission electron microscopy for studying the radiosensitizing effects of gold nanoparticles in vitro. Nanomaterials. 2021;11:1–19.
44. Pérez-Pérez Y, Carneros E, Berenguer E, Solís M-T, Bárány I, Pintos B, et al. Pectin de-methylesterification and AGP increase promote cell wall remodeling and are required during somatic embryogenesis of Quercus suber. Front Plant Sci. 2019;9:1–17.
45. Mollet J, Kim S, Jauh G-Y, Lord EM. Arabinogalactan proteins, pollen tube growth, and the reversible effects of Yariv phenylglycoside. Protoplasma. 2002;219:89–98.
46. Hu Y, Qin Y, Zhao J. Localization of an arabinogalactan protein epitope and the effects of Yariv phenylglycoside during zygotic embryo development of *Arabidopsis thaliana*. Protoplasma. 2006;229:21–31.
47. Cheng M, Zhou Q, Wang L, Jiao Y, Liu Y, Tan L, et al. A new mechanism by which environmental hazardous substances enhance their toxicities to plants. J Hazard Mater. 2022;421:1–11.
48. Wang R, Dobritsa AA. Microscopy: Looking below the surface in plants. eLife. 2020;9:1–3.
49. Sutherland P, Hallett I, Jones M. Probing cell wall structure and development by the use of antibodies: a personal perspective. N Z J For Sci. 2009;39:197–205.
50. Corral-Martínez P, García-Fortea E, Bernard S, Driouich A, Seguí-Simarro JM. Ultrastructural immunolocalization of arabinogalactan protein, pectin and hemicellulose epitopes through anther development in Brassica napus. Plant Cell Physiol. 2016;57:2161–74.
51. Mayhew TM, Lucocq JM, Griffiths G. Relative labelling index: a novel stereological approach to test for non-random immunogold labelling of organelles and membranes on transmission electron microscopy thin sections. J Microsc. 2002;205:153–64.
52. Sakamoto S, Putalun W, Vimolmangkang S, Phoolcharoen W, Shoyama Y, Tanaka H, et al. Enzyme-linked immunosorbent assay for the quantitative/qualitative analysis of plant secondary metabolites. J Nat Med. 2018;72:32–42.
53. Mahmood T, Yang PC. Western blot: technique, theory, and trouble shooting. N Am J Med Sci. 2012;4:429–34.
54. Kurien BT, Scofield RH. Western blotting. Methods. 2006;38:283–93.
55. Hauri HP, Bucher K. Immunoblotting with monoclonal antibodies: importance of the blocking solution. Anal Biochem. 1986;159:386–9.
56. Laemmli UK. Cleavage of structural proteins during the assembly of the head of bacteriophage T4. Nature. 1970;227:680–5.
57. Begum H, Murugesan P, Tangutur AD. Western blotting: A powerful staple in scientific and biomedical research. Biotechniques. 2022;73:59–70.
58. Masoodi KZ, Lone SM, Rasool RS. Blotting/hybridization and its types. In: Masoodi KZ, Lone SM, Rasool RS, editors. Advanced Methods in Molecular Biology and Biotechnology. Amsterdam: Academic Press; 2021. p. 117–22.
59. Santos-Hernández M, Recio I, Amigo L. Electrophoresis. In: McSweeney PLH, editor. Encyclopedia of Dairy Sciences. 3rd ed. Amsterdam: Academic Press; 2022. p. 370–81.
60. Masoodi KZ, Lone SM, Rasool RS. SDS-polyacrylamide gel electrophoresis. In: Masoodi LZ, Lone SM, Rasool RS, editors. Advanced methods in molecular biology and biotechnology. Amsterdam: Academic Press; 2021. p. 13–20.
61. Towbin H, Staehelint T, Gordon J. Electrophoretic transfer of proteins from polyacrylamide gels to nitrocellulose sheets: Procedure and some applications (ribosomal proteins/radioimmunoassay/fluorescent antibody assay/peroxidase-conjugated antibody/autoradiography). Proc Natl Acad Sci. 1979;76:4350–4.
62. Kurien BT, Scofield RH. Protein blotting: a review. J Immunol Methods. 2003;274:1–15.
63. Cannesan MA, Durand C, Burel C, Gangneux C, Lerouge P, Ishii T, et al. Effect of arabinogalactan proteins from the root caps of pea and Brassica napus on Aphanomyces euteiches zoospore chemotaxis and germination. Plant Physiol. 2012;159:1658–70.
64. Stott DI. Immunoblotting and dot blotting. J Immunol Methods. 1989;119:153–87.

65. Engvall E, Perlmann P. Enzyme-linked immunosorbent assay (ELISA) Quantitative assay of immunoglobulin G. Immunochemistry. 1971;8:871–4.
66. Mandal SM, Paul D. Enzyme-liked immunosorbent assay (ELISA). In: Mandal SM, Paul D, editors. Automation and basic techniques in medical microbiology. New York: Springer; 2022. p. 87–91.
67. Sengupta P, Wang CW, Ma ZF. Enzyme-linked immunosorbent assay (ELISA) technique for food analysis. In: Khan MS, Shafiur RM, editors. Techniques to measure food safety and quality. Springer; 2021. p. 91–115.
68. Happ K, Classen B. Arabinogalactan-proteins from the liverwort *Marchantia polymorpha* L., a member of a basal land plant lineage, are structurally different to those of angiosperms. Plants. 2019;8:1–14.
69. Leszczuk A, Kalaitzis P, Kulik J, Zdunek A. Review: structure and modifications of arabinogalactan proteins (AGPs). BMC Plant Biol. 2023;23:45.
70. Showalter AM, Keppler B, Lichtenberg J, Gu D, Welch LR. A bioinformatics approach to the identification, classification, and analysis of hydroxyproline-rich glycoproteins. Plant Physiol. 2010;153:485–513.
71. Classen B, Baumann A, Utermoehlen J. Arabinogalactan-proteins in spore-producing land plants. Carbohydr Polym. 2019;210:215–24.
72. Verhertbruggen Y, Marcus SE, Haeger A, Ordaz-Ortiz JJ, Knox JP. An extended set of monoclonal antibodies to pectic homogalacturonan. Carbohydr Res. 2009;344:1858–62.
73. Mohnen D. Pectin structure and biosynthesis. Curr Opin Plant Biol. 2008;11:266–77.
74. do Prado SBR, Ferreira GF, Harazono Y, Shiga TM, Raz A, Carpita NC, et al. Ripening-induced chemical modifications of p apaya pectin inhibit cancer cell proliferation. Sci Rep. 2017;7:1–17.
75. Posé S, Marcus SE, Knox JP. Differential metabolism of pectic galactan in tomato and strawberry fruit: detection of the LM26 branched galactan epitope in ripe strawberry fruit. Physiol Plant. 2018;164:95–105.
76. Tan L, Zhang L, Black I, Glushka J, Urbanowicz B, Heiss C, et al. Most of the rhamnogalacturonan-I from cultured *Arabidopsis* cell walls is covalently linked to arabinogalactan-protein. Carbohydr Polym. 2023;301: 120340.
77. Sanhueza D, Begum RA, Albenne C, Jamet E, Fry SC. An *Arabidopsis thaliana* arabinogalactan-protein (AGP31) and several cationic AGP fragments catalyse the boron bridging of rhamnogalacturonan-II. Biochem J. 2022;479:1967–84.
78. Leszczuk A, Szczuka E. Localization of arabinogalactan proteins in the cell walls of developing ovule in strawberry (*Fragaria* x *ananassaduch*). Int J Plant Biol Res. 2017;5:1066.
79. Moore JP, Fangel JU, Willats WGT, Vivier MA. Pectic-b(1,4)-galactan, extensin and arabinogalactan-protein epitopes differentiate ripening stages in wine and table grape cell walls. Ann Bot. 2014;114:1279–94.
80. Fragkostefanakis S, Dandachi F, Kalaitzis P. Expression of arabinogalactan proteins during tomato fruit ripening and in response to mechanical wounding, hypoxia and anoxia. Plant Physiol Biochem. 2012;52:112–8.
81. Suárez C, Zienkiewicz A, Castro AJ, Zienkiewicz K, Majewska-Sawka A, Rodríguez-García MI. Cellular localization and levels of pectins and arabinogalactan proteins in olive (*Olea europaea* L.) pistil tissues during development: Implications for pollen-pistil interaction. Planta. 2013;237:305–19.
82. Leszczuk A, Szczuka E, Wydrych J, Zdunek A. Changes in arabinogalactan proteins (AGPs) distribution in apple (*Malus* x *domestica*) fruit during senescence. Postharvest Biol Technol. 2018;138:99–106.
83. Pereira AM, Pereira LG, Coimbra S. Arabinogalactan proteins: rising attention from plant biologists. Plant Reprod. 2015;28:1–15.
84. Leszczuk A, Chylinska M, Zdunek A. Distribution of arabinogalactan proteins and pectins in the cells of apple (*Malus* x *domestica*) fruit during post-harvest storage. Ann Bot. 2019;123:47–55.
85. Kutyrieva-Nowak N, Leszczuk A, Zając A, Kalaitzis P, Zdunek A. Arabinogalactan protein is a molecular and cytological marker of particular stages of the tomato fruit ripening process. Sci Hortic. 2023;310:1–10.
86. Yariv J, Rapport MM, Graf L. The interaction of glycosides and saccharides with antibody to the corresponding phenylazo glycosides. Biochem J. 1962;85:383–8.
87. Classen B, Witthohn K, Blaschek W. Characterization of an arabinogalactan-protein isolated from pressed juice of *Echinacea purpurea* by precipitation with the β-glucosyl Yariv reagent. Carbohydr Res. 2000;327:497–504.
88. Kitazawa K, Tryfona T, Yoshimi Y, Hayashi Y, Kawauchi S, Antonov L, et al. β-galactosyl yariv reagent binds to the β-1,3-galactan of arabinogalactan proteins. Plant Physiol. 2013;161:1117–26.
89. Kaur D, Held MA, Smith MR, Showalter AM. Functional characterization of hydroxyproline-O-galactosyltransferases for *Arabidopsis* arabinogalactan-protein synthesis. BMC Plant Biol. 2021;21:1–24.
90. Lamport D. Preparation of arabinogalactan glycoproteins from plant tissue. Bio Protoc. 2013. https://doi.org/10.21769/BioProtoc.918.
91. Rueda S, Mccubbin TJ, Shieh M, Hoshing R, Braun DM, Basu A. A functionalizable analog of the Yariv reagent for AGP imaging using fluorescence microscopy. Bioconjug Chem. 2023;34:1398–406.

Publisher's Note

7. Tekst publikacji P.2

Kutyrieva-Nowak N., Leszczuk A., Zając A., Kalaitzis P., Zdunek A. 2023.

Arabinogalactan protein is a molecular and cytological marker of particular stages of the tomato fruit ripening process.

Scientia Horticulturae, 310: 111718.

Scientia Horticulturae 310 (2023) 111718

Contents lists available at ScienceDirect

Scientia Horticulturae

journal homepage: www.elsevier.com/locate/scihorti

Arabinogalactan protein is a molecular and cytological marker of particular stages of the tomato fruit ripening process

Nataliia Kutyrieva-Nowak [a], Agata Leszczuk [a,*], Adrian Zając [b], Panagiotis Kalaitzis [c], Artur Zdunek [a]

[a] Institute of Agrophysics, Polish Academy of Sciences, Doświadczalna 4, 20-290 Lublin, Poland
[b] Department of Functional Anatomy and Cytobiology, Institute of Biological Sciences, Maria Curie Skłodowska University, Akademicka 19, Lublin 20-400, Poland
[c] Department of Horticultural Genetics and Biotechnology, Mediterranean Agronomic Institute of Chania, Chania, P.O. Box 85, Chania 73100, Greece

ARTICLE INFO

Keywords:
Arabinogalactan proteins
Cell wall
Fruit
Proteoglycans
Ripening
Tomato

ABSTRACT

Arabinogalactan proteins (AGPs) are constituents of the plant cell walls, which are increasingly being considered as essential molecules in the formation of the extracellular matrix. Given their molecular structure and the advantage of the carbohydrate moiety, the glycosylation level and its modification is assumed as a cause of the functional diversity of AGPs. The aim of current work was to evaluate the molecular features of AGP as a potential molecule involved in the ripening process. For this purpose, tomato fruits were analyzed at specific five stages of ripening using microscopic and molecular tools. The experiment showed that the high content and the occurrence of the AGP molecule with molecular weight around 120 kDa are related to cell wall conditions and the intensity of ongoing glycosylation. At the breaker and/or turning stage, the processes of modification of the sugar moiety and depolymerization begin to prevail. At the red ripe/pink stage, the synthesis process is replaced by the degradation process, which is associated with the disappearance of AGPs with high molecular weights and the appearance of only single sugar residues with very low molecular weights. The occurrence of AGPs with low molecular weight (~30 kDa) may be used as a marker of the finalization of the ripening process in tomato fruits. All anatomical and morphological alterations in the cell wall confirm the presence of dependencies and connections between components of the cell wall network. We may presume that selected antibodies (JIM13, LM2, LM14) indicate very specific features of the fruit tissue at different stages of ripening; thus, AGP is a molecular and cytological marker of particular stages of the fruit ripening process.

1. Introduction

1.1. The cell wall in the fruit ripening process

Fruits are one of the main horticultural crops whose production is growing around the world every year. About 700 million tons of fruits are currently being produced worldwide. Tomato (*Solanum lycopersicum*) is an economically important fruit found as one of the most important crops globally valued at 124.6 billion US dollars annually and representing the largest sector of the fleshy fruit market (Osoria and Fernie, 2013; Skolik et al., 2019; Ling et al., 2021). Tomato fruit ripening is a complex biological process involving changes in the color, texture, and nutrient content (Hyodo et al., 2013; Wang and Seymour, 2022). These factors affect the quality and postharvest shelf life of tomato fruits, which has a direct impact on their economic value (Tucker et al., 2017; Jiang et al., 2019). For over 40 years, extensive research on various fruits has been done, where mostly tomato fruits have been used as a model organism to study the development and ripening processes (Hyodo et al., 2013; Feder et al., 2020), as these processes are controlled by the interaction between genetic and hormonal factors, and the general features of this ripening model appear to apply to many fruits (Osoria and Fernie, 2013; Tucker et al., 2017).

Generally, plant growth and development are important processes regulated and supported by the cell wall (CW) (Burton et al., 2010; Zhang et al., 2021). One of the important processes in fruit is ripening, which is associated with cell wall degradation. Degradation of the cell wall leads to reduced intercellular adhesion and depolymerization of polysaccharides. However, the spatial regulation and biochemical changes involved in cell wall transformation are not fully understood (Li et al., 2010; Tucker et al., 2017). It has been recognized that they are

* Corresponding author.
E-mail address: a.leszczuk@ipan.lublin.pl (A. Leszczuk).

https://doi.org/10.1016/j.scienta.2022.111718
Received 11 October 2022; Received in revised form 17 November 2022; Accepted 18 November 2022
Available online 26 November 2022

related to changes in cell wall properties resulting from modifications of polysaccharide components (Orfila et al., 2001). At the molecular level, the loss of carbohydrates, i.e. galactose and arabinose, seems to be the earliest detectable change (Tucker et al., 2017). However, the cell wall is composed not only of polysaccharides (Verhertbruggen et al., 2009). In the last few years, many studies have been performed to determine changes in proteins that occur in cell walls during fruit ripening. Moreover, there are reports that, during the ripening process, there are no major changes in the amount of the proteins in the cell wall, but they do change their structures and functions, for example, changing the activity of enzymes present in the cell wall (Ruiz-May and Rose, 2013; Shi et al., 2014).

1.2. Arabinogalactan proteins (AGPs) in plant development and fruit ripening

Arabinogalactan proteins (AGPs) are one of the most complex and diverse families of proteoglycans widely distributed in plants (Carpita et al., 2001; Fragkostefanakis et al., 2012; Peng et al., 2012; Tsumuraya et al., 2019). AGPs are found in all tissues, mainly in cell walls, plasma membranes (PMs), and intercellular spaces (Showalter, 2001; Lopez-Hernandez et al., 2020). There are reports that AGPs localized in cell walls act as modulators of cell expansion and differentiation, transducers of cell surface signals, and effectors of responses to environmental conditions and other organisms (Hromadová et al., 2021). The specific distribution of AGPs in the extracellular matrix allows formation of the cell wall-plasma membrane continuum, which may be essential to the external parts of the whole plant cell (Liu et al., 2015, Leszczuk et al., 2018a). AGPs are attached to the plasma membrane by glycosylphosphatidylinositol (GPI) in the C-terminal domain. The GPI anchor allows the transmission of information between the intracellular and extracellular space (Showalter, 2001). Therefore, the determination of the localization of AGPs at the level of tissues and cells in different plant organs may provide insight into their new functions. Also, AGPs are versatile in their biological roles, e.g. they exert an impact on cell division, cellular communication, programmed cell death, embryogenesis, plant-microbe interactions, plant growth, and reproductive processes (Tsumuraya et al., 2019).

AGPs belong to the family of cell wall hydroxyproline-rich proteoglycans (HRGPs) (Showalter, 2001). Their N-terminal domain is rich in proline/hydroxyproline, alanine, serine, and threonine (Showalter and Basu 2016). Protein moiety account for about 10% of the total molecular mass of the proteoglycan. About 90% of the molecules consist of arabinogalactan polysaccharides. As their name implies, AGPs are rich in arabinose, galactose, and glucuronic acid in some cases, along with other less-abundant sugars (Classen et al., 2000). AGP carbohydrates consist of β-(1→3)-galactan backbones that are replaced by side chains of (1→6)-linked β-galactosyl residues through O-6. The side chains have L-arabinose (L-Ara1) residues and other less-abundant sugars, such as D-glucouronic acid (GlcA), 4-O-methyl-glucuronic acid (4- Me-GlcA), L-fucose (L-Fuc), L-rhamnose (L-Rha), D-xylose (D-Xyl), D-mannose (Man), D-glucose (Glc), D-glucosamine (GlcN), and D-galacturonic acid (GalA). It has been recognized that AGPs serve biological functions through the presence of carbohydrate moiety. The polysaccharide chains appear to be attached to Hyp residues and possibly to Ser and Thr residues. In contrast, short arabinoses are joined to Hyp residues (Classen et al., 2000; Kitazawa et al., 2013; Showalter and Basu, 2016; Tsumuraya et al., 2019, Leszczuk et al., 2020a).

Research on AGPs conducted over the past three decades suggests that these proteins may affect the cell wall structure, which may influence fruit properties. It is known that AGPs undergo glycosylation and this molecular mechanism is well understood, but the effect of this process on the role of AGPs in the cell wall has currently been described in only a few experimental papers (Fragkostefanakis et al., 2012; Leszczuk et al., 2018b, 2020b). It is not clear whether AGP is connected with cell wall breakdown, which is unquestionably related to the process of fruit softening and ripening. Also, it is not specified how AGPs affect the processes of fruit development and ripening or whether these molecules are essential for these processes. In this paper, we report the molecular characterization of AGPs in tomato fruits collected at different, strictly defined stages of ripening, with focus on the occurring changes. Our research was based on '*in planta*' and '*ex planta*' studies, which provided a complete description of the alterations in AGPs. For this purpose, the AGP extraction with Yariv reagent, radial gel diffusion, immuno-dot blot assay, Western blotting, and ELISA were performed and the immunofluorescence technique imaged by CLSM was used. The assays are based on carefully tested antibodies that recognize the AGP carbohydrate moiety (Fig. 1).

2. Material and methods

2.1. Plant growth conditions and fruit characterization during development and ripening

Tomato plants (*Solanum lycopersicum* cv. 'Betalux') were grown in the greenhouse (Lublin, Poland). The tomato fruit at various stages of ripening was the object of study. Tomato fruit ripening can be divided into different stages by colour changes previously described by Nakatsuka et al. (1998): stage after development – 'mature green, GR' (1), pale-green colour on fruit surface – 'breaker, BR' (2), the first appearance of pink colour at blossom end – 'turning, TU' (3), red colour in two-thirds of fruit surface – 'pink, PINK' (4), the red colour on entire fruit surface – 'red ripe, RR' (5). The GR stage is considered to be the last stage of development, and in confirmation of this, we observed a lack of increase in fruit diameter at later stages. In the next stages, only the ripening and colour change of the fruit occurs, and the diameter of the fruit remains close to the last stage of development.

2.2. AGPs extraction with Yariv Reagent

AGPs from tomato fruit tissue were isolated by extraction protocol using Yariv reagent (β-GlcY, Biosupplies, Australia) according to Lamport (2013) and to our previous studies (Leszczuk et al., 2020c). Frozen, homogenized tissue was mixed with 2% (w/v) $CaCl_2$ at room temperatures (rt). After 3 h, tissue was centrifuged at 10 000 rpm at rt for 30 min. To supernatant was added 1 mg mL^{-1} Yariv reagent in 2% (w/v) $CaCl_2$ and left overnight at rt. The insoluble Yariv-AGP complex was collected after centrifugation at 2 000 rpm at rt for 10 min and mixed with sodium metabisulphite (Thermo Scientific, USA). Then the mixture was heated at 50°C until the red colour disappeared and transferred to dialysis tubing with a 12-kDa MW cut-off (32 mm flat width, Sigma, USA). The obtained dialysate was frozen in liquid nitrogen, lyophilized and then the product – AGPs was weight.

2.3. Radial gel diffusion assay

Radial gel diffusion was performed according to Holst and Clarke (1985), and Castilleux et al. (2020). After extraction, samples were dropped into wells in gel plate containing 0.002% (w/v) Yariv reagent (β-GlcY, Biosupplies), 1% (w/v) NaCl, 0.02% (w/v) sodium azide and 1% (w/v) agar. Samples were loaded in 40 µl per well and incubated for 48 h at rt. The relative reactivity of β-GlcY was quantified using gum arabic (Biosupplies) as the standard (positive control). The distilled water was used as a negative control. For quantitative analysis of reactivity of β-GlcY - AGPs concentration, the halo area around the wells was manually identified and counted with ImageJ 1.51 software (https://imagej.nih.gov/). The assay was performed in triplicate.

2.4. Immuno-dot-blot assay

The most common technique for the determination of the occurrence of AGP is an immunocytochemical reaction using specific antibodies

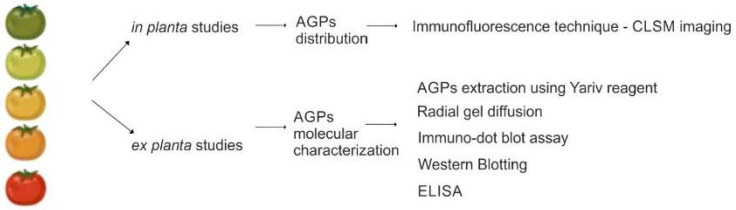

Fig. 1. Representative of the microscopic and molecular approaches including *ex situ* and *ex situ* investigations.

directed against the carbohydrate epitopes of AGPs. The primary monoclonal antibodies used were obtained from Plant Probes, Centre of Plant Sciences (University of Leeds, UK), and Kerafast (USA) (Table 1). For the second validation of the content of AGPs in supernatant obtained, immune-dot-blot assay with monoclonal antibodies against AGPs epitopes was carried out. Each sample was dotted onto a nitrocellulose membrane and subsequently blocked with 5% (w/v) BSA (Sigma, USA) in PBS (Sigma, USA). After washing with TBST (7.6 pH), samples were incubated with primary antibodies recognized specific AGPs epitopes diluted 1:500 in 2.5% (w/v) BSA in PBS for 2 h at rt. After three washes with TBST, samples were incubated with secondary anti-rat antibodies conjugated with alkaline phosphatase diluted 1:1000 in 2.5% (w/v) BSA in PBS for 2 h at rt. The optimal dilution was determined according to the antibody manufacturer. After immunochemical reactions, the membrane was washed in TBST and AP buffer, finally AGPs were detected with AP substrates: 5-bromo-4-chloro-3-indolyl-phosphate (Sigma) in water (4 mg/mL) (BCiP) and nitro-blue tetrazolium (NBT) (Sigma, USA) in water and N, N-dimethylformamide (DMF) (Thermo Scientific, USA) (9 mg/0.3 mL water/ 0.7 mL DMF) in the dark. All analyses of samples were performed in triplicate. In turn, the heat map analysis in which color intensity is proportional to a numerical value was prepared using the Image Lab Software version 6.1 (Bio-Rad, USA).

2.5. SDS-PAGE gel electrophoresis and protein detection with Western blotting

Total proteins extraction were performed using Laemmli buffer (1970) composed of 65 Mm Tris-HCl, pH 6.8, 2% (w/v) SDS, 2 mM EDTA, 1 mM PMSF, 700 mM β-mercaptoethanol and 1:10 protease inhibitor (Sigma, USA). Then protein sample quantification was performed with a standard Bradford assay. SDS-PAGE was used for protein separation with a mixture of 12.5% resolving gel and 4% stacking gel. After electrophoresis proteins were electroblotted onto a PVDF Transfer Membrane with a 0.2 μm pore size (Thermo Scientific, USA). Immunoblotting was performed on a mini-rocker shaker. After wet transfer, the membrane was washed in TBST. Membranes were blocked with 5% (w/v) BSA in PBS for 1 h at rt and incubated with primary antibodies at a concentration of 1:500 for 2 h at rt. After three washes with TBST, the membranes were incubated with secondary antibodies conjugated with alkaline phosphatase at a concentration of 1:1000 for 2 h at rt. The optimal dilution was determined according to the antibody manufacturer. The membrane was washed in TBST and next, in AP buffer. Visualization of bands was carried out with BCiP (Sigma, USA) in water (4 mg/mL) and NBT (Sigma, USA) in water and DMF (Thermo Scientific, USA) (9 mg/0.3 mL water/ 0.7 mL DMF) in the dark. Gel after Coomassie Blue staining and membranes visualization was performed using GelDoc Go Imaging System (Bio-Rad, USA). The results were analyzed qualitatively on the basis of the band thickness, width, and colour depth. For quantification of molecular mass, Pierce™ Prestained Protein MW Marker was used (Thermo Scientific, USA). The quantitative analysis of protein bands was performed using the Image Lab Software version 6.1 (Bio-Rad, USA). Three independent experiments were performed.

Table 1
Representative of the used monoclonal antibodies against the carbohydrate epitopes of AGPs.

mAb	EPITOPES	REFs.
JIM13	βGlcA(1→3)-αGalA(1→2)Rha	Knox et al. (1991), Yates et al. (1996)
JIM15	D-GlcA; GlcA-β(1-O-Me)	Yates et al. (1996)
LM2	β-D-GlcA units with terminal β-GlcA in AGP	Smallwood et al. (1996), Yates et al. (1996)
LM14	binds to arabinose- and galactose-enriched carbohydrate chains (AG type II)	Moller et al. (2008)

2.6. Enzyme-linked immunosorbent assay (ELISA)

According to Pfeifer et al. (2020), the binding of the different monoclonal AGP-antibodies JIM13, JIM15, LM2, and LM14 was investigated in an indirect ELISA. First, the 96-well plates (Nunc MaxiSorp™ flat-bottom, ThermoFisher Scientific, Denmark) were coated with different concentrations of AGP (0, 25, 50, 100 μg/mL in distilled water, 100 μl per well) at 37.5°C with open cover for 3 days. Then, the plates were washed three times with PBS (pH 7.4) with 0.05% Tween 20 (Sigma) and blocked with 0.1% (w/v) BSA in PBS (200 μL per well, 1 h at 37.5°C). The blocked plates were washed again with PBS. Next 100 μl of the different antibodies (JIM and LM series diluted 1:20) was added to each well and plates were incubated for 1 h at 37.5°C. Next, the plates were washed three times with the same washing buffer as described above. The secondary antibody (Anti-Rat-IgG conjugated with alkaline phosphatase, Sigma-Aldrich, USA) was pipetted in a dilution of 1:500 in PBS. After incubation and three-times washing steps, color was developed by addition of 1-Step p-nitrophenyl phosphate disodium salt - PNPP (100 μL well−1, ThermoFisher Scientific, USA). According to Thermo Scientific instructions, the reaction water-yellow product absorbs light at 405 nm. After incubation at room temperature for 5–20 min, the reaction was stopped with 2 N NaOH (50 μL well−1). The absorbance of each well was measured in an ELISA reader (MPP-96 Photometer, Biosan) and analyzed with Quant Assay Software. Samples were tested in triplicate.

2.7. Material preparation for immunocytochemistry

Overall, the microscopic analyses were performed according to our previous papers (Leszczuk et al., 2019). For immunolabelling protocols, the cube-shaped fruit tissue was fixed in 2% (w/v) paraformaldehyde (Sigma, USA) and 2.5% (w/v) glutaraldehyde (Sigma, USA) dissolved in PBS (pH 7.4, 0.15 M). The tissues were fixed under vacuum seven times for 10 min each and then overnight and then the material was dehydrated in graded ethanol series (from 30%, 50%, 70%, 90%, and 96% for 15 min to 99.8% for 30 min twice). For embedding, the LR White resin was used, and the polymerization was performed according to the manufacturer's instructions (Sigma Aldrich, USA). For CLSM imaging, 1 μm-thick sections were cut using an ultramicrotome (PowerTome XL, RMC Boeckeler, USA) equipped with a glass knife.

2.8. Immunofluorescence labelling technique for confocal laser scanning microscope (CLSM)

Thick sections (1 μm) mounted on poly-L-lysine coated slides (Sigma, USA) and circled with a liquid blocker PAP Pen (Daido Sangyo, Tokyo, Japan), were washed in PBS and pre-incubated with 1% (w/v) BSA in PBS at rt to block non-specific binding sites. Then, the samples were incubated with the primary rat antibody diluted 1:50 in 0.1% (w/v) BSA in PBS overnight at 4°C. Prior to the visualization of AGPs, the samples were incubated with sets of specific monoclonal antibodies directed to glycan moieties of AGPs. After washing with three changes of PBS, incubation with the secondary antibody, goat anti-rat IgM (heavy chain) cross – Alexa Fluor 488 (ThermoFisher Scientific) diluted 1:200 in 0.1% (w/v) BSA in PBS overnight at 4°C was performed. After the labeling procedure, the sections were washed with PBS and stained with Calcofluor White. Imaging of the immunofluorescence method was performed using an Olympus BX51 CLSM microscope equipped with corresponding software FluoView v. 5.0. (Olympus Corporation, Tokyo, Japan). Control reactions were carried out by omitting the primary antibody. All photographs and figures were edited using the CorelDrawX6 graphics program.

2.9. Statistical analysis

The data were statistically analyzed using Statistica v.13 (TIBCO Software Inc. USA). For comparisons of the mean values, an analysis of variance (one-way ANOVA) followed by post hoc Tukey's honestly significant difference (HSD) test was used. For all analyses, the significance level was estimated at $p < 0.05$.

3. Results

3.1. Determination of changes in AGP content during ripening progress - Isolation of AGPs using Yariv reagent

AGPs from tomato fruit tissue were isolated using the Yariv Reagent extraction technique (Yariv et al., 1962; Kitazawa et al., 2013; Lamport, 2013), which allows estimating AGP content in fruit tissue. The results showed the AGP content of 0.91 mg/g at the mature green stage, 0.98 mg/g at the breaker stage, 3.11 mg/g at the turning stage, 1.12 mg/g at the pink stage, and 1.18 mg/g at the red ripe stage (Fig. 2A). The results indicated the highest amount of AGPs at the turning stage; however, it declined during the consecutive ripening stages. The results of the radial gel diffusion assay confirmed the presence of AGPs in the extracted material. Moreover, the method highlighted differences in the AGP concentration in the tomato fruits at each stage during the ripening process. The results also showed a significantly higher concentration of AGPs extracted using Yariv reagent at the turning stage than at the mature green stage. The following values were determined: 0.13 ± 0.02 mg/mL at the mature green stage, 0.48 ± 0.09 mg/mL at the breaker stage, 0.84 ± 0.05 mg/mL at the turning stage, 0.71 ± 0.05 mg/mL at the pink stage, and 0.45 ± 0.1 mg/mL at the red ripe stage (Fig. 2B). The results of the radial gel diffusion demonstrated a decrease in the AGP concentration at the pink and red ripe stages, which confirms that the increase in the intensity of degradation processes is a typical event at the advanced stages of ripening.

3.2. Changes in the content of specific AGP epitopes – dot blot assay, ELISA test

The molecular traits of the AGPs from fruits at different stages of ripening were evaluated in several steps. A dot blot assay was performed to determine the appropriate starting concentration of primary antibody for Western blotting and to visualize an antibody that would reveal different types of AGP epitopes in the tested samples. Afterward, an immunoenzymatic test (ELISA) was conducted to obtain a direct proof of a proper use of the antibody and to visualize changes in the AGP participation at the different fruit ripening stages. The proportions of molecular weights in the protein mixture in the tested samples were determined with the use of the Western blotting method.

In order to quickly check the presence of specific epitopes of AGPs, an immuno-dot-blot assay with monoclonal antibodies against AGP epitopes was performed. We used four antibodies against AGP epitopes (JIM13, JIM15, LM2, and LM14) (Fig. 3). The analysis of the dot-blot membranes revealed that the concentrations of the tested samples were properly chosen. The simple heat map provides information that almost every antibody used, excluding JIM15, had high efficiency in AGP detection in the tested samples, which confirmed the correctness of the concentrations used, as presented in Fig. 3. The best visualization effect of AGPs in all extracts was achieved by the LM2 antibody in every sample, which suggested that the epitope with β-linked glucuronic acid in the polysaccharide moiety was present at every stage of the fruit ripening process. Interestingly, the highest amount of JIM13, LM2, and LM14 epitope were detected at the BR stage and gradually decreased with the progress of the ripening process.

Since there were differences between samples representing the different stages, the ELISA assay was used to determine the amount of the epitope in detail. The ELISA test was performed using the same antibodies (JIM13, JIM15, LM2, and LM14) for better visualization of differences in the occurrence of the epitopes between the particular stages of fruit ripening. The results shown in Fig. 4 indicate the lowest differences in the amount of the JIM13 epitope in all ripening stages,

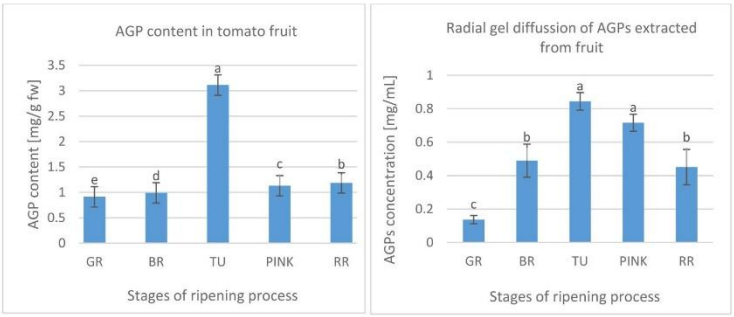

Fig. 2. Determination of changes in AGPs content during ripening process: Isolation of AGPs using Yariv reagent (A), Radial gel diffusion of AGPs (B). Abbreviations: GR – mature green stage, BR – breaker stage, TU – turning stage, PINK – pink stage, RR – red ripe stage. For comparisons of the mean values, an analysis of variance (one-way ANOVA) followed by post hoc Tukey's honestly significant difference (HSD) test was used, with the significance level at $p < 0.05$.

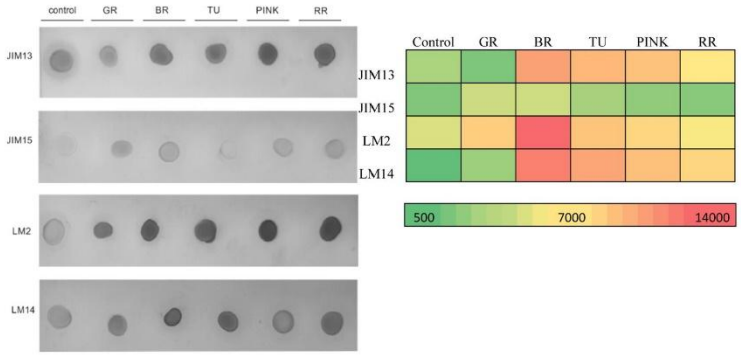

Fig. 3. Dot blot with heat map analysis of AGPs extracted from tomato fruit at examined stages of the ripening process. Abbreviations: GR – mature green stage, BR – breaker stage, TU – turning stage, PINK – pink stage, RR – red ripe stage.

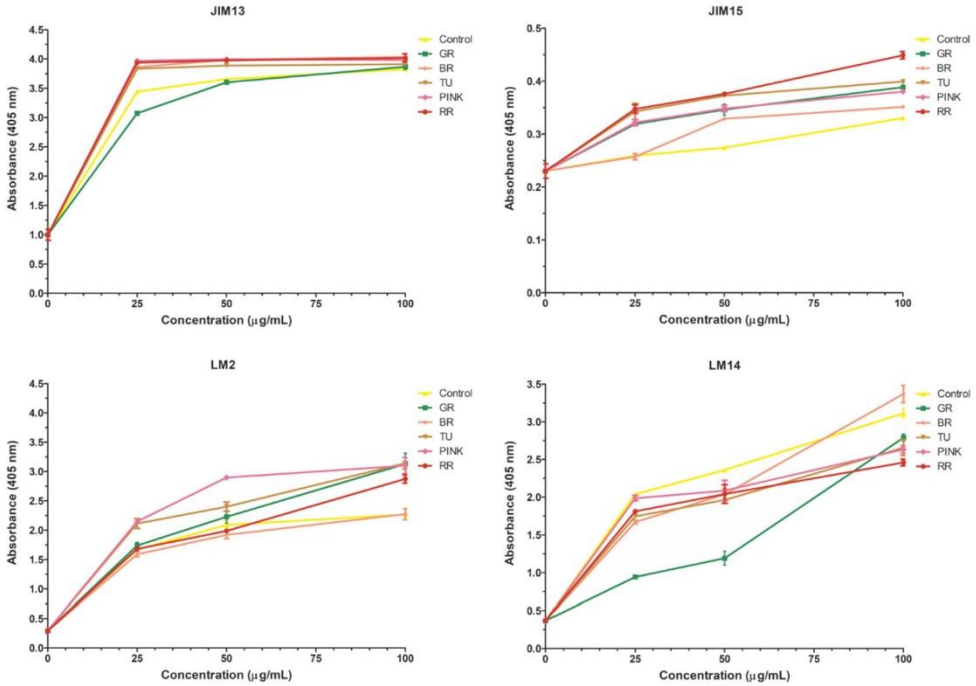

Fig. 4. ELISA test of AGPs extracted from tomato fruit at examined stages of the ripening process. Abbreviations: GR – mature green stage, BR – breaker stage, TU – turning stage, PINK – pink stage, RR – red ripe stage.

with the highest expression of this epitope in the TU, PINK, and RR stages. The lowest absorbance value was observed after using the JIM15 antibody, which correlates with the dot-blot analysis. The reaction with the JIM15 antibody was minimal, i.e. at the background level. The biggest changes in the exposure of the epitopes were observed after the incubation of the LM2 and LM14 antibodies with the tested samples, where the most significant differences were noticed in the LM14 epitope. The use of the LM14 antibody allowed observing increased absorbance during the stages of ripening, which is probably correlated with the release of type II AG from degraded carbohydrate chains of AGPs. The LM2 epitope was characterized by the highest exposure in the PINK stage of ripening, whereas the lowest exposure was observed at the BR stage. The most interesting results were obtained in the exposures of the LM14 epitope, which were the lowest at the GR stage of the ripening process and the highest at the BR stage

3.3. Determination of AGPs molecular mass

The Western blotting analyses estimated the differences in the molecular weights occurring during the ripening stages to identify the different AGP epitopes (Fig. 5). As in the previous analyses, the lowest expression was revealed for the epitope labeled with the JIM15 antibody. Small bands at ~30 kDa were observed only at the PINK and RR stages, where the expression in the case of the RR sample was stronger than in the PINK one. Low molecular weight bands (~30 kDa) were observed in all the epitope variants in the PINK and RR stages. Hence, these low molecular weight bands (Fig. 5, marked in red) should be considered a marker of the final advanced stage of the ripening process. The JIM13 epitope-labeled AGP was characterized by the highest differences in the molecular weights at each ripening stage. The JIM13 epitope labeling low and medium molecular weights (60–20 kDa) was present at all ripening stages; the lowest and the highest relative AGP level was determined at the BR and RR stages, respectively. Different results were obtained in the case of LM2, where the highest relative AGP level was noted for high molecular weights (120–60 kDa) and the lowest level was recorded at the TU stage. The LM14 epitope was characterized by AGP with medium molecular weights (60–25 kDa), and the strongest expression signal was observed at the BR and TU stages, whereas the weakest signal was noticed in the PINK and RR samples. Therefore, the LM14 antibody can be considered the most specific, as a decrease in the content and molecular weight of AGPs was observed as the ripening process progressed. Overall, the Western blotting analysis revealed heterogeneity of AGPs characterized by different molecular weights. The relative level of AGPs with the highest molecular weights was found to decline with the progress of ripening. At two stages, i.e. BR and TU, AGPs with 120–60 kDa and 60–25 kDa molecular weights

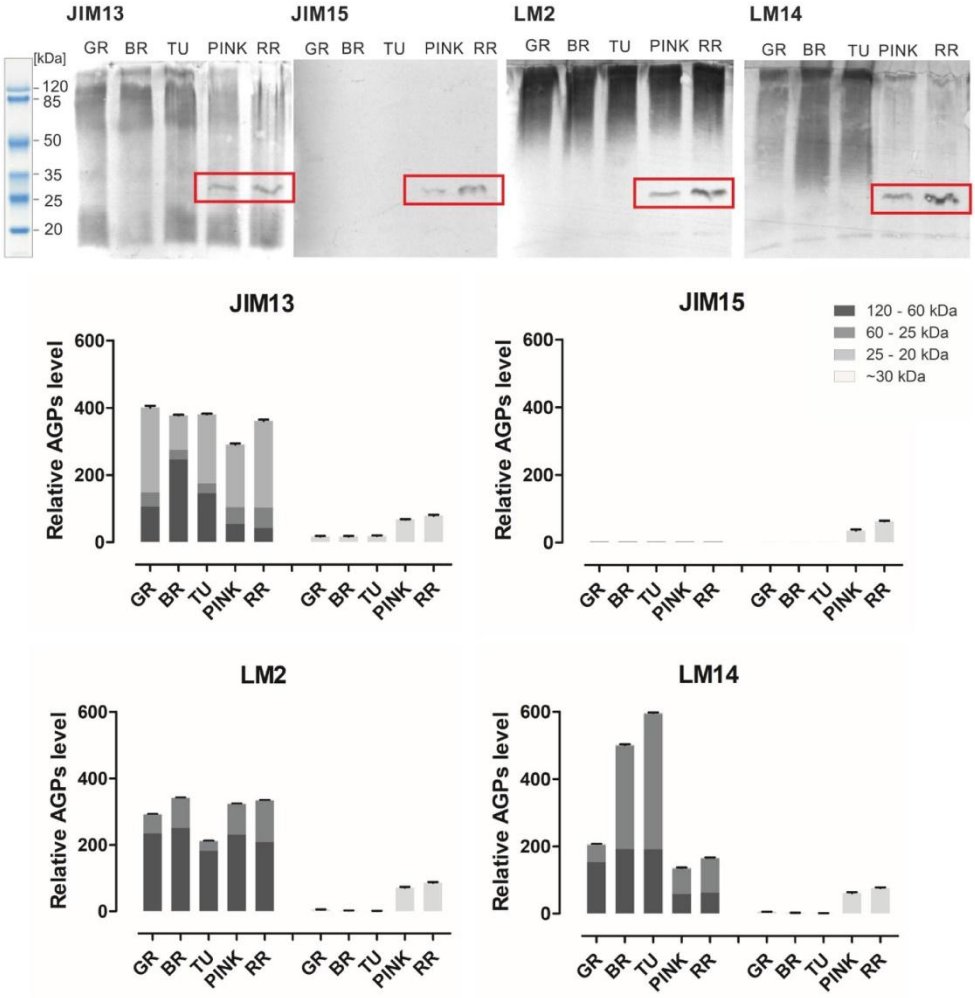

Fig. 5. SDS-PAGE – Western blotting of AGPs extracted from tomato fruit at examined stages of ripening process with analyses of molecular mass of AGPs. Specific bands around 30 kDa are marked in red. Abbreviations: GR – mature green stage, BR – breaker stage, TU – turning stage, PINK – pink stage, RR – red ripe stage.

predominated. At the PINK and RR stages, the sample contained 25–20 kDa AGPs (JIM13 epitope). Additionally, similarity between the relative AGP levels obtained by Western blotting using LM14 and the measurement of AGP content with the Yariv extraction protocol was noticeable.

3.4. Changes in AGPs distribution in situ at the cellular level

The *in planta* studies on AGPs were performed using the immunolabeling technique, which allowed showing alterations in the analyzed epitopes of AGPs. Figs. 6 and 7 show microscopic investigations of the AGP distribution in the epidermal/hypodermal layers and parenchymal tissue inside the fruit, respectively. Firstly, the microscopic observations demonstrated the anatomical changes in tissues at the cellular level. With the progress of the ripening process, the cell walls underwent modifications, and numerous detached cell wall compartments were located inside the cell. These changes were correlated with the well-known typical alterations in fruit cells as a result of the ongoing ripening process. Similar findings were obtained using the same antibodies as in previous analyses. AGP epitopes recognized by JIM13 and LM2 were present in the fruit at the GR and BR stages mainly in the periphery of the cell wall, in a close area to the plasma membrane. At the subsequent stages, the AGP epitopes were situated in the cellular remains, in the neighborhood of the cell wall-plasma membrane continuum. Also, the *in situ* analyses showed no JIM15 epitopes, even in the degraded cell wall of the fruit at the RR stage. In turn, after the immunocytochemical reaction using LM14, the strongest signal of fluorescence was visible in the fruit at the PINK and RR stages. To verify the correctness of the analysis, a control was performed without the step of incubation with primary antibodies, which showed no reaction (Fig. 6).

The tissue level analyses revealed that, at the initiation of the

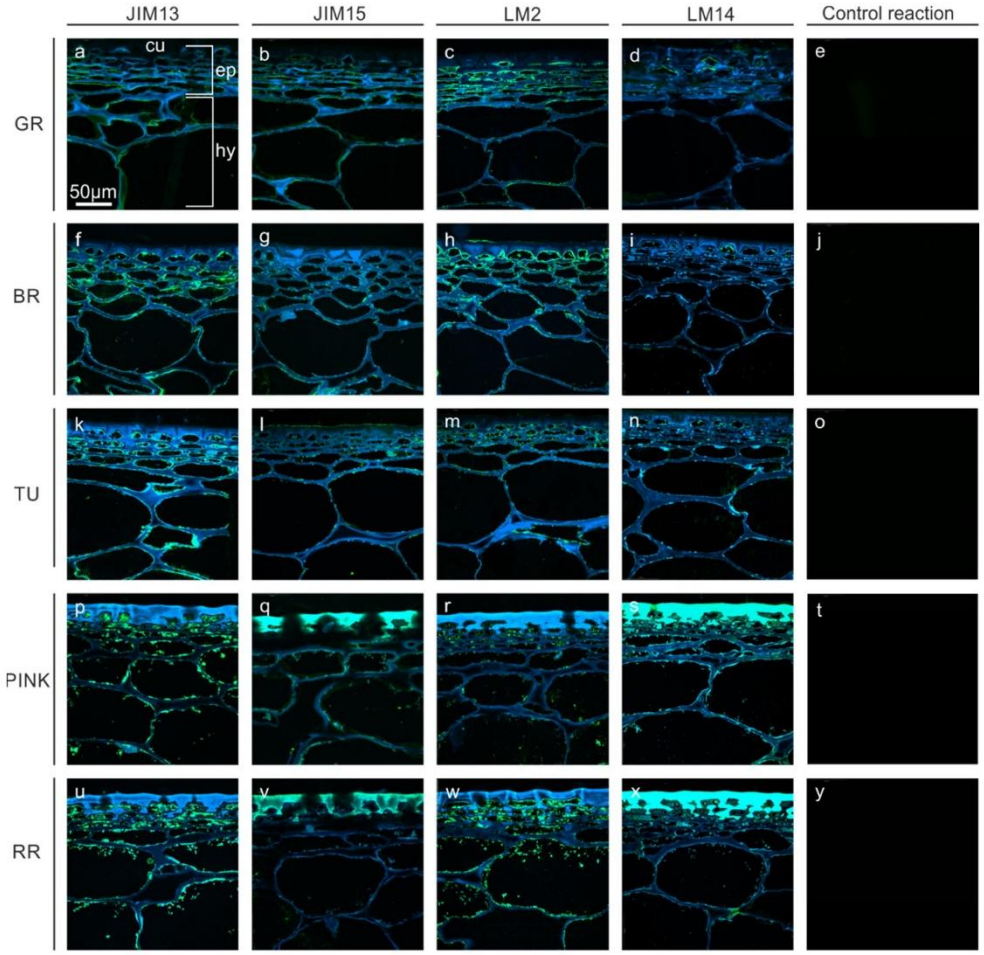

Fig. 6. Arabinogalactan proteins distribution in epidermal and hypodermal layers during the progress of the ripening process. AGPs localization in fruit at GR stage (a-e), BR stage (f-j), TU stage (k-o), PINK stage (p-t), and RR stage (u-y). Control reactions (e, j, o, t, y). Bar: 50 µm. Abbreviations: GR – mature green stage, BR – breaker stage, TU – turning stage, PINK – pink stage, RR – red ripe stage, cu – cuticle, ep – epidermal layer, hy – hypodermal layer. Immunofluorescence technique with Alexa Fluor-488 (green staining) and counterstaining using Calcofluor White (blue color).

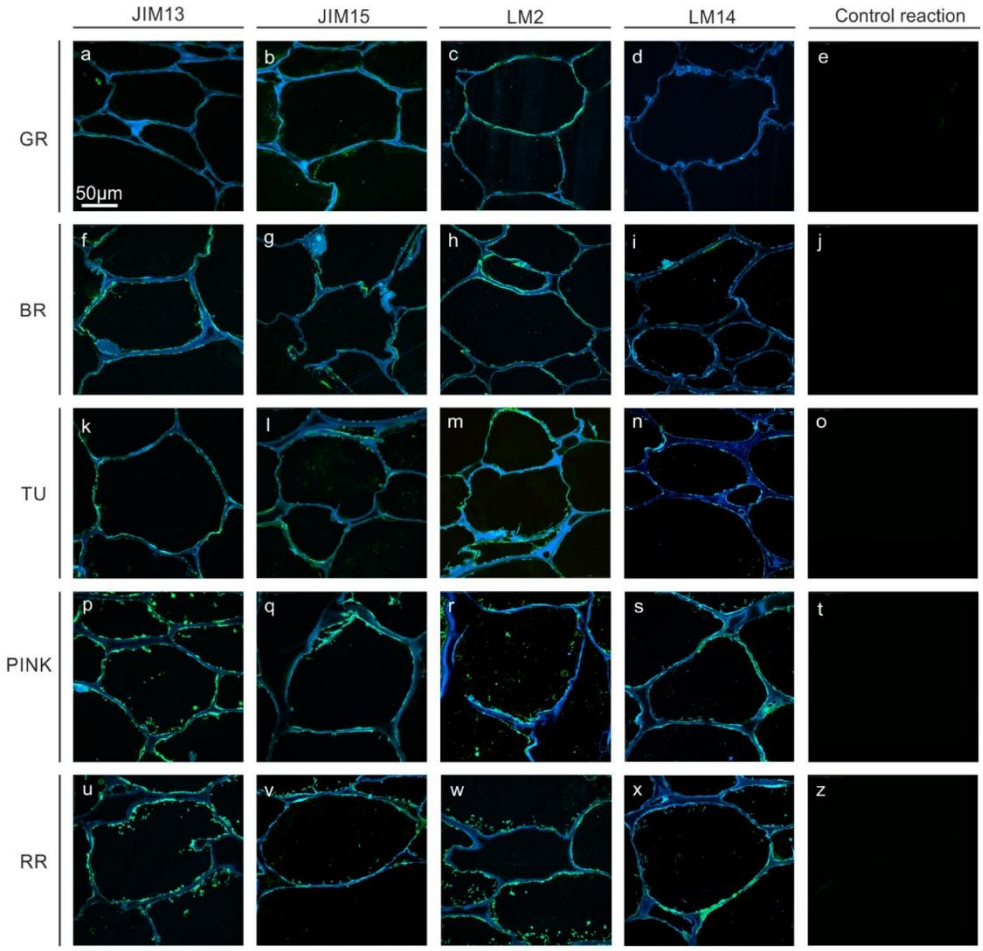

Fig. 7. Arabinogalactan proteins distribution in the parenchyma layer during the progress of the ripening process. AGPs localization in fruit at GR stage (a-e), BR stage (f-j), TU stage (k-o), PINK stage (p-t), and RR stage (u-z). Control reactions (e, j, o, t, z). Bar: 50 µm. Abbreviations: GR – mature green stage, BR – breaker stage, TU – turning stage, PINK – pink stage, RR – red ripe stage.

ripening process, AGPs were distributed mainly in the external parts of the fruit, i.e. the hypodermal layers, and were more visible in the parenchymal tissue with the progress of the process. The observations of the immunocytochemical reactions in parenchymal tissue sections showed that labeled epitopes were also present in the fruit at the PINK and RR stage, but not in the vicinity of the cell wall but in the degraded parts of the cell (Fig. 7). The results showing the relationship between the molecular properties of AGPs and the cellular changes in fruits during the ripening process are highly compatible with earlier results.

4. Discussion

It is well-known that, on the nanoscale, the ripening process is closely related to the association of cell wall components and covalent linkages among these components (Wang and Seymour, 2022). Alterations in polysaccharide domains, pectin depolymerization, and solubilization are closely linked to fruit softening, which is directly related to the texture of ripe fruit. Also, linkages of pectin, cellulose, and hemicellulose are fundamental for general mechanical features of fruits during the ripening process (Posé et al., 2019). On the other hand, AGPs are part of a strictly described model of a cell wall structure called the APAP1 complex (Tan et al., 2013). The authors of this theory suggest that, although AGP does not play a quantitatively significant role, its ability to bind to hemicelluloses and pectins has an impact on the final form of linkages in the plant matrix (Tan et al., 2013; Hijazi et al., 2014). For the same reason, cell wall remodeling during the ripening process is not only an outcome of changes in major cell wall constituents. The assembly of the cell wall is dependent on the interactions between all parts of the extracellular matrix (Tan et al., 2013; Hijazi et al., 2014). In our earlier studies, we focused mainly on the distribution of AGPs in fruit tissue and on creating the spatio-temporal pattern of their specific localization in apple fruits during ripening and senescence processes

(Leszczuk et al., 2018a, 2018b).

Previous studies have already shown that AGPs are changing with the progressing physiological processes in the fruit. The aim of the current research was to determine the molecular characteristics of AGP outside the fruit cell. It turns out that our current investigations are compatible with previous reports. Due to the presence of carbohydrate chains, AGPs should be considered as part of the polysaccharide network, not as a typical protein. The occurrence of a sugar moiety causes AGP to reside in the cell wall much longer than proteins during the ripening process, and changes in its molecular characteristics are the result of changes in their carbohydrate chains. The measurement of the AGP content using Yariv reagent showed the presence of AGPs during ripening at a level of approximately 3.11 mg/g at the turning stage. As the process progressed, the AGP content declined to around 1.18 mg/g at the red ripe stage. We may assume that this result is also correlated with the binding capacity of Yariv reagent. The appearance of the AGP-Yariv complex requires the presence of β-1,3-galactan chains, which are longer than five residues (Kitazawa et al., 2013). Disruption of the cell wall during the ripening process is inextricably linked with the destruction of long carbohydrate chains, thus we assume that the presence of only fully glycosylated AGPs can be assessed using this method. In the same way, the lower content of AGPs at the GR stage than at the BR stage is connected with the still ongoing synthesis and glycosylation process of AGPs. Any modifications that result in shortening of sugar chains affect the determination of the AGP content, and, the data on the estimation of the AGP amount by extraction with Yariv reagent underlined the ongoing degradation of the AGP molecule.

In line with the biochemical way of AGP content quantification are the results obtained with the molecular tools. Both Western blotting and the ELISA method revealed the decreasing molecular weight of AGPs during the ripening process. Generally, all immunocytochemical methods, both *in situ* and *ex situ*, revealed that the AGP modifications during the ripening process are correlated with the level of AGP molecule glycosylation. A similar observation on cell expansion events in grapes was described by Moore and coworkers (Moore et al., 2014). In these experiments, the abundance of AGP epitopes (JIM8, JIM13, and LM14) gradually increased throughout the grape ripening process as a ripening response. At the time of reaching full maturity, the decreasing signal represented the release of AGP molecules into the apoplast of the grapes. The authors assumed that the observed events are an excellent biomarker of grape ripening (Moore et al., 2014). Our experimental investigations are in agreement with the report on grapes. Moreover, the use of the four antibodies recognizing different AGP epitopes helped to reveal specific features common for the PINK and RR stages. Labeling with JIM15 and LM14 shows a strong fluorescence signal in the epidermal cells at the PINK and RR stage. We may assume that mentioned antibodies recognize specific AGPs which are expressed in the epidermal cells during ripening. Based on the analysis of the epitopes, we may conclude that sugar residues and arabinose- and galactose-enriched carbohydrate chains rather than long AG chains are mainly present in the fruit tissue at the end of the ripening process. As shown by the results of the quick check dot-blot and ELISA test, the JIM13 antibody can be used to determine the occurrence of AGP epitopes as a marker of AGPs in analyzed samples. The LM14 antibody, on the other hand, can be used as a marker of the ripening process. The occurrence of AGPs with low molecular weight (~30 kDa) may be regarded as a marker of the finalization of the ripening process in tomato fruits. Also, the JIM13 antibody can be used to determine the presence or absence of AGPs in plant tissue, as it shows the presence of the most frequent AGPs epitope with a molecular weight range of 120–20 kDa.

In summary, our results and conclusions have been based on glycome profiling, immunoprinting and epitope mapping, and the use of specific antibodies, which recognize carbohydrate chains of AGPs (Knox et al., 1991; Yates et al., 1996, Smallwood et al., 1996; Moller et al., 2008). We provide evidence that mentioned epitopes are a useful marker of particular stages of the fruit ripening process. Unfortunately, in AGPs studies, we should take into account that commercial anty-AGP antibodies can bind to glycan residues other than AGPs, i.a. AG type II. However, currently, only antibodies are specific and available tools for working on AGP. Moreover, this work highlights a lack of information and no research opportunities, indicating as yet undetermined approaches for the understanding of AGPs.

5. Conclusion

The results of our studies allowed formulation of three key conclusions:

(1) The high content and the occurrence of the AGP molecule with high molecular weight are related to cell wall conditions, such as high intensity of synthesis of particular carbohydrates and glycosylation. At the breaker and/or turning stage, the processes of modification of the sugar moiety and depolymerization begin to prevail. This is the cause of the appearance of AGPs with much lower molecular weights. At the red ripe/pink stage, the synthesis process is replaced by the degradation process, which is associated with the disappearance of AGPs with high molecular weights and the appearance of only fragments of carbohydrate parts and/or single sugar residues with very low molecular weights.
(2) AGPs as part of the polysaccharide cell wall network are involved in the ripening process. All anatomical and morphological alternations of the cell wall confirm the presence of dependencies and connections between components, which are then visible at the level of the whole tissue.
(3) All investigations presented in this study are based on the use of specific, commercial, and easily available antibodies. Given their results, we may presume that selected antibodies indicate very specific features of the fruit tissue at different stages of ripening. In addition, the Yariv reagent yields a fruit material exhibiting repeatable and specific features that are characteristic of each stage of the process. Thus, we assume that AGP is a molecular and cytological marker of particular stages of the fruit ripening process.

CRediT authorship contribution statement

Nataliia Kutyrieva-Nowak: Investigation, Data curation, Formal analysis, Writing – original draft. **Agata Leszczuk:** Investigation, Formal analysis, Supervision. **Adrian Zając:** Formal analysis. **Panagiotis Kalaitzis:** Writing – review & editing. **Artur Zdunek:** Writing – review & editing.

Declaration of Competing Interest

Authors have no competing interests to declare.

Data Availability

Data will be made available on request.

Acknowledgements

The authors gratefully acknowledge the financial support for this research by National Science Center Poland (SONATA16, 2020/39/D/NZ9/00232).

References

Burton, R.A., Gidley, M.J., Fincher, G.B., 2010. Heterogeneity in the chemistry, structure and function of plant cell walls. Nat. Chem. Biol. 6, 724–731.

Carpita, N.C, Tierney, M., Campbell, M., 2001. Molecular biology of the plant cell wall: searching for the genes that define structure, architecture and dynamics. Plant Mol. Biol. 47, 1–5.
Castilleux, R., Ropitaux, M., Mauasfi, Y., Bernard, S., Vicré-Gibouin, M., Driouich, A., Proper, Z., 2020. Contributions to arabinogalactan protein analysis. The Plant Cell Wall. Methods in Molecular Biology. Humana, New York, NY, p. 2149.
Classen, B., Witthohn, K., Blaschek, W., 2000. Characterization of an arabinogalactan-protein isolated from pressed juice of Echinacea purpurea by precipitation with the b-glucosyl Yariv reagent. Carbohydr. Res. 327, 497–504.
Feder, A., Jensen, S., Wang, A., Courtney, L., Middleton, L., Van Eck, J., Liu, Y., Giovannoni, J.J., 2020. Tomato fruit as a model for tissue-specific gene silencing in crop plants. Hortic. Res. 7, 142.
Fragkostefanakis, S., Dandachi, F, Kalaitzis, P., 2012. Expression of arabinogalactan proteins during tomato fruit ripening and in response to mechanical wounding, hypoxia and anoxia. Plant Physiol. Biochem. 52, 112–118.
Hijazi, M., Velasquez, S.M., Jamet, E., Estevez, J.M., Albenne, C., 2014. An update on post-translational modifications of hydroxyproline-rich glycoproteins: toward a model highlighting their contribution to plant cell wall architecture. Front. Plant Sci. 5 (395), 1–10.
Holst, G.J., Clarke, A.E., 1985. Quantification of arabinogalactan protein in plant extracts by single radial gel diffusion. Anal. Biochem. 148, 446–450.
Hromadová, D., Soukup, A., Tylová, E., 2021. Arabinogalactan proteins in plant roots – an update on possible functions. Front. Plant Sci. 12 (674010), 1–15.
Hyodo, H., Terao, A., Furukawa, J., Sakamoto, N., Yurimoto, H., Satoh, S., Iwai, H., 2013. Tissue specific localization of pecti Ca^{2+} cross linkages and pectin methyl esterification during fruit ripening in tomato (*Solanum lycopersicum*). PLoS One 8, 1–10.
Jiang, F., Lopez, A., Jeon, S., de Freitas, T., Yu, Q., Wu, Z., Labavitch, J., Tian, S., Powell, A., Mitcham, E., 2019. Disassembly of the fruit cell wall by the ripening-associated polygalacturonase and expansin influences tomato cracking. Hortic. Res. 6, 17.
Kitazawa, K., Tryfona, T., Yoshimi, Y., Hayashi, Y., Kawauchi, S., Antonov, L., Tanaka, H., Takahashi, T., Kaneko, S., Dupree, P., Tsumuraya, Y., Kotake, T., 2013. β Galactosyl Yariv reagent binds to the β 1,3 galactan of arabinogalactan proteins. Plant Physiol. 161, 1117–1126.
Knox, J.P., Linstead, P.J., Peart, J., Cooper, C., Roberts, K., 1991. Developmentally regulated epitopes of cell surface arabinogalactan proteins and their relation to root tissue pattern formation. Plant J. 1, 317–326.
Laemmli, U.K., 1970. Cleavage of structural proteins during the assembly of the head of bacteriophage T4. Nature 227, 680–685.
Lamport, D.T.A., 2013. Preparation of arabinogalactan glycoproteins from plant tissue. Bio-Protoc. 3 (19), 1–5.
Leszczuk, A., Chylińska, M., Zięba, E., Skrzypek, T., Szczuka, E., Zdunek, A., 2018a. Structural network of arabinogalactan proteins (AGPs) and pectins in apple fruit during ripening and senescence processes. Plant Sci. 275, 36–48.
Leszczuk, A., Szczuka, E., Wydrych, J., Zdunek, A., 2018b. Changes in arabinogalactan proteins (AGPs) distribution in apple (Malus x domestica) fruit during senescence. Postharvest Biol. Technol. 138, 99–106.
Leszczuk, A., Pieczywek, P.M., Gryta, A., Frąc, M., Zdunek, A., 2019. Immunocytochemical studies on the distribution of arabinogalactan proteins (AGPs) as a response to fungal infection in Malus x domestica fruit. Sci. Rep. 9 (17428), 1–14.
Leszczuk, A., Cybulska, J., Skrzypek, T., Zdunek, A., 2020a. Properties of arabinogalactan proteins (AGPs) in apple (Malus x domestica) fruit at different stages of ripening. Biology 9, 225.
Leszczuk, A., Kalaitzis, P., Blazakis, K.N., Zdunek, A., 2020b. The role of arabinogalactan proteins (AGPs) in fruit ripening – a review. Hortic. Res. 7, 176.
Leszczuk, A., Zając, A., Kurzyna-Szklarek, M., Cybulska, J., Zdunek, A., 2020c. Investigations of changes in the arabinogalactan proteins (AGPs) structure, size and composition during the fruit ripening process. Sci. Rep. 10, 20621.
Li, X., Xu, C., Korban, S.S., Chen, K.S., 2010. Regulatory mechanisms of textural changes in ripening fruits. Crit. Rev. Plant Sci. 29, 222–243.
Liu, Z., Persson, S., Sánchez-Rodríguez, C., 2015. At the border: the plasma membrane–cell wall continuum. J. Exp. Bot. 6, 1553–1563.
Ling, Q., Sadali, N.M., Soufi, Z., Zhou, Y., Huang, B., Zeng, Y., Rodriguez Concepcion, M., Jarvis, R.P., 2021. The chloroplast-associated protein degradation pathway controls chromoplast development and fruit ripening in tomato. Nat. Plants 7, 655–666.
Lopez-Hernandez, F., Tryfona, T., Rizza, A., Yu, X., Harris, M., Webb, A., Kotake, T., Dupree, P., 2020. Calcium binding by arabinogalactan polysaccharides is important for normal plant development. Plant Cell 32, 3346–3369.
Moller, I., Marcus, S.E., Haeger, A., Verhertbruggen, Y., Verhoef, R., Schols, H., Ulvskov, P., Mikkelsen, J.D., Knox, J.P., Willats, W., 2008. High-throughput screening of monoclonal antibodies against plant cell wall glycans by hierarchical clustering of their carbohydrate microarray binding profiles. Glycoconj. J. 25, 37–48.
Moore, J.P., Fangel, J.U., Willats, W.G.T., Vivier, M.A., 2014. Pectic-β(1,4)-galactan, extensin and arabinogalactan-protein epitopes differentiate ripening stages in wine and table grape cell walls. Ann. Bot. 114, 1279–1294.
Nakatsuka, A., Murachi, S., Okunishi, H., Shiomi, S., Nakano, R., Kubo, Y., Inaba, A., 1998. Differential expression and internal feedback regulation of 1-aminocyclopropane-1-carboxylate synthase, 1-aminocyclopropane-1-carboxyalte oxidase, and ethylene receptor genes in tomato fruit during development and ripening. Plant Physiol. 118, 1296–1305.
Orfila, C, Seymour, G.B, Willats, W.G., Huxham, I.M., Jarvis, M.C., Dover, C.J., Thompson, A.J., Knox, J.P., 2001. Altered middle lamella homogalacturonan and disrupted deposition of (1–>5) alpha L arabinan in the pericarp of Cnr, a ripening mutant of tomato. Plant Physiol. 126 (1), 210–221.
in: Osoria, S., Fernie, A.R, Seymour, G.B., Poole, M., Giovannoni, J.J., Tucker, G.A., 2013. Biochemistry of Fruit Ripening. The Molecular Biology and Biochemistry of Fruit Ripening. Blackwell Publishing Ltd, Hoboken, NJ, pp. 1–13.
Peng, Q., Song, J., Lv, X., Wang, Z., Huang, L., Du, Y., 2012. Structural characterization of an arabinogalactan-protein from the fruits of *Lycium ruthenicum*. J. Agric. Food Chem. 60, 9424–9429.
Pfeifer, L., Shafee, T., Johnson, K.L., Basic, A., Classen, B., 2020. Arabinogalactan-proteins of *Zostera marina* L. contain unique glycan structures and provide insight into adaption processes to saline environments. Sci. Rep. 10, 8232.
Posé, S., Paniagua, C., Matas, A.J., Gunning, A.P., Morris, V.J, Quesada, M.A., Mercado, J.A., 2019. A nanostructural view of the cell wall disassembly process during fruit ripening and postharvest storage by atomic force microscopy. Trends Food Sci. Technol. 87, 47–58.
Ruiz-May, E., Rose, J.K.C, Seymour, G.B., Poole, M., Giovannoni, J.J., Tucker, G.A., 2013. Cell wall architecture and metabolism in ripening fruit and the complex relationship with softening. The Molecular Biology and Biochemistry of Fruit Ripening. Blackwell Publishing Ltd, Hoboken, NJ, pp. 163–187.
Showalter, A.M., 2001. Arabinogalactan-proteins: structure, expression and function. CMLS Cell. Mol. Life Sci. 58, 1399–1417.
Showalter, A.M., Basu, D., 2016. Glycosylation of arabinogalactan-proteins essential for development in *Arabidopsis*. Commun. Integr. Biol. 9 (3), e1177687.
Shi, Y., Jiang, L., Zhang, L., Kang, R., Tu, Z., 2014. Dynamic changes in proteins during apple (*Malus* x *domestica*) fruit ripening and storage. Hortic. Res. 1 (6), 1–21.
Skolik, P., Morais, C.L., Martin, F.L., McAinsh, M.R., 2019. Determination of developmental and ripening stages of whole tomato fruit using portable infrared spectroscopy and Chemometrics. BMC Plant Biol. 19 (1), 1–15.
Smallwood, M., Yates, E.A., Willats, W.G.T., Martin, H., Knox, J.P., 1996. Immunochemical comparison of membrane-associated and secreted arabinogalactan-proteins in rice and carrot. Planta 198, 452–459.
Tan, L., Eberhard, S., Pattathil, S., Warder, C., Glushka, J., Yuan, C., Hao, Z., Zhu, X., Avci, U., Miller, J.S., Baldwin, D., Pham, C., Orlando, R., Darvill, A., Hahn, M.G., Kieliszewski, M.J., Mohnen, D., 2013. An arabidopsis cell wall proteoglycan consists of pectin and arabinoxylan covalently linked to an arabinogalactan protein. Plant Cell 25, 270–287.
Tsumuraya, Y., Ozeki, E., Ooki, Y., Yoshimi, Y., Hashizume, K., Kotake, T., 2019. Properties of arabinogalactan-proteins in European pear (*Pyrus communis* L.) fruits. Carbohydr. Res. 485 (107816), 1–9.
Tucker, G., Yin, X., Zhang, A., Wang, M.M., Zhu, Q., Liu, X., Xie, X., Chen, K., Grierson, D., 2017. Ethylene and fruit softening. Food Qual. Saf. 1 (4), 253–267.
Verhertbruggen, Y., Marcus, S.E., Haeger, A., Verhoef, R., Schols, H.A., McCleary, B.V., McKee, L., Gilbert, H.J., Knox, J.P., 2009. Developmental complexity of arabinan polysaccharides and their processing in plant cell walls. Plant J. 59, 413–425.
Wang, D., Seymour, G.B., 2022. Molecular and biochemical basis of softening in tomato. Mol. Hortic. 2 (5), 1–10.
Yariv, J., Rapport, M.M., Graf, L., 1962. The interaction of glycosides and saccharides with antibody to the corresponding phenylazo glycosides. Biochem. J. 85, 383.
Yates, E.A., Valdor, J., Haslam, S.M., Morris, H.R., Dell, A., Mackie, W., Knox, J.P., 1996. Characterization of carbohydrate structural features recognized by anti arabinogalactan-protein monoclonal antibodies. Glycobiology 6, 131–139.
Zhang, B., Gao, Y., Zhang, L., Zhou, Y., 2021. The plant cell wall: Biosynthesis, construction, and functions. J. Integr. Plant Biol. 63, 251–272.

8. Tekst publikacji P.3

Kutyrieva-Nowak N., Leszczuk A., Ezzat L., Kaloudas D., Zając A., Szymańska-Chargot M., Skrzypek T., Krokida A., Mekkaoui K., Lampropoulou E., Kalaitzis P., Zdunek A. 2024.

The modified activity of prolyl 4 hydroxylases reveals the effect of arabinogalactan proteins on changes in the cell wall during the tomato ripening process.

Frontiers in Plant Science, 15: 1365490.

frontiers | Frontiers in Plant Science

TYPE Original Research
PUBLISHED 20 March 2024
DOI 10.3389/fpls.2024.1365490

OPEN ACCESS

EDITED BY
Daniel V. Savatin,
University of Tuscia, Italy

REVIEWED BY
Jozef Mravec,
Institute of Plant Genetics and Biotechnology (SAS), Slovakia
Juan Pablo Martinez,
Agricultural Research Institute, Chile

*CORRESPONDENCE
Agata Leszczuk
a.leszczuk@ipan.lublin.pl
Panagiotis Kalaitzis
panagiot@maich.gr

RECEIVED 04 January 2024
ACCEPTED 08 March 2024
PUBLISHED 20 March 2024

CITATION
Kutyrieva-Nowak N, Leszczuk A, Ezzat L, Kaloudas D, Zając A, Szymańska-Chargot M, Skrzypek T, Krokida A, Mekkaoui K, Lampropoulou E, Kalaitzis P and Zdunek A (2024) The modified activity of prolyl 4 hydroxylases reveals the effect of arabinogalactan proteins on changes in the cell wall during the tomato ripening process. *Front. Plant Sci.* 15:1365490. doi: 10.3389/fpls.2024.1365490

The modified activity of prolyl 4 hydroxylases reveals the effect of arabinogalactan proteins on changes in the cell wall during the tomato ripening process

Nataliia Kutyrieva-Nowak[1], Agata Leszczuk[1]*, Lamia Ezzat[2], Dimitris Kaloudas[2], Adrian Zając[3], Monika Szymańska-Chargot[1], Tomasz Skrzypek[4], Afroditi Krokida[2], Khansa Mekkaoui[2], Evangelia Lampropoulou[2], Panagiotis Kalaitzis[2]* and Artur Zdunek[1]

[1]Institute of Agrophysics, Polish Academy of Sciences, Lublin, Poland, [2]Department of Horticultural Genetics and Biotechnology, Mediterranean Agronomic Institute of Chania, Chania, Greece, [3]Department of Functional Anatomy and Cytobiology, Institute of Biological Sciences, Maria Curie-Skłodowska University, Lublin, Poland, [4]Department of Biomedicine and Environmental Research, Institute of Biological Sciences, Faculty of Medicine, John Paul II Catholic University of Lublin, Lublin, Poland

Arabinogalactan proteins (AGPs) are proteoglycans with an unusual molecular structure characterised by the presence of a protein part and carbohydrate chains. Their specific properties at different stages of the fruit ripening programme make AGPs unique markers of this process. An important function of AGPs is to co-form an amorphous extracellular matrix in the cell wall-plasma membrane continuum; thus, changes in the structure of these molecules can determine the presence and distribution of other components. The aim of the current work was to characterise the molecular structure and localisation of AGPs during the fruit ripening process in transgenic lines with silencing and overexpression of *SlP4H3* genes (prolyl 4 hydroxylase 3). The objective was accomplished through comprehensive and comparative *in situ* and *ex situ* analyses of AGPs from the fruit of transgenic lines and wild-type plants at specific stages of ripening. The experiment showed that changes in prolyl 4 hydroxylases (P4H3) activity affected the content of AGPs and the progress in their modifications in the ongoing ripening process. The analysis of the transgenic lines confirmed the presence of AGPs with high molecular weights (120–60 kDa) at all the examined stages, but a changed pattern of the molecular features of AGPs was found in the last ripening stages, compared to WT. In addition to the AGP molecular changes, morphological modifications of fruit tissue and alterations in the spatio-temporal pattern of AGP distribution at the subcellular level were detected in the transgenic lines with the progression of the ripening process. The work highlights the impact of AGPs and their alterations on the fruit cell wall and changes in AGPs associated with the progression of the ripening process.

KEYWORDS

arabinogalactan proteins, cell wall, fruit, proteoglycans, ripening, tomato, transgenic lines

1 Introduction

1.1 Arabinogalactan proteins in the fruit ripening process

The tomato (*Solanum lycopersicum* L.) is one of the most widely cultivated crops worldwide and a well-studied model for tissue-specific gene modification and fruit ripening (Feder et al., 2020). In turn, studies of fruit ripening are useful for both practical agricultural applications and improvement of the understanding of physiological programmes. The ripening process is a complex phenomenon inducing changes in fruit tissues. Alterations in fruit texture and colour are attributed to different metabolic processes in the cell wall (Orfila et al., 2002). Our previous studies have shown that there are substantial changes in the structure and distribution of arabinogalactan proteins (AGPs) correlated with the ongoing ripening process (Kalaitzis et al., 2023; Kutyrieva-Nowak et al., 2023a). As common components in the plant extracellular matrix, AGPs are attached to the plasma membrane via glycosylphosphatidylinositol (GPI) anchors (Showalter, 2001; Lopez-Hernandez et al., 2020; Zhou, 2022; Leszczuk et al., 2023). The specific and mutable distribution of AGPs in the cell wall-plasma membrane continuum allows identification of the effects of these molecules on the specific arrangement of the cell wall assembly in fruit cells (Liu et al., 2015; Leszczuk et al., 2018). Moreover, in the newest concept of the cell wall model named the APAP1 complex, AGPs are considered as cross-linkers between other cell wall components in which they are covalently attached to other polysaccharides of the cell wall, such as hemicellulose and pectins (Tan et al., 2013; Hijazi et al., 2014a, Hijazi et al., 2014b; Leszczuk et al., 2020c). Furthermore, it should also be underlined that some processes of plant growth and development, including cell expansion, somatic embryogenesis, root and stem growth, signalling during cell-cell communication, salt tolerance, and programmed cell death, require the presence of AGPs (Showalter, 2001; Borassi et al., 2020; Zhang et al., 2020; Leszczuk et al., 2023). Although the involvement of AGPs in many aspects of plant growth and development is well understood, still little is known about their function in fruit development and ripening. It is well-known that hydroxyproline-rich glycoproteins (HRGPs), i.e. the group to which AGPs are classified, are involved in fruit softening and affect the progression of the ripening process (Fragkostefanakis et al., 2012; Kalaitzis et al., 2023). Moreover, our previous investigations conducted on apple fruit after colonisation of *Penicillium spinulosum* have shown that the amount of AGPs increased in infection-associated modifications in fruit tissue. The increased amount of AGPs during the development of fungal disease is correlated with their assumed contribution in response to biotic stress, i.e. structure of the mechanical barrier against plant pathogens (Leszczuk et al., 2019c; Leszczuk et al., 2020b).

1.2 Structure and biosynthesis of AGP

AGPs are one of the most complex protein families in the plant cell wall. Notably, AGPs contain carbohydrate chains in 90-95% of their molecular mass and the protein core constitutes only 5-10%. Among others, AGPs have unique characteristics, such as the presence of arabinogalactan type II (AG) chains attached to the protein core composed of hydroxyproline (Hyp) residues and typical Ala-Pro, Pro-Ala, Thr-Pro, Ser-Pro, Val-Pro, and Gly-Pro peptide repeats (Showalter, 2001; Liu et al., 2015; Leszczuk et al., 2020b). In turn, the β-1,3-galactose chains of AGPs are modified by linking β-1,6-galactose side chains, which are further modified by the addition of arabinose (Ara), rhamnose (Rha), fucose (Fuc), xylose (Xyl), and β-glucuronic acid (GlcA) residues.

AGP synthesis is a sequence of steps, including the inter-formation of both protein moiety and carbohydrate chains accompanied by multiple enzymes. The key stages are (1) protein backbone and GPI anchor synthesis in the endoplasmic reticulum (ER), (2) AG and other sugar residues synthesis in the Golgi apparatus, and (3) formation of the AGP molecule in the cell wall-plasma membrane compartments (Ellis et al., 2010; Fragkostefanakis et al., 2012). The first stage involves the synthesis of the AGP protein core by transcription of appropriate genes onto mRNA on ribosomes and transfer of newly created peptides to the ER. In the ER, AGPs have modification and attachment GPI anchor to their hydrophobic C-terminal domain. Among the required enzymes during the AGP protein domain modification, an important function is performed by prolyl 4 hydroxylases (P4Hs). P4Hs catalyse the hydroxylation of proline residues in the polypeptide to form hydroxyproline (Vlad et al., 2007; Perrakis et al., 2019; Konkina et al., 2021). After proper hydroxylation of proline catalysed by P4Hs, AGPs undergo glycosylation, and this molecular mechanism is well known, but the effect of changes in this mechanism on AGPs as well as the mechanism of disruption of the subsequent glycosylation process by changes in the protein domain need to be elucidated. In the AGP glycosylation involved seven enzymes which are codding by 17 different genes. This step of biosynthesis is initiated by hydroxyproline galactosyltransferase affecting the attachment of the first residue of galactose onto Hyp in the protein core. The activity of β-1,3-galactosyltransferase and β-1,6-galactosyltransferase initialise the addition of galactose to the β-1,3-galactan backbone and β-1,6-galactan side chains of AGP glycans. The attachment of arabinose residues to the β-1,3-galactan backbone is activated by the arabinosyltransferase enzyme. The glucuronosyltransferases initiate the addition of glucuronic acid to the main backbone and side chains of AGPs. And finally, the fucosyltransferases add fucose residues to AGPs. In addition, during this step, other glycosyltransferases in the Golgi activate decorating AGP structure by less frequent sugar residues, such as Rha and Xyl (Ellis et al., 2010; Showalter and Basu, 2016). The heterogeneity of sugar chains, types of bonds, chains length, and abbreviations occurring during synthesis are the reasons for the structural and functional diversity of AGPs (Ellis et al., 2010; Fragkostefanakis et al., 2012).

1.3 Modification of AGP carbohydrate chains

Moreover, it is assumed that the wide functionality of AGPs is the result of their complex glycome structure (Showalter, 2001). In

more detail, it is suggested that GlcA may confer functional properties on AGPs specifically linked to β-(1→6)-galactan chains (Tan et al., 2004). One of the presumed mechanisms of the alterations in the activity and distribution of AGPs is their interaction with Ca^{2+}, which depends on the bonds with GlcA (Lamport and Várnai, 2013). In β-glucuronyltransferase mutants (*GlcAT*), a reduction of Ca^{2+} binding, which affected the cell wall and plasma membrane stabilisation and caused less intensive plant growth, was revealed. Also, the AGP's ability to release Ca^{2+} contributes to the regulation of cellular signalling (Lopez-Hernandez et al., 2020), and as a reservoir of Ca^{2+} affecting plant development (Lamport et al., 2018). Furthermore, AGs from mutant plants exhibited reduced glucuronidation, which caused binding of less Ca^{2+} *in vitro* and development deficiencies in these plants (Lopez-Hernandez et al., 2020).

Interestingly, another proposed mechanism in which the primary factor is the carbohydrate part of AGP is related to the enzymatic activity of two exo-β-1,3-galactosidases (Nibbering et al., 2020). The aforementioned investigations showed that GlcA also forms a bridging residue between pectin and AGPs, confirming the presence of the APAP1 complex (Tan et al., 2013, Tan et al., 2023). Moreover, it can be concluded that APAP1 may be the target of GH43 activity, as it affects cell wall-bound AGPs (Nibbering et al., 2020).

1.4 Modification of the protein moiety of AGPs – effect of prolyl 4 hydroxylases

As mentioned above, P4Hs catalyse proline hydroxylation, a major post-translational modification of HRGPs (Kivirikko and Myllyharju, 1998; Hieta and Myllyharju, 2002; Koski et al., 2009; Leszczuk et al., 2020c, Leszczuk et al., 2023). The impact of P4Hs on plant growth and development was demonstrated in carrot root *in vivo* (Cooper and Varner, 1983). Structural alterations in HRGPs were correlated with abnormal cell division, which influenced the loosening of the cell wall matrix and the *de novo* synthesis and rearrangement of cell wall components (Cooper et al., 1994). In other studies, mutants of *Arabidopsis* with T-DNA knockout P4Hs had shorter root hair, which was caused by destruction of extensins, and were characterised by a disrupted *O*-glycosylation process (Velasquez et al., 2015). Overall, in plants with disturbed function of P4Hs, the total hydroxyproline content is changed, leading to structural and functional changes during cell division and expansion (Vlad et al., 2007; Perrakis et al., 2019; Konkina et al., 2021). Also, alterations in tomato P4H genes caused by Virus-Induced Gene Silencing (VIGS) allowed determination of the impact on the weight and size of leaves resulting in intensified biomass production (Fragkostefanakis et al., 2014). Transient suppression of three tomato P4Hs by using Virus Induced Gene Silencing (VIGS) resulted in a decrease in the content of JIM8-bound AGPs and JIM11-bound extensins (Fragkostefanakis et al., 2014). In three stable RNAi transgenic lines of *SlP4H3*, abscission was delayed in overripe tomato fruits indicating involvement in the progression of this developmental process (Perrakis et al., 2019). Moreover, suppression and overexpression of *SlP4H3* in stable tomato transgenic lines resulted in changes in the content of AGPs-bound epitopes in flower abscission zones and/or distal and proximal tissue (Perrakis et al., 2021). In addition, *Arabidopsis* mutants of the β-linked glucuronic acid transferases resulted in lower content of glucuronic acids on AGPs leading to severe developmental phenotypes such as limited seedling growth and sterility which were associated with perturbed calcium waves indicating reduced binding of calcium due to insufficient glucuronidation of AGPs (Lopez-Hernandez et al., 2020).

Despite the well-documented importance of HRGPs, there is still insufficient information on the impact of P4H activity on AGPs. Phenotypic analyses have confirmed that overexpression and silencing of P4H genes cause changes in the *O*-glycosylation process, and the role of AGPs in the fruit ripening process may be determined via genetic manipulation of the protein backbone which changes glycan moieties. The purpose of our study was to characterise the molecular structure, content and distribution of AGPs during the ongoing fruit ripening process. The aims were accomplished through *in situ* and *ex situ* analyses of AGPs in the fruit of transgenic lines and WT at different stages of ripening. Obtaining various research results, we considered the hypothesis whether changes in the molecular parameters of AGP influence deviations in the cell wall assembly by modifying interactions with other matrix components. Taking into account the significant role of the cell wall in the ripening and softening process, we could directly analyse the fundamental factors related to the arrangement of the cell wall. The development of transgenic lines with altered *SlP4H3* expression facilitated the determination of modification in the structure and distribution of AGPs, thus contributing to the elucidation of the effect of these molecules on the whole fruit extracellular matrix.

2 Materials and methods

2.1 The SlP4H3 RNAi and overexpression transgenic lines

Homozygous T2 and T3 generation tomato (*Solanum lycopersicum* cv. 'Ailsa Craig') plants of two RNAi, RNAi#1, RNAi#7, and four overexpression, OEX#1, OEX#2, and cGFP OEX (cGFP), nGFP OEX (nGFP), lines were prepared (Perrakis et al., 2021). Plants of the T2 and T3 tomato lines were grown under hydroponic conditions in perlite sacks in one glasshouse at Chania, Greece under standard conditions of temperatures at the range of 18-27°C and relative humidity at the range of 60-80% humidity for approximately one year. Approximately 10 plants per line were grown under identical environmental conditions. Fruits were collected at the four ripening stages from more than one plant per line. Fruits of only similar size were collected. Then, the material was collected from 10 tomato fruits from each stage. Next, ten cube-shaped fruit tissue samples were taken from each examined fruit and subjected to microscopic analysis in a minimum of 50 sections (CLSM) and 5 ultrathin sections (TEM). For molecular approaches, tissue was homogenized and frozen at -80°C.

Tomato fruits were harvested at the Breaker (BR), Turning (TU), Pink (PINK), and Red Ripe (RR) previously described by Nakatsuka and coworkers (1998). The ripening stages were identified by assessment of changes in the fruit colour as proposed by Batu (2004). The first stage of the ripening process is

BR. It is the stage after development, in which tomatoes have a pale-green surface and the first signs of ripening (an orange colour) are visible. The next stage is TU, in which the first appearance of a pale-pink colour of the fruit surface is evident on 10-30% of the surface. The next stage is PINK, in which two-thirds (above 60%) of the fruit surface is red. The last stage is RR, in which the fruit is red on the entire surface (Nakatsuka et al., 1998; Kutyrieva-Nowak et al., 2023a).

2.2 RNA extraction and cDNA synthesis

Total RNA was extracted from 200 mg of pericarp tissue at the fruit ripening stages of BR, TU, PINK, and RR from the RNAi#1, RNAi#7, OEX#1, OEX#2, cGFP, nGFP lines and wild-type (WT). The samples were pulverized in liquid nitrogen and RNA was extracted using the NucleoZOL reagent (MACHEREY-NAGEL, Germany), following the manufacturer's instructions. The RNA samples were treated with DNase I (NEB, RNase-free, Ipswich, MA, USA) and approximately 1 µg of RNA was reverse transcribed using SuperScriptTM II RT (Invitrogen, Carlsbad, CA, USA) for cDNA synthesis following the manufacturer's instructions.

2.3 Real-time qRT-PCR analysis

Real-time PCR analysis was conducted using the SYBR™ Select Master Mix (Thermo Fisher Scientific, Waltham, MA, USA) in a CFX Connect™ Real-Time PCR Detection System (Bio-Rad, Hercules, CA, USA). The cDNA samples were normalized with b-actin as the reference gene using the primers SlActinF 5′-GTCCC TATTTACGAGGGTTATGCT-3′, SlActinR 5′-GTTCA GCAGTGGTGGTGAACA-3′. The primers used to determine the *SlP4H3* expression in the RNA#1, RNA#7, OEX#1, OEX#2, cGFP, nGFP lines and WT were *SlP4H3* Forward 5′-GTGA AAGGAAGGCATTCTCG-3′ and SlP4H3 Reverse 5′-CTTT CTGAGAGC CCCTGTGA-3′. The PCR conditions started at 50° C for 2 minutes and 95°C for 5 minutes, followed by 40 cycles of denaturation at 95°C for 15 seconds, annealing at 60°C for 30 seconds, and extension at 72°C for 30 seconds. A final melt-curve stage was performed, with temperatures set at 95°C for 15 seconds, followed by 60°C for 30 seconds with a 0.5°C increment at each repeat. Data analysis was carried out using the 2-ΔΔCT method (Livak and Schmittgen, 2001), and the results were presented as relative levels of gene expression with actin as the internal standard. Standard errors were calculated for all mean values. Three biological replicates were used per sample.

2.4 Molecular analyses

2.4.1 Protein extraction

Protein extraction was conducted according to Ling's protocol (Ling et al., 2021) and with modifications described in our previous work (Kutyrieva-Nowak et al., 2023a). The fruit tissue was cut into cube-shaped pieces and frozen at -80°C before the extraction procedure. The tomato fruit tissue was homogenised to a fine powder in liquid nitrogen, and then Laemmli's extraction buffer (Laemmli, 1970) was added. The modified Laemmli's buffer contained 65mM Tris-HCl pH 6.8, 2% SDS, 2mM EDTA, 1mM PMSF, 700mM β-mercaptoethanol, and a 1:10 protease inhibitor. The samples were boiled at 95°C for 5 minutes and then clarified by centrifugation at 14000 rpm at 4°C for 20 minutes. The final step was to collect the supernatant and freeze it at -80°C for the next assays. The protein content was determined by the Bradford method using ready-to-used solution of Bradford reagent (Sigma-Aldrich, USA).

2.4.2 Dot blotting with quantitative analysis

For determination of the presence of AGPs in the supernatants, an immuno-dot-blot reaction using specific antibodies against the carbohydrate epitopes of AGPs was carried out. The commercial monoclonal antibodies used to study AGPs were provided by Kerafast (USA). The experiment was conducted using primary antibodies: JIM13, which recognises the trisaccharide epitope β-D-GlcA-(1,3)-α-D-GalA(1,2)-α-L-Rha (Knox et al., 1991; Yates and Knox, 1994; Yates et al., 1996), LM2, which recognises the epitope β-linked GlcA (Yates and Knox, 1994; Smallwood et al., 1996; Yan et al., 2015), LM14, which recognises the epitope arabinogalactan type II (Moller et al., 2008), and LM1, which recognises extensin glycoprotein (Smallwood et al., 1996). The volume of dotted samples on nitrocellulose membrane (PVDF) was dependent of protein concentrations and was around 0.3 µg of protein per dot. Each sample was dotted onto a pre-prepared nitrocellulose membrane with a 0.2 µm pore size (Thermo Scientific, USA) and blocked using a 5% solution of bovine serum albumin (BSA; Sigma, USA) in phosphate-buffered saline (PBS; Sigma, USA). After washing in Tris-buffered saline (TBST, 7.6 pH) three times, the membranes were incubated for 2 h at room temperature (RT) with primary antibodies diluted 1:500 in 2.5% BSA in PBS. After washing with TBST, the membranes were incubated for 2 h at RT with secondary antibodies Anti-Rat-IgG conjugated with alkaline phosphatase (AP) (Sigma-Aldrich, USA) at a dilution of 1:1000 in 2.5% BSA in PBS. After three washing steps in TBST and AP-buffer, AGPs were finally detected using the following substrates: 4 mg of 5-bromo-4-chloro-3-indolylphosphate (BCiP; Sigma, USA) in 1 mL water and 9 mg of nitro-blue tetrazolium (NBT; Sigma, USA) in 0.3 mL water and 0.7 mL N,N-dimethylformamide (DMF; Thermo Scientific, USA) in the dark. After membrane imaging using GelDoc Go Imaging System (Bio-Rad, USA), the measurement of the colour intensity of the dots was carried out using Image Lab Software v. 6.1 (Bio-Rad, USA). The heat map was prepared using Microsoft tools in which colour intensity is proportional to a numerical value. The numerical values are rearranged to $\times 10^3$ for better representation of results. Data for each sample were obtained from three independent experiments. Each experiment presented data from the same set of samples under identical conditions. Statistic analysis was performed by Statistica v.13 tools (TIBCO Software Inc. USA) using variance (one-way ANOVA) and Tukey's Honestly Significant Difference (HSD) *post hoc* test. For all analyses, the significance level was estimated at $p<0.05$.

2.4.3 SDS-PAGE and Western blotting with quantification

Gel electrophoresis and next Western blotting were performed for identification of the molecular weight of AGPs from the fruit tissue in the different stages of ripening. After total protein extraction, quantification of the protein content was carried out using the Bradford assay. Protein separation was performed using SDS-PAGE with 12.5% resolving gel and 4% stacking gel. After SDS-PAGE electrophoresis, proteins with the gel were electroblotted onto a PVDF membrane. After Western blotting wet transfer, the membrane was washed in TBST on a shaking platform. After washing, the preincubation step was performed for 1 h at RT with 5% BSA in PBS, and the membrane was incubated for 2 h at RT with primary antibodies at a concentration of 1:500 in 2.5% BSA in PBS. After washing with TBST, the membrane was incubated for 2 h at RT with secondary antibodies conjugated with AP at a concentration of 1:1000. After washing with TBST and AP-buffer three times, visualisation of bands was performed using BCiP and NBT at a concentration described above in the GelDoc Go Imaging System (Bio-Rad, USA). For qualitative and quantitative analysis, the Pierce™ Prestained Protein MW Marker (Thermo Scientific, USA) was used. The band thickness, width, and colour depth were used for qualitative analysis (different ranges of molecular weights – 3 points: high molecular range, medium and low ones). The quantitative analysis of protein bands was performed by measurements of obtained stripes using Image Lab Software v. 6.1 (Bio-Rad, USA). Three independent analyses were carried out.

2.4.4 ELISA with quantitative analysis

Based on the number of antigen-antibody interactions produced, ELISA is a fundamental test for both qualitative and quantitative identification of AGPs in samples (Pfeifer et al., 2020; Kutyrieva-Nowak et al., 2023b). First, the samples were added to each well on a 96-well plate (Nunc MaxiSorpTM flat-bottom, Thermo Fisher Scientific, Denmark) and immobilized at 37°C for 72 h with shaking (350 rpm). Then, the coated plate was washed three times with PBS (pH 7.4), preincubated for 1 h at 37°C with 0.1% BSA in PBS, and incubated for 1 h at 37°C with primary antibodies at a concentration of 1:20 in PBS. After the washing step, the plate was incubated for 1 h at 37°C with the secondary antibody (in a dilution of 1:500 in PBS). After the incubation and washing steps, the reaction was developed by adding a freshly prepared substrate solution of p-nitrophenol phosphate (PNPP) according to Thermo Scientific instructions. The reaction was run in the dark and stopped with 2M NaOH after 20 minutes. The absorbance was measured in an ELISA reader (MPP-96 Photometer, Biosan) at 405 nm. The AGPs concentration was calculated from a calibration curve for gum Arabic with the calibration coefficient $y=0.7231x$, $R^2=0.9871$ in the case of reaction with JIM13 antibody, $y=0.3417x$, $R^2=0.9873$ in the case of reaction with LM2 antibody, $y=0.6394x$, $R^2=0.9796$ in the case of reaction with LM14 antibody and $y=0.502x$, $R^2=0.9857$ in the case of reaction with LM1 antibody. Gum Arabic was treated as a standard for AGPs. Analysis of variance (one-way ANOVA) and Tukey's Honestly Significant Difference (HSD) *post hoc* test (Statistica v.13 tools (TIBCO Software Inc. USA)) were used to compare the mean results. For all analyses, the significance level was estimated at $p<0.05$. Three independent analyses were carried out.

2.5 Biochemical–structural analyses

2.5.1 Extraction of AGPs using β-glucosyl Yariv Reagent

AGPs were isolated from tomato fruit tissue using the β-glucosyl Yariv Reagent (β-GlcY; Biosupplies, Australia) according to the extraction protocol proposed by Lamport (2013) and used in our previous studies (Leszczuk et al., 2020a, b; Kutyrieva-Nowak et al., 2023a). The liquid-nitrogen pre-frozen and homogenised fruit tissue was added to 2% $CaCl_2$ and incubated at RT. After 3 h, the homogenate was centrifuged at 10000 rpm for 30 minutes at RT. The supernatant was retained and added to 1 mg/mL β-GlcY in 2% $CaCl_2$ and left overnight at RT. The insoluble Yariv-AGP complex was centrifuged for 15 minutes at 2000 rpm, and the precipitate was resuspended in MiliQ water. Next, sodium metabisulphite (Thermo Scientific, USA) was gradually added to the precipitate and heated at 50°C to reduce the diazo linkage until the suspension was decolourised. After obtaining a clear yellow solution, the suspension was transferred to dialysis tubing with a 12-kDa MW cut-off (32 mm flat width; Sigma, USA) and stirred overnight. The dialysate was lyophilized, and then the AGPs were weighed.

2.5.2 FTIR analyses

FTIR spectra were collected on a Nicolet 6700 FTIR spectrometer (Thermo Scientific, Madison, WI, USA). The Smart iTR ATR sampling accessory was used. The spectra of the lyophilized AGP extracts were collected over the range of 4000–650 cm^{-1}. Three samples of each material were examined in the same conditions. For each sample, 200 scans were averaged with a spectral resolution of 4 cm^{-1}. Then, a final average spectrum was calculated for a given material. These spectra were baseline corrected and normalized to 1.0 at 1019 cm^{-1}. To highlight the differences between the samples, the principal component analysis (PCA) of the spectra was performed in the mid-infrared region of 4000–400 cm^{-1} using Unscrambler 10.1 (Camo Software AS., Norway). The maximum number of components taken for the analysis was five, and the NIPALS algorithm was used (Szymanska-Chargot et al., 2015; Chylińska et al., 2016). The visualisation of FTIR spectra and PCA analysis were performed using the OriginPro program (Origin Lab v. 8.5 Pro, Northampton, USA).

2.6 Microscopic analyses

2.6.1 SEM imaging

For morphological description, AGPs extracted using β-glucosyl Yariv Reagent from fruit tissue at different stages of the ripening process (the BR and RR stages) were imaged with a scanning electron microscope (SEM, Zeiss Ultra Plus, Oberkochen,

Germany) in high vacuum (5×10^{-3} Pa) using a secondary electron detector at 3 kV.

2.6.2 Preparation of material for immunocytochemistry

The microscopic analyses were carried out in accordance with our previous papers (Leszczuk et al., 2019a; Kutyrieva-Nowak et al., 2023a, Kutyrieva-Nowak et al., 2023b). For the microscopic examination, the fruit tissue was subjected to the procedure of fixation, resin embedding, and sectioning. Cube-shaped pieces of the fruit tissue were fixed in 2% paraformaldehyde (Sigma, USA) and 2.5% glutaraldehyde (Sigma, USA) in PBS and placed in vacuum (0.7 bar) seven times for 10 minutes each and then left overnight. Next, the samples were washed in PBS and distilled water and dehydrated in graded series of ethanol solutions (30%, 50%, 70%, 90%, and 96% for 15 minutes each and 99.8% twice for 30 minutes). The tissue was placed in 99.8% ethanol and LR White resin (at a ratio of 3:1, 1:1, 1:3; Sigma Aldrich, USA), and next in 100% resin LR White. The polymerisation was carried out for 48 h at 55°C. For CLSM imaging, the samples were cut into semi-thin sections (1 µm) using a glass knife-equipped ultramicrotome (PowerTome XL, RMC Boeckeler, USA). Next, the sections were placed on poly-L-lysine coated glass slides (Sigma, USA). For TEM imaging, the samples were cut into ultra-thin sections (70 nm) using a diamond knife-equipped ultramicrotome, and the sections were placed on formvar film-coated nickel square grids (EM Resolutions Ltd, UK).

2.6.3 Immunofluorescence method with confocal laser scanning microscopy (CLSM imaging)

Immunofluorescence imaging of AGP epitopes at the tissue/cellular level facilitates evaluation of changes in the distribution of AGPs in fruit at different ripening stages. The experiment was conducted using JIM13, LM2, and LM14 antibodies. Semi-thin sections on poly-L-lysine coated glass slides were circled with a liquid blocker Dako-Pen (Sigma Aldrich, USA). The samples were washed and pre-incubated for 30 minutes at RT with 2% BSA in PBS to block non-specific binding sites. After the washing step, the sections were incubated with primary antibody diluted 1:50 in 0.1% BSA in PBS overnight at 4°C. After washing with PBS three times, secondary Alexa Fluor 488 antibodies (diluted 1:200 in 0.1% BSA in PBS, goat Anti-Rat-IgM, Thermo Fisher Scientific, Denmark) were added and the sections were incubated overnight at 4°C. Then, the incubated sections were washed in PBS and MiliQ water and finally counterstained with Calcofluor White (Sigma Aldrich, USA). An Olympus BX51 CLSM microscope with corresponding software FluoView v.5.0. (Olympus Corporation, Tokyo, Japan) was used for imaging. In order to perform control reactions, the incubation with the primary antibody was omitted. All photographs, figures, and schemes were edited using the CorelDrawX6 graphics program.

2.6.4 Immunogold labelling technique with the transmission electron microscope (TEM imaging) and quantitative analysis

Immunogold labelling of AGP epitopes facilitates identification and visualization of changes in their distribution at the subcellular level. The experiment was conducted using JIM13, which recognises the most common and specific AGP epitope in fruits. Ultra-thin sections placed on grids (5 grids per sample) were washed in distilled water, and next pre-incubated for 30 minutes at RT with 1% BSA in PBS. Then, the grids were incubated for 3 h at 37°C with the primary antibody (diluted 1:10 in 0.1% BSA in PBS), washed in the blocking solution, and labelled with the secondary antibody (diluted 1:50 in 0.1% BSA in PBS, Anti-Rat-IgG – Gold antibody; Sigma, USA) for 1 h at 37°C. After washing in PBS and distilled water, the samples were stained with a 1% uracyl acetate solution (for 10 minutes) and Reynold's reagent (for 7 minutes). The observations were carried out using a transmission electron microscope (TEM Zeiss EM900) operating at 80 kV acceleration voltage (Carl Zeiss AG, Oberkochen, Germany) and equipped with a digital camera with corresponding software ImageSP v. 1.1.2.5. In the quantitative analysis of AGP labelling density, gold particles on the same size (2048 × 2048 pixels) micrographs were manually identified and counted with the software ImageJ v. 1.51. The results were expressed as the number of gold particles per 1 μm^2 area of the examined cell compartment (Corral-Martínez et al., 2016; Leszczuk et al., 2018). The statistical analysis consisted of comparing the content of AGPs in the cell wall–plasma membrane and in the cytoplasm to indicate significant differences among the transgenic lines and WT within ripening stages (according to ANOVA and Tukey's Honestly Significant Difference (HSD) *post hoc* test with the significance level $p<0.05$). All photographs, figures, and schemes were edited using the CorelDrawX6 graphics program.

3 Results

3.1 Expression of *SlP4H3* at fruit ripening stages in overexpression and silencing lines

Two *SlP4H3* RNAi independent lines, #1 and #7, and two *SlP4H3* overexpression lines, OEX#1, OEX#2 were previously produced (Perrakis et al., 2019, 2021). Moreover, two additional, independent overexpression lines were created, cGFP OEX (cGFP) and nGFP OEX (nGFP), comprising a construct in which a GFP tag was either at the C- or the N-terminus of the *SlP4H3* cDNA under the control of the 35S promoter (Perrakis et al., 2021). The expression levels of *SlP4H3* in the two silencing and the four overexpression lines were determined at the four ripening stages (Figure 1). Lower expression levels were observed by approximately 50% at the RNAi#1 and RNAi #7 fruits in all ripening stages (Figure 1). In the overexpression lines, the highest levels of expression were detected in the cGFP and nGFP lines up to approximately 92- and 20-fold, respectively (Figure 1). In the OEX#1 and OEX#2 lines, the *SlP4H3* transcript abundance was higher up to 4- and 8-fold, respectively (Figure 1).

3.2 Molecular differences between AGPs in the fruit of the transgenic lines

The molecular differences between AGPs in the fruit of the transgenic lines and WT at different stages of ripening were evaluated in several steps. Firstly, an immuno-dot-blot assay was

performed to quickly check the presence of AGP epitopes. The Western blotting method helped to determine the proportions of the molecular weights of the AGP epitopes in the fruit samples. Afterwards, selective glycome profiling of AGPs using the enzyme-linked immunosorbent assay (ELISA test) was conducted to visualise quantitative changes in the AGP content in the fruit of the examined transgenic lines during the ongoing ripening process.

3.2.1 Presence/absence of AGP epitopes during the ripening process

To validate the protein extraction and check the presence of specific AGP epitopes in the samples, an immuno-dot-blot assay was performed (Figure 2) and monoclonal antibodies against AGP epitopes (JIM13, LM2, and LM14) and against extensin (LM1) were used. The heat map obtained showed that the examined epitopes were present in different concentrations depending on the stage of the ripening process and the modification of P4H3 activity caused changes in the content of particular epitopes in the tested samples.

First of all, when analysing the ripening process itself, it is clear that the highest amount of all examined epitopes was detected at the BR stage, regardless of the line being tested. Additionally, in all cases, the number of all epitopes gradually decreased with the progression of the ripening process.

Secondly, the analysis of individual epitopes makes it possible to find differences in their content between individual lines. The assay of the fruit tissue of the RNAi#7 line with all the antibodies used indicated that silencing of the *SlP4H3* gene resulted in reduced intensity of the dots, compared to WT. In the same way, the analysis of the overexpression lines also revealed increased content of the tested epitopes in comparison to WT. The best visualisation effect of AGPs in all samples was achieved with the use of the LM2 antibody, which may indicate that modification of P4H3 activity does not significantly affect the presence of β-linked GlcA at every stage of the fruit ripening process. Despite this, the silencing of the *SlP4H3* gene in the RNAi#7 line resulted in a 5-20% reduction in the intensity of the dots, depending on the stage of ripening. The most effective demonstration of the progression of the ripening process was observed in the case of JIM13 in WT. Furthermore, an increase in the amount of the JIM13 epitope in the fruit tissue of the OEX#1 and OEX#2 lines was found. This content was 20-30% higher than in WT, even at the last stages of ripening. Also, the analysis of LM14 confirmed that the *SlP4H3* overexpression resulted in an increased number of LM14 epitopes. During the analysis of the LM1 epitopes, no significant differences in dot intensity were identified between the transgenic lines and WT and between the particular stages of ripening. It was also observed that the LM1 epitope was the least abundant and underwent the fastest degradation process, compared to the other epitopes.

3.2.2 Molecular mass disruption of AGPs during the ripening process

The Western blotting analysis also revealed the presence of all examined epitopes of AGPs, which were characterized by different molecular weights depending on the ripening stage (Figure 3). In the WT and transgenic lines, AGPs with high molecular weight (between 120 and 60 kDa) were observed as smeared bands, which are characteristic for separation of AGPs in the electric field during electrophoresis. In the analysis of Western blot membranes, special attention was paid to the bands representing low molecular weight AGPs (~30 kDa), which are markers of the finalisation of the ripening process in tomato fruit. The use of all the examined antibodies revealed the absence or trace quantities of low

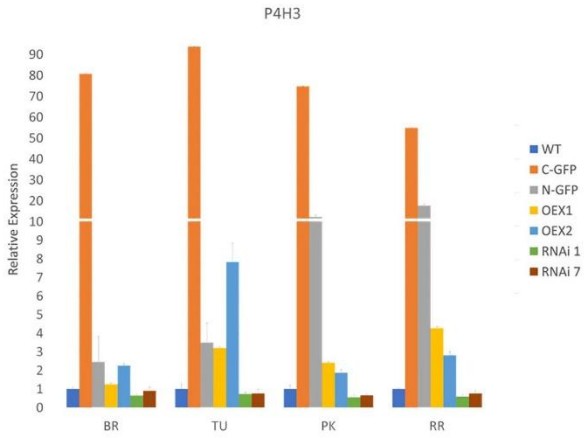

FIGURE 1
Expression of *SlP4H3* at Breaker (BR), Turning (TU), Pink (PK) and Red Ripe (RR) fruit ripening stages in cGFP, nGFP, OEX#1, OEX#2 and RNAi#1, RNAi#7 lines and WT. The relative expression was calculated based on the comparative CT method and actin was used as the internal standard. The relative fold differences for each sample were determined by normalizing the Ct value for the *SlP4H3* gene to the Ct value for actin and calculated using the formula $2^{-\Delta\Delta Ct}$. Three biological replicates were performed. Error bars represent standard error.

10.3389/fpls.2024.1365490

	BR	TU	PINK	RR	
WT	41.96 ± 1.95^{a}	35.7 ± 4.92^{ab}	33.64 ± 4.01^{ab}	28.14 ± 4.74^{bc}	JIM13
RNAi#1	27.09 ± 3.65^{b}	26.91 ± 2.82^{b}	24.64 ± 1.61^{b}	24.88 ± 1.65^{c}	
RNAi#7	38.57 ± 3.31^{a}	38.28 ± 4.65^{a}	36.88 ± 5.03^{a}	32.75 ± 3.65^{abc}	
OEX#1	42.81 ± 1.01^{a}	41.45 ± 3.74^{a}	40.98 ± 2.55^{a}	39.54 ± 5.25^{a}	
OEX#2	41.88 ± 1.31^{a}	41.51 ± 2.59^{a}	40.06 ± 1.82^{a}	36.35 ± 1.51^{ab}	
cGFP	37.67 ± 0.61^{a}	33.9 ± 3.63^{ab}	31.83 ± 5.45^{ab}	30.61 ± 5.57^{abc}	
nGFP	39.67 ± 1.01^{a}	36.34 ± 2.01^{ab}	36.23 ± 1.81^{a}	34.5 ± 1.31^{abc}	
WT	35.58 ± 2.25^{a}	33.36 ± 2.31^{a}	32.73 ± 1.51^{a}	31.7 ± 1.87^{a}	LM1
RNAi#1	32.58 ±6.25^{a}	32.41 ± 4.87^{a}	32.02 ± 6.98^{a}	32.07 ± 8.99^{a}	
RNAi#7	34.37 ± 3.23^{a}	33.15 ± 3.91^{a}	31.92 ± 1.78^{a}	31.79 ± 3.75^{a}	
OEX#1	38.72 ± 1.11^{a}	37.57 ± 0.95^{a}	36.28 ± 3.39^{a}	33.04 ± 5.56^{a}	
OEX#2	34.22 ± 1.43^{a}	33.65 ± 2.86^{a}	31.04 ± 1.62^{a}	28.08 ± 2.19^{a}	
cGFP	37.18 ± 4.04^{a}	36.91 ± 3.02^{a}	36.59 ± 3.81^{a}	35.4 ± 5.56^{a}	
nGFP	31,15 ± 2,36^{a}	28.37 ± 2.36^{a}	27.298 ± 1.22^{a}	25.397 ± 2.46^{a}	
WT	59.51 ± 0.61^{a}	49.29 ± 5.22^{a}	43.79 ± 5.08^{a}	40.58 ± 7.44^{a}	LM2
RNAi#1	48.85 ± 3.85^{ab}	48.81 ± 4.47^{a}	45.29 ± 5.43^{a}	41.62 ± 6.15^{a}	
RNAi#7	42.47 ± 7.91^{b}	40.85 ± 5.75^{a}	40.81 ± 5.12^{a}	38.94 ± 6.15^{a}	
OEX#1	48.44 ± 3.49^{ab}	45.35 ± 3.69^{a}	41.83 ± 5.31^{a}	39.88 ± 5.51^{a}	
OEX#2	47.19 ± 2.81^{ab}	43.46 ± 6.11^{a}	42.47 ± 5.58^{a}	41.63 ± 5.55^{a}	
GFP	44.24 ± 5.95^{b}	41.16 ± 6.44^{a}	39.08 ± 6.03^{a}	38.19 ± 5.95^{a}	
nGFP	41.53 ± 4.15^{b}	40.13 ± 4.64^{a}	39.23 ± 6.23^{a}	38.13 ± 6.51^{a}	
WT	36.24 ± 0.54^{a}	34.03 ± 0.43^{a}	33.85 ± 0.86^{a}	32.64 ± 1.84^{a}	LM14
RNAi#1	40.38 ± 9.15^{a}	37.61 ± 9.76^{a}	36.96 ± 8.69^{a}	36.63 ± 7.36^{a}	
RNAi#7	34.91 ± 2.04^{a}	33.04 ± 3.88^{a}	32.15 ± 3.36^{a}	31.34 ± 3.66^{a}	
OEX#1	45.25 ± 2.57^{a}	43.07 ± 2.21^{a}	41.29 ± 2.89^{a}	39.83 ± 1.29^{a}	
OEX#2	36.55 ± 1.35^{a}	36.27 ± 4.36^{a}	34.65 ± 2.28^{a}	34.54 ± 3.48^{a}	
cGFP	41.41 ± 0.95^{a}	39.41 ± 4.23^{a}	36.06 ± 3.67^{a}	34.53 ± 1.45^{a}	
nGFP	35.61 ± 3.14^{a}	34.38 ± 2.91^{a}	34.17 ± 2.47^{a}	33.17 ± 2.68^{a}	

FIGURE 2
Examination of samples using JIM13, LM1, LM2 and LM14 antibodies at different ripening stages from the fruit of wild-type plants (WT) and transgenic lines: RNAi#1, RNAi#7, OEX#1, OEX#2, cGFP, and nGFP. The numerical value in the heatmap is $\times 10^{-3}$. Letters indicate differences among the transgenic lines and WT within particular ripening stages (according to ANOVA and Tukey's Honestly Significant Difference (HSD) *post hoc* test with the significance level $p<0.05$). BR, Breaker stage; TU, Turning stage; PINK, Pink stage; RR, Red Ripe stage.

molecular weight epitopes. Interestingly, the aforementioned specific bands were not present in all the transgenic lines.

The next observation was that the different epitopes with various molecular weights had impaired participation in the composition of the examined lines, in comparison to WT. Both the JIM13 and LM2 epitopes were the most abundant in the fruit of the WT and in the transgenic lines, with the highest expression level in the fruit tissue of the cGFP (JIM13 epitope) and nGFP lines (LM2 epitope). The highest LM2 expression was recorded in the nGFP transgenic line, compared to WT and the other lines. In turn, the lowest expression of the LM2 and JIM13 epitopes was observed in the fruit tissue of the RNAi#1 and RNAi#7 lines. All the transgenic lines differed from WT in the abundance of LM14 epitopes with different molecular weights. AGPs extracted from WT exhibited low expression of the LM14 epitope, while all the transgenic lines showed a significant increase in its level. The weakest participation in the sample composition in both the WT and transgenic lines was noted in the case of LM1. Only several thick bands with low molecular weight in WT (~40kDa) and with high molecular weight (~120 kDa) in the OEX#1 and cGFP lines were observed. The most significant result of the quantitative Western Blotting analysis showed that AGPs extracted from the transgenic lines were characterised by a more variable structure in comparison to AGPs extracted from WT. Generally, in the same ripening stages, a higher amount of AGPs with diverse molecular masses were noted in the transgenic lines than in WT.

3.2.3 Changes in selective glycome profiling of AGPs during ripening process

The results presented above identified molecular differences between samples representing the various transgenic lines, thus the ELISA test was performed to confirm the presence of the AGP epitopes and to achieve better visualisation of differences between the particular stages of fruit ripening in each line (Figure 4).

The results shown in Figure 4 indicate the lowest differences in the amount of the JIM13 epitope in the fruit of transgenic lines

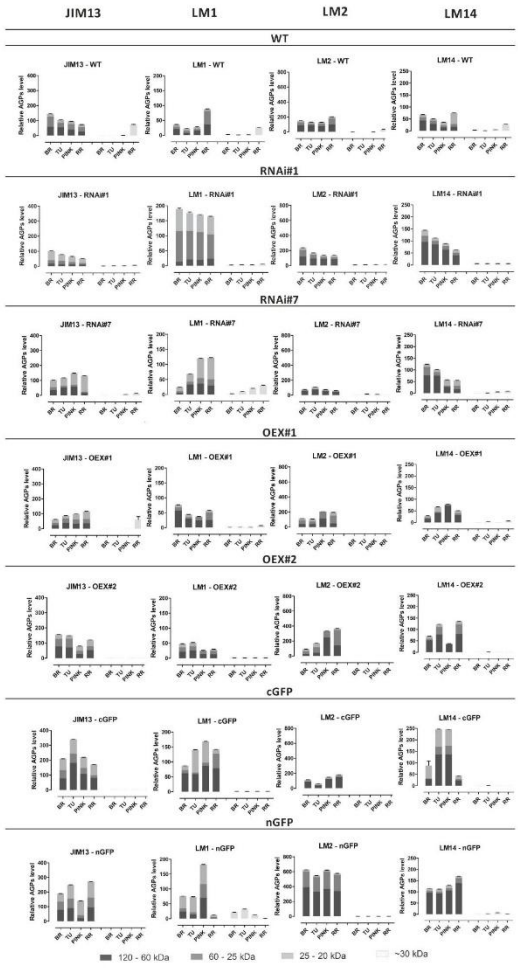

FIGURE 3
Western Blotting with quantitative analysis. Characterisation of molecular mass of AGPs from fruit at different ripening stages in wild-type plants (WT) and transgenic lines: RNAi#1, RNAi#7, OEX#1, OEX#2, cGFP, and nGFP. Western Blotting raw data (Supplementary Material). BR, Breaker stage; TU, Turning stage; PINK, Pink stage; RR, Red Ripe stage.

during the ripening process. The amount of the JIM13 epitope in the fruit tissue of the RNAi#7 line was not significantly different from that detected in WT. Besides, significant reduction of JIM13 epitope concentration in the case of RNAi#1 line. The highest concentration of the JIM13 epitope was obtained for the overexpression lines (around 55 μg/mL), and this dependence persisted to the last stages of ripening. Interesting results were obtained with the use of the LM2 antibody, as the concentration of the epitopes was significantly higher than in the analyses using the other antibodies. Only in the fruit of RNAi#1 line, the content was much lower than in other samples. Using the LM2 antibody, it was shown that the *SlP4H3* gene silencing had a significant effect on the concentration of this epitope. The AGP concentration was from approx. 700 μg/mL in WT to 1200 μg/mL for AGPs in the GFP lines, indicating that β-linked GlcA epitopes were the most abundant in the fruit AGPs. Also, the data showed that this epitope was predominant in all stages of the ongoing ripening process. In the case of overexpression of P4H3, the LM2 epitope was present in higher concentrations in comparison to native AGPs (around 20% higher for the fruit tissue of the OEX lines and around

40% for the fruit tissue of the GFP lines). The lowest absorbance value was observed after using the LM14 antibody, which correlated with the results of the dot blot analysis and Western blotting. The concentration of the LM14 epitopes had the lowest value, i.e. around 20 μg/mL in all the ripening stages and in all the tested samples. In the analyses with the LM1 antibody, significant increases in epitope concentrations were identified in the fruit tissue of the cGFP line at all the ripening stages. In turn, the fruit tissue of the RNAi#1 and RNAi#7 lines were characterised by lower LM1 epitope concentrations in comparison to WT. Also, the greatest fluctuations in the content of the LM1 epitopes were observed along with the progression of the ripening process.

3.3 Biochemical/structural differences

3.3.1 Various AGP amount in fruit at different ripening stages

For biochemical analyses, AGPs were isolated using β-glucosyl Yariv Reagent. After extraction, AGPs were lyophilised and weighed. Figure 5A shows the AGP content in tomato fruit at the BR and RR stages (mg of AGPs per g of fresh tissue). This procedure made it possible to confirm that the AGP amount decreased with the ongoing ripening process both in the WT and transgenic lines. The biochemical assay using β-GlcY determined the AGP content in the tomato fruit at the BR stage: 0.38 mg/g of WT, 0.31 mg/g of

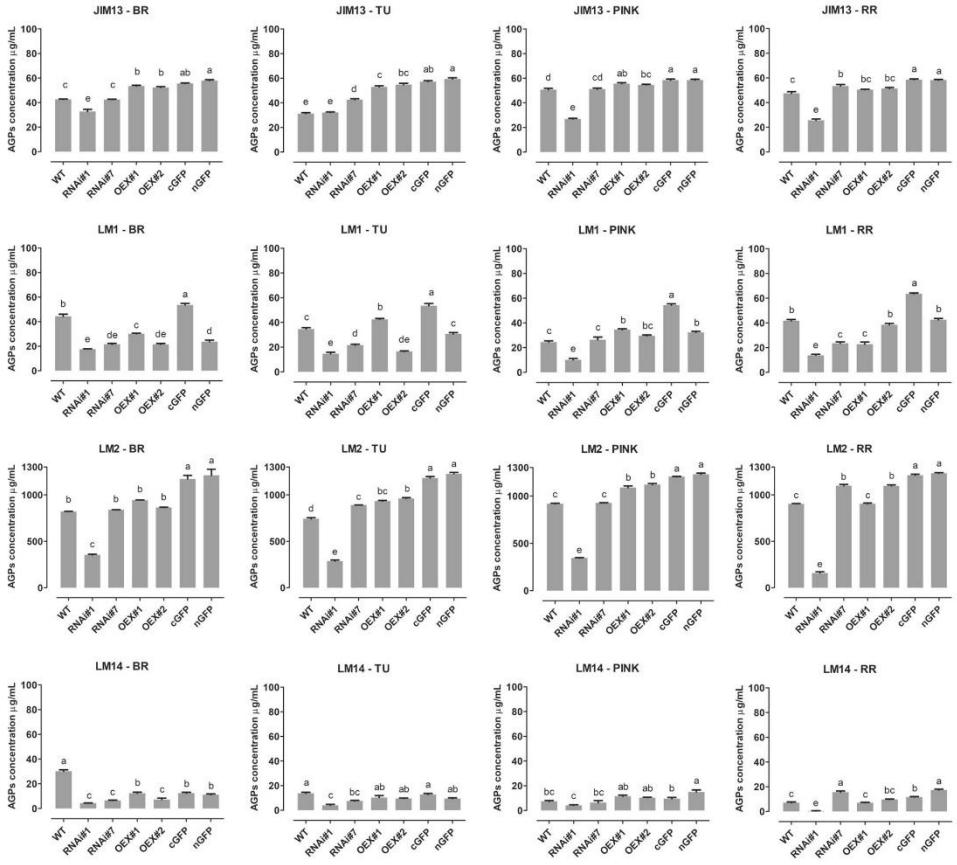

FIGURE 4
ELISA of AGPs extracted from fruit at different ripening stages from wild-type plants (WT) and transgenic lines: RNAi#1, RNAi#7, OEX#1, OEX#2, cGFP, and nGFP. Different letters indicate significant differences among the transgenic lines and WT within ripening stages (according to ANOVA and Tukey's Honestly Significant Difference (HSD) *post hoc* test with the significance level $p<0.05$). BR, Breaker stage; TU, Turning stage; PINK, Pink stage; RR, Red Ripe stage.

RNAi#7, 4.28 mg/g of OEX#1, and 0.59 mg/g of OEX#2 and at the RR stage: 0.28 mg/g of WT, 0.29 mg/g of RNAi#7, 0.75 mg/g of OEX#1, and 0.37 mg/g of OEX#2. It revealed the most intensive degradation process in the fruit tissue of the OEX#1 line, as around 82.3% of AGPs were degraded during the progression of the ripening process. In comparison, around 26.5% in WT, 7.48% in RNAi#7, and 37.5% AGPs in OEX#2 were degraded.

3.3.2 Morphological characterisation of AGPs

Figure 5B shows microphotographs of AGPs extracted from fruit at the initiation (BR) and finalisation (RR) of the ripening process. Despite the detailed observations of morphological features performed using SEM imaging, no differences between AGPs extracted from the BR and RR stages were noted. Interestingly, a high aggregation ability was visible. Thus, AGPs were imaged as compact oval aggregates composed of numerous smaller granules. The approximate diameter of the aggregates of AGPs was 1–3 μm in all the examined samples, regardless of the ripening stage.

3.3.3 Structural characterisation of AGPs

The FTIR spectra of AGPs isolated from the tomato WT and transgenic lines can be divided into several regions (Figure 6-I). The 4000–2750 region is characteristic for O-H vibrations typical for all substances and CH_2 and CH_3 stretching vibrations typical for lipids, proteins, and carbohydrates. The region from 1800 – 1400 is typical for bands assigned to C=O carbonyl stretching vibrations (1740 cm^{-1}), carboxyl ion symmetric and asymmetric vibrations (1620 and 1416 cm^{-1}, respectively), and characteristic for uronic acids. It is also typical for bands characteristic for proteins and denoted as C=O stretching in Amide I (1630 cm^{-1}), as N-H bending in Amide II (1547 cm^{-1}), and C-N stretching vibration in proteins (~1450 cm^{-1}) (Zhou et al., 2009; Szymanska-Chargot and Zdunek, 2013; Yamassaki et al., 2018). The region below 1400 cm^{-1} is called the fingerprint region and contains bands characteristic mostly for carbohydrates. The band at 1367 cm^{-1} is assigned to C-H vibrations and CH_2 bending, 1331 cm^{-1} – to bending of O-H groups in the pyranose ring of pectins, 1316 cm^{-1} – to CH_2 symmetric bending or CH_2 rocking vibration, 1230 cm^{-1} – to bending of O-H groups in the pyranose ring of pectins and proteins, 1147 cm^{-1} – to ring vibrations (C-OH) overlapped with stretching vibrations of side groups and glycosidic bond vibrations (C-O-C), 1000–1200 cm^{-1} – to skeletal vibrations of the ring or the glycoside bond, 1019 cm^{-1} – to C-O stretching and C-C stretching (Boulet et al., 2007; Szymanska-Chargot and Zdunek, 2013; Szymanska-Chargot et al., 2015; Chylińska et al., 2016). The bands at approx. 896, 835, and 776 cm^{-1} are characteristic for β-glycosidic linkages (hemicelluloses and cellulose), α-glycosidic linkages (uronic acids), 1–4 linkage of galactose, and 1–6 linkage of mannose (Bashir and Haripriya, 2016). The bands below 700 cm^{-1} are attributed to the skeletal vibrations of pyranose rings (Szymanska-Chargot et al., 2015; Bashir and Haripriya, 2016).

In the case of the AGPs isolated from the BR and RR stages of WT, the FTIR spectra did not show substantial differences (Figure 6A). Generally, in addition to arabinogalactans (β-glycosidic linkage vibrations at 776 cm^{-1}) and proteins (amide bands at 1630 cm^{-1}, 1547 cm^{-1}, and 1450 cm^{-1}), the isolates also contained uronic acids and pectins (bands at 1367 cm^{-1}, 1331 cm^{-1}, 1316 cm^{-1}, 1230 cm^{-1}, and especially 835 cm^{-1} characteristic for α-glycosidic linkages).

In the case of the RNAi#7 line, the differences in the FTIR spectra between the BR and RR stages were apparently more pronounced (Figure 6B). The spectrum for the BR stage of the RNAi#7 line was very similar to the BR stage of WT with a difference that the band at 1740 cm^{-1} for the mutant was more intense than for WT, which may evidence the presence of more esterified pectins. This band was even more intense in the spectrum for the RR stage of the RNAi#7 line. The spectrum for the RR stage of RNAi#7 line bands at 1377, 1339, 1318, 1230, 1093, 958, and 837 cm^{-1} characteristic for pectic polysaccharides, especially rhamnogalacturonans type I and II (Boulet et al., 2007), and 896 cm^{-1} characteristic for most of the hemicellulosic polysaccharides increased, while those characteristic for pure arabinogalactan glycoprotein (Arabic gum spectrum, Figure 6) at 810 and 776 cm^{-1} decreased (Szymanska-Chargot and Zdunek, 2013).

Less clear differences between spectra were obtained for the BR and RR stages in the OEX#1 line (Figure 6C). The spectra were characterized by relatively high intensity of the band at 1740 cm^{-1} assigned to esterified pectins. In turn, the bands at 1062 and 1030

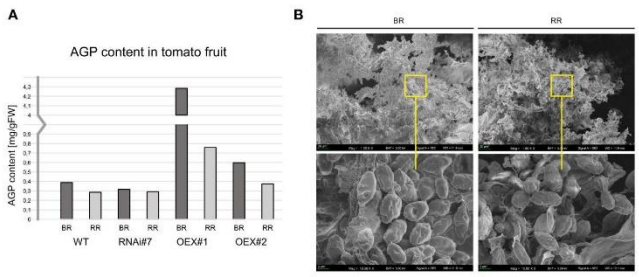

FIGURE 5
AGP content in tomato fruit at different ripening stages **(A)**. Morphological imaging using SEM with visible AGPs with high aggregation ability **(B)**. BR, Breaker stage; RR, Red Ripe stage.

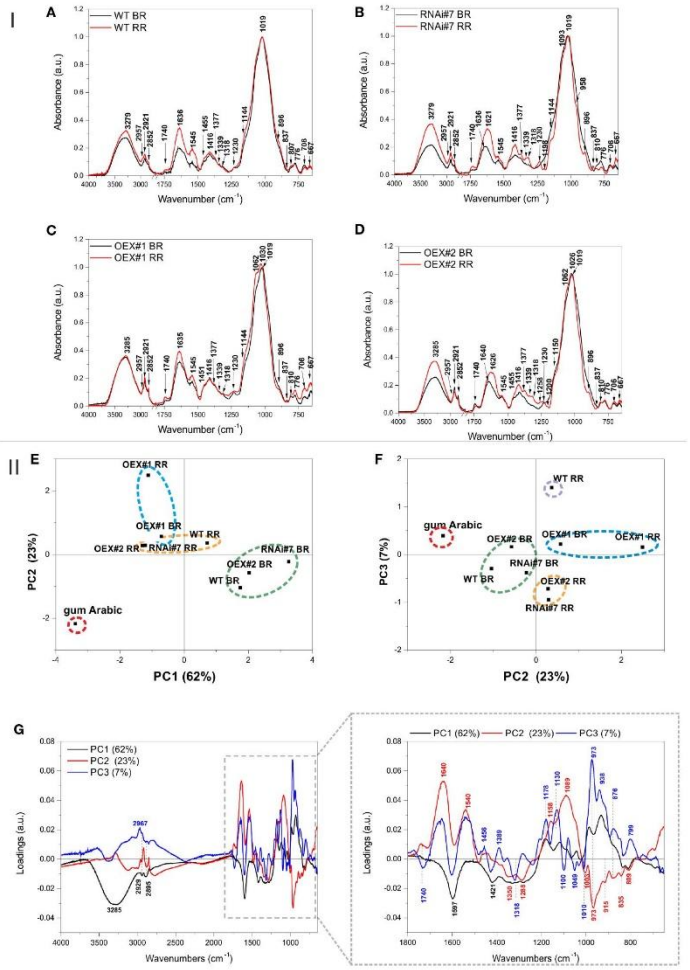

FIGURE 6
I. FTIR spectra in the range of 4000 – 650 cm^{-1} of AGP isolates obtained from tomato fruit at different ripening stages in wild-type plants (WT) **(A)** and transgenic lines: RNAi#7 **(B)**, OEX#1 **(C)**, and OEX#2 **(D)**. The 2750 – 1800 cm^{-1} region was cut out as it did not show any spectral features. The most characteristic wavenumbers are highlighted in the spectra. II. PCA of the FTIR spectra of AGP isolates from tomato fruit at different ripening stages in wild-type plants (WT) and transgenic lines: RNAi#7, OEX#1, and OEX#2. Gum Arabic was added to the analysis as the AGP standard. Scatter of PC1xPC2 **(E)** and PC2xPC3 **(F)** scores are shown together with the loading profile of components PC1, PC2, and PC3 **(G)**. The most characteristic wavenumbers are highlighted in the loadings; different colours (black, blue, and red) denote the different PC (PC1, PC2, and PC3) loadings, respectively (some of the wavenumbers are characteristic for more than one PC loading). BR, Breaker stage; RR, Red Ripe stage.

cm^{-1} that appeared in the spectrum for the RR stage of the OEX#1 line can be assigned to the vibrations of pyranose in gum Arabic and arabinogalactan polysaccharide, respectively (Wu et al., 2020). Moreover, the band at 837 cm^{-1} characteristic for pectic polysaccharides diminished and bands at 896, 810, and 776 cm^{-1} characteristic for arabinogalactans were more visible in the spectrum for the RR stage of the OEX#1 line.

Interestingly, the band at 1740 cm^{-1} declines and the band at 1640 cm^{-1} is shifted to 1626 cm^{-1} in the spectrum for the RR stage of the OEX#2 line, compared with the BR stage of the OEX#2 line (Figure 6D). This may evidence demethylation of pectic polysaccharides present in the AGP isolate from the OEX#2 line. Additionally, as in the case of the RR stage of the RNAi#7 line, the bands characteristic for pectic polysaccharides, especially

rhamnogalacturonans type I and II, also appeared in the RR stage of the OEX#2 line. However, the AGP isolate from the RR stage of the OEX#2 line was also rich in arabinogalactan polysaccharide and protein, as the bands visible at 1150, 1062, 1026, 896, 810, and 776 cm^{-1} were intense.

The PCA analysis of the obtained FTIR spectra was performed for better comparison and highlighting of the samples (Figure 6-II). Figures 6E and F present the scatter plots of the scores of the first three principal components PC1, PC2, and PC3, which together explain 92% of variability. The scores are scattered along all axes and the grouping effect of scores can be observed. The gum Arabic is separated from the other samples, which is clear evidence that the spectra of the obtained isolates differ from the AGP standard (Figure 6E, F). The samples from the BR stages of WT, RNAi#7, and OEX#2 and samples from the RR stages of WT, RNAi#7, and OEX#2 form two separate clusters in the PC1xPC2 score plot, which proves that there are spectral similarities between the samples, while the samples from the BR and RR stages of the OEX#1 line form a separate cluster (Figure 6E). In the PC2xPC3score plot, the same samples groups were obtained; however the RR stage of WT form a new separate group (Figure 6F).

Loadings that influence the differentiation of the scores are presented in Figure 6G. The wavenumbers of PC1 negative loadings that mostly influenced the sample scores lying on the negative side of PC1 (gum Arabic, the BR and RR stages of the OEX#1 line, the RR stages of the OEX#2 and RNAi#7 lines) were 3285, 2929, 2895, 1597, 1421, 1350, 1018, 1288, 835, and 810 cm^{-1}, which are mostly characteristic for esterified pectins and for AGP protein (gum Arabic spectrum), while the positive influence was associated with the following wavenumbers: 1181, 1119, 1042, 977, and 938 cm^{-1}, mostly characteristic for gum Arabic (Figure 6). On the other hand, the gum Arabic was located on the negative side of PC2, on which wavenumbers 1350, 1288, 973, 835, and 809 cm^{-1}, also characteristic for pure AGP from gum Arabic, had an influence. The other samples lying on the negative side of PC2 (but closer to PC2 = 0) were the BR stages of WT, OEX#2, and RNAi#7 lines. The wavenumbers having a positive influence on the scores of samples scattered on the positive side of PC2 were 1740, 1640, 1540, 1158, and 1089 cm^{-1}. The negative influence on the scores scattered along PC3 (the RR stages of the OEX#2 and RNAi#7 lines) had wavenumbers 1740, 1597, 1421, 1318, 1100, 1049, and 1010 cm^{-1} – characteristic mostly for pectic polysaccharides. In turn, wavenumbers 1178, 1130, 973, 938, 876, and 799 cm^{-1}, characteristic for arabinogalactans and for some phospholipids, had a positive influence.

3.4 Differences in AGP arrangement in the cell wall assembly – analyses *in situ*

3.4.1 Changed spatio-temporal localisation of AGPs at the cellular level

In planta studies were performed using the immunofluorescence technique to identify presumed changes in the spatio-temporal pattern of the AGP distribution in the fruit tissue of the examined lines. Figures 7–9 show microscopic investigations of the AGP arrangement in the tissue of WT, OEX#1, and OEX#2; RNAi#1, and RNAi#7; cGFP and nGFP lines, respectively. Our decision to focus on the two distant stages of ripening (BR and RR) was based on the fact that the differences did not appear between particular successive stages.

The microscopic observations demonstrated the anatomic changes in fruit tissues and cell walls at the cellular level. In all the fruit lines, modifications of cell walls occurred with the progression of the ripening process and were visualised as degraded cellular compartments adjacent to swollen cell walls. These modifications were correlated with typical processes of decay in fruit during the ongoing ripening process. The specific pattern of arrangement of AGPs was labelled as a line at the border between the cell wall and the plasma membrane. With the subsequent stages of ripening, the localisation of AGPs changed and the immunofluorescence intensity was lower. For WT, this correlation persisted for the samples labelled with all the antibodies.

The interpretation of microscopic results consisted in finding differences between the analysed lines after the reactions with three antibodies against AGPs. In the initial ripening stages, the fluorescence intensity in the OEX#1 fruit tissue was higher than in WT. The increased number of labelled AGP epitopes was confirmed using all antibodies. The fruit tissue of the OEX#2 line also showed an increase in the number of labelled AGP epitopes compared to WT, although the number was lower than in the fruit tissue of the OEX#1 line. The increase in the amount of AGP epitopes (mainly JIM13 and LM2) disturbed the typical pattern of localisation of AGPs, and the epitopes were visible in the whole area of the cell wall-plasma membrane continuum. Similarly, the striking typical anatomical changes in the tissue during the ripening process coincide with a decrease in the occurrence of AGP epitopes. However, the immunofluorescence signal is clearly higher compared to WT.

In samples with the silenced expression of the *SlP4H3* gene, intrusive alterations in the tissue morphology were imaged as a result of ripening progress. Significant changes in the macrostructure were found in the fruit tissue of the RNAi#1 and RNAi#7 lines. At first, compared to all lines, the tissue in the mutants mentioned above was looser even at the BR stage. In addition, at the RR stage, the tissue was disordered, the cell wall was less integrated, unevenly thickened, more undulating, and swelled. The rearrangement of epitopes was correlated with cellular dissociation. In the fruit tissue of the RNAi# lines, a decrease in all AGP epitopes was observed at both the BR and RR stages.

In the fruit tissue of the cGFP line, substantially increased fluorescence intensity was observed after the reaction performed using JIM13, LM2, and LM14, compared to WT. Moreover, AGP epitopes were present at the last stage of ripening. In the fruit tissue of the nGFP line, loosening of the cell wall was observed from the first ripening stage. With the progression of the ripening process, the cell wall became even more unevenly undulating and thickened. The number of AGP epitopes decreased, which distinguished this line from the fruit tissue of the OEX and cGFP lines.

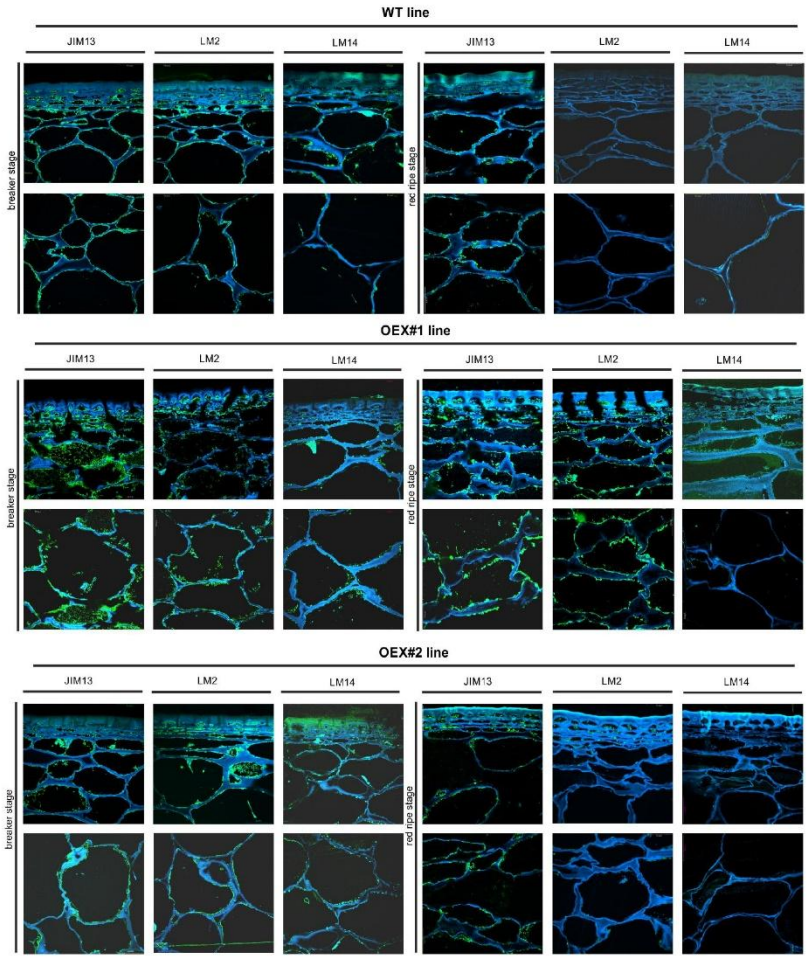

FIGURE 7
Spatio-temporal localisation of AGPs in tomato fruit tissue at different ripening stages in wild-type plants (WT) and transgenic lines OEX#1 and OEX#2. Immunofluorescence method using JIM13, LM2, and LM14 antibodies (green color) and counterstaining with Calcofluor White (blue color). Negative control for immunocytochemical reactions (Supplementary Material).

3.4.2 Disturbed localisation of AGPs at subcellular level

The immunogold labelling analysis and TEM imaging (40 kx magnification) allowed localisation of AGPs in the individual compartments of the fruit cell at the subcellular level. The analysis was carried out using the JIM13 antibody. Figure 10 shows analyses of the correlation between the localisation of AGPs in the cellular compartments and the stages of the ripening process. JIM13 epitopes, visible as dark points marked with red circles (Figure 10A), were observed in the entire cell, and labelling mainly occurred in the cell wall-plasma membrane continuum and the cytoplasm. For consistency, we analysed two cell compartments (cell wall-plasma membrane and cytoplasm) in all cases. Since there were no significant differences between all the subsequent stages of the ripening process noted by CLSM imaging at the cellular level, the analysis at the subcellular level was carried out in two distant stages of ripening. Generally, AGP epitopes were detected less frequently in the RR stage of ripening than in the BR stage. In almost every case, the cell wall-plasma membrane continuum exhibited the largest amounts of AGP epitopes, with the exception of the RR stage in the fruit tissue of the cGFP and nGFP lines.

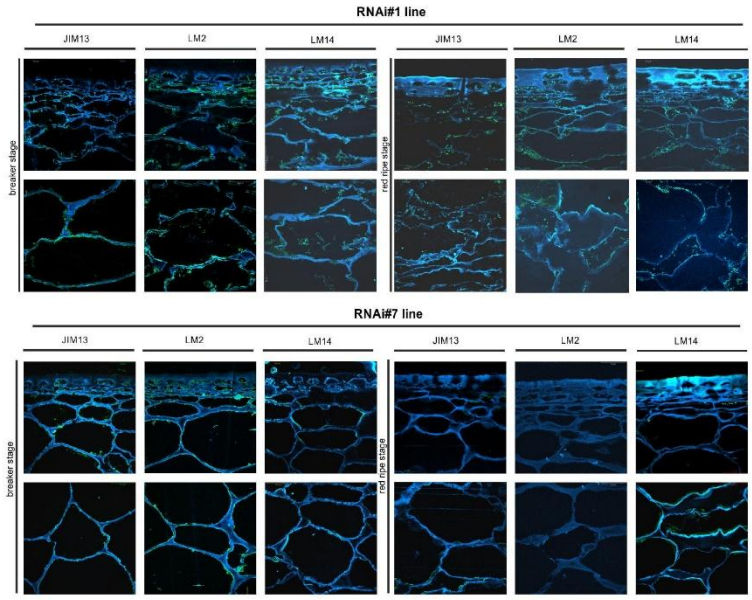

FIGURE 8
Spatio-temporal localisation of AGPs in tomato fruit tissue at different ripening stages in transgenic lines RNAi#1 and RNAi#7. Immunofluorescence method using JIM13, LM2, and LM14 antibodies (green color) and counterstaining with Calcofluor White (blue color).

The quantitative analysis of immunogold labelling confirmed the specific spatio-temporal pattern of distribution of AGPs and indicated changes in the amount of AGPs in the cell wall and cytoplasm in the transgenic lines during the ripening process (Figure 10B). Once again, the most characteristic distribution of AGPs was obtained in the WT fruit tissue. At the BR stage, the AGP epitopes were more organized and localised mainly in the cell wall-plasma membrane continuum. Only 10% of gold particles were localised in the cytoplasm. However, during the ripening process, the number of gold particles increased in the cytoplasm and accounted for nearly 40% at the RR stage. This may evidence the process of degradation of the cell wall and release of residues of cell wall compartments into the cytoplasm.

The AGP distribution pattern was disrupted in the fruit of the transgenic lines, where AGPs were dispersed in the whole area of the extracellular matrix. It was shown that modifications of *SlP4H3* gene activity caused changes in the number of gold particles in particular cell parts. Moreover, different proportions of gold particles in the cell wall-plasma membrane and in the cytoplasm were found in the examined samples, compared to WT. In lines with the overexpression of the *SlP4H3* gene, an increased amount of AGPs in the cytoplasm was found. Furthermore, the subcellular localisation of the AGP epitope in the fruit tissue of the cGFP and nGFP lines at the BR stage showed the presence of half of the amount of gold particles in the continuum cell wall-plasma membrane (0.38 and 0.14 particles per μm^2, respectively), and the rest was distributed in the cytoplasm (0.29 and 0.15 particles per μm^2, respectively). On the other hand, a significant reduction in the number of gold particles in the cell wall-plasma membrane (almost 80%) was observed in the lines with silenced *SlP4H3* gene expression (RNAi#1 and RNAi#7) at the BR stage. Similarly, at the RR stage, the AGP assembly disorder was assessed, and a higher amount of gold particles was noted in the cytoplasm than in the cell wall-plasma membrane.

5 Discussion

The ripening process is the subject of extensive research, but the role of AGPs in this process is still poorly known (Seymour et al., 2013). In our research, the genetic modification in the AGP biosynthesis process by changes in the activity of the P4H enzyme allowed identification of AGP alterations during the ripening process. First of all, the disruption in hydroxylation and subsequent AGP glycosylation processes most probably induce a sequence of modifications in the arrangement of cell walls. In the current work, we did the work step by step to investigate how changes in the process of forming the protein moiety may influence the subsequent phase of the AGP molecule synthesis pathway, such as the attachment of carbohydrate chains. The analyses performed using molecular, structural, and microscopic tools in *ex situ* and then *in situ* studies revealed crucial changes in AGP features in the

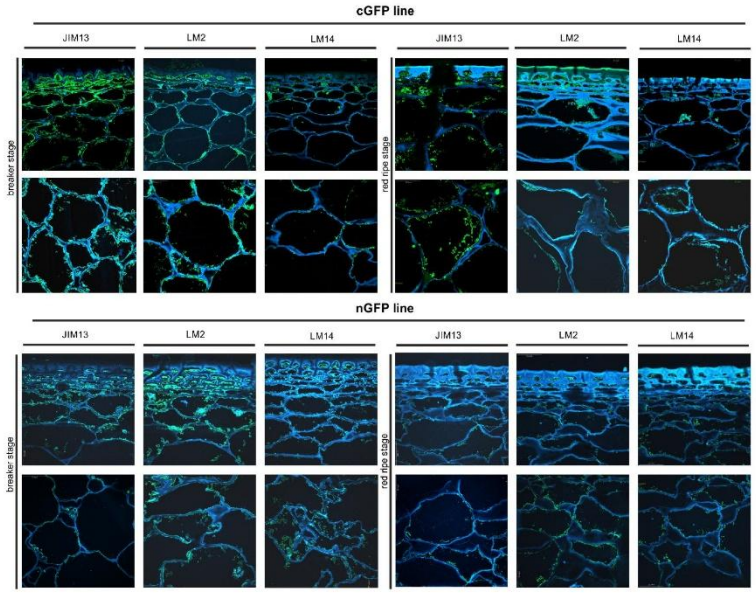

FIGURE 9
Spatio-temporal localisation of AGPs in tomato fruit tissue at different ripening stages in transgenic lines cGFP and nGFP. Immunofluorescence method using JIM13, LM2, and LM14 antibodies (green color) and counterstaining with Calcofluor White (blue color).

fruit of the transgenic lines in comparison to the wild-type plants. Based on the results obtained, a meticulous pattern of consecutive events in fruit cells that is associated with P4H3 was developed.

The development of the overexpressing and silenced P4H3 tomato lines facilitated the determination of alterations in the AGP carbohydrate design that induced changes in their localisation in the cell wall, allowing identification of AGP structural functions in the fruit tissue. So far, it has been demonstrated that hydroxyproline-rich glycoproteins are involved in fruit ripening (Moore et al., 2014; Kalaitzis et al., 2023). One of the major findings of a study conducted by Moore and coworkers on the anti-extensin LM1 antibody showed an increasing amount of extensin epitopes in ripe grapes as a response to the ripening process (Moore et al., 2014). These observations were consistent with the results of the analysis carried out by Nunan and coworkers that protein components rich in arginine and hydroxyproline also accumulate in grapes at the last stages of ripening (Nunan et al., 1997; Nunan et al., 1998). Similarly, our previous studies on apple and tomato fruit have shown that the amount of AGPs during the fruit ripening process changed with a significant concentration increase at the particular stages of the ripening programme (Leszczuk et al., 2020c; Kutyrieva-Nowak et al., 2023a). The analysis carried out with the use of β-glucosyl Yariv Reagent, whose reactivity is one of the most important criteria in the identification of AGPs (Seifert and Roberts, 2007; Kitazawa et al., 2013; Tsumuraya et al., 2019), also confirmed the differences in the AGP content between the specific stages of ripening. The confirmation was found also in the present work, as the content of AGPs decreased with the ongoing ripening process both in WT and in all the examined transgenic lines. Interestingly, an increased amount of AGPs in the overexpression lines was observed, indicating the influence of P4Hs in the AGP biosynthetic pathway.

The next research step involved comprehensive structural analyses on extracted AGPs aimed at revising changes that may have appeared as a result of the P4H3 modifications. The FTIR technique used for this purpose provided information about carbohydrate chains in AGPs during the fruit ripening process. Previous single FTIR reports of monosaccharide compositional analysis of AGPs isolated from *Lycium ruthenicum* Murr fruit revealed that arabinose and galactose represented by absorbance regions at 1060-1040, 975 cm^{-1}, and 945 cm^{-1}, respectively, were the major AGP sugars (Coimbra et al., 1998). The results obtained in the current work also confirm the occurrence of these carbohydrates in the isolated AGPs. The FTIR spectra showed that the AGP isolates from tomato fruit contained pure arabinogalactan proteins and a trace of pectic polysaccharides (uronic acids, rhamnogalacturonan) and hemicelluloses. The PCA analysis in the current work identified three PC groups with different polysaccharide compositions. The result obtained for the analysis of AGPs from the OEX#1 line seems interesting, as samples collected at different ripening stages formed a common group, compared to the two separate groups of the BR and RR stages.

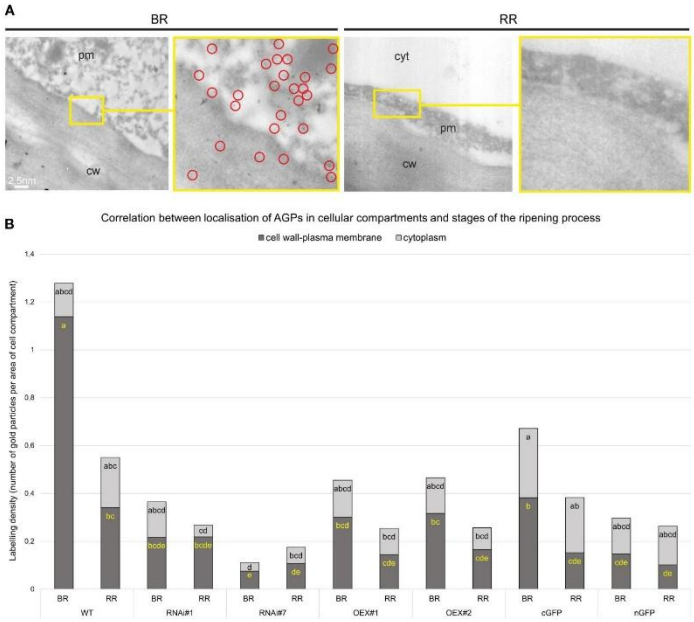

FIGURE 10
Ultrastructural TEM imaging of immunogold labeling of AGPs in tomato fruit at different ripening stages. Gold particles marked with red circles **(A)**. Quantitative data derived from analyses of the density of gold particles **(B)**. Different letters (yellow letters for cell wall – plasma membrane and black letters for cytoplasm) indicate significant differences among the transgenic lines and WT within ripening stages (according to ANOVA and Tukey's Honestly Significant Difference (HSD) *post hoc* test with the significance level $p<0.05$). cw, cell wall; pm, plasma membrane; cyt, cytoplasm; BR, Breaker stage; RR, Red Ripe stage.

Besides, the PC2xPC3 analysis identified a disruption of the 'native' ripening pattern of the transgenic lines, as they did not form a common group with the WT RR. In both PCA analyses, samples at the BR stage from the OEX#2 and RNAi#7 lines formed one group with WT. We conclude that the modification of *SlP4H3* significantly affects the progression of the ripening process, causing changes in the profiles of the AGPs structure.

Molecular studies were performed for the verification of the differences between the tomato lines in detail. In contrast to the β-glucosyl Yariv Reagent assays, anti-AGP antibodies recognizing specific carbohydrate epitopes used in these methods constitute a differentiating factor (Gao et al., 1999). Firstly, the immunoprinting on the nitrocellulose membrane confirmed the presence of AGP epitopes in tomato extracts and highlighted that the overexpression lines were characterised by a general trend towards increased content of the tested AGP epitopes. Secondly, a detailed analysis of the composition of individual epitopes showed further differences indicating disturbance in the carbohydrate chains of AGPs as a result of the modifications in P4H3 activities. In the study conducted by Fragkostefanakis and coworkers on tomato pericarp tissue with a ripening process without disorders, changes in the amount of AGP epitopes and a significantly higher number of the JIM13 epitope were noted (Fragkostefanakis et al., 2012). Western blotting analyses of the JIM13 epitopes revealed a slight decrease in high molecular weight epitopes in the last ripening stages. In the case of the JIM8 antibody, a gradually decrease in the presence of AGPs was also observed after the turning stage (Fragkostefanakis et al., 2012). On the other hand, in the study carried out by Sun and coworkers, only one fraction contained AGPs with a molecular weight of 48 kDa was collected using the LeAGP-1 antibody (Sun et al., 2004). In the first report on the molecular mass of AGPs extracted from fruit, AGP epitopes recognised by JIM8 and JIM13 epitopes in tomato pericarp tissue were in the range of 210-55 kDa and 300-45 kDa, respectively (Fragkostefanakis et al., 2012). In our previous papers, the molecular mass of AGPs was about 250-70 kDa from apple fruit (Leszczuk et al., 2020c) and 120-20 kDa from tomato fruit (Kutyrieva-Nowak et al., 2023a), which may indicate a variable pattern of AGPs in different fruits. In addition, in the case of the JIM13 epitope in WT at the beginning ripening stages, AGPs with 120–60 kDa and 60–25 kDa molecular weight predominated, and at the last stages contained 30–20 kDa AGPs, which were considered a marker of the finalisation of the ripening process (Kutyrieva-Nowak et al., 2023a). In the current work, AGPs from the transgenic lines were characterised by an altered molecular mass in comparison to WT. The molecular differences and the absence of single low molecular weight bands in the last stages of ripening

indicate an effect of the P4H3 activity disruption on AGP structural modifications. The changes observed also pointed to the disturbed process of degradation of 'native' carbohydrate chains with the ripening progress.

Selective glycome profiling of AGPs using an enzyme-linked immunosorbent assay allows rapid analysis of carbohydrate epitopes (Pattathil et al., 2010). Data from previous papers provided information about the relative absorbance of AGP epitopes for the JIM13 antibody. The strength of ELISA signals was characterised by absorbance at 0.05-0.08 in the case of banana fruit and at 0.71-1.18 in the case of mango fruit (Rongkaumpan et al., 2019). Research on tomato fruit from wild-type plants showed an average absorbance level of 0.5-3.5, with significant changes correlated with the ongoing ripening process (Kutyrieva-Nowak et al., 2023a). The present data showed that the absorbance level dependent on the tested lines was different from that of AGPs extracted from fruit in previous studies. This mainly involved the use of JIM13 and LM2 antibodies, where we noted absorbance levels at 2.5-4 and 2.9-4.2, respectively. The results obtained with the LM14 antibody seemed interesting as the absorbance of the transgenic lines was 0.5-0.9 compared to the absorbance of around 2.0 for WT. The glycome profiling with the LM1 antibody did not allow definite determination of the dependence of absorbance changes during the ripening process, as it was quite variable at the different stages of ripening. The changes found were related to disruptions in the concentration of specific epitopes caused by modifications in *SlP4H3* gene expression. Interestingly, the increase in the AGP concentration in the overexpression lines and the decrease in the AGP concentration in the lines with silenced P4H3 expression were confirmed by this method as well. All structural and molecular approaches used in this part of the work clearly indicate a linkage between P4H3 activity and the AGP carbohydrate moiety structure.

Ex situ studies showed that AGPs extracted from the examined transgenic lines were characterised by different molecular structures of carbohydrate chains, which is also connected with particular alterations linked with the stages of ripening. Thus, our next goal was to investigate how the structural changes affected the AGP localisation in the cell wall area. This issue is even more interesting and necessary to analyse, as previous studies have identified the characteristic spatio-temporal pattern of AGP distribution in the cell wall-plasma membrane continuum at the cellular and subcellular levels (Leszczuk et al., 2018; Kutyrieva-Nowak et al., 2023a). Next, subcellular studies of fruit proved that AGP epitopes changed their location and demonstrated a decrease in the number of AGP epitopes with the progression of the fruit senescence process, which is linked to degradative processes in the cell wall and the release of its cellular compartments (Leszczuk et al., 2018). Research conducted by Szymanska-Chargot and coworkers provided information on changes in polysaccharide distribution during post-harvest apple storage (Szymanska-Chargot et al., 2016). Also, comprehensive microarray polymer profiling demonstrated an increase in JIM13 and LM2 epitopes during the ripening process of grapes (Moore et al., 2014). Moreover, the ripening-associated changes had an impact on not only the localisation and distribution of AGPs and other cell wall components but also the fruit texture, causing differences in the anatomical features in the fruit tissue (Winisdorffer et al., 2015; Leszczuk et al., 2019b). This confirms that the correct glycosylation is essential for proper cell wall assembly and extracellular matrix functioning (Velasquez et al., 2011). Also, the analyses conducted in the present work revealed a decrease in the total number of epitopes during the ripening process with a concomitant increase in AGPs in the cytoplasm, compared to the cell wall-membrane continuum. Nevertheless, the significant disruption of the specific and well-documented AGP localisation pattern in all the examined transgenic lines must be underlined. In addition, the disorder of the proportion of AGPs attached to the cell wall and placed in other cellular compartments was also observed for all the transgenic lines. Numerous observations at the tissue level allow concluding that the overall appearance and structure of fruit tissue are also modified. The visible different localisation of AGPs related to the structural and molecular disruption caused by the change in the P4H3 activity is connected with modifications of fruit tissue morphology.

All analyses performed in the present study create complementary evidence that the effect of modifications of *SlP4H3* gene expression is supported by changes in the AGP amount, structure, and compositional properties, and thus impaired distribution of AGPs in fruit cells.

6 Conclusions

To sum up, the study demonstrated the disturbance i.e. changes in the AGP content, disruption of AGP molecular mass, alterations in the molecular composition, changes in the amount of AGPs bound by Yariv Reagent, structural differences indicating various degrees of ripening progress, and the disordered distribution pattern in the cell wall, plasma membrane, and cellular compartments.

Based on the obtained results, we focused on presenting the sequence of events that may take place in the fruit cells in response to changed P4H3 activity:

1) Disturbance of the 'native' AGP structure. The changed content of hydroxyproline residues affects the protein moiety of AGPs, which is associated with altered attachment of carbohydrate chains;
2) Disruption of the AGP molecular structure (mainly carbohydrate chains) causes changes in their localisation at the subcellular level;
3) Changes in the spatio-temporal AGP distribution may be related to the formation of a stable network between AGPs with other cell wall components (APAP1).
4) The lack of properly formulated carbohydrate chains affects the interlinking in the APAP1 network. In turn, the modified stability of the cell wall assembly has an influence on anatomical changes visible at the cellular level.
5) Changes in the continuity and durability of the cell wall affect the entire fruit tissue and the sequence of tissue transformation during the progression of the ripening process.

We conclude that the impaired P4H3 activity has an effect on the AGP molecular and structural features and, consequently, affects the degradation of AGPs during the ongoing ripening process. We may suppose that the 'native' structure of AGPs, mainly their carbohydrate moieties, is important for the strictly scheduled extracellular matrix arrangement and is essential for the correct course of the fruit ripening process. An interesting result is that the modifications caused changes in the anatomical image of the entire fruit tissue. In subsequent studies, it is necessary to focus on other components of the cell wall as part of the APAP1 complex that may be changed as a result of disturbed P4H activity.

Data availability statement

The raw data supporting the conclusions of this article will be made available by the authors, without undue reservation.

Author contributions

NK-N: Data curation, Investigation, Methodology, Software, Visualization, Writing – original draft, Writing – review & editing. AL: Conceptualization, Data curation, Formal analysis, Funding acquisition, Investigation, Methodology, Project administration, Resources, Software, Supervision, Validation, Visualization, Writing – original draft, Writing – review & editing. LE: Investigation, Writing – review & editing. DK: Investigation, Writing – review & editing. AZa: Data curation, Investigation, Writing – original draft. MS-C: Investigation, Writing – review & editing. TS: Investigation, Writing – review & editing. AK: Investigation, Writing – review & editing. KM: Writing – review & editing. EL: Writing – review & editing. PK: Conceptualization, Investigation, Writing – review & editing. AZd: Writing – review & editing.

Funding

The author(s) declare that financial support was received for the research, authorship, and/or publication of this article. The authors gratefully acknowledge the financial support by the National Science Center Poland (Sonata16, no 2020/39/D/NZ9/00232). Also, this work has been financed by the European Regional Development Fund of the European Union and Greek national funds through the Operational Competitiveness, Entrepreneurship and Innovation, under the call RESEARCH-CREATE-INNOVATE (T2EDK-01332: n-Tomatomics - Development of new tomato cultivars by using -omics technologies).

Acknowledgments

We would like to thank Mr Emil Zięba for his excellent technical assistance.

Conflict of interest

The authors declare that the research was conducted in the absence of any commercial or financial relationships that could be construed as a potential conflict of interest.

The author(s) declared that they were an editorial board member of Frontiers, at the time of submission. This had no impact on the peer review process and the final decision.

Publisher's note

All claims expressed in this article are solely those of the authors and do not necessarily represent those of their affiliated organizations, or those of the publisher, the editors and the reviewers. Any product that may be evaluated in this article, or claim that may be made by its manufacturer, is not guaranteed or endorsed by the publisher.

Supplementary material

The Supplementary Material for this article can be found online at: https://www.frontiersin.org/articles/10.3389/fpls.2024.1365490/full#supplementary-material

References

Bashir, M., and Haripriya, S. (2016). Assessment of physical and structural characteristics of almond gum. *Int. J. Biol. Macromol* 93, 476–482. doi: 10.1016/j.ijbiomac.2016.09.009

Batu, A. (2004). Determination of acceptable firmness and colour values of tomatoes. *J. Food Eng.* 61, 471–475. doi: 10.1016/S0260-8774(03)00141-9

Borassi, C., Gloazzo Dorosz, J., Ricardi, M. M., Carignani Sardoy, M., Pol Fachin, L., Marzol, E., et al. (2020). A cell surface arabinogalactan-peptide influences root hair cell fate. *New Phytol.* 227, 732–743. doi: 10.1111/nph.16487

Boulet, J. C., Williams, P., and Doco, T. (2007). A Fourier transform infrared spectroscopy study of wine polysaccharides. *Carbohydr Polym* 69, 79–85. doi: 10.1016/j.carbpol.2006.09.003

Chylińska, M., Szymanska-Chargot, M., and Zdunek, A. (2016). FT-IR and FT-Raman characterization of non-cellulosic polysaccharides fractions isolated from plant cell wall. *Carbohydr Polym* 154, 48–54. doi: 10.1016/j.carbpol.2016.07.121

Coimbra, M. A., Barros, A., Barros, M., Rutledge, D. N., and Delgadillo, I. (1998). Multivariate analysis of uronic acid and neutral sugars in whole pectic samples by FT-IR spectroscopy. *Carbohydr Polym* 37, 241–248. doi: 10.1016/S0144-8617(98)00066-6

Cooper, J. B., Heuser, J. E., and Varner, J. E. (1994). 3,4-Dehydroproline inhibits cell wall assembly and cell division in tobacco protoplasts. *Plant Physiol.* 104, 747–752. doi: 10.1104/pp.104.2.747

Cooper, J. B., and Varner, J. E. (1983). Insolubilization of hydroxyproline-rich cell wall glycoprotein in aerated carrot root slices. *Biochem. Biophys. Res. Commun.* 112, 161–167. doi: 10.1016/0006-291X(83)91811-9

Corral-Martínez, P., García-Fortea, E., Bernard, S., Driouich, A., and Seguí-Simarro, J. M. (2016). Ultrastructural immunolocalization of arabinogalactan protein, pectin and hemicellulose epitopes through anther development in *Brassica napus*. *Plant Cell Physiol.* 57, 2161–2174. doi: 10.1093/pcp/pcw133

Ellis, M., Egelund, J., Schultz, C. J., and Bacic, A. (2010). Arabinogalactan-proteins: Key regulators at the cell surface? *Plant Physiol.* 153, 403–419. doi: 10.1104/pp.110.156000

Feder, A., Jensen, S., Wang, A., Courtney, L., Middleton, L., Eck, J. V., et al. (2020). Tomato fruit as a model for tissue-specific gene silencing in crop plants. *Hortic. Res.* 7, 142–148. doi: 10.1038/s41438-020-00363-4

Fragkostefanakis, S., Dandachi, F., and Kalaitzis, P. (2012). Expression of arabinogalactan proteins during tomato fruit ripening and in response to mechanical wounding, hypoxia and anoxia. *Plant Physiol. Biochem.* 52, 112–118. doi: 10.1016/j.plaphy.2011.12.001

Fragkostefanakis, S., Sedeek, K. E. M., Raad, M., Zaki, M. S., and Kalaitzis, P. (2014). Virus induced gene silencing of three putative prolyl 4-hydroxylases enhances plant growth in tomato (*Solanum lycopersicum*). *Plant Mol. Biol.* 85, 459–471. doi: 10.1007/s11103-014-0197-6

Gao, M., Kieliszewski, M. J., Lamport, D. T. A., and Showalter, A. (1999). Isolation, characterization and immunolocalization of a novel, modular tomato arabinogalactan-protein corresponding to the LeAGP-1 gene. *Plant J.* 18, 43–55. doi: 10.1046/j.1365-313X.1999.00428.x

Hieta, R., and Myllyharju, J. (2002). Cloning and characterization of a low molecular weight prolyl 4-hydroxylase from *Arabidopsis thaliana*. Effective hydroxylation of proline-rich, collagen-like, and hypoxia-inducible transcription factor alpha-like peptides. *J. Biol. Chem.* 277, 23965–23971. doi: 10.1074/jbc.M201865200

Hijazi, M., Roujol, D., Nguyen-Kim, H., Del Rocio Cisneros Castillo, L., Saland, E., Jamet, E., et al. (2014a). Arabinogalactan protein 31 (AGP31), a putative network-forming protein in *Arabidopsis thaliana* cell walls? *Ann. Bot.* 114, 1087–1097. doi: 10.1093/aob/mcu038

Hijazi, M., Velasquez, S. M., Jamet, E., Estevez, J. M., and Albenne, C. (2014b). An update on post-translational modifications of hydroxyproline-rich glycoproteins: Toward a model highlighting their contribution to plant cell wall architecture. *Front. Plant Sci.* 5, 1–10. doi: 10.3389/fpls.2014.00395

Kalaitzis, P., Giannoutsou, E., and Konkina, A. (2023). "Role of the cell wall in the regulation of fruit ripening," in *Plant Cell Walls: Research Milestones and Conceptual Insights* (Boca Raton: CRC Press), 147–161.

Kitazawa, K., Tryfona, T., Yoshimi, Y., Hayashi, Y., Kawauchi, S., Antonov, L., et al. (2013). β-galactosyl Yariv reagent binds to the β-1,3-galactan of arabinogalactan proteins. *Plant Physiol.* 161, 1117–1126. doi: 10.1104/pp.112.211722

Kivirikko, K. I., and Myllyharju, J. (1998). Prolyl 4-hydroxylases and their protein disulfide isomerase subunit. *Matrix Biol.* 16, 357–368. doi: 10.1016/S0945-053X(98)90009-9

Knox, J. P., Linstead, P. J., Peart, J., Cooper, C., and Roberts, K. (1991). Developmentally regulated epitopes of cell surface arabinogalactan proteins and their relation to root tissue pattern formation. *Plant J.* 1, 317–326. doi: 10.1046/j.1365-313X.1991.t01-9-00999.x

Konkina, A., Klepadlo, M., Lakehal, A., Zein, Z. E., Krokida, A., Botros, M., et al. (2021). An *Arabidopsis* prolyl 4-hydroxylase is involved in the low oxygen response. *Front. Plant Sci.* 12, 1–12. doi: 10.3389/fpls.2021.637352

Koski, M. K., Hieta, R., Hirsilä, M., Rönkä, A., Myllyharju, J., and Wierenga, R. K. (2009). The crystal structure of an algal prolyl 4-hydroxylase complexed with a proline-rich peptide reveals a novel buried tripeptide binding motif. *J. Biol. Chem.* 284, 25290–25301. doi: 10.1074/jbc.M109.014050

Kutyrieva-Nowak, N., Leszczuk, A., Zając, A., Kalaitzis, P., and Zdunek, A. (2023a). Arabinogalactan protein is a molecular and cytological marker of particular stages of the tomato fruit ripening process. *Sci. Hortic.* 310, 1–10. doi: 10.1016/j.scienta.2022.111718

Kutyrieva-Nowak, N., Leszczuk, A., and Zdunek, A. (2023b). A practical guide to in *situ* and *ex situ* characterisation of arabinogalactan proteins (AGPs) in fruits. *Plant Methods* 19, 1–18. doi: 10.1186/s13007-023-01100-3

Laemmli, U. K. (1970). Cleavage of structural proteins during the assembly of the head of bacteriophage T4. *Nature* 227, 680–685. doi: 10.1038/227680a0

Lamport, D. T. A. (2013). Preparation of arabinogalactan glycoproteins from plant tissue. *Bio Protoc.* 3. doi: 10.21769/BioProtoc.918

Lamport, D. T. A., Tan, L., Held, M., and Kieliszewski, M. J. (2018). Pollen tube growth and guidance: Occam's razor sharpened on a molecular arabinogalactan glycoprotein Rosetta Stone. *New Phytol.* 217, 491–500. doi: 10.1111/nph.14845

Lamport, D. T. A., and Várnai, P. (2013). Periplasmic arabinogalactan glycoproteins act as a calcium capacitor that regulates plant growth and development. *New Phytol.* 197, 58–64. doi: 10.1111/nph.12005

Leszczuk, A., Chylinska, M., and Zdunek, A. (2019a). Distribution of arabinogalactan proteins and pectins in the cells of apple (*Malus* × *domestica*) fruit during post-harvest storage. *Ann. Bot.* 123, 47–55. doi: 10.1093/aob/mcy133

Leszczuk, A., Chylińska, M., and Zdunek, A. (2019b). Enzymes and vitamin C as factors influencing the presence of arabinogalactan proteins (AGPs) in *Solanum lycopersicum* fruit. *Plant Physiol. Biochem.* 139, 681–690. doi: 10.1016/j.plaphy.2019.04.035

Leszczuk, A., Chylińska, M., Zięba, E., Skrzypek, T., Szczuka, E., and Zdunek, A. (2018). Structural network of arabinogalactan proteins (AGPs) and pectins in apple fruit during ripening and senescence processes. *Plant Sci.* 275, 36–48. doi: 10.1016/j.plantsci.2018.07.019

Leszczuk, A., Cybulska, J., Skrzypek, T., and Zdunek, A. (2020a). Properties of arabinogalactan proteins (AGPs) in apple (*Malus* × *domestica*) fruit at different stages of ripening. *Biology* 9, 1–12. doi: 10.3390/biology9080225

Leszczuk, A., Kalaitzis, P., Blazakis, K. N., and Zdunek, A. (2020b). The role of arabinogalactan proteins (AGPs) in fruit ripening – a review. *Hortic. Res.* 7, 1–12. doi: 10.1038/s41438-020-00397-8

Leszczuk, A., Kalaitzis, P., Kulik, J., and Zdunek, A. (2023). Review: structure and modifications of arabinogalactan proteins (AGPs). *BMC Plant Biol.* 23, 45. doi: 10.1186/s12870-023-04066-5

Leszczuk, A., Pieczywek, P. M., Gryta, A., Frąc, M., and Zdunek, A. (2019c). Immunocytochemical studies on the distribution of arabinogalactan proteins (AGPs) as a response to fungal infection in *Malus* × *domestica* fruit. *Sci. Rep.* 9, 1–14. doi: 10.1038/s41598-019-54022-3

Leszczuk, A., Zając, A., Kurzyna-Szklarek, M., Cybulska, J., and Zdunek, A. (2020c). Investigations of changes in the arabinogalactan proteins (AGPs) structure, size and composition during the fruit ripening process. *Sci. Rep.* 10, 1–14. doi: 10.1038/s41598-020-77749-w

Ling, Q., Mohd. Sadali, N., Soufi, Z., Zhou, Y., Huang, B., Zeng, Y., et al. (2021). The chloroplast-associated protein degradation pathway controls chromoplast development and fruit ripening in tomato. *Nat. Plants* 7, 655–666. doi: 10.1038/s41477-021-00916-y

Liu, Z., Persson, S., and Sánchez-Rodríguez, C. (2015). At the border: the plasma membrane-cell wall continuum. *J. Exp. Bot.* 66, 1553–1563. doi: 10.1093/jxb/erv019

Livak, K. J., and Schmittgen, T. D. (2001). Analysis of relative gene expression data using real-time quantitative PCR and the 2-ΔΔCT method. *Methods* 25, 402–408. doi: 10.1006/meth.2001.1262

Lopez-Hernandez, F., Tryfona, T., Rizza, A., Yu, X. L., Harris, M. O. B., Webb, A. A. R., et al. (2020). Calcium binding by arabinogalactan polysaccharides is important for normal plant development. *Plant Cell* 32, 3346–3369. doi: 10.1105/tpc.20.00027

Moller, I., Marcus, S. E., Haeger, A., Verhertbruggen, Y., Verhoef, R., Schols, H., et al. (2008). High-throughput screening of monoclonal antibodies against plant cell wall glycans by hierarchical clustering of their carbohydrate microarray binding profiles. *Glycoconj J.* 25, 37–48. doi: 10.1007/s10719-007-9059-7

Moore, J. P., Fangel, J. U., Willats, W. G. T., and Vivier, M. A. (2014). Pectic-b(1,4)-galactan, extensin and arabinogalactan-protein epitopes differentiate ripening stages in wine and table grape cell walls. *Ann. Bot.* 114, 1279–1294. doi: 10.1093/aob/mcu053

Nakatsuka, A., Murachi, S., Okunishi, H., Shiomi, S., Nakano, R., Kubo, Y., et al. (1998). Differential expression and internal feedback regulation of 1-aminocyclopropane-1-carboxylate synthase, 1-aminocyclopropane-1-carboxylate oxidase, and ethylene receptor genes in tomato fruit during development and ripening. *Plant Physiol.* 118, 1295–1305. doi: 10.1104/pp.118.4.1295

Nibbering, P., Petersen, B. L., Motawia, M. S., Jørgensen, B., Ulvskov, P., and Niittylä, T. (2020). Golgi-localized exo-β1,3-galactosidases involved in cell expansion and root growth in *Arabidopsis*. *J. Biol. Chem.* 295, 10581–10592. doi: 10.1074/jbc.RA120.013878

Nunan, K. J., Sims, I. M., Bacic, A., Robinson, S. P., and Fincher, G. B. (1997). Isolation and characterization of cell walls from the mesocarp of mature grape berries (*Vitis vinifera*). *Planta* 203, 93–100. doi: 10.1007/s00050169

Nunan, K. J., Sims, I. M., Bacic, A., Robinson, S. P., and Fincher, G. B. (1998). Changes in cell wall composition during ripening of grape berries. *Plant Physiol.* 118, 783–792. doi: 10.1104/pp.118.3.783

Orfila, C., Huisman, M. M. H., Willats, W. G. T., van Alebeek, G.-J. W. M., Schols, H. A., Seymour, G. B., et al. (2002). Altered cell wall disassembly during ripening of Cnr tomato fruit: implications for cell adhesion and fruit softening. *Planta* 215, 440–447. doi: 10.1007/s00425-002-0753-1

Pattathil, S., Avci, U., Baldwin, D., Swennes, A. G., Mcgill, J. A., Popper, Z., et al. (2010). A comprehensive toolkit of plant cell wall glycan-directed monoclonal antibodies. *Plant Physiol.* 153, 514–525. doi: 10.1104/pp.109.151985

Perrakis, A., Bita, C. E., Arhondakis, S., Krokida, A., Mekkaoui, K., Denic, D., et al. (2019). Suppression of a prolyl 4 hydroxylase results in delayed abscission of overripe tomato fruits. *Front. Plant Sci.* 10, 1–11. doi: 10.3389/fpls.2019.00348

Perrakis, A., Denic, D., Blazakis, K. N., Giannoutsou, E., Kaloudas, D., Bita, C. E., et al. (2021). A tomato prolyl-4-hydroxylase causes relocation of abscission zone and alters abscission kinetics. *bioRxiv*, 1–36. doi: 10.1101/2021.04.20.440677

Pfeifer, L., Shafee, T., Johnson, K. L., Bacic, A., and Classen, B. (2020). Arabinogalactan-proteins of *Zostera marina* L. contain unique glycan structures and provide insight into adaption processes to saline environments. *Sci. Rep.* 10, 1–10. doi: 10.1038/s41598-020-65135-5

Rongkaumpan, G., Amsbury, S., Andablo-Reyes, E., Linford, H., Connell, S., Knox, J. P., et al. (2019). Cell wall polymer composition and spatial distribution in ripe banana and mango fruit: implications for cell adhesion and texture perception. *Front. Plant Sci.* 10, 1–11. doi: 10.3389/fpls.2019.00858

Seifert, G. J., and Roberts, K. (2007). The biology of arabinogalactan proteins. *Annu. Rev. Plant Biol.* 58, 137–161. doi: 10.1146/annurev.arplant.58.032806.103801

Seymour, G. B., Chapman, N. H., Chew, B. L., and Rose, J. K. C. (2013). Regulation of ripening and opportunities for control in tomato and other fruits. *Plant Biotechnol. J.* 11, 269–278. doi: 10.1111/j.1467-7652.2012.00738.x

Showalter, A. (2001). Arabinogalactan – proteins: Structure, expression and function. *Cell Mol. Life Sci.* 58, 1399–1417. doi: 10.1007/PL00000784

Showalter, A. M., and Basu, D. (2016). Extensin and arabinogalactan-protein biosynthesis: Glycosyltransferases, research challenges, and biosensors. *Front. Plant Sci.* 7, 814. doi: 10.3389/fpls.2016.00814

Smallwood, M., Yates, E. A., Willats, W. G. T., Martin, H., and Knox, J. P. (1996). Immunochemical comparison of membrane-associated and secreted arabinogalactan-proteins in rice and carrot. *Planta* 198, 452–459. doi: 10.1007/BF00620063

Sun, W., Zhao, Z. D., Hare, M. C., Kieliszewski, M. J., and Showalter, A. M. (2004). Tomato LeAGP-1 is a plasma membrane-bound, glycosylphosphatidylinositol-anchored arabinogalactan-protein. *Physiol. Plant* 120, 319–327. doi: 10.1111/j.0031-9317.2004.0236.x

Szymanska-Chargot, M., Chylinska, M., Kruk, B., and Zdunek, A. (2015). Combining FT-IR spectroscopy and multivariate analysis for qualitative and quantitative analysis of the cell wall composition changes during apples development. *Carbohydr Polym* 115, 93–103. doi: 10.1016/j.carbpol.2014.08.039

Szymanska-Chargot, M., Chylińska, M., Pieczywek, P. M., Rösch, P., Schmitt, M., Jürgen, P., et al. (2016). Raman imaging of changes in the polysaccharides distribution in the cell wall during apple fruit development and senescence. *Planta* 243, 935–945. doi: 10.1007/s00425-015-2456-4

Szymanska-Chargot, M., and Zdunek, A. (2013). Use of FT-IR spectra and PCA to the bulk characterization of cell wall residues of fruits and vegetables along a fraction process. *Food Biophys.* 8, 29–42. doi: 10.1007/s11483-012-9279-7

Tan, L., Eberhard, S., Pattathil, S., Warder, C., Glushka, J., Yuan, C., et al. (2013). An *Arabidopsis* cell wall proteoglycan consists of pectin and arabinoxylan covalently linked to an arabinogalactan protein. *Plant Cell* 25, 270–287. doi: 10.1105/tpc.112.107334

Tan, L., Qiu, F., Lamport, D. T. A., and Kieliszewski, M. J. (2004). Structure of a hydroxyproline (Hyp)-arabinogalactan polysaccharide from repetitive Ala-Hyp expressed in transgenic *Nicotiana tabacum*. *J. Biol. Chem.* 279, 13156–13165. doi: 10.1074/jbc.M311864200

Tan, L., Zhang, L., Black, I., Glushka, J., Urbanowicz, B., Heiss, C., et al. (2023). Most of the rhamnogalacturonan-I from cultured *Arabidopsis* cell walls is covalently linked to arabinogalactan-protein. *Carbohydr Polym* 301, 1–12. doi: 10.1016/j.carbpol.2022.120340

Tsumuraya, Y., Ozeki, E., Ooki, Y., Yoshimi, Y., Hashizume, K., and Kotake, T. (2019). Properties of arabinogalactan-proteins in European pear (*Pyrus communis* L.) fruits. *Carbohydr Res.* 485, 1–9. doi: 10.1016/j.carres.2019.107816

Velasquez, S. M., Ricardi, M. M., Dorosz, J. G., Fernandez, P. V., Nadra, A. D., Pol-Fachin, L., et al. (2011). O-glycosylated cell wall proteins are essential in root hair growth. *Sci. (1979)* 332, 1401–1403. doi: 10.1126/science.1206657

Velasquez, S. M., Ricardi, M. M., Poulsen, C. P., Oikawa, A., Dilokpimol, A., Halim, A., et al. (2015). Complex regulation of prolyl-4-hydroxylases impacts root hair expansion. *Mol. Plant* 8, 734–746. doi: 10.1016/j.molp.2014.11.017

Vlad, F., Spano, T., Vlad, D., Daher, B., Ouelhadj, A., and Kalaitzis, P. (2007). Arabidopsis prolyl 4-hydroxylases are differentially expressed in response to hypoxia, anoxia and mechanical wounding. *Physiol. Plant* 130, 471–483. doi: 10.1111/j.1399-3054.2007.00915.x

Winisdorffer, G., Musse, M., Quellec, S., Barbacci, A., Gall, S. L., Mariette, F., et al. (2015). Analysis of the dynamic mechanical properties of apple tissue and relationships with the intracellular water status, gas distribution, histological properties and chemical composition. *Postharvest Biol. Technol.* 104, 1–16. doi: 10.1016/j.postharvbio.2015.02.010

Wu, J., Xu, Y., Zhu, B., Liu, K., Wang, S., Sheng, Y., et al. (2020). Characterization of an arabinogalactan from the fruit hulls of *Ficus pumila* Linn. and its immunomodulatory effect. *J. Funct. Foods* 73(104091), 1–11. doi: 10.1016/j.jff.2020.104091

Yamassaki, F. T., Campestrini, L. H., Zawadzki-Baggio, S. F., and Maurer, J. B. B. (2018). Chemical characterization and complement modulating activities of an arabinogalactan-protein-rich fraction from an aqueous extract of avocado leaves. *Int. J. Biol. Macromol* 120, 513–521. doi: 10.1016/j.ijbiomac.2018.08.072

Yan, Y., Takáč, T., Li, X., Chen, H., Wang, Y., Xu, E., et al. (2015). Variable content and distribution of arabinogalactan proteins in banana (*Musa* spp.) under low temperature stress. *Front. Plant Sci.* 6, 1–14. doi: 10.3389/fpls.2015.00353

Yates, E. A., and Knox, J. P. (1994). Investigations into the occurrence of plant cell surface epitopes in exudate gums. *Carbohydr Polym* 24, 281–286. doi: 10.1016/0144-8617(94)90072-8

Yates, E. A., Valdor, J.-F., Haslam, S. M., Morris, H. R., Dell, A., Mackie, W., et al. (1996). Characterization of carbohydrate structural features recognized by anti-arabinogalactan-protein monoclonal antibodies. *Glycobiology* 6, 131–139. doi: 10.1093/glycob/6.2.131

Zhang, Y., Held, M. A., and Showalter, A. M. (2020). Elucidating the roles of three β-glucuronosyltransferases (GLCATs) acting on arabinogalactan-proteins using a CRISPR-Cas9 multiplexing approach in *Arabidopsis*. *BMC Plant Biol.* 20, 1–20. doi: 10.1186/s12870-020-02420-5

Zhou, K. (2022). The regulation of the cell wall by glycosylphosphatidylinositol-anchored proteins in *Arabidopsis*. *Front. Cell Dev. Biol.* 10, 1–8. doi: 10.3389/fcell.2022.904714

Zhou, X.-L., Sun, P.-N., Bucheli, P., Huang, T.-H., and Wang, D. (2009). FT-IR methodology for quality control of arabinogalactan protein (AGP) extracted from green tea (*Camellia sinensis*). *J. Agric. Food Chem.* 57, 5121–5128. doi: 10.1021/jf803707a

9. Tekst publikacji P.4

Kutyrieva-Nowak N., Leszczuk A., Denic D., Bellaidi S., Blazakis K., Gemeliari P., Lis M., Kalaitzis P., Zdunek A. 2024.

***In vivo* and *ex vivo* study on cell wall components as part of the network in tomato fruit during the ripening process.**

Horticulture Research, 11: uhae145.

Horticulture Research

Horticulture Research, 2024, **11**: uhae145
https://doi.org/10.1093/hr/uhae145

Article

In vivo and *ex vivo* study on cell wall components as part of the network in tomato fruit during the ripening process

Nataliia Kutyrieva-Nowak[1], Agata Leszczuk[1,*], Dusan Denic[2], Samia Bellaidi[2], Konstantinos Blazakis[2], Petroula Gemeliari[2], Magdalena Lis[3], Panagiotis Kalaitzis[2,*] and Artur Zdunek[1]

[1]Institute of Agrophysics, Polish Academy of Sciences, 20-290 Lublin, Poland
[2]Department of Horticultural Genetics and Biotechnology, Mediterranean Agronomic Institute of Chania, Chania 73100, Greece
[3]Department of Biomedicine and Environmental Research, Institute of Biological Sciences, Faculty of Medicine, John Paul II Catholic University of Lublin, 20-708 Lublin, Poland
* Corresponding authors. E-mails: a.leszczuk@ipan.lublin.pl; panagiot@maich.gr

Abstract

Ripening is a process involving various morphological, physiological, and biochemical changes in fruits. This process is affected by modifications in the cell wall structure, particularly in the composition of polysaccharides and proteins. The cell wall assembly is a network of polysaccharides and proteoglycans named the arabinoxylan pectin arabinogalactan protein1 (APAP1). The complex consists of the arabinogalactan protein (AGP) core with the pectin domain including arabinogalactan (AG) type II, homogalacturonan (HG), and rhamnogalacturonan I (RG-I). The present paper aims to determine the impact of a disturbance in the synthesis of one constituent on the integrity of the cell wall. Therefore, in the current work, we have tested the impact of modified expression of the *SlP4H3* gene connected with proline hydroxylase (P4H) activity on AGP presence in the fruit matrix. Using an immunolabelling technique (CLSM), an immunogold method (TEM), molecular tools, and calcium mapping (SEM-EDS), we have demonstrated that disturbances in AGP synthesis affect the entire cell wall structure. Changes in the spatio-temporal AGP distribution may be related to the formation of a network between AGPs with other cell wall components. Moreover, the modified structure of the cell wall assembly induces morphological changes visible at the cellular level during the progression of the ripening process. These results support the hypothesis that AGPs and pectins are required for the proper progression of the physiological processes occurring in fruits.

Introduction

Ripening is a postdevelopment process composed of different morphological, physiological, and biochemical changes [1]. It includes a series of changes that alter a green unripe fruit into a red ripe fruit with an appropriate appearance, taste, and soft texture. The softening and textural modifications are due to changes in the composition of polymers and their binding in the cell matrix in fruit tissue [2]. The alterations include modification of the cell wall structure from the degradation of pectin and hemicellulose to the synthesis of new polymers [3, 4]. Fruit ripening is a coordinated developmental programme undoubtedly related to changes in the architecture of the primary cell wall mainly due to softening progression [5]. Recent research has challenged individual cell wall models and suggests that specific components are closely related to each other and have a much more direct impact on defining fruit properties [6,7]. On the other side, the complexity of the fruit tissue provides opportunities to improve mature fruit characteristics. Currently, it is desirable to select varieties whose fruits are tolerant to cracking, epidermal shrivelling, delay acceleration of softening progression, characterized by higher nutritional value, and resilient to climate change. Also, the analysis demonstrated that fruit disruption rate is associated most significantly with cellulose content and its interaction with other components [8]. It is also necessary to emphasize that the ripening programme is coordinated by the effects of epigenetic modifications, transcription factors, and plant hormones [9]. Moreover, studies at the molecular level show that biochemical changes coordinated by proteins entangled in signal transduction and membrane interactions also influence fruit quality. Therefore, in this context, structural studies such as subcellular localization of a protein and general bio-imaging are essential steps toward understanding its activities [10]. Only focusing on explaining the connections with cell wall metabolism, hormonal activity, and genetic modifications in fruit ripening allows for a complete description of the programmes taking place in fruit.

The structure of the cell wall is investigated in ongoing studies, and the functions of particular polysaccharides and proteins are being debated [11, 12]. The cell wall is a complex assembly consisting mainly of cellulose, hemicelluloses accompanied by pectins, and proteins [4, 13]. Cellulose is composed of a linear chain of 500–7500 of β-(1 → 4)-D-glucose (Glc) monomers assembled by hydrogen bonding to constitute microfibrils [14]. Also

Received: 25 January 2024; **Accepted:** 13 May 2024; **Published:** 24 May 2024; **Corrected and Typeset:** 1 July 2024

within the cell wall, there are numerous matrix glycans, known as hemicelluloses, i.e. a group of polysaccharides composed of Glc, xylose (Xyl) or mannose (Man), and xyloglucan (XyG) [15]. It is well known that XyG binds to the surface of microfibrils forming a network with cellulose [16]. Structural changes and rearrangements of linkages in hemicellulose and cellulose disrupt the middle lamella. The disruption of xyloglucan and other glycans affects the ripening progress by inducing the softening process in fruits [17]. Other hemicellulosic polymers, i.e. xylans with β-(1 → 4)-xylosyl backbone cross-linking polysaccharides in the structure of the cell wall, also affect cell wall integrity and architecture [18–20]. As linear glycan chains of β-(1,4)-linked mannose residues [18], mannans play a role in the softening and degradation of the cell wall during fruit ripening [21]. Another heterogeneous group of structural cell wall components are pectins composed of α-(1,4)-linked galacturonic acids (GalA). They are divided into three polymers: homogalacturonan (HG), rhamnogalacturonan I (RG-I), and complex rhamnogalacturonan II (RG-II) [18, 22, 23]. HG is an abundant linear pectic subtype, representing 55%–70% of pectin. It is classified according to the esterification degree into high-methoxylated HG and low-methoxylated HG [24, 25]. RG-I and RG-II are pectin subtypes mainly found in primary plant cell walls. RG-I is composed of GalA and rhamnose (Rha) residues with side chains of arabinan, arabinogalactan, and galactan [26]. RG-II is composed of glycosyl residues comparable to the repeating GalA and Rha residues in RG-I. It has a highly conserved and complex structure with approximately ten different saccharides in side chains [27].

Modifications of carbohydrate chains have a significant effect on the ripening process [4]. The cell wall degradation is associated with pectin solubilization and depolymerization and a decrease in the number of pectic side chains [28, 29]. The HG depolymerization reduces intercellular adhesion, thereby having an impact on turgor and contributing to tissue softening [30–32]. In turn, the degradation of HG molecules during the ripening process leads to the disassembly of the links between cellulose and hemicellulose [23, 25]. Also, RG-I and RG-II are involved in cell-to-cell signalling and the formation of the pectic network, and degradation of these pectins exerts an effect on the cell wall mechanical properties [33, 34].

Furthermore, cell wall proteins (CWPs) are important structural and functional constituents of the plant cell walls [13]. Proteins are categorized as hydroxyproline-rich glycoproteins (HRGPs) with arabinogalactan proteins (AGPs), glycine-rich proteins (GRPs), and proline-rich proteins (PRPs) [18, 35, 36]. They have numerous functions in the plant cell, including signal transduction, cell-to-cell interactions, cell wall-to-plasma membrane interactions, and provide additional support and rigidity to the cell wall [13, 37]. Extensins, belonging to HRGP, are involved in plant cell development as regulators of cell wall expansion, chains binding the cell wall with the plasma membrane, and polymers forming the cellular architecture [38, 39]. AGPs are unusual proteoglycans localized between the cell wall and plasma membrane and have a variety of biological functions, whose basis has not been definitively identified [40]. They have a role in cell differentiation and cellular communication [41]. Also, AGPs probably have an impact on cell division, plant growth and development, reproductive processes, and programmed cell death [42]. Our previous research has shown that AGPs may have an effect on anatomical and morphological alterations in the fruit cell wall during the ripening process. In the last stages of ripening, we noted a decrease in the number of AGPs associated with disruption of the native cell wall structure [43, 44].

To emphasize the importance of the cell wall, it is necessary to mention that cell wall components interact with each other and form complex extracellular networks that control cell growth and help maintain cell shape. Generally, non-covalent interactions are found between pectic HG domains, cellulose chains, and cellulose with xylan and xyloglucan [20, 23, 45]. In turn, covalent interactions are found between HRGPs, pectin RG-I and RG-II monomers, and polysaccharides with lignins [23, 45, 46]. In the cell wall integrity context, AGPs play an important role, as they form the system of polysaccharides and proteoglycans in the cell wall–plasma membrane continuum [47] by creating the arabinoxylan pectin arabinogalactan protein1 (APAP1) [45]. The APAP1 is an AGP core with the classical AG attached. The APAP1 pectin domain includes HG and RG-I, in which short HG oligosaccharides are located around RG-I (graphic scheme in Fig. 1). In addition, the APAP1 contains arabinoxylan, which is attached to the Ara residue from AG and to Rha in RG-I [12, 45]. The synthesis of the APAP1 probably occurs in the extracellular matrix by binding pectin and arabinoxylan glycans to AGPs [45,48]. The components of the APAP1 are synthesized in different cellular compartments. For example, AGP synthesis proceeds in several stages, starting with the synthesis of the protein backbone, the glycosylphosphatidylinositol (GPI) anchor in the endoplasmic reticulum, and the sugar chains in the Golgi apparatus and ending in the formation of the AGP molecule in the space between the cell wall and plasma membrane [35, 47]. Pectin and xylan synthesis proceeds in the Golgi apparatus [34, 45]. Scientific reports have so far confirmed that changes in the pathways for the synthesis of the particular components of the APAP1 can cause disruptions in its structure and function. Interestingly, changes in the binding between the components also affect the cell wall structure, and these alterations are associated with the shape, turgor, and size of fruit cells [4, 49, 50]. These connections provide strength and stiffness to the cell walls, which have an influence on the fruit structure during the developmental programme, ripening process, and senescence in postharvest storage [51]. For example, ripening is correlated with alterations in the fruit texture and firmness, i.e. a process of swelling of the middle lamella [52], which is related to changes in the negative charge and structure of pectin polymers [51]. The research conducted by Castro and coworkers revealed an inverse correlation between fruit firmness and depolymerization of cell walls [4].

Another feature emphasizing the important role of the connections between the cell wall components is the binding of calcium ions. Currently, it has been proved that GalA residues from pectins and GlcA residues from AGPs bind Ca^{2+} and form calcium bridges between cells [48, 53–56]. The hypothetical molecular basis of the mechanism of AGP action is based on calcium cross-linking. AGPs take part in physiological processes by interacting with Ca^{2+}, followed by the release of Ca^{2+} [57, 58]. This was confirmed by a study on β-glucuronyltransferase mutants (GlcAT) where the depletion of Ca^{2+} binding affected the stability of the cell wall–plasma membrane continuum, which stopped plant development [59, 60]. Other investigations of GLCAT14A, GLCAT14B, and GLCAT14C mutants showed that β-glucuronyltransferases 14 (GT) were accountable for the binding of GlcA residues to AGPs [61]. Besides, the decrease in GlcA in the double and triple mutants affected cell differentiation and plant growth. Most likely, these changes are related to reduced Ca^{2+} influx into particular cells [60, 61]. Thus, it can be concluded that, as part of AGP and pectins in the APAP1, GlcA has an effect on cell wall integrity and cell-to-cell signalling via Ca^{2+} binding [53, 56]. It is well-known that calcium ions are implicated in biological processes,

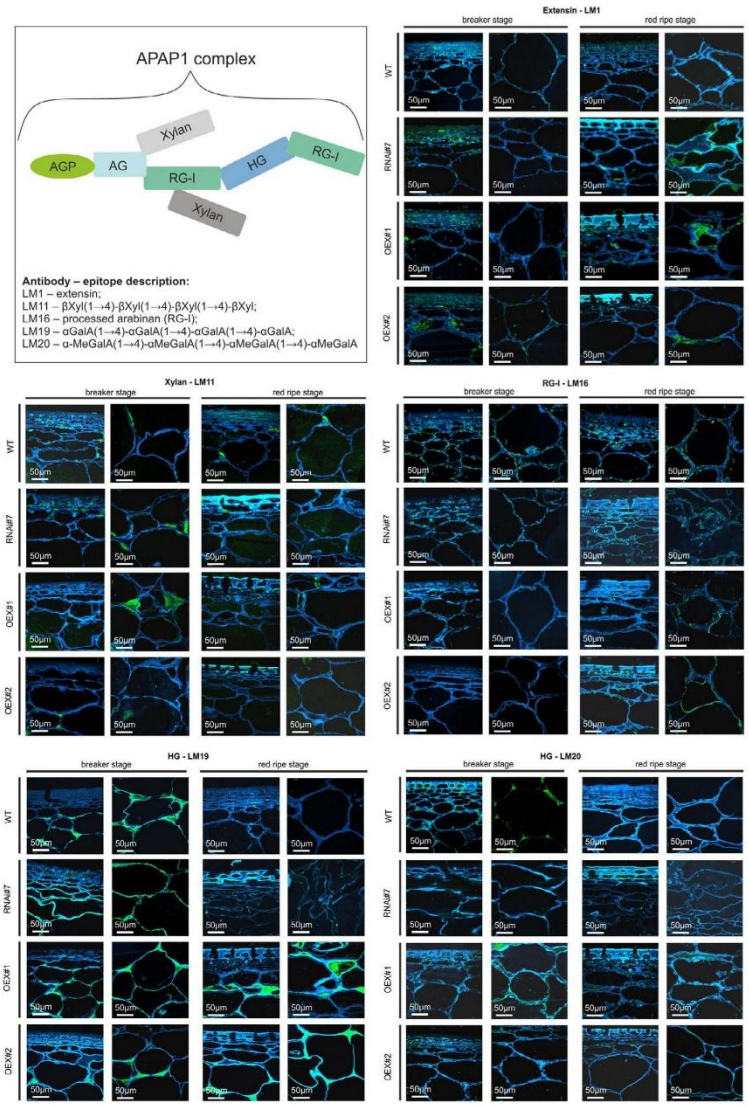

Figure 1. Hypothetical and simplified structure of the APAP1 [45, 75] with a description of the antibodies used. The spatio-temporal localization of extensin (LM1), xylan (LM11), rhamnogalacturonan type I (LM16), low methyl-esterified homogalacturonan (LM19), and high methyl-esterified homogalacturonan (LM20) in the fruit tissue of the WT plants and transgenic lines RNAi#7, OEX#1, and OEX#2 in different ripening stages. Abbreviations: AG, arabinogalactan; RG-I, rhamnogalacturonan I; HG, homogalacturonan Bars 50 μm for all images.

including cell division and elongation, and stabilization of the cell wall [62]. Moreover, calcium helps maintain the structural integrity of the cell wall and is a cofactor for various enzymes involved in fruit ripening, such as pectin methylesterase (PME) and polygalacturonase (PG) [33, 63]. The structural integrity is related to the ability of calcium ions to form cross-links between pectin molecules, which helps strengthen the cell walls and prevent the breakdown of cells during ripening, maintaining the firmness of fruit [63, 64]. Moreover, calcium ions interact as single signalling molecules or co-interact with plant hormones, such as abscisic acid (ABA), to regulate biochemical changes associated with ripening [65]. In addition, calcium ions control the synthesis and breakdown of various compounds, such as pigments, flavour compounds, and aroma volatiles. A study conducted by Xu and coworkers demonstrated that calcium ions have the ability to modulate fruit polyphenolic biosynthesis, e.g. anthocyanins in

strawberries, whose content increases significantly as the fruit ripens [66].

Combining all the above-mentioned features of the cell wall, structure of components, connections between them, and the calcium ion binding ability as well as their impact on the ripening process, we aim to determine the effect of a disturbance in the synthesis of one constituent on the integrity of the cell wall at the molecular level and, consequently, at the level of the entire fruit organ. In our previous studies on modified tomato fruits, we focused on analysis of the effect of modification of *SlP4H3* expression encoding the P4H3 enzyme, which is responsible for the posttranslational modification of AGP, on the presence of AGP in the cell wall [67]. The physiological role of *SlP4H3* in developmental programmes such as fruit ripening and abscission was well demonstrated in silencing and overexpression lines [67–69]. In these *SlP4H3* lines, changes were observed in the spatio-temporal AGP distribution in the red ripe fruit pericarp tissue as well as disruption of the AGP molecular structure and disturbance of the native AGP structure [67]. Moreover, silencing of *SlP4H3* resulted in a delay of overripe fruit abscission progression [69] and alterations in the position of the flower abscission zone [68]. In addition, the silencing of two tomato P4Hs, SlP4H5 and SlP4H7, by VIGS (Virus-Induced Gene Silencing) indicated a delay in ripening progression [7].

In our previous paper, we described that this modification affected the amount and spatio-temporal pattern of distribution of AGPs during the ripening process. We noted changes that led to disruption of the whole-cell wall structure [67]. Therefore, in the current work, we have tested the effect of this AGP modification on the APAP1 for the first time. The purpose of the present work is to identify changes in the content and distribution of other cell wall constituents during the fruit ripening process in transgenic lines with modified *SlP4H3* gene expression.

Results

Localization of cell wall components at the cellular level

Fruit visualization at the tissue level allows finding differences in morphology between WT and transgenic lines. The tissues of the modified fruits were more damaged in the RR stage than the tissue of the WT fruits. Moreover, the cell walls in the OEX#1, OEX#2, and RNAi#7 lines after the ripening process were more disturbed with visible interrupted continuity and excessive swelling (Fig. 1). Furthermore, the microscopic studies allowed the determination of the localization of the cell wall components, constituents of the APAP1, and changes in their distribution during the ripening process in the WT fruits and in the transgenic lines OEX#1, OEX#2, and RNAi#7. The use of specific antibodies and the CLSM observations revealed that the modification associated with the changes in the expression of the *SlP4H3* gene affected the assembly of extensin (LM1), xylan (LM11), rhamnogalacturonan (LM16), low methyl-esterified homogalacturonan (LM19), and high methyl-esterified homogalacturonan (LM20) in the cell walls. Representative photographs with immunocytochemical labelling are presented in Fig. 1 (cellular localization) and Fig. 2 (subcellular localization).

The analysis of immunocytochemical labelling with LM1 demonstrated the typical presence of extensin epitopes across the cell wall–plasma membrane continuum. In addition, the occurrence of single conglomerates of the LM1 epitope in the cytoplasm close to the border with the plasma membrane was detected. Moreover, high amounts of extensin epitopes were detected in the cells of the epidermal layer in the BR stages of all the examined lines. The ripening process resulted in a decrease in the number of extensin in the cell wall–plasma membrane continuum. In the RR stage, an increased number of epitopes were observed in the cytoplasm in all the tested lines. Most probably, the localization was associated with degradative processes in the cell wall and the release of previously bound epitopes. The comparison of fruit WT and transgenic lines at each ripening stage showed a significantly higher fluorescence signal in sections from fruit with the overexpression of the *SlP4H3* gene. Also, in the BR stage, the presence of a bigger accumulation of epitopes in the cytoplasm was observed. There were no noticeable differences in the abundance of LM1 epitopes between fruits with the silenced expression of the *SlP4H3* gene and WT.

The immunofluorescence labelling with the LM11 antibody localized the epitopes of xylan in the corners and at cellular junctions in fruit tissues of WT. In the case of all the transgenic lines, the immunolabelling analyses showed a slight increase in fluorescence intensity and revealed an increasing abundance of xylan epitopes during the progress of the ripening process. In addition, an increase in the number of groups of the LM11 epitope was observed near the plasma membrane.

The fluorescence signal after the immunofluorescence reaction with the LM16 antibody was quite weak and was mainly noted along the plasma membrane in association with the cell wall. The ripening process did not affect the presence of the epitope, and similar amounts of the LM16 epitope were observed in the BR and RR stages. The immunofluorescence intensity in the lines with the *SlP4H3* gene overexpression was similar to that in WT. However, the changes in the expression of the *SlP4H3* gene caused higher dispersion of the RG-I epitope within the plasma membrane. In line with the silenced expression of the *SlP4H3* gene, the LM16 epitope was visualized as single larger aggregations rather than a line at the cell wall periphery.

The immunofluorescence analysis with the LM19 and LM20 antibodies recognizing homogalacturonan with various esterification levels revealed the most considerable differences as a result of the alteration in the *SlP4H3* expression. Low methyl-esterified HG (LM19 epitope) in the fruit tissue in the different ripening stages was distributed according to specific spatial patterns in corners and at cellular junctions in the BR stage. The ripening process resulted in a decreased amount of the LM19 epitope forming single dots in the intercellular area. In the fruit tissue with the overexpression of the *SlP4H3* gene, significantly higher fluorescence intensity was observed compared to WT in both the first and last stages of the ripening process. In turn, the silencing of the *SlP4H3* gene caused the occurrence of HG epitopes without characteristic labelled corners. In addition, in the fruits with the silenced expression of the *SlP4H3* gene, a decrease in fluorescence intensity was found from the beginning of the ripening process.

The immunofluorescence reaction with LM20 antibody which recognized high methyl-esterified HG allows discrimination between high- and low-esterified HGs. In the WT fruits, the LM20 epitope was labelled in the cellular junctions and corners, and the immunofluorescence decreased with the ongoing ripening process. However, no significant changes in the immunofluorescence intensity were observed in the transgenic lines compared to WT. At the beginning of the ripening process, a slightly reduced amount of HG epitopes was identified in the fruits with the silenced expression of the *SlP4H3* gene; they were present as single dots in the fruit tissue within the cell wall. In the RR stage, the

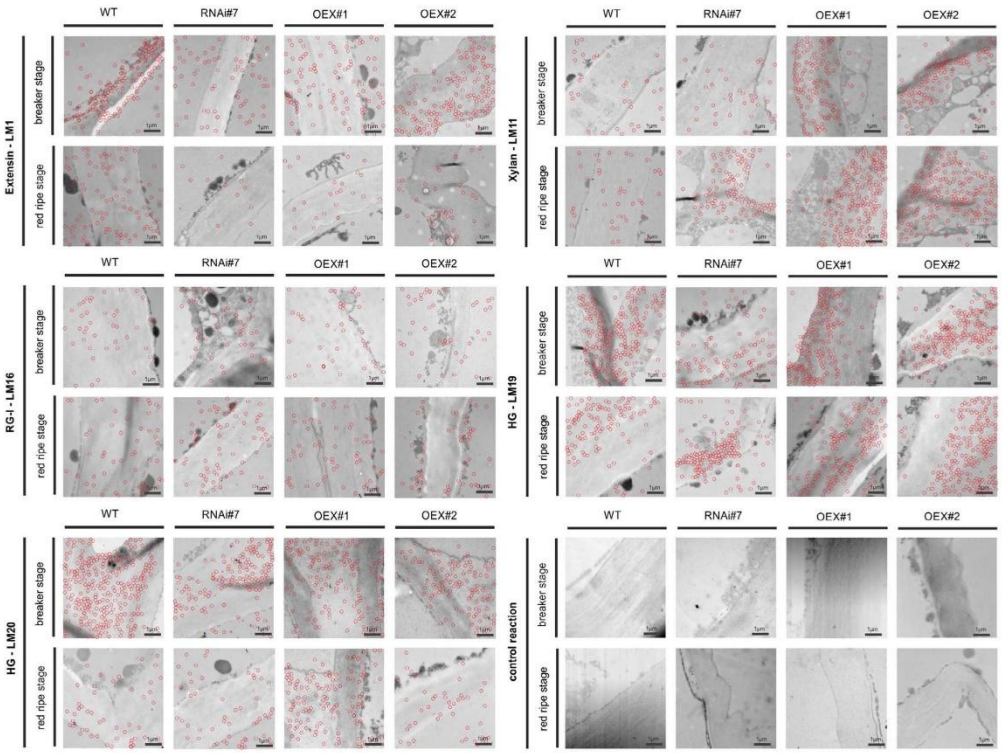

Figure 2. Immunogold labelling distribution of extensin (LM1), xylan (LM11), rhamnogalacturonan type I (LM16), low methyl-esterified homogalacturonan (LM19), and high methyl-esterified homogalacturonan (LM20) in the fruit tissue of the WT plants and transgenic lines RNAi#7, OEX#1, and OEX#2 in different ripening stages. Abbreviations: RG-I, rhamnogalacturonan I; HG, homogalacturonan. Control reaction with lack of incubation with primary antibody. Bars 1 μm for all images. Gold particles marked with red circles.

LM20 epitopes in the fruits with the overexpression of the *SlP4H3* gene were detected as single conglomerates.

Localization of cell wall components at the subcellular level

The localization of the LM1, LM11, LM16, LM19, and LM20 epitopes analysed by immunogold labelling imaged with TEM also confirmed changes in the distribution of these epitopes during the ripening process. Detection coupled with TEM allows mapping the arrangement of particular epitopes at the subcellular level (Fig. 2). Our interpretation focused mainly on quantitative alterations in their localization in the cell wall–plasma membrane and cytoplasm compartments (Fig. 3).

Epitopes visible as red circled dots were noted in all the samples as clusters accumulated mainly in the cell wall–plasma membrane continuum. TEM imaging showed alterations in their distribution, i.e. there was an increase in the number of epitopes dispersed along the cell wall and cytoplasm in the RR stage compared to the BR stage (Fig. 2). Briefly, the comparative analyses of the examined tomato lines revealed differences in the localization of specific epitopes between the fruits of the transgenic lines and WT. In the case of extensin recognized by LM1, there are visible differences between the stage of ripening. It should be emphasized that there was a significant decrease in the LM1 epitope content in transgenic lines in the RR stage, both in the cell wall and in the cytoplasm compared to WT. In the case of xylan recognized by LM11, there is a clear accumulation of epitopes in the cell walls in OEX lines. Subcellular detection of RG-I recognized by LM16 showed no changes. However, completely different images were detected in the case of homogalacturonans recognized by LM19 and LM20. LM19 epitopes formed irregular aggregates but were mainly observed in the cell wall and middle lamella. Interestingly, in the tissue of the OEX lines, the mapping indicated a higher content of dots in comparison to WT and showed agglomerates over the entire surface of the cells. During the microscopic observations of LM20 epitopes, it was difficult to note parts of the cell without labelled HG. Also, abundant dispersion throughout the cell was correlated with the progress of the ripening process (Fig. 2).

To evaluate the mentioned changes in more detail, a quantitative analysis was performed (Fig. 3). The immunogold labelling with the LM1 antibody identified epitopes within the cell wall–plasma membrane and in the cytoplasm. In the case of WT, a 30% decrease in the number of extensin epitopes was observed during the ripening process with a simultaneous increase in their presence in the cytoplasm. Moreover, in the fruit with the silenced expression of the *SlP4H3* gene, no LM1 epitopes were observed at any cellular compartments in the RR stage. In turn, the analyses

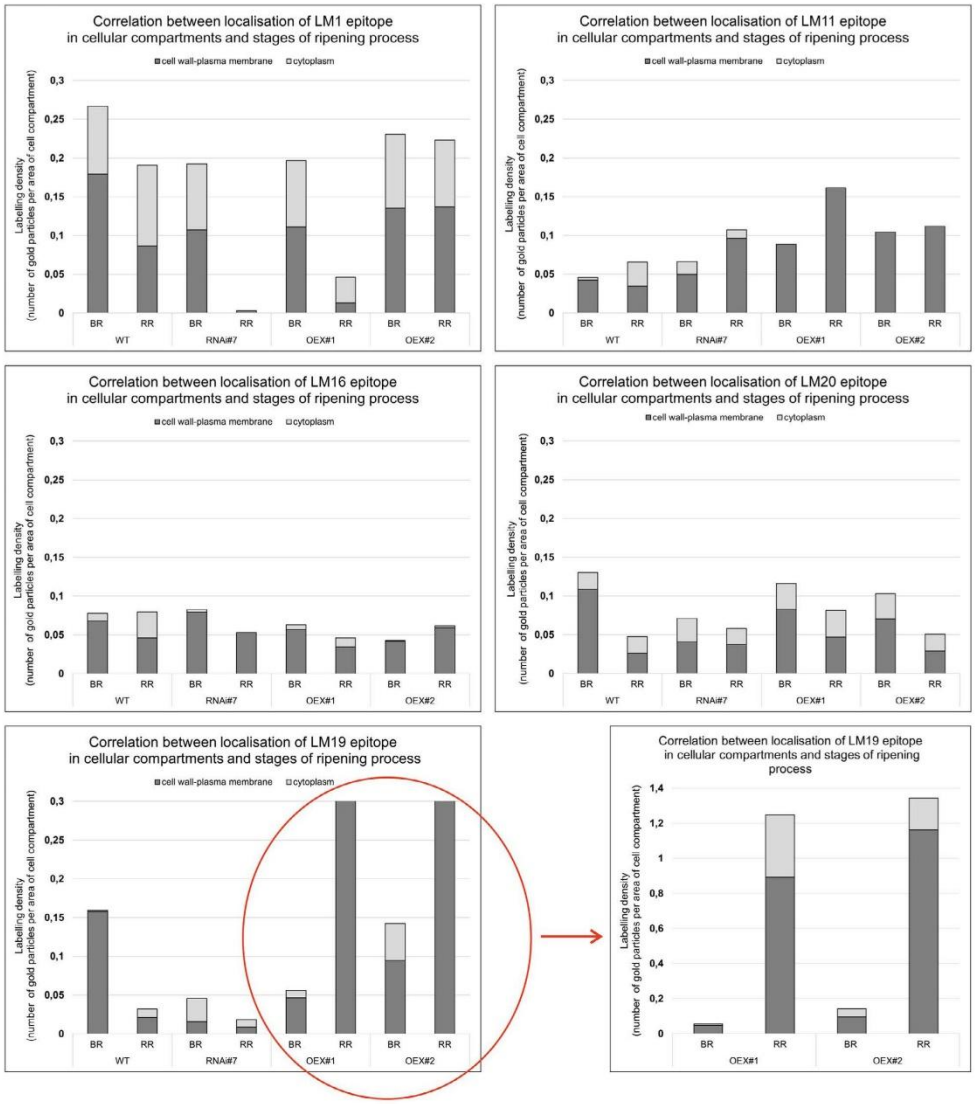

Figure 3. Quantitative analysis of immunogold labelling – analysis of changes in the distribution of epitopes (examined APAP1 components) in individual cellular compartments during the ripening process in the fruits of the WT plants and transgenic lines RNAi#7, OEX#1, and OEX#2.

of the OEX#1 fruits showed that almost 80% of LM1 epitopes underwent degradation during the ripening process. However, in the OEX#2 line, there were no significant differences in the number of labelled epitopes in the examined compartments in both ripening stages.

The subcellular analysis performed by immunogold labelling demonstrated the presence of LM11 epitopes mainly within the cell wall. In the case of WT, an increase in the number of epitopes in the cytoplasm in the last stage of ripening associated with the cell wall degradation process was found. Interestingly, the results of the immunogold analysis of the lines with the overexpression of the *SlP4H3* gene revealed the absence of the LM11 epitope in the cytoplasm in the ripening process. Besides, compared to WT, a higher number of LM11 epitopes were identified in the case of all transgenic lines in the BR and RR stages. The results obtained in the RR stage showed an increase in the total number of labelled LM11 epitopes (40% in WT, 60% in RNAi#7, 80% in OEX#1, and 10% in OEX#2).

The immunogold labelling with the LM16 antibody confirmed that epitopes RG-I dispersed along the cell wall–plasma

membrane continuum. In the WT fruits, the progress of the ripening process was accompanied by a significant increase in the number of LM16 epitopes in the cytoplasm (from 10% to 43% labelling density). The analyses of the transgenic lines did not show such a significant increase in the proportion of RG-I epitopes in the cytoplasm in the last stage of ripening. In the fruits with the silenced expression of the *SlP4H3* gene, the overall quantity of RG-I epitopes was not different from that in WT and no LM16 epitopes were observed in the cytoplasm in the RR stage. The result of the lines with the overexpression of the *SlP4H3* gene was interesting, as the total number of labelled LM16 epitopes decreased on average by 40% in comparison to WT.

The subcellular analysis of the distribution of the LM19 epitopes showed their presence in the whole area of the cell wall with a low number in the cytoplasm. In WT, a significant decrease in the number of labelled gold particles was observed with the progress of the ripening process. The results obtained in the fruit with the overexpression of the *SlP4H3* gene are interesting, as a significant increase in the number of LM19 epitopes was observed in the last stages of ripening compared to the BR stages (10-fold and 24-fold in OEX#1 and OEX#2, respectively) and the WT fruits.

The immunogold labelling with the LM20 antibody showed a similar spatial pattern of epitope distribution as in the case of LM19 mAb. However, it should be added that the number of labelled LM20 epitopes was lower compared to low methyl-esterified HG. Generally, in the case of the transgenic lines and WT, a decreased number of labelled epitopes was identified in the last stage of the ripening process. Moreover, an increase in the content of labelled HG epitopes in the cytoplasm was observed in the RR stage. In contrast, the analyses of the fruits with the silenced expression of the *SlP4H3* gene in the BR stage revealed an almost 2-fold decrease in the amount of labelled epitopes in comparison to WT. In turn, compared to WT, no significant changes in the number of LM20 epitopes were detected in the fruits with the overexpression of the *SlP4H3* gene.

Cell wall glycome profiling using ELISA

The microscopic analyses showed differences between specific epitopes in samples representing the different transgenic lines in the BR and RR stages of fruit ripening, suggesting that the glycome profiling using the ELISA facilitated better quantitative visualization of changes in the cell wall components. The results shown in Fig. 4 indicate the concentration of p-nitrophenol (PNP, mg/ml) obtained through alkaline phosphatase activity linked to the secondary antibody recognizing different primary antibodies. Generally, numerous disorders in the content of all the analysed constituents were confirmed, underlining the different degrees of their presence in comparison to WT. The analysis of the results obtained with the LM1 antibody revealed statistical differences between the WT and transgenic lines in the BR stage. We observed an increase in bound antibodies based on an increase in alkaline phosphatase activity in OEX#1 and OEX#2 (15 and 10 mg/ml PNP, respectively), compared to 5 mg/ml PNP in the case of WT. No significant differences were identified between the samples analysed in the RR stage, except RNAi#7. The analysis of the samples in the BR and RR stages allowed us to identify an increase in the LM11 epitope content in the transgenic lines. The alkaline phosphatase activity increased from 3–5 to 5–8 mg/ml PNP. In the RG-I analysis, an increase in LM16 epitopes was observed in the transgenic lines compared to WT. However, no significant changes in the presence of LM16 epitopes were identified during the progress of the ripening process. The glycome profiling of low methyl-esterified HG identified lower LM19 epitope content in the lines with the overexpression of the *SlP4H3* gene compared to WT. This was confirmed by the increase in alkaline phosphatase activity bound to antibodies from 6–11 to 11–14 mg/ml PNP. Surprisingly, as in previous *in vivo* analyses of the OEX lines, an increase in the number of LM19 labelled epitopes was observed as the ripening process progressed. Interestingly, the number of LM20 epitopes was lower than that of LM19 epitopes. The statistical analysis of the presence of the LM20 epitopes at the beginning of the ripening process showed no significant differences between the transgenic lines and WT. During the ongoing ripening process, an increased number of HG epitopes was observed in the transgenic lines compared to WT.

In vitro binding assay with glycome profiling

The presented assay of '*in vitro* reaction' between particular components of the cell wall and isolated AGPs from tomato fruits allows analyses of the potential binding between the components in the *in vitro* environment. The immunoprinting on nitrocellulose membranes shown in Table 1 demonstrates changes in the reaction intensity representing the presence or absence of possible binding. Overall, a strong signal of the immunoblotting reaction was observed for the binding of AGPs to RG-I and cellulose. In the case of binding with RG-I, only the reaction with AGPs isolated from RNAi#7 was slightly less intensive. In the other cases, the strongest signal was recorded for AGPs isolated from the WT and transgenic lines, regardless of the stage of ripening. In the case of binding between cellulose and AGPs isolated from the WT and RNAi#7 line, the reaction indicates high signal intensity. An exception was the samples from the OEX# fruit lines where there was a low-intensity reaction.

The analysis of the AGP binding to commercial cell wall components showed that xyloglucan and xylan did not yield an immunoprinting reaction signal in the transgenic lines and WT. Interestingly, the use of AGPs isolated from the fruits in different stages of ripening had no significant effect on the presence of reactions in the *in vitro* binding assay. It should be added that the increased concentrations of the commercial cell wall components had no effect on the binding with AGPs either.

The subsequent binding assay performed using the glycome profiling approach confirmed the ability of AGPs to bind to the cell wall components (Fig. 5a). The level of absorbance demonstrates the presence/absence of binding between AGPs and other cell wall components *in vitro*. Interestingly, the analysis again showed binding between AGPs and RG-I, cellulose, and arabinogalactan. The presence of binding of AGPs with the analysed polysaccharides was represented as a heat map (Fig. 5b), which helped to find differences between particular AGPs isolated from the WT and transgenic lines and two distinct ripening stages. The analysis of the AGP binding to arabinogalactan showed an increase in absorbance in the transgenic lines with the overexpression of the *SlP4H3* gene. Similar results were obtained in the analysis of binding to RG-I. In both RG-I and AG, the level of absorbance in the line with the silenced expression of the *SlP4H3* gene was similar to that in WT. In the case of the reaction between AGPs and cellulose, a decrease in binding was found in the transgenic lines, as the highest level of absorbance was recorded in WT.

The lowest level of absorbance was determined for AGP binding with xylan and xyloglucan. This analysis did not identify significant differences in the binding of AGPs isolated from the different ripening stages.

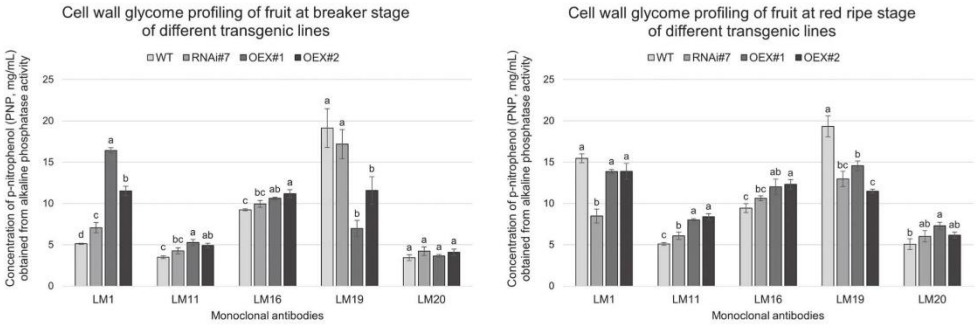

Figure 4. ELISA of cell wall components extracted from the fruits of the WT plants and transgenic lines RNAi#7, OEX#1, and OEX#2 in different ripening stages. ELISA with LM1, LM11, LM16, LM20, and LM19 antibodies. Different letters indicate significant differences amongst the WT and transgenic lines within a specific antibody (one-way ANOVA and Tuckey's HSD *post hoc* test with $P < 0.05$).

Table 1. Binding assay between commercial cell wall components (arabinogalactan, rhamnogalacturonan, xylan, xyloglucan, cellulose) and AGPs isolated from the fruits of WT plants and transgenic lines RNAi#7, OEX#1, and OEX#2 in different ripening stages

		Arabinogalactan (mg/ml)			Rhamnogalacturonan (mg/ml)			Xylan (mg/ml)			Xyloglucan (mg/ml)			Cellulose (mg/ml)		
		5	10	20	5	10	20	5	10	20	5	10	20	5	10	20
		–	±	±	+	+	+	–	–	–	±	±	±	+	+	+
WT	BR	–	–	–	+	+	+	–	–	–	–	–	–	+	+	+
	RR	–	±	+	±	±	±	–	–	–	±	±	+	+	+	+
RNAi#7	BR	–	–	–	+	+	+	–	–	–	–	–	–	+	+	+
	RR	–	–	–	+	+	+	–	–	–	–	–	–	+	+	+
OEX#1	BR	–	–	–	+	+	+	–	–	–	–	–	–	+	+	+
	RR	–	–	–	+	+	+	–	–	–	–	–	–	±	±	±
OEX#2	BR	–	–	–	+	+	+	–	–	–	–	–	–	±	±	±
	RR	–	–	–	+	+	+	–	–	–	–	–	–	±	±	±

Immunoprinting on nitrocellulose membrane using the JIM13 antibody. Abbreviations: BR, Breaker stage; RR, Red Ripe stage; '+', high signal intensity; '±', low signal intensity; '–', no signal.

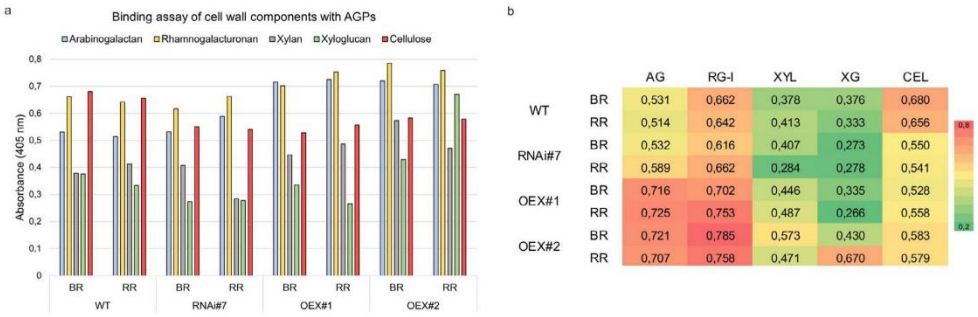

Figure 5. Binding assay between commercial cell wall components (arabinogalactan, rhamnogalacturonan I, xylan, xyloglucan, cellulose) and AGPs isolated from the fruits of the WT plants and transgenic lines RNAi#7, OEX#1, and OEX#2 (a) in different ripening stages. Glycome profiling with ELISA using JIM13 antibody. Heat map analysis of binding of cell wall components with AGPs (b). The numerical value in the heat map is the level of absorbance at 405 nm. Abbreviations: BR, Breaker stage; RR, Red Ripe stage; AG, arabinogalactan; RG-I, rhamnogalacturonan I; XYL, xylan; XG, xyloglucan; CEL, cellulose.

Calcium amount at the tissue level

The analysis of calcium in the tomato tissue revealed a statistically significant increase in calcium ions during ripening in all the transgenic lines and WT (Fig. 6). Compared to WT, higher content of calcium-normalized mass was observed in the transgenic lines with the progress of the ripening process. The representative spectral plots helped to conduct an elemental composition analysis directed at estimation of the total amount of calcium (Fig. 6). In the case of the WT fruits, two EDS spectra at different peak levels of the voltage range of elemental calcium were observed. In the BR stage, the first one was the peak level of 400 × 0.001 cps/eV and the other one was located at 50 × 0.001 cps/eV. Also, two peaks

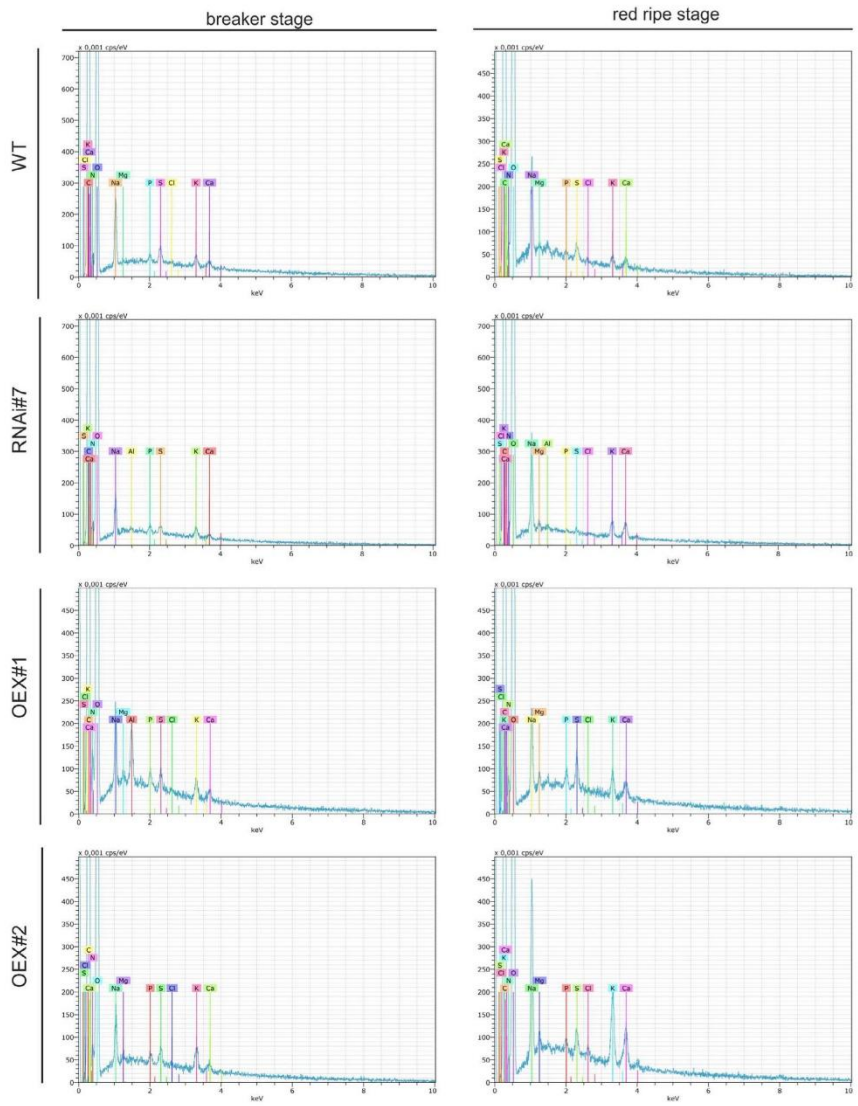

Figure 6. The spectral plots for the elemental composition of WT, RNAi#7, OEX#1, and OEX#2 tomato fruits.

at the levels of 300 × 0.001 cps/eV and 50 × 0.001 cps/eV were observed in the RR stage. A very similar EDS spectrum with two peaks for calcium was also observed in the tissue of the RNAi#7 line, but the peak levels were slightly lower in both BR and RR stages. However, the spectra in the OEX#1 and OEX#2 lines were the same in the BR and RR stages. Moreover, the peak levels were noted at 200 × 0.001 cps/eV and 50 × 0.001 cps/eV, significantly discriminating between the overexpressed line and the WT tissue.

By staining with the Fluo-3 AM indicator, the arrangement of calcium ions in the fruit tissue was visualized and the cellular changes occurring during the ripening process were determined (Fig. 7). The analysis of the tissues from all the transgenic lines and WT showed an increase in fluorescence intensity with the progress of the ripening process. High amounts of calcium ions were detected in epidermal layer cells in the RR stages in all the examined lines, compared to the BR stages. It should also be added that the fluorescence intensity in the fruit tissue of the lines with the overexpression of the *SlP4H3* gene was higher than in the WT and RNAi#7 line.

The results obtained allowed us to confirm the previously presented data showing that the ripening process was accompanied by changes in the distribution of calcium ions in the cell wall.

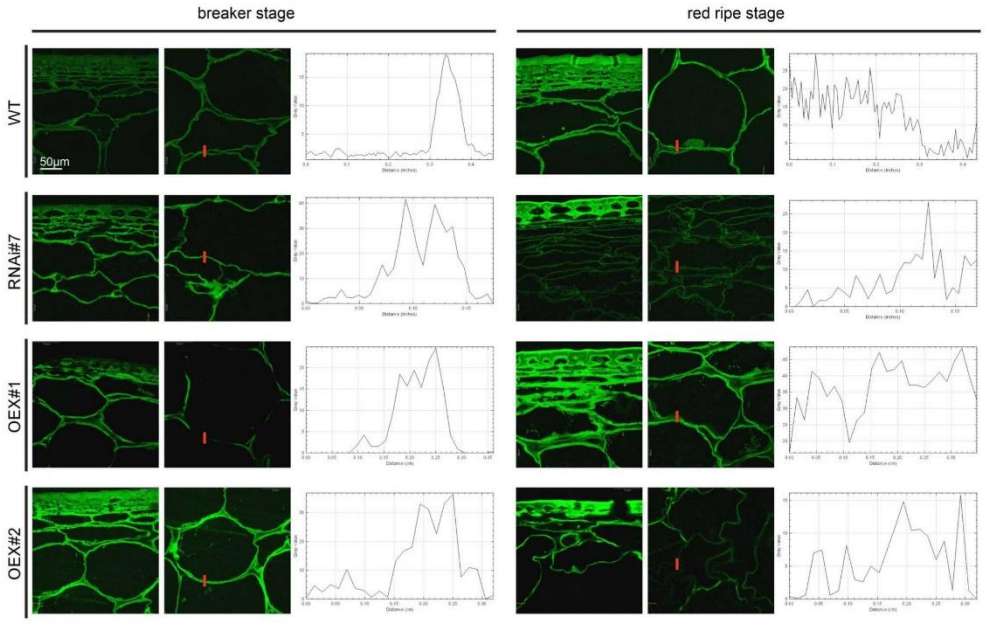

Figure 7. The calcium arrangement in the cell wall assembly of the fruits of the WT plants and transgenic lines RNAi#7, OEX#1, and OEX#2 in different ripening stages. Labelling with the Fluo-3 AM indicator imaged with CLSM with plots of the grey value profile (marked with a red line).

The prepared profiles are plots of the grey values of pixels along a line drawn across the cells that measure the intensity of calcium arrangement. The analyses of the profiles across the cell wall from the tomato fruits showed a significant increase in fluorescence intensity within the border of the cell wall–plasma membrane continuum. The higher fluorescence signal at the border of the cell wall was visible as one peak in the tissue of the WT and transgenic lines in the BR stage. As is well known, the ripening process disrupts the continuity of the cell wall. Analyses of calcium distribution also allow finding structural changes, which are confirmed by the lack of a single characteristic fluorescence peak. In the RR stage, the plots of the grey value profile from the labelled cell walls were featured as a disturbed pattern of numerous peaks along the whole cell walls.

Discussion

The complex ripening process is inextricably linked with structural, morphological, and functional modifications of fruit tissue. Genetically programmed changes during ripening include hormonal and ethylene regulations, cell wall loosening, polysaccharide disruption, and pigment and aroma development [2]. Both the interactions between cell wall components and their spatio-temporal distribution have an impact on the proper functioning of the whole cell assembly [70]. The progress of ripening is linked with a lower cell-to-cell adhesion and changes in the cell wall mechanical properties [33, 71, 72]. The degradation of polysaccharides and linkages between the particular components cause softening of the cell wall [1, 49, 73]. These changes mainly result in the loss of fruit firmness [17].

Given the numerous studies on the cell wall in the successful course of the ripening process, in the current paper, we intended to determine the effect of the lack of one cell wall component on its assembly, which in turn affects the progress of the process. Thus, tomato fruits with altered *SlP4H3* expression and changed AGP content and structure were used as the research material. Detailed studies on AGP modifications in tomato fruits were reported in our previous paper [67]. In the current paper, we focused on other constituents of the APAP1.

The starting point in our analysis was the finding of clear morphological differences between the fruits of the WT and transgenic lines. Regardless of whether we analysed the silencing or overexpression of *SlP4H3*, the progress of the ripening process resulted in a different appearance of the fruit tissue. This gives grounds for concluding that the structure of the cell wall changed, and the progression of processes related to ripening deviated from the native process. The literature provides ample information about the composition of the cell wall and changes caused by fruit ripening. In the analysis of *Lycium barbarum* L. carried out by Liu and coworkers, the content of cell wall polysaccharide components decreased during the ripening process. This caused changes in the structure of the cell wall with intercellular adhesion and the resultant deformation of the parenchyma tissue [74]. Other studies carried out by Rosli and coworkers also confirmed decreased amounts of polysaccharides during strawberry ripening [73]. In summary, the reduction of cell wall components causes the disappearance of adequate support for the fruit tissues, which leads to the progression of softening [4, 74]. Other detailed analyses allowed the conclusion that changes in the amount of cellulose and hemicellulose have no significant effect on softening during the ripening process, and mainly the amount of pectins and the degree of their depolymerization and solubilization had an effect on the modification of the cell wall during the ongoing strawberry ripening [29, 73]. The data mentioned above were

also confirmed in our work. The *in situ* and *ex situ* immunocytochemical approaches demonstrated quantitative and qualitative changes in the cell wall composition during the ripening process. A higher number of analysed epitopes was detected in the BR stage than in the RR stage, confirming the occurrence of degradation processes during ripening. However, the modification of P4H3 had an influence on the cell wall composition, and the changes in its content correlated with the progress of ripening. Firstly, the most pronounced disturbances were observed in the case of HG. In-depth molecular analyses showed that low methyl-esterified HG is the most distinctive component in the analysed tomato fruit lines at the beginning and end of the examined process. Low methyl-esterified HG (LM19) was present in much higher amounts than high methyl-esterified HG (LM20). Moreover, the ELISA, CLSM, and TEM analyses revealed that low methyl-esterified HG was characterized by longer persistence (RR stage) in the cell walls of the transgenic lines in comparison to WT. Especially the results of the OEX lines indicate that low methyl-esterified HG undergoes a slower degradation process with the progress of ripening. As is known, low methyl-esterified HGs are associated with the binding of calcium ions; thus, the obtained data indicated the need to perform an analysis of the content of calcium ions in the analysed tissues.

Subsequently, compared to WT, the cell walls of the transgenic lines had modified spatio-temporal distribution of particular components. *In situ* analyses were performed to verify these changes during the ripening process. An immunofluorescence analysis carried out by Ning and coworkers demonstrated changes in pectin localization during the banana fruit (*Musa* spp.) ripening process. The JIM5 (recognizes partially methyl-esterified HG (up to 40%)) and JIM7 (recognizes methyl-esterified HG (40%–80%)) antibodies used in the study increased slightly with the development of the fruits. In the case of JIM7, the signal of immunofluorescence became stronger during the development and was higher at harvest. However, after ripening, the signal significantly decreased. It was also found that the amount of LM18 antibody epitopes (which recognizes low methyl-esterified HG) was higher than that of JIM15 and JIM7 [25]. Recent evidence in strawberries and tomatoes suggests that pectin disassembly is a key factor in textural changes [22, 75]. A study on the abscission zone (AZ) during olive fruit abscission (*Olea europaea* L.) found that AZ cell separation was linked with the decreased level of JIM19 epitopes (extensin). Moreover, JIM19 labelling was present in the cell wall and the cytoplasm and absent in the cell junction regions [38]. In the present study, we found an increase in immunofluorescence intensity in tissues of the lines with the overexpression of the *SlP4H3* gene. LM19 epitopes were mainly present in the corners and cellular junctions in the BR stage, changing the location to the intercellular area in the RR stage. The location of another HG epitope, LM20, seemed to be interesting, as it was densely distributed in the cellular junctions, but the signal was significantly lower than in the case of LM19. The ripening process mainly did not affect the distribution of this epitope. Nevertheless, in the lines with the overexpression of the *SlP4H3* gene, we detected the occurrence of single conglomerates in the RR stage. In the current study, the increased *SlP4H3* expression also affected extensin distribution causing increased signal intensity in the cell wall. Extensins were visible as large conglomerates in the cytoplasm compartments, but they were absent in WT. During the progress of the ripening process, a decrease in the intensity of LM1 epitopes was determined.

Another unique disorder was noted in the microscopic observations of xylan recognized by LM11. The analyses at the subcellular level demonstrated that the LM11 epitopes in both overexpression lines were distributed mainly in the cell wall–plasma membrane. In the WT fruits in the RR stage, the examined epitopes were noted also in the cytoplasm. In the modified fruits, no such localization of xylan was observed. Furthermore, in our study, a 20%–30% increase in Xyl and a 10% increase in RG-I were determined in the transgenic lines. We may conclude that this result also proves a disturbance in the native degradation process of cell walls. An explanation can be found in available studies in which the use of mutants with the disrupted synthesis of different cell wall components made it possible to determine the role of the cell wall components in cell structure and function. Studies conducted by Biswal and coworkers showed an accumulation of HG and RG-I in the cell wall upon overexpression of the *PtGAUT12.1* gene in *Populus deltoides*. Moreover, the analyses of the *PtGAUT12.1* gene also showed a 14%–20% increase in Xyl and a 12%–17% increase in GalA. This process was accompanied by a reduction in the amount of galactose (Gal), Man, and Glc. The study also found that the tested polymers were distributed more tightly in the cell walls, which affected the plant height [76]. The study carried out by Peña and coworkers presented a modified xylan localization and distribution pattern in *Arabidopsis thaliana irregular xylem8 (irx8)* mutant, which had an impact on the morphology of plant tissue [77, 78]. In addition, the new xylan distribution pattern exerted an effect on the interactions between xylan and pectin polymers [79]. Thus, results obtained suggested that changes in expression of *SlP4H3* gene may affect other cell wall components. This is most likely due to the resulting disruption in the amount and function of AGPs. Fragkostefanakis and coworkers determined the effect of modifying P4Hs activity on the distribution of xylan and pectins in leaf epidermal cells [80].

SlP4H1, *SlP4H7*, and *SlP4H9* gene silencing was associated with a decreased amount of the JIM8 epitope (AGP) as well as the JIM11 epitope (extensin) in the case of the last two genes [80]. A study on *S. lycopersicum* presented changes in the morphology of leaf epidermal cells probably as a result of the modification of the xyloglucan and pectin epitope distribution. In addition, the results obtained are most likely related to changes in AGPs and extensins because they are covalently linked to other cell wall polymers [80]. The results obtained by Nibbering and coworkers indicate that AGPs may affect cell wall matrix properties [81], and defects in AGP synthesis may cause changes in the structure and function of the cell wall [82]. Therefore, the use of GH43 loss-of-function (the glycosyl hydrolase 43 family) mutants of *A. thaliana (gh43null)* allowed determination of the contents of cellulose, hemicellulose, and pectic sugars during AGP changes. The amount of these polymers was similar in *gh43null* and WT, but there were changes in their distribution and localization. In addition, increased signal intensity of the CoMMP microarray was observed for the pectin (LM5), xyloglucan (LM25), and extensin (JIM20) antibodies. These results indicated that the defect caused by the loss of GH43 activity had an impact on the abundance of cell wall-associated AGPs and on the content of other polymers [81]. Our previous analyses also confirmed the presence of a different amount of AGPs in fruit of lines with overexpression and silencing of the *SlP4H3* gene compared to WT [67]. The analyses of the overexpression of the *SlP4H3* gene showed that the increased P4H3 enzyme activity resulted in a higher number of AGP epitopes [67]. In the current research, we observed a disorder in the amount of all the epitopes tested in the lines with the modified *SlP4H3* gene. This correlation persisted during the ripening process. Therefore, it can be hypothesized that changes in the quantity and quality of AGPs affect other cell wall components. Mentioned disorders

can disrupt fruit ripening. A great example of this might be the *Cnr* mutant, in which the aberrant localization of polysaccharide domains occurred in the cell wall, but cell wall swelling did not occur during the ripening process. In addition, in the mutant cells, there was no degradation process that takes place during proper ripening. It can be concluded that *Cnr* mutants exhibited a blocked progress of the fruit ripening process [31]. The complex structure of the cell wall with high interactions between its components is important for maintaining tissue firmness, and changing their binding ability can induce irreversible changes [29, 45, 48].

The second step of the work was to determine whether AGP from the modified fruits could be related to *ex situ* binding to other constituents. Nibbering and coworkers put forward a similar theory that APAP1 and/or cell wall-bound AGPs are targets of GH43 activity, and their modification changes the structure of the cell wall [81]. The APAP1 is a proteoglycan in which AGP binds to matrix polysaccharides [45]. Thus, the structure and function of the cell wall are affected by the present polymers and the bonds between them. However, the complete spectrum of binding is not definitively known [45, 48]. To determine the effect of the modifications of the APAP1 core protein on the whole cell wall structure, *SALK_070113c/apapap1*–3 and *SALK_002144/apapap1*–4 mutants were created. Using the glycome profiling method, a 5- to 83-fold increase in RG-I and HG epitopes and a 9- to 49-fold increase in xylan, compared to WT, were determined. Also, higher amounts of Rha and GalA were detected in addition to the increase in pectin and xylan in mutant extracts. Moreover, the analyses indicated less tight binding of these polymers to the cell wall due to the absence of the core protein [45]. Taking into account previous analyses and the hypothesis that AGPs have the ability to bind with other polymers, we conducted *in vitro* binding tests of extracted AGPs and commercial cell wall components. Our results indicated the ability of AGPs to bind with RG-I, AG, and cellulose. AGPs were found to have the lowest binding affinity to xylan. This was most likely related to the ability of xylan to bind to RG-I, but not AGPs, in the APAP1, as demonstrated by Tan and coworkers [45]. Whilst comparing the results obtained from the AGPs extracted from the fruits of the transgenic lines and WT, we detected stronger binding to RG-I and AG in the case of AGPs extracted from the overexpression lines. The analysis confirmed the AGP binding to AG and RG-I as showed that the intensity of the immunoreactions was higher than in the case of AGPs extracted from WT. Our data are in line with a study carried out by Hijazi and coworkers [83]. The authors also found *in vitro* interactions between AGP31 and commercial saccharides, mainly RG-I, cellulose, AG, and xylan. Hence, we can hypothesize that the APAP1 is a proteoglycan whose undisturbed structure allows proper mechanisms to take place in the cells.

The last phase of our work was to assess the content of calcium ions in the examined fruits. It is well known that pectins and AGPs have the ability to bind Ca^{2+} and form intramolecular and intermolecular calcium bridges [48, 53–56]. Research performed by Ajayi and coworkers in *glcat14* mutants showed a ~50% reduction in the amount of GlcA with a corresponding increase in galactose content and a significant reduction in calcium content [60]. Another study performed by Lopez-Hermandez and coworkers showed that glucuronidation of AG polysaccharides had an effect on the AGP-Ca^{2+} interaction [53]. The triple mutants (*glcat14a/b/d* and *glcat14a/b/e*) exhibited a significant decrease in the glucuronidation level, compared to the single and double mutants. Consequently, this had an impact on Ca^{2+} binding, as an 80% reduction in Ca^{2+} binding in triple mutants was shown, in contrast to WT. Also, in the case of the double and triple mutants, the authors observed numerous developmental and morphological defects [53]. Considering the information about the ability of pectins to bind Ca^{2+} [56] and the results of the study, the authors proposed a theory that GlcA, which bind AGPs and pectins in the APAP1, have an effect on cell wall integrity and cell-to-cell signalling [53]. In our study, we determined an increase in the calcium content during the ripening process, which was similar to the results obtained by Hyodo and coworkers. Their observations performed with the use of quantitative imaging by secondary ion-microprobe mass spectrometry (SIMS) confirmed the presence of Ca^{2+} bound by pectins in tomato fruits [29]. In all the samples of the transgenic lines and WT, the amount of calcium was higher in the RR stage compared to the beginning of the ripening process. However, the analysis of the calcium content in the cell wall of the transgenic lines confirmed the increase in the amount of this element, in comparison to WT. The SEM-EDS analysis allowed a conclusion that, in the overexpression lines, the changes in the calcium distribution as a result of ripening progress were less visible, and signals indicating calcium occurrence were observed in the whole cell surface. Given our earlier results on higher content of HG in modified lines, we may conclude that it is related to the binding affinity between calcium and pectins. An explanation of the obtained data may be provided by the information published in previous reports, in which the changes in the content of pectins and AGPs had a direct effect on the amount and distribution of Ca^{2+} ions in plant cells [57, 84].

Fruit ripening is a developmental programme strictly regulated by hormones, mainly ethylene as well as abscisic acid, jasmonic acid, and brassinosteroids [85–90]. An *Arabidopsis* P4H3 might be implicated in the oxygen-sensing pathway, and its function in plants under low oxygen has been examined [91]. In turn, oxygen sensing is coordinated by the regulation of ERF protein stability (Ethylene Response Factor) cluster of transcription factors [92, 93]. Moreover, several AGPs are upregulated during fruit ripening in tomato [7, 40, 44] suggesting putative regulation by climacteric ethylene. In this context, changes in the molecular properties of AGPs as a result of modification in P4H3 activities are associated with the assembly of the entire fruit cell wall, and we assume that the molecular changes in the cell walls may be regulated by ethylene through changes in the organization of the individual components. Such observations outline further research perspectives aimed at determining a pathway for subsequent changes in fruit metabolism and structure along with all factors that influence the fruit pericarp tissue. Correlations between oxygen concentration, ethylene level, ripening stage, P4H3 activity, AGP changes, and disruption in APAP1 organization are completely new and require extensive research.

Conclusion

Overall, these results support the hypothesis that AGPs and pectins are responsible for the proper progression of the physiological ripening process occurring in fruits. Disorders in their quantity, structure, and temporal–spatial distribution can disrupt fruit ripening.

Here, we presumed the following order of events in response to changed *SlP4H3* expression: (1) Disruption of the AGP molecular structure causes changes in their localization in the cell wall–plasma membrane continuum [67]. Alterations in spatio-temporal AGP distribution affect the creation of connections between AGPs and other cell wall components that are included in the APAP1. (2) The disorder in the typical presence of low methyl-esterified homogalacturonan affects the presence of calcium ions

in the cell wall compartments. (3) In turn, the modified structure of the cell wall matrix induces morphological variations during the progression of the ripening process.

Material

Tomato plants (*Solanum lycopersicum* cv. 'Ailsa Craig') were grown in a greenhouse (Greece). The objects of the study were fruits in different stages of the ripening process. The ripening stages were classified by alternations in fruit colour [94, 95]. The first stage is Breaker (BR)—tomatoes have a pale-green colour. The next stage is Turning (TU) when tomatoes have a pale-pink colour on 10%–30% of the surface, and Pink (PINK) when 60% of the surface of tomatoes has a red colour. The last stage is Red Ripe (RR) when the entire fruits are red [95].

In the present study, we used transgenic lines with modified expression of the *SlP4H3* gene [68]. Lines with the overexpression of the *SlP4H3* gene (OEX#1 and OEX#2), which are characterized by increased activity of the P4H3 enzyme, were studied. For contrast, a line with silenced *SlP4H3* gene expression (RNAi#7), which is characterized by significantly decreased activity of the P4H3 enzyme, was analysed. A detailed description of the P4H3 effect on AGP structure was studied in our previous work [67]. Moreover, preliminary experiments suggested that there are differences in the postharvest behaviour of tomato fruits from the *SlP4H3* RNAi#7, OEX#1, and OEX#2 lines. Fruits were harvested at the Breaker+3 days and stored at 23°C for 1 month. A higher degree of fruit epidermis shrivelling was observed for both the overexpression and silencing lines whilst the softening seemed to be delayed compared to the wild type (WT). However, these experiments need to be further validated using a texture analyser.

Methods

Immunofluorescence labelling and CLSM imaging

The immunofluorescence method is used to evaluate changes in the cellular localization of APAP1 components in fruits in different ripening stages. Monoclonal antibodies recognizing extensin (LM1), xylan (LM11), RG-I (LM16), low methyl-esterified HG (LM19), and high methyl-esterified HG (LM20) epitopes were selected in this work. Samples were prepared according to the protocol described in our previous paper [96], i.e. fixation in paraformaldehyde (2%, Sigma, USA) and glutaraldehyde (2.5%, Sigma, USA), dehydration in a graded series of ethanol solutions, polymerization in LR White (Sigma, USA), and cutting into 1-μm-thin sections using a ultramicrotome (PowerTome XL, RMC Boeckeler, USA). The semi-thin sections were placed on poly-L-lysine–coated glass slides (Sigma Aldrich, USA) and preincubated using bovine serum albumin (2% BSA; Sigma, USA) for 30 minutes at room temperature (RT). After the washing steps, the sections were incubated with the primary antibody (diluted 1:50; Goat Anti-Rat-IgM, Kerafast, USA) overnight at 4°C. The next day, after the washing step, the sections were incubated with secondary Alexa Fluor 488 antibodies (diluted 1:200; Thermo Fisher Scientific, Denmark) overnight at 4°C. Then, the sections were counterstained with Calcofluor White (Sigma Aldrich, USA). In the control reaction, labelling with the primary antibody was omitted. An Olympus BX51 CLSM microscope with software FluoView v. 5.0. (Olympus Corporation, Tokyo, Japan) was used for imaging. Figures were prepared using the CorelDrawX6.

Immunogold labelling and TEM imaging with quantitative analysis

Immunogold labelling of APAP1 components helps to identify changes in their localization at the subcellular level during the fruit ripening process. As in the CLSM analysis, we used LM1, LM11, LM16, LM19, and LM20 antibodies. Ultrathin sections were prepared using a diamond knife-equipped ultramicrotome (PowerTome XL, RMC Boeckeler, USA) and placed on nickel grids with formwar film. Then, the grids were preincubated using 1% BSA for 30 minutes at RT, then incubated with the primary antibody (1:10) for 3 hours at 37°C as well as with the secondary antibody diluted (1:50; Anti-Rat-IgG – Gold antibody; Sigma, USA) for 1 hour at 37°C. Before microscopic analysis, the grids were stained with a 1% uracyl acetate solution and Reynold's reagent for 10 and 7 minutes, respectively. Control reactions were carried out by omitting the primary antibody. A TEM Zeiss EM900 transmission electron microscope operating at 80-kV acceleration voltage (Carl Zeiss AG, Oberkochen, Germany) equipped with a digital camera and software ImageSP v. 1.1.2.5 was used. The quantitative analysis revealed the correlation between the number of gold particles per 1-μm^2 area of the cell compartment. The labelling density of the gold particles on the same size micrographs (2048 × 2048 pixels square) was counted with ImageJ v. 1.51.

Cell wall glycome profiling – ELISA test

Enzyme-linked immunosorbent assay (ELISA) is a test for qualitative and quantitative glycan epitope profiling [96]. The preprepared samples (homogenized fruit tissue in liquid nitrogen and diluted in PBS with subsequent centrifugation at 6000 rpm for 15 minutes and 15 000 rpm for 15 minutes at RT) were added to each well on a 96-well plate (NaxiSorpTM flat-bottom, Sigma-Aldrich, USA) and incubated for immobilization for 72 hours at 37°C with shaking (350 rpm). Then, the coated plate was washed with PBS and preincubated using 0.1% BSA for 1 hour at 37°C in a plate lab shaker. After the blocking and washing steps, the plate was incubated with the primary antibody (1:20) for 1 hour at 37°C and with the secondary antibody, Anti-Rat-IgG conjugated with alkaline phosphatase (AP) (Sigma-Aldrich, USA) (1:500) for 1 hour at 37°C. The enzymatic reaction was run in the dark using a solution of p-nitrophenol phosphate (PNPP; Thermo Scientific). The absorbance at 405 nm was measured using an ELISA reader (MPP-96 Photometer, Biosan) and analysed with Statistica tools (Statistica v.13; TIBCO Software Inc. USA). Alkaline phosphatase activity was determined by the release of p-nitrophenol (PNP; Thermo Scientific) ions from PNPP. The reaction was carried out for 10 minutes at RT and then stopped by adding 2 M NaOH. In an alkaline medium, PNP takes on a yellow colour. The amount of PNP ions released was calculated from a calibration curve with the calibration coefficient $y = 0.0808x$, $R^2 = 0.9854$. Analysis of variance (one-way ANOVA) and Tukey's Honestly Significant Difference (HSD) *post hoc* test were used to compare the mean results. In all the analyses, the significance level was set at $P < 0.05$.

In vitro binding assay – immunoprinting on the nitrocellulose membrane

The *in vitro* binding assays of AGPs extracted from the fruits with Yariv Reagent (β-GlcY; Biosupplies, Australia) with commercial cell wall components on nitrocellulose membranes were carried out according to the protocol prepared by Hijazi [83] and Moller [97]. To isolate AGPs, frozen fruit tissue was homogenized, mixed with 2% $CaCl_2$, and incubated at RT for 3 hours. After the incubation step, the homogenate was centrifuged (10 000 rpm 30 minutes

at RT) and the supernatant was collected. β-GlcY in 2% $CaCl_2$ was added to the supernatant (an equal volume to the supernatant) and incubated at RT overnight. After the incubation step, the supernatant was centrifuged (2000 rpm 15 minutes at RT) and next the precipitate was collected. The precipitate was mixed with sodium metabisulphite and heated at 50°C to reduce the diazo linkage. The solution was dialysed (dialysis tubing, 12-kDa MW cut-off, 32 mm flat width; Sigma, USA) for 48 hours. Finally, the resulting dialysate was freeze-dried. Samples of commercial cell wall components (concentration 5–20 mg/ml) were dotted onto a preprepared nitrocellulose membrane (PVDF) (Thermo Scientific, USA) and incubated for 30 minutes at RT. In the present work, the following elements of the APAP1 were selected: arabinogalactan (Megazyme, USA), rhamnogalacturonan (Megazyme, USA), partially acetylated xylan (Megazyme, USA), xyloglucan (Megazyme, USA), and cellulose (Sigma, USA) to check the ability to bind with the isolated AGPs. After washing with Tris-buffered saline (TBST, 7.6 pH), the membrane was incubated with the solution of isolated AGPs (a concentration of 20 μg/ml was selected experimentally) overnight at 4°C. After the washing steps, the membrane was blocked using 3% BSA in TBST for 1 hour at RT. After the blocking and washing steps, the membrane was incubated with the primary antibody diluted in 1.5% BSA (1:200) for 2 hours at RT and with the secondary antibody diluted in 1.5% BSA (1:1000) for 1 hour at RT. The membrane was treated with 20 ml of AP buffer with substrates: 9 mg of nitro-blue tetrazolium (NBT; Sigma, USA) in 0.3 ml of water and 0.7 ml of N, N-dimethylformamide (DMF; Thermo Scientific, USA) and 4 mg of 5-bromo-4-chloro-3-indolylphosphate (BCiP; Sigma, USA) in 1 ml of water. Measurements and analysis of colour intensity were carried out using GelDoc Go Imaging System (Bio-Rad, USA) and Image Lab Software v. 6.1 (Bio-Rad, USA). Data for each sample were obtained from the results of three independent experiments and represented in the table as the presence and absence of binding. The measurements were classified into 3 categories: '+' – high signal intensity, '±' – low signal intensity, and '–' – no signal.

Binding assay and screening by ELISA

The results of the binding assay described by Biswal and coworkers [76] based on the use of glycome profiling with screening with ELISA-based monoclonal antibodies were shown in histograms and heat maps. Samples of commercial cell wall components at a concentration of 20 mg/ml were added to each well on a 96-well plate and incubated for immobilization for 72 hours at 37°C with shaking (350 rpm). Then, the coated plate was washed with PBS, and AGP solutions (concentration 20 μg/ml) were added to each well overnight at RT. After blocking with 0.1% BSA for 1 hour and washing steps, the plate was incubated with the primary antibody diluted in PBS (1:20) for 1 hour at 37°C and with the secondary antibody Anti-Rat-IgG conjugated with AP diluted in PBS (1:500) for 1 hour at 37°C. After the washing step, the enzymatic reaction was run in the dark using PNPP; the reaction was then stopped with 2 M NaOH. The absorbance at 405 nm was measured using an ELISA reader (MPP-96 Photometer, Biosan) and analysed with Microsoft tools. The heat map presenting the colour intensity is proportional to the numerical value of absorbance.

Estimation of the calcium amount at the tissue level – SEM-EDS

The elemental composition analysis was performed with the use of the energy-dispersive X-ray microanalysis method and scanning electron microscope (SEM). The surface of the fruit sample was examined using energy-dispersive X-ray spectroscopy (EDS) with a Bruker X-ray detector equipped with an SEM with operating conditions of the electron microprobe of 20 kV (SEM, Zeiss Ultra Plus, Oberkochen, Germany). After the fixation step (2% paraformaldehyde and 2.5% glutaraldehyde), the samples were washed 2 times in PBS and dehydrated in a graded ethanol series. Next, the samples were dried in a critical point dryer using liquid CO_2 to redraw water (CPD7501, Polaron Range, UK) and coated with gold using a sputter coater. SEM-EDS imaging allows semiquantitative measurements of the amount of calcium. Each sample had at least five replicates of X-ray line scans, and then data analysis was done as in Li and coworkers [98].

Determination of the intracellular calcium level – Imaging with the Fluo-3 AM indicator

As in the studies performed by Li [98] and Qiu [99], the Fluo 3-AM (Sigma Aldrich, USA) indicator was used as a reagent to detect the localization of calcium at the cellular level and to estimate the different calcium content by measurement of the fluorescence intensity. Briefly, slices of the fruits were rinsed twice with dimethyl sulfoxide (DMSO; Sigma Aldrich, USA) and incubated in a working solution of Fluo 3-AM for 2 hours at 4°C in darkness. The Fluo 3-AM (1 mM in DMSO) was mixed with Pluronic F-127 (10% solution in DMSO; Thermo Fisher Scientific). Calcium detection was performed using an Olympus BX51 Confocal Laser Scanning Microscope equipped with software Fluo-View v. 5.0. (Olympus Corporation, Tokyo, Japan). The plots of the grey value profile were counted with ImageJ 1.51 software.

Acknowledgements

This research was funded by the National Science Center, Poland (SONATA 16, grant number 2020/39/D/NZ9/00232). Also, this work has been supported by the COST Action 'Roxy-COST' (CA:18210) which is funded by the European Cooperation in Science & Technology. Also, work has been financed by the European Regional Development Fund of the European Union and Greek national funds through the Operational Competitiveness, Entrepreneurship and Innovation, under the call RESEARCH-CREATE-INNOVATE (project code: T2EDK-01332: n-Tomatomics - Development of new tomato cultivars by using -omics technologies).

Author contributions

N.K. Investigation, Methodology, Data curation, Visualization, Writing—original draft; A.L. Supervision, Project administration, Funding acquisition, Formal analysis, Writing—review & editing; M.L. Investigation (TEM imaging); D.D., S.B., K.B., P.G. Investigation (created the transgenic lines); P.K. Investigation (created the transgenic lines), Writing—review & editing; and A.Z. Writing—review & editing.

Conflict of interest statement

The authors declare that they have no conflict of interest.

Data availability statement

The data underlying this article are available in the RepOD database [Leszczuk Agata, 2023, Studies on arabinogalactan proteins (AGPs) in fruits, file folder no A_6] at https://doi.org/10.18150/KMG7WI.

References

1. Wang D, Seymour GB. Molecular and biochemical basis of softening in tomato. *Mol Hortic*. 2022;**2**:1–10
2. Osorio S, Scossa F, Fernie AR. Molecular regulation of fruit ripening. *Front Plant Sci*. 2013;**4**:1–8
3. Mo Y, Jiang B, Huo J. *et al.* Quantitative ubiquitylomic analysis of the dynamic changes and extensive modulation of ubiquitylation in papaya during the fruit ripening process. *Front Plant Sci*. 2022;**13**:1–11
4. Castro RI, Morales-Quintana L. Study of the cell wall components produced during different ripening stages through thermogravimetric analysis. *Cellulose*. 2019;**26**:3009–20
5. Li S, Chen K, Grierson D. Molecular and hormonal mechanisms regulating fleshy fruit ripening. *Cells*. 2021;**10**:1–34
6. Huang B, Hu G, Wang K. *et al.* Interaction of two MADS-box genes leads to growth phenotype divergence of all-flesh type of tomatoes. *Nat Commun*. 2021;**12**:1–14
7. Kalaitzis P, Giannoutsou E, Konkina A. Role of the cell wall in the regulation of fruit ripening. In: *Plant Cell Walls: Research Milestones and Conceptual Insights*. Boca Raton: CRC Press, 2023,147–61
8. Jiang F, Lopez A, Jeon S. *et al.* Disassembly of the fruit cell wall by the ripening-associated polygalacturonase and expansin influences tomato cracking. *Hortic Res*. 2019;**6**:1–15
9. Li X, Wang X, Zhang Y. *et al.* Regulation of fleshy fruit ripening: from transcription factors to epigenetic modifications. *Hortic Res*. 2022;**9**:1–12
10. Guo Y, Bao Z, Deng Y. *et al.* Protein subcellular localization and functional studies in horticultural research: problems, solutions, and new approaches. *Hortic Res*. 2023;**10**:1–5
11. Tucker MR, Lou H, Aubert MK. *et al.* Exploring the role of cell wall-related genes and polysaccharides during plant development. *Plan Theory*. 2018;**7**:1–17
12. Hijazi M, Velasquez SM, Jamet E. *et al.* An update on post-translational modifications of hydroxyproline-rich glycoproteins: toward a model highlighting their contribution to plant cell wall architecture. *Front Plant Sci*. 2014;**5**:1–10
13. Srivastava V, McKee LS, Bulone V. Plant cell walls. In: *eLS*. Chichester; John Wiley & Sons, Ltd, 2017,1–17
14. Tucker G, Yin X, Zhang A. *et al.* Ethylene and fruit softening. *Food Qual Saf*. 2017;**1**:253–67
15. Posé S, Paniagua C, Matas AJ. *et al.* A nanostructural view of the cell wall disassembly process during fruit ripening and postharvest storage by atomic force microscopy. *Trends Food Sci Technol*. 2019;**87**:47–58
16. Scheller HV, Ulvskov P. Hemicelluloses. *Annu Rev Plant Biol*. 2010;**61**:263–89
17. Goulao LF, Oliveira CM. Cell wall modifications during fruit ripening: when a fruit is not the fruit. *Trends Food Sci Technol*. 2008;**19**:4–25
18. Zhang B, Gao Y, Zhang L. *et al.* The plant cell wall: biosynthesis, construction, and functions. *J Integr Plant Biol*. 2021;**63**:251–72
19. Curry TM, Peña MJ, Urbanowicz BR. An update on xylan structure, biosynthesis, and potential commercial applications. *Cell Surf*. 2023;**9**:1–4
20. Pauly M, Albersheim P, Darvill A. *et al.* Molecular domains of the cellulose/xyloglucan network in the cell walls of higher plants. *Plant J*. 1999;**20**:629–39
21. del Carmen Rodriguez-Gacio M, Iglesias-Fernandez R, Carbonero P. *et al.* Softening-up mannan-rich cell walls. *J Exp Bot*. 2012;**63**:3976–88
22. Paniagua C, Posé S, Morris VJ. *et al.* Fruit softening and pectin disassembly: an overview of nanostructural pectin modifications assessed by atomic force microscopy. *Ann Bot*. 2014;**114**:1375–83
23. Caffall KH, Mohnen D. The structure, function, and biosynthesis of plant cell wall pectic polysaccharides. *Carbohydr Res*. 2009;**344**:1879–900
24. Engle KA, Amos RA, Yang JY. *et al.* Multiple *Arabidopsis* galacturonosyltransferases synthesize polymeric homogalacturonan by oligosaccharide acceptor-dependent or de novo synthesis. *Plant J*. 2022;**109**:1441–56
25. Ning T, Chen C, Yi G. *et al.* Changes in homogalacturonan metabolism in banana peel during fruit development and ripening. *Int J Mol Sci*. 2022;**23**:1–20
26. Yapo BM. Rhamnogalacturonan-I: a structurally puzzling and functionally versatile polysaccharide from plant cell walls and mucilages. *Polymer Rev*. 2011;**51**:391–413
27. Barnes WJ, Koj S, Black IM. *et al.* Protocols for isolating and characterizing polysaccharides from plant cell walls: a case study using rhamnogalacturonan-II. *Biotechnol Biofuels*. 2021;**14**:1–20
28. Brummell DA, Dal Cin V, Crisosto CH. *et al.* Cell wall metabolism during maturation, ripening and senescence of peach fruit. *J Exp Bot*. 2004;**55**:2029–39
29. Hyodo H, Terao A, Furukawa J. *et al.* Tissue specific localization of pectin-Ca^{2+} cross-linkages and pectin methyl-esterification during fruit ripening in tomato (*Solanum lycopersicum*). *PLoS One*. 2013;**8**:1–10
30. Brummell DA. Sensing when the wall comes tumbling down. *J Exp Bot*. 2020;**71**:6865–8
31. Orfila C, Seymour GB, Willats WG. *et al.* Altered middle lamella homogalacturonan and disrupted deposition of (1-5)-L-arabinan in the pericarp of *Cnr*, a ripening mutant of tomato. *Plant Physiol*. 2001;**126**:210–21
32. Orfila C, Huisman MMH, Willats WGT. *et al.* Altered cell wall disassembly during ripening of *Cnr* tomato fruit: implications for cell adhesion and fruit softening. *Planta*. 2002;**215**:440–7
33. Brummell DA, Harpster MH. Cell wall metabolism in fruit softening and quality and its manipulation in transgenic plants. *Plant Mol Biol*. 2001;**47**:311–39
34. Harholt J, Suttangkakul A, Scheller HV. Biosynthesis of pectin. *Plant Physiol*. 2010;**153**:384–95
35. Silva J, Ferraz R, Dupree P. *et al.* Three decades of advances in arabinogalactan-protein biosynthesis. *Front Plant Sci*. 2020;**11**:1–18
36. Cooper JB, Heuser JE, Varner JE. 3,4-Dehydroproline inhibits cell wall assembly and cell division in tobacco protoplasts. *Plant Physiol*. 1994;**104**:747–52
37. Jamet E, Canut H, Boudart G. *et al.* Cell wall proteins: a new insight through proteomics. *Trends Plant Sci*. 2006;**11**:33–9
38. Parra R, Gomez-Jimenez MC. Spatio–temporal immunolocalization of extensin protein and hemicellulose polysaccharides during olive fruit abscission. *Planta*. 2020;**252**:1–15
39. Kieliszewski MJ, Lamport DTA. Entensin: repetitive motifs, functional sites, post-translational codes, and phylogeny. *Plant J*. 1994;**5**:157–72
40. Leszczuk A, Kalaitzis P, Kulik J. *et al.* Review: structure and modifications of arabinogalactan proteins (AGPs). *BMC Plant Biol*. 2023;**23**:1–12
41. Hromadova D, Soukup A, Tylova E. Arabinogalactan proteins in plant roots – an update in possible functions. *Front Plant Sci*. 2021;**12**:1–15
42. Tsumuraya Y, Ozeki E, Ooki Y. *et al.* Properties of arabinogalactan-proteins in European pear (*Pyrus communis* L.) fruits. *Carbohydr Res*. 2019;**485**:1–9

43. Kutyrieva-Nowak N, Leszczuk A, Zając A. *et al.* Arabinogalactan protein is a molecular and cytological marker of particular stages of the tomato fruit ripening process. *Sci Hortic.* 2023;**310**: 111718–0
44. Leszczuk A, Kalaitzis P, Blazakis KN. *et al.* The role of arabinogalactan proteins (AGPs) in fruit ripening – a review. *Hort Res.* 2020;**7**:1–12
45. Tan L, Eberhard S, Pattathil S. *et al.* An *Arabidopsis* cell wall proteoglycan consists of pectin and arabinoxylan covalently linked to an arabinogalactan protein. *Plant Cell.* 2013;**25**:270–87
46. Fry SC. Isodityrosine, a new cross-linking amino acid from plant cell-wall glycoprotein. *Biochem J.* 1982;**204**:449–55
47. Ellis M, Egelund J, Schultz CJ. *et al.* Arabinogalactan-proteins: key regulators at the cell surface? *Plant Physiol.* 2010;**153**:403–19
48. Tan L, Zhang L, Black I. *et al.* Most of the rhamnogalacturonan-I from cultured *Arabidopsis* cell walls is covalently linked to arabinogalactan-protein. *Carbohydr Polym.* 2023;**301**:120340–12
49. Brummell DA. Cell wall disassembly in ripening fruit. *Funct Plant Biol.* 2006;**33**:103–19
50. Zhang W, Guo M, Yang W. *et al.* The role of cell wall polysaccharides disassembly and enzyme activity changes in the softening process of Hami melon (*Cucumis melo* L.). *Food Secur.* 2022;**11**:1–20
51. Forlani S, Masiero S, Mizzotti C. Fruit ripening: the role of hormones, cell wall modifications, and their relationship with pathogens. *J Exp Bot.* 2019;**70**:2993–3006
52. Redgwell RJ, MacRae E, Hallett I. *et al. In vivo* and *in vitro* swelling of cell walls during fruit ripening. *Planta.* 1997;**203**:162–73
53. Lopez-Hernandez F, Tryfona T, Rizza A. *et al.* Calcium binding by arabinogalactan polysaccharides is important for normal plant development. *Plant Cell.* 2020;**32**:3346–69
54. Pfeifer L, Shafee T, Johnson KL. *et al.* Arabinogalactan-proteins of *Zostera marina* L. contain unique glycan structures and provide insight into adaption processes to saline environments. *Sci Rep.* 2020;**10**:1–10
55. Tan L, Qiu F, Lamport DTA. *et al.* Structure of a hydroxyproline (Hyp)-arabinogalactan polysaccharide from repetitive ala-Hyp expressed in transgenic *Nicotiana tabacum*. *J Biol Chem.* 2004;**279**: 13156–65
56. Willats WGT, Orfila C, Limberg G. *et al.* Modulation of the degree and pattern of methyl-esterification of pectic homogalacturonan in plant cell walls: implications for pectin methyl esterase action, matrix properties, and cell adhesion. *J Biol Chem.* 2001;**276**:19404–13
57. Lamport DTA, Várnai P. Periplasmic arabinogalactan glycoproteins act as a calcium capacitor that regulates plant growth and development. *New Phytol.* 2013;**197**:58–64
58. Lamport DTA, Tan L, Held M. *et al.* Pollen tube growth and guidance: Occam's razor sharpened on a molecular arabinogalactan glycoprotein Rosetta Stone. *New Phytol.* 2018;**217**:491–500
59. Knoch E, Dilokpimol A, Tryfona T. *et al.* A β-glucurono syltransferase from *Arabidopsis thaliana* involved in biosynthesis of type II arabinogalactan has a role in cell elongation during seedling growth. *Plant J.* 2013;**76**:1016–29
60. Ajayi OO, Held MA, Showalter AM. Three β-glucurono syltransferase genes involved in arabinogalactan biosynthesis function in *Arabidopsis* growth and development. *Plan Theory.* 2021;**10**:1–19
61. Zhang Y, Held MA, Showalter AM. Elucidating the roles of three β-glucuronosyltransferases (GLCATs) acting on arabinogalactan-proteins using a CRISPR-Cas9 multiplexing approach in *Arabidopsis*. *BMC Plant Biol.* 2020;**20**:1–20
62. Demarty M, Morvan C. Calcium and the cell wall. *Plant Cell Environ.* 1984;**7**:441–8
63. Michailidis M, Karagiannis E, Tanou G. *et al.* Novel insights into the calcium action in cherry fruit development revealed by high-throughput mapping. *Plant Mol Biol.* 2020;**104**: 597–614
64. Hocking B, Tyerman SD, Burton RA. *et al.* Fruit calcium: transport and physiology. *Front Plant Sci.* 2016;**7**:1–17
65. Xiong T, Tan Q, Li S. *et al.* Interactions between calcium and ABA signaling pathways in the regulation of fruit ripening. *J Plant Physiol.* 2021;**256**:153309–30
66. Xu W, Peng H, Yang T. *et al.* Effect of calcium on strawberry fruit flavonoid pathway gene expression and anthocyanin accumulation. *Plant Physiol Biochem.* 2014;**82**:289–98
67. Kutyrieva-Nowak N, Leszczuk A, Ezzat L. *et al.* The modified activity of prolyl 4 hydroxylases reveals the effect of arabinogalactan proteins on changes in the cell wall during the tomato ripening process. *Front Plant Sci.* 2024;**15**:1–21
68. Perrakis A, Denic D, Blazakis KN. *et al.* A tomato prolyl-4-hydroxylase causes relocation of abscission zone and alters abscission kinetics. *bioRxiv.* 2021;**04.20.440677**;1–36
69. Perrakis A, Bita CE, Arhondakis S. *et al.* Suppression of a prolyl 4 hydroxylase results in delayed abscission of overripe tomato fruits. *Front Plant Sci.* 2019;**10**:1–11
70. Stafstrom JP, Staehelin LA. Antibody localization of extensin in cell walls of carrot storage roots. *Planta.* 1988;**174**:321–32
71. Barrelt DM, Gonzalez C. Activity of softening enzymes during cherry maturation. *J Food Sci.* 1994;**59**:574–7
72. Jarvis MC. Structure of native cellulose microfibrils, the starting point for nanocellulose manufacture. *Philos Trans Royal Soc A.* 2018;**376**:1–13
73. Rosli HG, Civello PM, Martínez GA. Changes in cell wall composition of three *Fragaria* × *ananassa* cultivars with different softening rate during ripening. *Plant Physiol Biochem.* 2004;**42**: 823–31
74. Liu J, Ma Q, Liu D. *et al.* Identification of the cell wall proteins associated with the softening of *Lycium barbarum* L. fruit by using iTRAQ technology. *Food Chem: Mol Sci.* 2022;**4**:100–10
75. Posé S, Marcus SE, Knox JP. Differential metabolism of pectic galactan in tomato and strawberry fruit: detection of the LM26 branched galactan epitope in ripe strawberry fruit. *Physiol Plant.* 2018;**164**:95–105
76. Biswal AK, Atmodjo MA, Pattathil S. *et al.* Working towards recalcitrance mechanisms: increased xylan and homogalacturonan production by overexpression of GAlactUronosylTransferase12 (GAUT12) causes increased recalcitrance and decreased growth in Populus Mike Himmel. *Biotechnol Biofuels.* 2018;**11**: 1–26
77. Persson S, Caffall KH, Freshour G. *et al.* The *Arabidopsis* irregular xylem8 mutant is deficient in glucuronoxylan and homogalacturonan, which are essential for secondary cell wall integrity. *Plant Cell.* 2007;**19**:237–55
78. Peña MJ, Zhong R, Zhou GK. *et al. Arabidopsis* irregular xylem8 and irregular xylem9: implications for the complexity of glucuronoxylan biosynthesis. *Plant Cell.* 2007;**19**:549–63
79. Brown DM, Goubet F, Wong VW. *et al.* Comparison of five xylan synthesis mutants reveals new insight into the mechanisms of xylan synthesis. *Plant J.* 2007;**52**:1154–68
80. Fragkostefanakis S, Sedeek KEM, Raad M. *et al.* Virus induced gene silencing of three putative prolyl 4-hydroxylases enhances plant growth in tomato (*Solanum lycopersicum*). *Plant Mol Biol.* 2014;**85**:459–71
81. Nibbering P, Petersen BL, Motawia MS. *et al.* Golgi-localized exo-b1,3-galactosidases involved in cell expansion and root growth in *Arabidopsis*. *J Biol Chem.* 2020;**295**:10581–92

82. Tryfona T, Liang H-C, Kotake T. *et al.* Structural characterization of *Arabidopsis* leaf arabinogalactan polysaccharides. *Plant Physiol.* 2012;**160**:653–66
83. Hijazi M, Roujol D, Nguyen-Kim H. *et al.* Arabinogalactan protein 31 (AGP31), a putative network-forming protein in *Arabidopsis thaliana* cell walls? *Ann Bot.* 2014;**114**:1087–97
84. De Freitas ST, Handa AK, Wu Q. *et al.* Role of pectin methylesterases in cellular calcium distribution and blossom-end rot development in tomato fruit. *Plant J.* 2012;**71**: 824–35
85. Chirinos X, Ying S, Rodrigues MA. *et al.* Transition to ripening in tomato requires hormone-controlled genetic reprogramming initiated in gel tissue. *Plant Physiol.* 2023;**191**: 610–25
86. Liu Y, Shi Y, Su D. *et al.* SlGRAS4 accelerates fruit ripening by regulating ethylene biosynthesis genes and SlMADS1 in tomato. *Hortic Res.* 2021;**8**:1–11
87. Gan L, Song M, Wang X. *et al.* Cytokinins are involved in regulation of tomato pericarp thickness and fruit size. *Hortic Res.* 2022;**9**:1–10
88. Zou J, Li N, Hu N. *et al.* Co-silencing of ABA receptors (SlRCAR) reveals interactions between ABA and ethylene signaling during tomato fruit ripening. *Hortic Res.* 2022;**9**:1–15
89. Su D, Liu K, Yu Z. *et al.* Genome-wide characterization of the tomato GASA family identifies SlGASA1 as a repressor of fruit ripening. *Hortic Res.* 2023;**10**:1–11
90. Wu M, Liu K, Li H. *et al.* Gibberellins involved in fruit ripening and softening by mediating multiple hormonal signals in tomato. *Hortic Res.* 2024;**11**:1–11
91. Konkina A, Klepadlo M, Lakehal A. *et al.* An *Arabidopsis* prolyl 4-hydroxylase is involved in the low oxygen response. *Front Plant Sci.* 2021;**12**:1–12
92. Gibbs DJ, Lee SC, Md Isa N. *et al.* Homeostatic response to hypoxia is regulated by the N-end rule pathway in plants. *Nature.* 2011;**479**:415–8
93. Weits DA, Giuntoli B, Kosmacz M. *et al.* Plant cysteine oxidases control the oxygen-dependent branch of the N-end-rule pathway. *Nat Commun.* 2014;**5**:1–10
94. Batu A. Determination of acceptable firmness and colour values of tomatoes. *J Food Eng.* 2004;**61**:471–5
95. Nakatsuka A, Murachi S, Okunishi H. *et al.* Differential expression and internal feedback regulation of 1-aminocyclopropane-1-carboxylate synthase, 1-aminocyclopropane-1-carboxylate oxidase, and ethylene receptor genes in tomato fruit during development and ripening. *Plant Physiol.* 1998;**118**:1295–305
96. Kutyrieva-Nowak N, Leszczuk A, Zdunek A. A practical guide to in situ and ex situ characterisation of arabinogalactan proteins (AGPs) in fruits. *Plant Methods.* 2023;**19**:1–18
97. Moller I, Sørensen I, Bernal AJ. *et al.* High-throughput mapping of cell-wall polymers within and between plants using novel microarrays. *Plant J.* 2007;**50**:1118–28
98. Li W, Xu F, Chen S. *et al.* A comparative study on Ca content and distribution in two Gesneriaceae species reveals distinctive mechanisms to cope with high rhizospheric soluble calcium. *Front Plant Sci.* 2014;**5**:1–14
99. Qiu L, Wang Y, Qu H. Loading calcium fluorescent probes into protoplasts to detect calcium in the flesh tissue cells of *Malus domestica*. *Hortic Res.* 2020;**7**:1–11

10. Bibliografia

1) Baldwin TC, Mccann MC, Roberts K. 1993. A novel hydroxyproline-deficient arabinogalactan protein secreted by suspension-cultured cells of *Daucus carota* (Purification and Partial Characterization). *Plant Physiology* 103: 115–123.
2) Batu A. 2004. Determination of acceptable firmness and colour values of tomatoes. *Journal of Food Engineering* 61: 471–475.
3) Biswal AK, Atmodjo MA, Pattathil S, *et al.* 2018. Working towards recalcitrance mechanisms: increased xylan and homogalacturonan production by overexpression of *GAlactUronosylTransferase12 (GAUT12)* causes increased recalcitrance and decreased growth in Populus. *Biotechnology for Biofuels* 11: 9.
4) Bradford MM. 1976. A rapid and sensitive method for the quantitation of microgram quantities of protein utilizing the principle of protein-dye binding. *Analytical Biochemistry* 72: 248–254.
5) Brummell DA. 2006. Cell wall disassembly in ripening fruit. *Functional Plant Biology* 33: 103–119.
6) Castilleux R, Ropitaux M, Manasfi Y, *et al.* 2020. Contributions to arabinogalactan protein analysis. *Methods in Molecular Biology* 2149: 383–402.
7) Chen W, Chen J, Xu Y, *et al.* 2024. Applications of the Yariv reagent in polysaccharide analysis and plant physiology from theory to practice. *Carbohydrate Polymers* 329: 121781.
8) Chromiński A. 1971. Stan badań nad zastosowaniem kwasu 2-chloroetylofosfonowego w przyspieszaniu dojrzewania owoców pomidorów. *Postępy Nauk Rolniczych* 5: 91–110.
9) Cooper JB, Varner JE. 1983. Insolubilization of hydroxyproline-rich cell wall glycoprotein in aerated carrot root slices. *Biochemical and Biophysical Research Communications* 112: 161–167.
10) Corral-Martínez P, García-Fortea E, Bernard S, *et al*. 2016. Ultrastructural immunolocalization of arabinogalactan protein, pectin and hemicellulose epitopes through anther development in *Brassica napus*. *Plant and Cell Physiology* 57: 2161–2174.
11) Duruflé H, Hervé V, Balliau T, *et al.* 2017. Proline hydroxylation in cell wall proteins: Is it yet possible to define rules? *Frontiers in Plant Science* 8: 1–10.
12) Ellis M, Egelund J, Schultz CJ, *et al.* 2010. Arabinogalactan-proteins: Key regulators at the cell surface? *Plant Physiology* 153: 403–419.

13) Feder A, Jensen S, Wang A, *et al.* 2020. Tomato fruit as a model for tissue-specific gene silencing in crop plants. *Horticulture Research* 7: 142.

14) Fragkostefanakis S, Dandachi F, Kalaitzis P. 2012. Expression of arabinogalactan proteins during tomato fruit ripening and in response to mechanical wounding, hypoxia and anoxia. *Plant Physiology and Biochemistry* 52: 112–118.

15) Fragkostefanakis S, Kaloudas D, Kalaitzis P. 2018. Pyridine 2,4-dicarboxylic acid suppresses tomato seedling growth. *Frontiers in Chemistry* 6: 3.

16) Fragkostefanakis S, Sedeek KEM, Raad M, *et al.* 2014. Virus induced gene silencing of three putative prolyl 4-hydroxylases enhances plant growth in tomato (*Solanum lycopersicum*). *Plant Molecular Biology* 85: 459–471.

17) Gao Q, Xiong T, Li X, *et al.* 2019. Calcium and calcium sensors in fruit development and ripening. *Scientia Horticulturae* 253: 412–421.

18) Georgiadou EC, Antoniou C, Majak I, *et al.* 2021. Tissue-specific elucidation of lycopene metabolism in commercial tomato fruit cultivars during ripening. *Scientia Horticulturae* 284: 110144.

19) Ghosh K, Takahashi D, Kotake T. 2023. Plant type II arabinogalactan: Structural features and modification to increase functionality. *Carbohydrate Research* 529: 10828.

20) Göllner EM, Blaschek W, Classen B. 2010. Structural investigations on arabinogalactan-protein from wheat, isolated with Yariv reagent. *Journal of Agricultural and Food Chemistry* 58: 3621–3626.

21) Hijazi M, Roujol D, Nguyen-Kim H, *et al.* 2014a. Arabinogalactan protein 31 (AGP31), a putative network-forming protein in *Arabidopsis thaliana* cell walls? *Annals of Botany* 114: 1087–1097.

22) Hijazi M, Velasquez SM, Jamet E, *et al.* 2014b. An update on post-translational modifications of hydroxyproline-rich glycoproteins: toward a model highlighting their contribution to plant cell wall architecture. *Frontiers in Plant Science* 5: 395.

23) van Holst GJ, Clarke AE. 1985. Quantification of arabinogalactan-protein in plant extracts by single radial gel diffusion. *Analytical Biochemistry* 148: 446–450.

24) Hoshing R, Leeber BW, Kuhn H, *et al.* 2022. The chirality of aggregated Yariv reagents correlates with their AGP-binding ability. *ChemBioChem* 23: e202100532.

25) Hoshing R, Saladino M, Kuhn H, *et al.* 2020. An improved protocol for the synthesis and purification of Yariv reagents. *Journal of Organic Chemistry* 85: 16236–16242.

26) Hyodo H, Terao A, Furukawa J, *et al.* 2013. Tissue specific localization of pectin-Ca^{2+} cross-linkages and pectin methyl-esterification during fruit ripening in tomato (*Solanum lycopersicum*). *PLoS ONE* 8: e78949.

27) Inaba M, Maruyama T, Yoshimi Y, *et al.* 2015. L-Fucose-containing arabinogalactan-protein in radish leaves. *Carbohydrate Research* 415: 1–11.

28) Johnson KL, Cassin AM, Lonsdale A, *et al.* 2017. A motif and amino acid bias bioinformatics pipeline to identify hydroxyproline-rich glycoproteins. *Plant Physiology* 174: 886–903.

29) Kalaitzis P, Fragkostefanakis S, Dandachi F, *et al.* 2010. The role of prolyl 4-hydroxylases in tomato fruit ripening. *Acta Horticulturae* 877: 999–1004.

30) Kalaitzis P, Giannoutsou E, Konkina A. 2023. Role of the cell wall in the regulation of fruit ripening In: Geitmann A, ed. *Plant Cell Walls. Research Milestones and Conceptual Insights* . CRC Press, 147–161.

31) Kawai Y, Ono E, Mizutani M. 2014. Evolution and diversity of the 2-oxoglutarate-dependent dioxygenase superfamily in plants. *The Plant Journal* 78: 328–343.

32) Kieliszewski MJ. 2001. The latest hype on Hyp-O-glycosylation codes. *Phytochemistry* 57: 319–323.

33) Kitazawa K, Tryfona T, Yoshimi Y, *et al.* 2013. β-galactosyl Yariv reagent binds to the β-1,3-galactan of arabinogalactan proteins. *Plant Physiology* 161: 1117–1126.

34) Klee HJ, Giovannoni JJ. 2011. Genetics and control of tomato fruit ripening and quality attributes. *Annual Review of Genetics* 45: 41–59.

35) Knox JP, Linstead PJ, Peart J, *et al.* 1991. Developmentally regulated epitopes of cell surface arabinogalactan proteins and their relation to root tissue pattern formation. *The Plant Journal* 1: 317–326.

36) Konkina A, Klepadlo M, Lakehal A, *et al.* 2021. An *Arabidopsis* prolyl 4 hydroxylase is involved in the low oxygen response. *Frontiers in Plant Science* 12: 637352.

37) Koski MK, Hieta R, Böllner C, *et al.* 2007. The active site of an algal prolyl 4-hydroxylase has a large structural plasticity. *Journal of Biological Chemistry* 282: 37112–37123.

38) Koski MK, Hieta R, Hirsilä M, *et al.* 2009. The crystal structure of an algal prolyl 4-hydroxylase complexed with a proline-rich peptide reveals a novel buried tripeptide binding motif. *Journal of Biological Chemistry* 284: 25290–25301.

39) Laemmli U.K. 1970. Cleavage of structural proteins during the assembly of the head of bacteriophage T4. *Nature* 227: 680–685.

40) Lamport D. 2013. Preparation of arabinogalactan glycoproteins from plant tissue. *BIO-PROTOCOL* 3: 1–5.

41) Lampugnani ER, Khan GA, Somssich M, *et al.* 2018. Building a plant cell wall at a glance. *Journal of Cell Science* 131: jcs207373.

42) Leszczuk A, Chylińska M, Zdunek A. 2019a. Distribution of arabinogalactan proteins and pectins in the cells of apple (*Malus* × *domestica*) fruit during post-harvest storage. *Annals of Botany* 123: 47–55.

43) Leszczuk A, Chylińska M, Zięba E, *et al.* 2018. Structural network of arabinogalactan proteins (AGPs) and pectins in apple fruit during ripening and senescence processes. *Plant Science* 275: 36–48.

44) Leszczuk A, Cybulska J, Skrzypek T, *et al.* 2020a. Properties of arabinogalactan proteins (AGPs) in apple (*Malus* × *domestica*) fruit at different stages of ripening. *Biology* 9: 1–12.

45) Leszczuk A, Kalaitzis P, Blazakis KN, *et al.* 2020b. The role of arabinogalactan proteins (AGPs) in fruit ripening – a review. *Horticulture Research* 7: 1–12.

46) Leszczuk A, Kalaitzis P, Kulik J, *et al.* 2023. Review: structure and modifications of arabinogalactan proteins (AGPs). *BMC Plant Biology* 23: 45.

47) Leszczuk A, Kozioł A, Szczuka E, *et al.* 2019b. Analysis of AGP contribution to the dynamic assembly and mechanical properties of cell wall during pollen tube growth. *Plant Science* 281: 9–18.

48) Leszczuk A, Pieczywek PM, Gryta A, *et al.* 2019c. Immunocytochemical studies on the distribution of arabinogalactan proteins (AGPs) as a response to fungal infection in *Malus* × *domestica* fruit. *Scientific Reports* 9: 1–14.

49) Leszczuk A, Zając A, Kurzyna-Szklarek M, *et al.* 2020c. Investigations of changes in the arabinogalactan proteins (AGPs) structure, size and composition during the fruit ripening process. *Scientific Reports* 10: 20621.

50) Li W, Xu F, Chen S, *et al.* 2014. A comparative study on Ca content and distribution in two *Gesneriaceae* species reveals distinctive mechanisms to cope with high rhizospheric soluble calcium. *Frontiers in Plant Science* 5: 647.

51) Ling Q, Mohd. Sadali N, Soufi Z, *et al.* 2021. The chloroplast-associated protein degradation pathway controls chromoplast development and fruit ripening in tomato. *Nature Plants* 7: 655–666.

52) Liu Z, Persson S, Sánchez-Rodríguez C. 2015. At the border: the plasma membrane-cell wall continuum. *Journal of Experimental Botany* 66: 1553–1563.

53) Ma Y, Johnson K. 2023. Arabinogalactan proteins – Multifunctional glycoproteins of the plant cell wall. *The Cell Surface* 9: 100102.

54) Ma Y, Zeng W, Bacic A, *et al.* 2018. AGPs through time and space. *Annual Plant Reviews Online* 1: 1–38.

55) McCartney L, Marcus SE, Knox JP. 2005. Monoclonal antibodies to plant cell wall xylans and arabinoxylans. *Journal of Histochemistry & Cytochemistry* 53: 543–546.

56) Moller I, Marcus SE, Haeger A, *et al.* 2008. High-throughput screening of monoclonal antibodies against plant cell wall glycans by hierarchical clustering of their carbohydrate microarray binding profiles. *Glycoconjugate Journal* 25: 37–48.

57) Moore JP, Fangel JU, Willats WGT, *et al.* 2014. Pectic-β(1,4)-galactan, extensin and arabinogalactan-protein epitopes differentiate ripening stages in wine and table grape cell walls. *Annals of Botany* 114: 1279–1294.

58) Nagata M, Yamashita I. 1992. Simple method for simultaneous determination of chlorophyll and carotenoids in tomato fruit. *Journal of The Japanese Society For Food Science and Technology – Nippon Shokuhin Kagaku Kogaku Kaishi* 39: 925–928.

59) Nakatsuka A, Murachi S, Okunishi H, *et al.* 1998. Differential expression and internal feedback regulation of 1-aminocyclopropane-1-carboxylate synthase, 1-aminocyclopropane-1-carboxylate oxidase, and ethylene receptor genes in tomato fruit during development and ripening. *Plant Physiology* 118: 1295–1305.

60) Nibbering P, Petersen BL, Motawia MS, *et al.* 2020. Golgi-localized exo-β1,3-galactosidases involved in cell expansion and root growth in *Arabidopsis*. *Journal of Biological Chemistry* 295: 10581–10592.

61) Nothnagel EA. 1997. Proteoglycans and related components in plant cells. *International Review of Cytology* 174: 195–291.

62) Orfila C, Seymour GB, Willats WG, *et al.* 2001. Altered middle lamella homogalacturonan and disrupted deposition of (1→5)-α-l-arabinan in the pericarp of *Cnr*, a ripening mutant of tomato. *Plant Physiology* 126: 210–221.

63) Ortiz A, Graell J, Lara I. 2011. Cell wall-modifying enzymes and firmness loss in ripening 'Golden Reinders' apples: A comparison between calcium dips and ULO storage. *Food Chemistry* 128: 1072–1079.

64) Osorio S, Scossa F, Fernie AR. 2013. Molecular regulation of fruit ripening. *Frontiers in Plant Science* 4: 198.

65) Oxley D, Bacic A. 1999. Structure of the glycosylphosphatidylinositol anchor of an arabinogalactan protein from *Pyrus communis* suspension-cultured cells. *PNAS* 96: 14246–14251.

66) Paniagua C, Posé S, Morris VJ, *et al.* 2014. Fruit softening and pectin disassembly: An overview of nanostructural pectin modifications assessed by atomic force microscopy. *Annals of Botany* 114: 1375–1383.

67) Paulsen BS, Craik DJ, Dunstan DE, *et al.* 2014. The Yariv reagent: behaviour in different solvents and interaction with a gum arabic arabinogalactan-protein. *Carbohydrate Polymers* 106: 460–468.

68) Perrakis A, Bita CE, Arhondakis S, *et al.* 2019. Suppression of a prolyl 4 hydroxylase results in delayed abscission of overripe tomato fruits. *Frontiers in Plant Science* 10: 348.

69) Perrakis A, Denic D, Blazakis KN, *et al.* 2021. A tomato prolyl-4-hydroxylase causes relocation of abscission zone and alters abscission kinetics. *bioRxiv*: 1–36.

70) Pfeifer L, Shafee T, Johnson KL, *et al.* 2020. Arabinogalactan-proteins of *Zostera marina* L. contain unique glycan structures and provide insight into adaption processes to saline environments. *Scientific Reports* 10: 8232.

71) Piński A, Betekhtin A, Kwasniewska J, *et al.* 2021. 3,4-Dehydro-L-proline induces programmed cell death in the roots of *Brachypodium distachyon*. *International Journal of Molecular Sciences* 22: 7548.

72) Přerovská T, Pavlů A, Pavlů P, *et al.* 2021. Structural basis of the function of Yariv reagent-an important tool to study arabinogalactan proteins. *Frontiers in Molecular Biosciences* 8: 682858.

73) Popper ZA. 2011. Extraction and detection of arabinogalactan proteins In: Popper ZA, ed. *The Plant Cell Wall. Methods in molecular biology*. Humana Press, 245–254.

74) Posé S, Marcus SE, Knox JP. 2018. Differential metabolism of pectic galactan in tomato and strawberry fruit: detection of the LM26 branched galactan epitope in ripe strawberry fruit. *Physiologia Plantarum* 164: 95–105.

75) Posé S, Paniagua C, Matas AJ, *et al.* 2019. A nanostructural view of the cell wall disassembly process during fruit ripening and postharvest storage by atomic force microscopy. *Trends in Food Science & Technology* 87: 47–58.

76) Qiu L, Wang Y, Qu H. 2020. Loading calcium fluorescent probes into protoplasts to detect calcium in the flesh tissue cells of *Malus domestica*. *Horticulture Research* 7: 91.

77) Quinet M, Angosto T, Yuste-Lisbona FJ, *et al.* 2019. Tomato fruit development and metabolism. *Frontiers in Plant Science* 10: 1554.

78) Rueda S, Mccubbin TJ, Shieh M, *et al.* 2023. A functionalizable analog of the Yariv reagent for AGP imaging using fluorescence microscopy. *Bioconjugate Chemistry* 34: 1398–1406.

79) Schultz CJ, Johnson KL, Currie G, *et al.* 2000. The classical arabinogalactan protein gene family of Arabidopsis. *The Plant Cell* 12: 1751–1767.

80) Schultz CJ, Rumsewicz MP, Johnson KL, *et al.* 2002. Using genomic resources to guide research directions. The arabinogalactan protein gene family as a test case. *Plant Physiology* 129: 1448–1463.

81) Seymour GB, Chapman NH, Chew BL, *et al.* 2013. Regulation of ripening and opportunities for control in tomato and other fruits. *Plant Biotechnology Journal* 11: 269–278.

82) Showalter A. 2001. Arabinogalactan – proteins: Structure, expression and function. *CMLS, Cellular and Molecular Life Sciences* 58: 1399–1417.

83) Showalter AM, Basu D. 2015. Glycosylation of arabinogalactan-proteins essential for developmentin *Arabidopsis*. *Communicative & Integrative Biology* 10: e1177687.

84) Showalter A, Basu D. 2016. Extensin and arabinogalactan-protein biosynthesis: Glycosyltransferases, research challenges, and biosensors. *Frontiers in Plant Science* 7: 814.

85) Silva J, Ferraz R, Dupree P, *et al.* 2020. Three decades of advances in arabinogalactan-protein biosynthesis. *Frontiers in Plant Science* 11: 610377.

86) Skolik P, Morais CLM, Martin FL, *et al.* 2019. Determination of developmental and ripening stages of whole tomato fruit using portable infrared spectroscopy and chemometrics. *BMC Plant Biology* 19: 236.

87) Smallwood M, Yates EA, Willats WGT, *et al.* 1996. Immunochemical comparison of membrane-associated and secreted arabinogalactan-proteins in rice and carrot. *Planta* 198: 452–459.

88) Srivastava V, McKee LS, Bulone V. 2017. Plant Cell Walls In: *eLS.* John Wiley & Sons, 1–17.

89) Strasser R, Seifert G, Doblin MS, *et al.* 2021. Cracking the ‘sugar code’: A snapshot of N- and O-glycosylation pathways and functions in plants cells. *Frontiers in Plant Science* 12: 640919.

90) Svetek J, Yadav MP, Nothnagel EA. 1999. Presence of a glycosylphosphatidylinositol lipid anchor on rose arabinogalactan proteins. *Journal of Biological Chemistry* 274: 14724–14733.

91) Tan L, Cheng J, Zhang L, *et al.* 2024. Pectic-AGP is a major form of *Arabidopsis* AGPs. *Carbohydrate Polymers* 330: 121838.

92) Tan L, Eberhard S, Pattathil S, *et al.* 2013. An *Arabidopsis* cell wall proteoglycan consists of pectin and arabinoxylan covalently linked to an arabinogalactan protein. *The Plant Cell* 25: 270–287.

93) Tan L, Leykam JF, Kieliszewski MJ. 2003. Glycosylation motifs that direct arabinogalactan addition to arabinogalactan-proteins. *Plant Physiology* 132: 1362–1369.

94) Tan L, Zhang L, Black I, *et al.* 2023. Most of the rhamnogalacturonan-I from cultured *Arabidopsis* cell walls is covalently linked to arabinogalactan-protein. *Carbohydrate Polymers* 301: 120340.

95) Tsien RY. 1980. New calcium indicators and buffers with high selectivity against magnesium and protons: Design, synthesis, and properties of prototype structures? *Biochemistry* 19: 3768–3770.

96) de Tullio MC, Paciolla C, Vecchia FD, *et al.* 1999. Changes in onion root development induced by the inhibition of peptidyl-prolyl hydroxylase and influence of the ascorbate system on cell division and elongation. *Planta* 209: 424–434.

97) Velasquez SM, Ricardi MM, Dorosz JG, *et al.* 2011. O-glycosylated cell wall proteins are essential in root hair growth. *Science* 332: 1401–1403.

98) Velasquez SM, Ricardi MM, Poulsen CP, *et al.* 2015. Complex regulation of prolyl 4-hydroxylases impacts root hair expansion. *Molecular Plant* 8: 734–746.

99) Verhertbruggen Y, Marcus SE, Haeger A, *et al.* 2009. Developmental complexity of arabinan polysaccharides and their processing in plant cell walls. *The Plant Journal* 59: 413–425.

100) Vlad F, Spano T, Vlad D, *et al.* 2007. *Arabidopsis* prolyl 4-hydroxylases are differentially expressed in response to hypoxia, anoxia and mechanical wounding. *Physiologia Plantarum* 130: 471–483.

101) Vlad F, Tiainen P, Owen C, *et al.* 2010. Characterization of two carnation petal prolyl 4 hydroxylases. *Physiologia Plantarum* 140: 199–207.

102) Wang D, Seymour GB. 2022. Molecular and biochemical basis of softening in tomato. *Molecular Horticulture* 2: 5.

103) Yariv J, Rapport MM, Graf L. 1962. The interaction of glycosides and saccharides with antibody to the corresponding phenylazo glycosides. *Biochemical Journal* 85: 383–388.

104) Yates EA, Valdor J-F, Haslam SM, *et al.* 1996. Characterization of carbohydrate structural features recognized by anti-arabinogalactan-protein monoclonal antibodies. *Glycobiology* 6: 131–139.

105) Zhang B, Gao Y, Zhang L, *et al.* 2021. The plant cell wall: Biosynthesis, construction, and functions. *Journal of Integrative Plant Biology* 63: 251–272.

106) Zhou K. 2022. The regulation of the cell wall by glycosylphosphatidylinositol-anchored proteins in *Arabidopsis*. *Frontiers in Cell and Developmental Biology* 10: 1–8.

11. Oświadczenia

INSTYTUT AGROFIZYKI PAN

HR EXCELLENCE IN RESEARCH

Lublin, 08.01.2025

mgr Nataliia Kutyrieva-Nowak
Zakład Fizykochemii Materiałów Porowatych
Instytut Agrofizyki im. Bohdana Dobrzańskiego PAN
ul. Doświadczalna 4, 20-290 Lublin

Oświadczenie

Niniejszym oświadczam, że w niżej wymienionych pracach inicjatywa podjęcia badań jest moim wkładem intelektualnym:

P.1: **Kutyrieva-Nowak N.**, Leszczuk A., Zdunek A. 2023. A practical guide to *in situ* and *ex situ* characterisation of arabinogalactan proteins (AGPs) in fruits. Plant Methods, 19: 117.

P.2: **Kutyrieva-Nowak N.**, Leszczuk A., Zając A., Kalaitzis P., Zdunek A. 2023. Arabinogalactan protein is a molecular and cytological marker of particular stages of the tomato fruit ripening process. Scientia Horticulturae, 310: 111718.

P.3: **Kutyrieva-Nowak N.**, Leszczuk A., Ezzat L., Kaloudas D., Zając A., Szymańska-Chargot M., Skrzypek T., Krokida A., Mekkaoui K., Lampropoulou E., Kalaitzis P., Zdunek A. 2024. The modified activity of prolyl 4 hydroxylases reveals the effect of arabinogalactan proteins on changes in the cell wall during the tomato ripening process. Frontiers in Plant Science, 15: 1365490.

P.4: **Kutyrieva-Nowak N.**, Leszczuk A., Denic D., Bellaidi S., Blazakis K., Gemeliari P., Lis M., Kalaitzis P., Zdunek A. 2024. *In vivo* and *ex vivo* study on cell wall components as part of the network in tomato fruit during the ripening process. Horticulture Research, 11: uhae145.

Mój wkład w poniższe prace obejmował:

- szczegółową analizę danych literaturowych,
- współudział w opracowaniu koncepcji badań,
- współudział w opracowaniu metodyki wykorzystanej w badaniach,
- przeprowadzenie zaplanowanych badań laboratoryjnych,
- analizę i interpretację wyników badań,
- statystyczne i graficzne opracowanie danych,
- przygotowanie manuskryptu,
- współudział w edycji i korekcie manuskryptu,
- uczestnictwo w odpowiedziach do recenzentów.

Nataliia Kutyrieva-Nowak

Czytelny podpis

INSTYTUT AGROFIZYKI PAN

HR EXCELLENCE IN RESEARCH

Lublin, 08.01.2025

dr hab. Agata Leszczuk
Zakład Fizykochemii Materiałów Porowatych
Instytut Agrofizyki im. Bohdana Dobrzańskiego PAN
ul. Doświadczalna 4, 20-290 Lublin

Oświadczenie

Niniejszym oświadczam, że w niżej wymienionych pracach inicjatywa podjęcia badań jest wkładem intelektualnym mgr Natalii Kutyrieva-Nowak:

P.1: **Kutyrieva-Nowak N.**, Leszczuk A., Zdunek A. 2023. A practical guide to *in situ* and *ex situ* characterisation of arabinogalactan proteins (AGPs) in fruits. Plant Methods, 19: 117.

P.2: **Kutyrieva-Nowak N.**, Leszczuk A., Zając A., Kalaitzis P., Zdunek A. 2023. Arabinogalactan protein is a molecular and cytological marker of particular stages of the tomato fruit ripening process. Scientia Horticulturae, 310: 111718.

P.3: **Kutyrieva-Nowak N.**, Leszczuk A., Ezzat L., Kaloudas D., Zając A., Szymańska-Chargot M., Skrzypek T., Krokida A., Mekkaoui K., Lampropoulou E., Kalaitzis P., Zdunek A. 2024. The modified activity of prolyl 4 hydroxylases reveals the effect of arabinogalactan proteins on changes in the cell wall during the tomato ripening process. Frontiers in Plant Science, 15: 1365490.

P.4: **Kutyrieva-Nowak N.**, Leszczuk A., Denic D., Bellaidi S., Blazakis K., Gemeliari P., Lis M., Kalaitzis P., Zdunek A. 2024. *In vivo* and *ex vivo* study on cell wall components as part of the network in tomato fruit during the ripening process. Horticulture Research, 11: uhae145.

Mój wkład w powyższe prace polegał na:

- pełnieniu funkcji kierownika Projektu, w ramach którego realizowano badania,
- określeniu problematyki i zakresu badań,
- opracowaniu koncepcji badań zgodnie z założeniami realizowanego Projektu,
- zapewnieniu materiałów i aparatury umożliwiających realizację badań,
- współudziale w przeprowadzeniu badań oraz interpretacji wyników badań,
- nadzorowaniu procesu przygotowania manuskryptu,
- współudziale w edycji i korekcie manuskryptu,
- pełnieniu funkcji autora korespondencyjnego.

Jednocześnie wyrażam zgodę, aby prace zostały wykorzystane w rozprawie doktorskiej mgr Natalii Kutyrieva-Nowak.

Agata Leszczuk

Czytelny podpis

Chania, 08.01.2025

Panagiotis Kalaitzis, PhD
Studies & Research Coordinator
Department of Horticultural Genetics & Biotechnology
Mediterranean Agronomic Institute of Chania
Alsyllio Agrokepio, 1 Makedonias str Chania,
Crete, 73100 Greece

Statement

I declare that in the publications listed below, the initiative to undertake the research is the intellectual contribution of MSc Nataliia Kutyrieva-Nowak:

P.2: **Kutyrieva-Nowak, N.**, Leszczuk, A., Zając, A., Kalaitzis, P., Zdunek, A., 2023. Arabinogalactan protein is a molecular and cytological marker of particular stages of the tomato fruit ripening process. *Scientia Horticulturae* 310, 111718.

P.3: **Kutyrieva-Nowak, N.**, Leszczuk, A., Ezzat, L., Kaloudas, D., Zając, A., Szymańska-Chargot, M., Skrzypek, T., Krokida, A., Mekkaoui, K., Lampropoulou, E., Kalaitzis, P., Zdunek, A., 2024. The modified activity of prolyl 4 hydroxylases reveals the effect of arabinogalactan proteins on changes in the cell wall during the tomato ripening process. *Frontiers in Plant Science* 15, 1365490.

P.4: **Kutyrieva-Nowak, N.**, Leszczuk, A., Denic, D., Bellaidi, S., Blazakis, K., Gemeliari, P., Lis, M., Kalaitzis, P., Zdunek, A., 2024. *In vivo* and *ex vivo* study on cell wall components as part of the network in tomato fruit during the ripening process. *Horticulture Research* 11, uhae145.

My contribution and my research team, including:
Lamia Ezzat, Dimitris Kaloudas, Afroditi Krokida, Khansa Mekkaoui, Evangelia Lampropoulou, Dusan Denic, Samia Bellaidi, Kostas Blazakis, Petroula Gemielari

to the above works involved:

• Preparation, cultivation, and genetic characterization of the research material.

I hereby give my consent for the publications to be used in the doctoral dissertation of MSc Nataliia Kutyrieva-Nowak.

Signature

Lublin, 08.01.2025

dr Adrian Zając
Katedra Anatomii Funkcjonalnej i Cytobiologii
Wydział Biologii i Biotechnologii
Uniwersytet Marii Curie-Skłodowskiej
ul. Akademicka 19, 20-400 Lublin

Oświadczenie

Niniejszym oświadczam, że w niżej wymienionych pracach inicjatywa podjęcia badań jest wkładem intelektualnym mgr Natalii Kutyrieva-Nowak:

P.2: **Kutyrieva-Nowak N.**, Leszczuk A., Zając A., Kalaitzis P., Zdunek A. 2023. Arabinogalactan protein is a molecular and cytological marker of particular stages of the tomato fruit ripening process. Scientia Horticulturae, 310: 111718.

P.3: **Kutyrieva-Nowak N.**, Leszczuk A., Ezzat L., Kaloudas D., Zając A., Szymańska-Chargot M., Skrzypek T., Krokida A., Mekkaoui K., Lampropoulou E., Kalaitzis P., Zdunek A. 2024. The modified activity of prolyl 4 hydroxylases reveals the effect of arabinogalactan proteins on changes in the cell wall during the tomato ripening process. Frontiers in Plant Science, 15: 1365490.

Mój wkład w powyższe prace polegał na:

- współudziale w interpretacji wyników badań.

Jednocześnie wyrażam zgodę, aby prace zostały wykorzystane w rozprawie doktorskiej mgr Natalii Kutyrieva-Nowak.

Adrian Zając

Czytelny podpis

INSTYTUT AGROFIZYKI PAN

HR EXCELLENCE IN RESEARCH

Lublin, 08.01.2025

dr hab. Monika Szymańska-Chargot
Zakład Mikrostruktury i Mechaniki Biomateriałów
Instytut Agrofizyki im. Bohdana Dobrzańskiego PAN
ul. Doświadczalna 4, 20-290 Lublin

Oświadczenie

Niniejszym oświadczam, że w niżej wymienionej pracy inicjatywa podjęcia badań jest wkładem intelektualnym mgr Natalii Kutyrieva-Nowak:

P.3: **Kutyrieva-Nowak N.**, Leszczuk A., Ezzat L., Kaloudas D., Zając A., Szymańska-Chargot M., Skrzypek T., Krokida A., Mekkaoui K., Lampropoulou E., Kalaitzis P., Zdunek A. 2024. The modified activity of prolyl 4 hydroxylases reveals the effect of arabinogalactan proteins on changes in the cell wall during the tomato ripening process. Frontiers in Plant Science, 15: 1365490.

Mój wkład w powyższe prace polegał na:

- przeprowadzeniu analiz strukturalnych za pomocą spektroskopii w podczerwieni z transformacją Fouriera (FTIR),
- współudziale w interpretacji wyników badań.

Jednocześnie wyrażam zgodę, aby prace zostały wykorzystane w rozprawie doktorskiej mgr Natalii Kutyrieva-Nowak.

Czytelny podpis

Lublin, 08.01.2025

dr hab. Tomasz Skrzypek prof. KUL
Katedra Biomedycyny i Badań Środowiskowych
Instytut Nauk Biologicznych
Wydział Medyczny
Katolicki Uniwersytet Lubelski Jana Pawła II
ul. Konstantynów 1 H, 20-708 Lublin

Oświadczenie

Niniejszym oświadczam, że w niżej wymienionej publikacji inicjatywa podjęcia badań jest wkładem intelektualnym mgr Natalii Kutyrieva-Nowak:

P.3: **Kutyrieva-Nowak N.**, Leszczuk A., Ezzat L., Kaloudas D., Zając A., Szymańska-Chargot M., Skrzypek T., Krokida A., Mekkaoui K., Lampropoulou E., Kalaitzis P., Zdunek A. 2024. The modified activity of prolyl 4 hydroxylases reveals the effect of arabinogalactan proteins on changes in the cell wall during the tomato ripening process. Frontiers in Plant Science, 15: 1365490.

Mój wkład w powyższą pracę polegał na:

- współudziale w wykonaniu analiz mikroskopowych za pomocą transmisyjnego mikroskopu elektronowego (TEM) oraz skaningowego mikroskopu elektronowego (SEM).

Jednocześnie wyrażam zgodę, aby prace zostały wykorzystane w rozprawie doktorskiej mgr Natalii Kutyrieva-Nowak.

Czytelny podpis

Lublin, 08.01.2025

dr Magdalena Lis
Katedra Biomedycyny i Badań Środowiskowych
Instytut Nauk Biologicznych
Wydział Medyczny
Katolicki Uniwersytet Lubelski Jana Pawła II
ul. Konstantynów 1 H, 20-708 Lublin

Oświadczenie

Niniejszym oświadczam, że w niżej wymienionej publikacji inicjatywa podjęcia badań jest wkładem intelektualnym mgr Natalii Kutyrieva-Nowak:

P.4: **Kutyrieva-Nowak N.**, Leszczuk A., Denic D., Bellaidi S., Blazakis K., Gemeliari P., Lis M., Kalaitzis P., Zdunek A. 2024. *In vivo* and *ex vivo* study on cell wall components as part of the network in tomato fruit during the ripening process. Horticulture Research, 11: uhae145.

Mój wkład w powyższe prace polegał na:

- współudziale w wykonaniu analiz mikroskopowych za pomocą transmisyjnego mikroskopu elektronowego (TEM).

Jednocześnie wyrażam zgodę, aby prace zostały wykorzystane w rozprawie doktorskiej mgr Natalii Kutyrieva-Nowak.

Magdalena Lis

Czytelny podpis

INSTYTUT AGROFIZYKI PAN

HR EXCELLENCE IN RESEARCH

Lublin, 31.01.2025

prof. dr hab. Artur Zdunek
Zakład Mikrostruktury i Mechaniki Biomateriałów
Instytut Agrofizyki im. Bohdana Dobrzańskiego PAN
ul. Doświadczalna 4, 20-290 Lublin

Oświadczenie

Niniejszym oświadczam, że w niżej wymienionych pracach inicjatywa podjęcia badań jest wkładem intelektualnym mgr Natalii Kutyrieva-Nowak:

P.1: **Kutyrieva-Nowak N.**, Leszczuk A., Zdunek A. 2023. A practical guide to *in situ* and *ex situ* characterisation of arabinogalactan proteins (AGPs) in fruits. Plant Methods, 19: 117.

P.2: **Kutyrieva-Nowak N.**, Leszczuk A., Zając A., Kalaitzis P., Zdunek A. 2023. Arabinogalactan protein is a molecular and cytological marker of particular stages of the tomato fruit ripening process. Scientia Horticulturae, 310: 111718.

P.3: **Kutyrieva-Nowak N.**, Leszczuk A., Ezzat L., Kaloudas D., Zając A., Szymańska-Chargot M., Skrzypek T., Krokida A., Mekkaoui K., Lampropoulou E., Kalaitzis P., Zdunek A. 2024. The modified activity of prolyl 4 hydroxylases reveals the effect of arabinogalactan proteins on changes in the cell wall during the tomato ripening process. Frontiers in Plant Science, 15: 1365490.

P.4: **Kutyrieva-Nowak N.**, Leszczuk A., Denic D., Bellaidi S., Blazakis K., Gemeliari P., Lis M., Kalaitzis P., Zdunek A. 2024. *In vivo* and *ex vivo* study on cell wall components as part of the network in tomato fruit during the ripening process. Horticulture Research, 11: uhae145.

Mój wkład w powyższe prace polegał na:

- współudziale w edycji i korekcie manuskryptu.

Jednocześnie wyrażam zgodę, aby prace zostały wykorzystane w rozprawie doktorskiej mgr Natalii Kutyrieva-Nowak.

Czytelny podpis

12. Aneks – życiorys naukowy

WYKSZTAŁCENIE

2022 – 2025 Uniwersytet Marii Curie-Skłodowskiej w Lublinie, Szkoła Doktorska Nauk Ścisłych i Przyrodniczych
Kształcenie w dyscyplinie naukowej – rolnictwo i ogrodnictwo
Tytuł rozprawy doktorskiej: *„Badania białek arabinogalaktanowych (AGP) jako istotnych składników ściany komórkowej w procesie dojrzewania owoców”.*
Promotor: dr hab. Agata Leszczuk

2015 – 2017 Uniwersytet Marii Curie-Skłodowskiej w Lublinie, Wydział Biologii i Biotechnologii
Studia magisterskie na kierunku biotechnologia o specjalności biotechnologia ogólna
uzyskanie tytułu zawodowego magistra na podstawie pracy magisterskiej pt. *„Egzopolimery i metabolity oraz aktywność enzymatyczna w hodowlach niepatogenicznych szczepów Fusarium spp. na różnych źródłach C i N”.*
Promotor: dr hab. Jolanta Jaroszuk-Ściseł, prof. UMCS

2012 – 2015 Uniwersytet Marii Curie-Skłodowskiej w Lublinie, Wydział Biologii i Biotechnologii
Studia licencjackie na kierunku biotechnologia
uzyskanie tytułu zawodowego licencjata na podstawie pracy licencjackiej pt. *„Od środowiska glebowego do biopreparatów grzybowych”.*
Promotor: dr hab. Jolanta Jaroszuk-Ściseł, prof. UMCS

DOŚWIADCZENIE ZAWODOWE

2018 – 2022 „BIOMED-LUBLIN” Wytwórnia Surowic i Szczepionek S.A., Lublin (obecnie Synthaverse S.A.)
Lider Produkcji oraz Zastępca Kierownika Wydziału Produkcyjnego po awansie ze stanowiska Operator urządzeń do produkcji farmaceutycznej.

PROJEKTY BADAWCZE

2022 – 2024 Instytut Agrofizyki im. Bohdana Dobrzańskiego Polskiej Akademii Nauk w Lublinie
Członkini zespołu projektowego na stanowisku Stypendysta – Student/Doktorant – Projekt finansowany przez Narodowe Centrum Nauki nr 2020/39/D/NZ9/00232 w ramach konkursu SONATA 16 pt. „Badania białek arabinogalaktanowych (AGP) jako istotnych składników ściany komórkowej podczas procesu dojrzewania owoców”.

STAŻE ZAGRANICZNE

18.03.2024 – 18.05.2024 Uniwersytet w Belgradzie, Serbia
Institute of Molecular Genetics and Genetic Engineering
Laboratory for Plant Molecular Biology
Staż finansowany w ramach projektu NAWA STER „UMCS Doctoral Schools – Your Success in Globalize World of Science" nr 1/STAZ/spozaOECD2.
Opiekun naukowy: dr Marija Vidović

NAGRODY I WYRÓŻNIENIA

01.04.2024 – 30.09.2024 Stypendium dla najlepszych zagranicznych doktorantów, kształcących się w Szkołach Doktorskich UMCS w ramach Projektu pt. „UMCS Doctoral Schools – Your Success in Globalized World of Science" nr STYP/2022/14.

14.12.2023 Wyróżnienie za referat wygłoszony podczas VI Konferencji Doktorantów „Cztery Żywioły – współczesne problemy w naukach o życiu" pod tytułem „Dystrybucja i zawartość Ca^{2+} w tkankach owoców pomidora z zaburzonym procesem syntezy AGP". Lublin, Polska.

AKTYWNOŚĆ PUBLIKACYJNA

Lista publikacji stanowiących podstawę rozprawy doktorskiej

1. **Kutyrieva-Nowak N.**, Leszczuk A., Zdunek A. 2023. A practical guide to *in situ* and *ex situ* characterisation of arabinogalactan proteins (AGPs) in fruits. Plant Methods, 19: 117.
Wskaźnik Impact Factor (2023): 4.7; punktacja MNiSW: 140 punktów.

2. **Kutyrieva-Nowak N.**, Leszczuk A., Zając A., Kalaitzis P., Zdunek A. 2023. Arabinogalactan protein is a molecular and cytological marker of particular stages of the tomato fruit ripening process. Scientia Horticulturae, 310: 111718.
Wskaźnik Impact Factor (2023): 3.9; punktacja MNiSW: 140 punktów.

3. **Kutyrieva-Nowak N.**, Leszczuk A., Ezzat L., Kaloudas D., Zając A., Szymańska-Chargot M., Skrzypek T., Krokida A., Mekkaoui K., Lampropoulou E., Kalaitzis P., Zdunek A. 2024. The modified activity of prolyl 4 hydroxylases reveals the effect of arabinogalactan proteins on changes in the cell wall during the tomato ripening process. Frontiers in Plant Science, 15: 1365490.
Wskaźnik Impact Factor (2023): 4.1; punktacja MNiSW: 100 punktów.

4. **Kutyrieva-Nowak N.**, Leszczuk A., Denic D., Bellaidi S., Blazakis K., Gemeliari P., Lis M., Kalaitzis P., Zdunek A. 2024. *In vivo* and *ex vivo* study on cell wall components as part of the network in tomato fruit during the ripening process. Horticulture Research, 11: uhae145.

Wskaźnik Impact Factor (2023): 7.6; punktacja MNiSW: 200 punktów.

Pozostałe publikacje

5. Leszczuk A., **Kutyrieva-Nowak N.**, Nowak A., Nosalewicz A., Zdunek A. 2024. Low oxygen environment effect on the tomato cell wall composition during the fruit ripening process. BMC Plant Biology, 24: 503.
Wskaźnik Impact Factor (2023): 4.3; punktacja MNiSW: 140 punktów.

6. Nowak A., Majewska M., Marzec-Grządziel A., Ozimek E., Przybyś M., Słomka A., **Kutyrieva-Nowak N.**, Galązka A., Jaroszuk-Ściseł J. 2024. Effect of long-term radish (*Raphanus sativus* var. *sativus*) monoculture practice on physiological variability of microorganisms in cultivated soil. Journal of Environmental Management, 367: 122007.
Wskaźnik Impact Factor (2023): 8.0; punktacja MNiSW: 200 punktów.

7. **Kutyrieva-Nowak N.**, Leszczuk A., Zdunek A. 2024. Metody molekularne i mikroskopowe w badaniach ściany komórkowej. XII Ogólnopolski Sympozjum „Nauka i przemysł – lubelskie spotkanie studenckie". str. 82-85. ISBN 978-83-227-9806-5.
Punktacja MNiSW: 20 punktów.

8. **Kutyrieva-Nowak N.**, Pantelić A., Isaković S., Kanellis A.K., Vidović M., Leszczuk A. 2025. Effect of the overexpression of the *GGP1* gene on tomato fruit cell walls (manuskrypt w recenzji).

9. Leszczuk A., **Kutyrieva-Nowak N.**, Rueda S., Basu A. 2025. Changes in *Arabidopsis thaliana* seedling cell wall polysaccharides induced by treatment with Yariv reagent – visualization with immunocytochemistry and a fluorescent Yariv reagent (manuskrypt w recenzji).

10. Zając A., Leszczuk A., **Kutyrieva-Nowak N.**, Kalaitzis P. 2025. An insight into functional pro-health abilities of glycoproteins: underlying mechanisms of arabinogalactan proteins isolated from plants (manuskrypt w recenzji).

AKTYWNOŚĆ ORGANIZACYJNA

2023 – 2025 Członek Rady Szkoły Doktorskiej Nauk Ścisłych i Przyrodniczych (Reprezentantka doktorantów) powołana decyzją Rektora prof. dr hab. Radosława Dobrowolskiego na podstawie § 5 Regulaminu Szkoły Doktorskiej Nauk Ścisłych i Przyrodniczych Uniwersytetu Marii Curie-Skłodowskiej w Lublinie stanowiącego załącznik do Uchwały Nr XXIV – 26.6/19 Senatu Uniwersytetu Marii Curie-Skłodowskiej w Lublinie.

AKTYWNOŚĆ REDAKCYJNA

2023 Projekt i skład książki „Cztery Żywioły – współczesne problemy w naukach o życiu”. Wydawnictwo: Instytut Agrofizyki im. Bohdana Dobrzańskiego Polskiej Akademii Nauk, ul. Doświadczalna 4, Lublin 20-290; ISBN 978-83-89969-83-5.

AKTYWNOŚĆ POPULARYZACYJNA

2024 Uczestnictwo w warsztatach biologicznych podczas XIII Nocy Biologów na Wydziale Biologii i Biotechnologii Uniwersytetu Marii Curie-Skłodowskiej w Lublinie, Polska.

2023 Uczestnictwo w Komitecie Organizacyjnym VI Konferencji Doktorantów „Cztery Żywioły – współczesne problemy w naukach o życiu”. Lublin, Polska.

UDZIAŁ W KONFERENCJACH NAUKOWYCH – 16 doniesień konferencyjnych

Referaty wygłoszone na konferencjach międzynarodowych

1. **Kutyrieva N.**, Leszczuk A., Zdunek A. Molecular studies on changes of arabinogalactan proteins (AGPs) during tomato ripening process. 21st International Workshop for Young Scientists „BioPhys Spring”. 30-31.05.2022, Nitra, Słowacja.
Abstrakt został opublikowany w materiałach konferencyjnych na str. 61-62.

2. **Kutyrieva-Nowak N.**, Leszczuk A., Kalaitzis P., Zdunek A. 2023. Prolyl 4 hydroxylases (P4Hs) affect cell wall changes during the fruit ripening process. 22nd International Workshop for Young Scientists „BioPhys Spring”. 15-16.06.2023, Gödöllő, Węgry.
Abstrakt został opublikowany w materiałach konferencyjnych na str. 43.

3. **Kutyrieva-Nowak N.**, Leszczuk A., Zdunek A. Molecular & microscopic tools to study fruit cell walls. 14th International Conference on Agrophysics. 11-13.09.2023, Lublin, Polska.
Abstrakt został opublikowany w materiałach konferencyjnych na str. 35.

4. **Kutyrieva-Nowak N.**, Leszczuk A., Nowak A., Nosalewicz A., Zdunek A. Physiological changes in tomato fruit during storage in stressful oxygen condition. 23rd International Workshop for Young Scientists „BioPhys Spring 2024”, 23-24.05.2024, Lublin, Polska.
Abstrakt został opublikowany w materiałach konferencyjnych na str. 87-89.

Referaty wygłoszone na konferencjach krajowych

1. **Kutyrieva-Nowak N.**, Leszczuk A., Kalaitzis P., Zdunek A. Rola hydroksylazy prolinowej (P4H3) w biosyntezie AGP w procesie dojrzewania owoców pomidora. Warsztaty dla młodych badaczy. 28-29.11.2022, Lublin, Polska.
Abstrakt został opublikowany w materiałach konferencyjnych na str.17-18.

2. **Kutyrieva-Nowak N.**, Leszczuk A., Kalaitzis P., Zdunek A. Wpływ aktywności hydroksylazy prolinowej (P4H3) na dystrybucję AGP w ścianie komórkowej podczas procesu dojrzewania owoców pomidora. Konferencja „Cztery Żywioły – współczesne problemy w naukach o życiu". 14.12.2022, Warszawa, Polska.
Abstrakt został opublikowany w materiałach konferencyjnych na str. 28.

3. **Kutyrieva-Nowak N.**, Leszczuk A., Zdunek A. Lokalizacja i czasowo-przestrzenna dystrybucja składników kompleksu APAP1 podczas procesu dojrzewania owoców pomidora. Warsztaty dla młodych badaczy. 30.11-01.12.2023, Lublin, Polska.
Abstrakt został opublikowany w materiałach konferencyjnych na str. 10-11.

4. **Kutyrieva-Nowak N.**, Leszczuk A., Kalaitzis P., Zdunek A. Dystrybucja i zawartość Ca^{2+} w tkankach owoców pomidora z zaburzonym procesem syntezy AGP. Konferencja „Cztery Żywioły – współczesne problemy w naukach o życiu". 14.12.2023, Lublin, Polska.
Abstrakt został opublikowany w materiałach konferencyjnych na str. 35-36.

Postery zaprezentowane na konferencjach międzynarodowych

1. **Kutyrieva-Nowak N.**, Leszczuk A., Zając A., Kaloudas D., Kalaitzis P., Zdunek A. The role of proline hydroxylase (P4H3) in AGP biosynthesis and distribution during the tomato fruit ripening process. XVI Cell Wall Meeting. 18-22.06.2023, Malaga, Hiszpania.
Abstrakt został opublikowany w materiałach konferencyjnych na str. 223.

2. **Kutyrieva-Nowak N.**, Leszczuk A., Nowak A., Nosalewicz A., Zdunek A. How does a low oxygen environment impact the tomato fruit cell walls? International Conference of Soil and Agriculture, ICSA 2024 Towards Soil Sustainability, 11-13.06.2024, Lublin, Polska.
Abstrakt został opublikowany w materiałach konferencyjnych doi.org/10.24326/ICSA1.PP.19

Postery zaprezentowane na konferencjach krajowych

1. **Kutyrieva-Nowak N.**, Leszczuk A., Zdunek A. Metody molekularne i mikroskopowe w badaniach ściany komórkowej. XII Ogólnopolski Sympozjum „Nauka i przemysł – lubelskie spotkanie studenckie", 03.06.2024, Lublin, Polska.
Abstrakt został opublikowany w materiałach konferencyjnych na str. 82-85.

Współautorstwo doniesień konferencyjnych

1. Jaroszuk-Ściseł J., Nowak A., **Kutyrieva N.**, Perzanowski M., Słomka A. Potencjał stymulacyjny i bioremediacyjny niepatogenicznego, endofitycznego szczepu *Fusarium oxysporum* DEMFo14 zależny od warunków hodowli i obecności metalu ciężkiego (Cd, Pb lub Zn). VI Ogólnopolskie Sympozjum Mikrobiologiczne „Metagenomy różnych środowisk". 23-24.06.2022, Puławy, Polska.
Abstrakt został opublikowany w materiałach konferencyjnych na str. 87.

2. Leszczuk A., **Kutyrieva-Nowak N.**, Kalaitzis P. Arabinogalactan protein is a molecular and cytological marker of the fruit ripening process. COST Action CA18210 'Oxygen sensing a novel mean for biology and technology of fruit quality' Annual Meeting. 03-07.10.2022, Belgrad, Serbia.

3. Leszczuk A., **Kutyrieva-Nowak N.**, Sampathianaki M., Kalaitzis P., Zdunek A. Effect of modification of AGP structure on the cell wall assembly. XVI Cell Wall Meeting. 18-22.06.2023, Malaga, Hiszpania.
Abstrakt został opublikowany w materiałach konferencyjnych na str. 205.

4. Leszczuk A., Pieczywek P.M., **Kutyrieva-Nowak N.**, Zdunek A. Molecular & microscopic studies on fruit microstructure during the ripening program and postharvest senescence. 14th International Conference on Agrophysics. 11-13.09.2023, Lublin, Polska.
Abstrakt został opublikowany w materiałach konferencyjnych na str. 35.

5. Nowak A., **Kutyrieva-Nowak N.**, Majewska M., Jaroszuk-Ściseł J. Zmienność fizjologiczna mikroorganizmów zasiedlających glebę uprawną pobraną spod monokultury rzodkiewki (*Raphanus sativus* var. *sativus*). 55 Jubileuszowa Konferencja Mikrobiologiczna „Mikrobiologia w badaniach środowiskowych – rys historyczny i perspektywy na przyszłość". 14-15.09.2023, Puławy, Polska.
Abstrakt został opublikowany w materiałach konferencyjnych na str. 87.